

# NASA CONTRACTOR REPORT



NASA CR

LV. 51  
C.1

0060864



TECH LIBRARY KAFB, NM

LOAN COPY: RETURN TO  
AFWL (WLOL)  
KIRTLAND AFB, N MEX

NASA CR-1607

## DETERMINATION OF WELDABILITY AND ELEVATED TEMPERATURE STABILITY OF REFRACTORY METAL ALLOYS

### *I - Weldability of Refractory Metal Alloys*

*by G. G. Lessmann*

*Prepared by*  
WESTINGHOUSE ASTRONUCLEAR LABORATORY  
Pittsburgh, Pa. 15236  
*for Lewis Research Center*



0060864

1. Report No. NASA CR-1607		2. Government Accession No.		3. Recipient's Catalog No.	
4. Title and Subtitle DETERMINATION OF WELDABILITY AND ELEVATED TEMPERATURE STABILITY OF REFRACTORY METAL ALLOYS. I - WELDABILITY OF REFRACTORY METAL ALLOYS				5. Report Date August 1970	
				6. Performing Organization Code	
7. Author(s) G. G. Lessmann				8. Performing Organization Report No. WANL-PR-(P)-013	
9. Performing Organization Name and Address  Westinghouse Astronuclear Laboratory Pittsburgh, Pennsylvania 15236				10. Work Unit No.	
				11. Contract or Grant No. NAS 3-2540	
12. Sponsoring Agency Name and Address  National Aeronautics and Space Administration Washington, D. C. 20546				13. Type of Report and Period Covered  Contractor Report	
				14. Sponsoring Agency Code	
15. Supplementary Notes					
16. Abstract Refractory metal alloys commercially available and several experimental alloys were included in this program. Both sheet and plate were welded by GTA (gas-tungsten-arc) and EB (electron beam) weld processes. Tantalum alloys showed excellent weldability, followed by the columbium alloy which showed variable weldability, followed by the tungsten alloys which showed generally poor weldability. Weldability was interpreted in terms of its effect on mechanical and metallurgical characteristics rather than merely the ease of joining. Reliable methods were developed for control of the weld atmosphere. A statistical sampling showed that the refractory metal alloys can be welded without contamination. The factors causing weld porosity were determined and procedures to eliminate it were developed to avoid it. The importance of balance between matrix and grain boundary strength in high temperature applications was demonstrated. Alloys with large weld grains (solid solution alloys), low recrystallization temperatures, and relatively weak grain boundaries (yttrium modified alloys) had the least desirable tensile fracture characteristics.					
17. Key Words (Suggested by Author(s))  Refractory metals Welding Thermal stability				18. Distribution Statement  Unclassified - unlimited	
19. Security Classif. (of this report)  Unclassified		20. Security Classif. (of this page)  Unclassified		21. No. of Pages  293	
				22. Price*  \$3.00	



## FOREWORD

This evaluation was conducted by the Westinghouse Astronuclear Laboratory under NASA contract NAS 3-2540. Mr. P. E. Moorhead, of the Lewis Research Center Space Power Systems Division, was the NASA Project Manager for the program. Mr. G. G. Lessmann was responsible for performance of the program at the Westinghouse Astronuclear Laboratory.

The objectives delineated and results reported herein represent the requirements of Tasks I and II of contract NAS 3-2540. Additional comprehensive investigations which were conducted as a part of this program are the subjects of additional reports. The final reports for this contract are the following:

- I - Weldability of Refractory Metal Alloys (CR-1607)
- II - Long-Time Elevated Temperature Stability of Refractory Metal Alloys (CR-1608)
- III - Effect of Contamination Level on Weldability of Refractory Metal Alloys (CR-1609)
- IV - Post Weld Annealing Studies of T-111 (CR-1610)
- V - Weldability of Tungsten Base Alloys (CR-1611)

Additional salient features of this program have been summarized in the following reports:

G. G. Lessmann, "The Comparative Weldability of Refractory Metal Alloys," The Welding Journal Research Supplement, Vol. 45 (12), December, 1966.

G. G. Lessmann and R. E. Gold, "The Weldability of Tungsten Base Alloys," The Welding Journal Research Supplement.

D. R. Stoner and G. G. Lessmann, "Measurement and Control of Weld Chamber Atmospheres," The Welding Journal Research Supplement, Vol. 30 (8), August, 1965.

G. G. Lessmann and D. R. Stoner, "Welding Refractory Metal Alloys for Space Power System Applications," Presented at the 9th National SAMPE Symposium on Joining of Materials for Aerospace Systems, November, 1965.



D. R. Stoner and G. G. Lessmann, "Operation of  $10^{-10}$  Torr Vacuum Heat Treating Furnaces in Routine Processing," Transactions of the 1965 Vacuum Metallurgy Conference of the American Vacuum Society, L. M. Bianchi, Editor.

G. G. Lessmann and R. E. Gold, "Thermal Stability of Refractory Metal Alloys", NASA Symposium on Recent Advances in Refractory Metals for Space Power Systems, June, 1969.

D. R. Stoner, "Welding Behavior of Oxygen Contaminated Refractory Metal Alloys," Presented at Annual AWS Meeting, April, 1967.

## TABLE OF CONTENTS

	<u>Page No.</u>
I. INTRODUCTION	1
II. SUMMARY AND CONCLUSIONS	3
WELDABILITY	3
THERMAL RESPONSE TO WELDING	4
WELD ATMOSPHERE CONTROL	5
POST WELD ANNEALING	6
III. TECHNICAL APPROACH AND PROCEDURES	7
ALLOYS	7
TECHNICAL APPROACH	12
WELDING PROCEDURES AND CONTROLS	17
SPECIAL TEST PROCEDURES	26
INVENTORY AND LOGISTICS MANAGEMENT	31
IV. RESULTS	33
RESTRAINT TESTS	33
DUCTILITY RESPONSE TO WELDING	33
ALLOY WELDABILITY LIMITATIONS	42
TUNGSTEN AND TUNGSTEN-25 RHENIUM	44
THERMAL WELD RESPONSES IN COLUMBIUM ALLOYS	55
WELD POROSITY AND EDGE PREPARATION	75
POST WELD ANNEALING	80
TENSILE EVALUATION	84
V. REFERENCES	96
APPENDICES	97

## LIST OF ILLUSTRATIONS

<u>Figure No.</u>	<u>Title</u>	<u>Page No.</u>
1	Typical GTA Sheet Butt Weld Schedule for Welding Parameter Study	14
2	Typical EB Sheet Butt Weld Schedule	15
3	Gas Tungsten Arc Butt Weld Tooling	19
4	Weld Set-up for GTA Sheet Butt Welds	20
5	Torch and Internal Chamber Arrangement for Manual Plate Welding	22
6	Plate Butt Weld Joint Designs and Typical Macrosections	24
7	Welding Schedule for SCb-291 Butt Weld in 3/8 Inch Plate Material	25
8	Bend Test Parameters	27
9	Bend Test Fixture. Top, Open View. Bottom, With Liquid Nitrogen Cryostat	28
10	Plate Weldments Bend Tested at Room Temperature	29
11	Plate Bend Test Fixture	30
12	Sheet and Plate Weld Restraint Specimens. Top, Circular Groove Test in FS-85 Plate. Bottom, Bead-on-Plate Patch Test in T-111 Sheet	34
13	Weld Restraint Test Specimens for 0.035 Inch Sheet (A), and 0.375 Inch Plate (B)	35
14	Summary of Bend Test Results for Gas Tungsten Arc and Electron Beam Butt Welds in 0.035 Inch Sheet. Twelve Welding Conditions for Each Alloy and Process. Weld Tested in both Longitudinal and Transverse Directions	38
15	Categorized Weld Bend Transition Behavior	39

# LIST OF ILLUSTRATIONS (Continued)

<u>Figure No.</u>	<u>Title</u>	<u>Page No.</u>
16	Plate Weld Room Temperature Bend Test Summary. For Post Weld Anneals See Table 7	41
17	Defected Gas Tungsten Arc Weld Microstructures for Alloys Displaying Particular Weldability Limitations	45
18	GTA Weld Structure in Unalloyed Tungsten, Weld No. 1 (Welded at 7.5 ipm Without Preheat)	48
19	Typical Sections of Electron Beam Welds in Tungsten	49
20	Typical Dye-Penetrant Results of Electron Beam Welds in Unalloyed Tungsten Sheet	50
21	The Effect of Weld Parameters on Ductility of Gas Tungsten Arc Welds in W-25Re Alloy Sheet	51
22	Photomicrographs of Cast Weld Area in Gas Tungsten Arc Welded W-25Re Sheet	53
23	Photomicrographs of Cast Weld Area in Gas Tungsten Arc Welded W-25Re Sheet	54
24	Observed Heat Input Requirements for Welding 0.035 Inch Sheet as a Function of Welding Speed, Weld Size Constant	56
25	Typical Sheet Butt Weld Configurations for Gas Tungsten Arc (top) and Electron Beam Welds	57
26	Effect of Electron Beam Welding Variables on FS-85 Weld Ductility in 0.035 Inch Sheet	59
27	Relationship of Weld Size to Bend Transition Temperature of Electron Beam Welds in Columbium Alloys. Data for all Columbium Alloy Welds Produced with 60~Longitudinal Deflection (Regardless of Amplitude) Included. Welding Speeds as Indicated.	60

## LIST OF ILLUSTRATIONS (Continued)

<u>Figure No.</u>	<u>Title</u>	<u>Page No.</u>
28	Change in Bend Transition Temperature with Increasing Heat Affected Zone Size of Gas Tungsten Arc Welds in the Solid Solution Columbium Alloy, SCb-291	63
29	Effect of Gas-Tungsten-Arc-Weld Heat Input on Ductility in the Solid Solution plus Dispersion (Reactive Element) Strengthened Columbium Alloys. Welding Speeds as Indicated.	64
30	Change in Bend Transition Temperature with Size of Gas Tungsten Arc Welds in the Solid Solution plus Dispersion Strengthened Columbium Alloys. Welding Speeds as Indicated.	65
31	Effect of Gas-Tungsten-Arc-Weld Heat Input on Ductility in the Yttrium Modified Alloys C-129Y and D-43Y. Welding Speeds as Indicated.	66
32	Change in Bend Transition Temperature with Size of Gas Tungsten Arc Welds in the Yttrium Modified Alloys C-129Y and D-43Y.	67
33	Effect of Annealing Temperature on the Grain Size and Ductility of B-66	69
34	Isothermal Discontinuous Grain Growth in Arc Cast Molybdenum (after J.H. Bechtold <sup>9</sup> )	70
35	Effect of Increased Weld Size in Reducing Heat Affected Zone Size and Increasing the Cooling Rate Through this Zone	71
36	Interface of Gas Tungsten Arc Weld (top) and Electron Beam Weld (bottom) in FS-85, Showing Thermal Effects of Higher Arc Weld Heat Input: Increased Weld Cell Size, Heat Affected Zone Grain Growth, Heat Affected Zone Size, and Dissolution of Fine Precipitates Along Ghost Structure in the Heat Affected Zone	74

LIST OF ILLUSTRATIONS (Continued)

<u>Figure No.</u>	<u>Title</u>	<u>Page No.</u>
37	Process Flow Diagram for Weld Porosity Evaluation of D-43	77
38	Summary Showing the Effect of Annealing on GTA Weld Bend Ductility	81
39	Summary Showing the Effect of Annealing on EB Weld Bend Ductility	82
40	Room Temperature Tensile Strength	86
41	Elevated Temperature Tensile Strength of Annealed Base Metal and Arc Welds	87
42	Elevated Temperature Yield Strength of Annealed Base Metal and Arc Welds	88
43	Elevated Temperature Tensile Elongation of Annealed Base Metal and Arc Welds	89
44	Fracture Characteristics of Welds in Tantalum Alloys and the Highest Strength Columbium Alloys (FS-85 and D-43).	92
45	Fracture Characteristics of Yttrium Modified Alloys Tensile Tested at 2400°F. Fracture by Grain Boundary Separation.	94
46	Base Metal Fractures for B-66 (top) and Cb-752 (bottom) Tensile Tested at 2400°F	95

## LIST OF TABLES

<u>Table No.</u>	<u>Title</u>	<u>Page No.</u>
1	Alloys Included in the Weldability Study	8
2	Chemistry of As-Received Material	10
3	Metallurgical Data on As-Received Material	11
4	Summary of Sheet Weld Chemical Surveillance	18
5	Summary of Plate Weld Chemical Surveillance	21
6	Restraint Test Summary	36
7	One Hour Post Weld Annealing Temperatures Used on Plate Weld Specimens	42
8	Bend Transition Data for the Sheet Weld Study Based on Mechanically Acceptable Welds Only	43
9	Gas Tungsten Arc Weld Porosity Count	76
10	Pickling and Rinsing Schedules for Weld Porosity Evaluation	78
11	Optimized Weld Conditions for 0.035 Inch Sheet	83
12	Room Temperature Tensile Properties for Welded Plate	90

## I. INTRODUCTION

This weldability study is one of a number of broad based programs sponsored by the Space Power System Division which were designed to upgrade refractory metal alloy technology in terms of space power system requirements. Contemplated systems will convert thermal energy to electric power using Brayton or Rankine thermodynamic cycles or direct conversion. The major design objective of high thermal efficiency at minimum system weight can be realized by operating at the highest possible temperature and at moderate working fluid pressures. In this respect, liquid alkali metals are excellent working fluids, while refractory metal alloys, combining superior high temperature strength and excellent corrosion resistance in alkali metals, are uniquely suited for system structures. The most severe shortcomings of refractory metals, poor oxidation resistance and adverse ductility response to atmospheric contamination, are avoided in the high vacuum space environment.

This weldability study was application oriented. Hence, requirements of long life structures deployed in high vacuum environments were emphasized. This emphasis represents a considerable departure from the short-life aerospace applications for which the alloys were originally designed, and, in part, justified the need for this program. A more pressing necessity, however, arose because these alloys had accrued negligible service time in actual hardware. Hence, this program was conceived as a major comparative review of a new group of promising materials, and as the first evaluation emphasizing an application for which these materials are ideally suited.

The primary objective of this study was to provide the essential information required for rating all the refractory metal alloys on the basis of weldability. For this purpose the program was designed to provide a comparison of alloys based on the following information:

1. A measure of weld hot tear sensitivity.
2. The degree of impairment of alloy ductility resulting from welding.
3. The sensitivity of weld properties to weld process and parameter variations.



4. The effect of section size on weldability.
5. The degree of recovery obtainable by post weld annealing.
6. Tensile joint efficiencies throughout the anticipated application temperature range.

The secondary objective of this program was to provide guidelines for the welding of these materials. Particular emphasis was placed on developing joint preparation techniques and methods for controlling welding environments to minimize contamination. The joint preparation studies are described in this report. The results of the weld atmosphere control studies are summarized in this report but the detailed test data were previously reported<sup>(5)</sup>.

## II. SUMMARY AND CONCLUSIONS

### WELDABILITY

- (1) Good weldability was exhibited by the second generation columbium and tantalum alloys as demonstrated by restrained weld tests and general accommodation in welding both sheet and plate. Few unusual complications arose within a nominal range of welding conditions even though weldability limitations were exceeded for several alloys. Room temperature and elevated temperature weld strength approached base metal strength for these alloys demonstrating joint efficiencies at all temperatures of nearly 100%. Within the respective alloy groups, FS-85 and T-111 demonstrated superior combinations of strength and fabricability.
- (2) Welding resulted in a loss of ductility in all alloys as measured by the bend ductile-to-brittle transition temperature. The comparative degradation of ductility occurring with welding provides a convenient measure of weldability in these systems. Plate weldability was comparable to sheet weldability for the more fabricable alloys. However, with the less weldable alloys, adverse welding characteristics were exaggerated in plate welding.
- (3) Tantalum alloys were considerably less sensitive to welding than columbium alloys, and as a result have superior fabricability.
- (4) The tungsten alloys had poor weldability and were difficult to handle because of their low ductility at ambient temperatures. Weld cleavage failures occurred frequently during weld cooling through the ductile-brittle transition range to room temperature. In this respect, variability in weld ductility for different welding conditions seemed to result from differences in the magnitude and distribution of residual weld stress levels. W-25Re displayed an apparent tendency toward hot tearing as well as cleavage during welding.

- (5) The importance of attaining balance between matrix and grain boundary strengths for high temperature application was demonstrated. Alloys with large weld grains (solid solution alloys), low recrystallization temperatures, and relatively weak grain boundaries (yttrium modified alloys) had the least desirable tensile fracture characteristics.
- (6) Considerable alloy-to-alloy variability in porosity sensitivity was demonstrated. In the most sensitive alloys porosity is eliminated by preparing edges by machining prior to pickling and vacuum degassing after pickling whereas in the least sensitive alloys sheared and pickled edges are satisfactory. Hydrogen adsorption during pickling, and release during welding, is the most probable cause of porosity. Procedures reducing the "pre-weld" joint surface area reduce porosity.

#### THERMAL RESPONSE TO WELDING

- (1) Columbium alloy weld behavior was rationalized with a thermal response analysis. Welding conditions which tend to stimulate development of the heat affected zone and grain size in this zone increase the weld ductile-to-brittle transition temperature. Consequently, differences in alloy responses can be related to the metallurgical characteristics affecting grain stability and growth phenomena. Weld process and metallurgical factors combine such that a heat input threshold for ductility impairment is observed for alloys which are dispersion strengthened. With increased grain stability, as realized with the yttrium modified alloys, this threshold occurs at a higher heat input. The solid solution alloy did not display this threshold but rather a continuous ductility loss with increasing size of the heat affected zone. This implies that the observed differences between solid solution and dispersion strengthened alloys is continuous vs. discontinuous grain growth in the heat affected zone.
- (2) The thermal analysis interpreted in terms of a heat input threshold, provided a sensible rationale to which the general improved ductility of electron beam welds can be ascribed.

## WELD ATMOSPHERE CONTROL

- (1) Using optimum evacuation and backfilling techniques, a high quality inert welding atmosphere having less than 1.25 ppm total active impurities can be obtained in vacuum purged chambers. Following backfilling, the welding atmosphere gradually deteriorates permitting 6 or more hour use depending on the contamination limit established for the particular run.
- (2) The sources of moisture and oxygen contamination in weld chamber atmospheres differ considerably. Consequently, these contaminants are not related and must be considered independently.
- (3) The oxygen level in the backfilled weld chamber atmosphere depends on the gas quality, weld box tightness, a moderate evacuation of  $10^{-4}$  -  $10^{-5}$  torr, and the backfill techniques employed. The oxygen level increases following backfilling mainly by diffusion through the weld box gloves.
- (4) Low moisture levels in the backfilled weld chamber atmosphere are obtained by using extended pumpdown cycles, conveniently overnight for 16 to 18 hours to the low  $10^{-6}$  torr range. Atmosphere stability with respect to this impurity is enhanced by longer and lower pressure pumpdowns since outgassing of the chamber interior and tooling surfaces is the primary source of moisture.
- (5) The leak rate (pressure rise rate of a sealed chamber) is an excellent measure of the adequacy of a pumpdown cycle since it represents the sum of leakage and outgassing rates. Hence, a low leak rate assures low moisture and oxygen rise rates in the backfilled chamber. A 1 minute pressure rise in the evacuated chamber of  $3 \times 10^{-5}$  torr is required for reasonably good stability of the backfilled chamber atmosphere. In this respect double purge cycles are not beneficial. Contrary to a widely held opinion, welding can be accomplished under a slightly negative pressure (below 1 atm) without increasing the contamination rate if a good leak rate is obtained and sound gloves are used.

- (6) Nitrogen as a contaminant appears to be present in the weld atmosphere in roughly the same ratio with respect to oxygen as in air. Hence, oxygen can be monitored and nitrogen contamination assumed by implication to be x4 the oxygen level. The source of nitrogen, like oxygen, must be air leaks and diffusion through gloves.
- (7) Other active atmospheric contaminants which are not generally airborne, such as hydrocarbons, are avoided by judicious selection of materials, lubricants, and cleaning techniques for internal chamber components.
- (8) Neoprene gloves provided the best over-all performance of those tested. These were however prone to degassing of sulfur during chamber evacuation. Degassing subsides with use. Further, it never caused any problem after chamber backfilling. Clean copper tooling reacts with the sulfur vapors during chamber evacuation and can be protected with line-of-sight shielding such as loosely wrapped aluminum foil. All the gloves tested were permeable to air. Hence, for the same size and thickness glove, the greater the number of gloves used and the smaller the weld chamber the more rapid will be the deterioration of a weld box atmosphere.

#### POST WELD ANNEALING

- (1) Columbium base alloys generally require post weld annealing to improve weld ductility and enhance thermal stability.
- (2) Tantalum alloys do not require post weld annealing based on the ductility data generated in this welding study. However, liquid metal corrosion resistance is enhanced by post weld annealing and thermal stability considerations established in the more advanced studies in this program demonstrate the need for post weld annealing.
- (3) The ductility of tungsten and W-25Re alloy weldments is modestly improved by post weld stress relief.

### III. TECHNICAL APPROACH AND PROCEDURES

#### ALLOYS

Commercially available high strength alloys and several experimental alloys were included in this program. These are listed in Table 1. Except for the tungsten alloys these were purchased in the recrystallized condition and in uniform sheet and plate thicknesses of 0.035 and 0.375 inch respectively. The recrystallized condition is generally favored for strength and stability in long time application.

Eight columbium base alloys comprise the major portion of this group reflecting the emphasis of government and industry sponsored alloy development. This emphasis stemmed from the importance of the density advantage of columbium over tantalum (0.31 lb/cu.in. vs. 0.60 lb/cu.in.) and also availability. Inclusion of the two high strength tantalum alloys, T-111 and T-222, reflects a growing interest in these because of greater fabricability combined with promise of an eventual tantalum system with a superior high temperature strength-density ratio. The weaker solid solution strengthened Ta-10W and SCb-291 alloys were included as reference alloys. The three tungsten alloys were included primarily to ascertain the state of the welding art in joining extremely brittle materials, and to determine if recent improvements in tungsten technology would translate into improved weldability. Therefore, both unalloyed tungsten and tungsten-25 rhenium were produced using recently developed techniques for conversion from arc cast ingots. The arc cast material was selected because it provided porosity free welds in a preliminary comparison with several grades of powder metallurgy tungsten. Sylvania "A" is the only powder metallurgy product evaluated in this program. It is designed for high strength but proved to be essentially unweldable and is therefore not a fabricable material. For this reason weld data on this alloy is given in the appendix only.

TABLE 1. Alloys Included in the Weldability Study

Alloy	Nominal Composition Weight Percent
AS-55	Cb-5W-1Zr-0.06C+Y
B-66	Cb-5Mo-5V-1Zr
C-129Y	Cb-10W-10Hf+Y
Cb-752	Cb-10W-2.5Zr
D-43	Cb-10W-1Zr-0.1C
FS-85	Cb-27Ta-10W-1Zr
SCb-291	Cb-10W-10Ta
D-43+Y	Cb-10W-1Zr-0.1C+Y
T-111	Ta-8W-2Hf
T-222	Ta-9.6W-2.4Hf-0.01C
Ta-10W	Ta-10W
W-25Re	W-25Re
W	Unalloyed
Sylvania "A"	W-0.5Hf-0.025C

NOTE: All alloys from arc-cast and/or electron beam melted material.

This list of alloys investigated appears formidable. However, a few comments on the phase relationships involved, which are basically uncomplicated, prove helpful in this respect. Complete solid solubility is demonstrated by all combinations of Cb, Mo, Ta, W and V, as employed in these systems. Hence, these are mutual single phase solid solution strengtheners. The predominant element of this group in both the columbium and tantalum alloys is tungsten. Two columbium alloys also contain tantalum, and one contains molybdenum and vanadium instead of tungsten.

One or the other of the reactive elements, zirconium or hafnium, is a necessary component in all the high strength columbium and tantalum alloys. These form complex systems with the other elements but are alloyed at levels below their equilibrium solid solubility limit. Hence, wrought structures are single phase while cored weld structures may be multiphased. Strengthening is realized through both solid solution and dispersion strengthening since hafnium and zirconium tend to form very stable precipitates with the residual interstitials. A detailed understanding of the dispersion strengthening mechanism involved is lacking.

Several alloys also contain intentional carbon additions. These alloys respond to thermal treatment during processing and realize their strength in part from carbide dispersions. In this respect a knowledge of the probable phase relations is important and have been investigated for T-222 by R. L. Ammon, et al,<sup>(1)</sup> and for D-43 by Ostermann and Bollenrath.<sup>(2)</sup>

Additions of minor amounts of yttrium in several columbium alloys provide an interesting modification of mechanical properties resulting primarily in improved ductility. Yttrium is essentially insoluble in columbium and is very reactive with oxygen. Hence, the most probable mechanisms for improved ductility are an effective reduction in matrix oxygen level by preferential combination with yttrium, purification during melting and welding by slagging of the oxide, and grain refinement resulting from the presence of the highly stable oxide.<sup>(3,4)</sup> Among the yttrium containing alloys only C-129Y is commercial. AS-55 was procured on a "best effort" basis and D-43Y was specially produced only for this program. The grain refining influence of yttrium was evident in as-received material. AS-55 and C-129Y were recrystallized at the highest temperatures among the columbium alloys yet had the smallest grain size.

The pertinent data on composition and metallurgical condition of material procured for this program are listed in Tables 2 and 3. Check analyses were run on interstitials because of their important influence on ductility, and, hence, as a quality assurance measure. Hardness and grain size data along with final anneals are also listed, providing a relative comparison of grain size stability.



TABLE 2 - Chemistry of As-Received Material

Alloy	Form	Heat No.	Certified Analysis (Avg.)										Check Chemistry					
			w/o										ppm					
			Zr	Hf	Mo	V	Y	Re	W	Ta	Cb	C	O	N	C	O <sub>2</sub>	N <sub>2</sub>	
A5-55 B-66	Sheet	430-7	1.07				0.02-0.3		4.74		Bal.	306	190-600	155	440	630-930	200	
	Plate	DX-609	1.00		5.17	4.89					Bal.	95	110	63	37	120	70	
	Sheet	DX-609	1.00		5.17	4.89					Bal.	95	110	63	44	150	30	
	Wire	DX-569	1.10		5.23	5.61					Bal.	17	70	64	130	140	90	
C-129Y		DX-603	0.92		4.55	4.85					Bal.	40	82	75	130	190	60	
	Plate	6.6-57033		10.25					10.8		Bal.	65	160	15	58	200	30	
		610-57204		10.10					10.85		Bal.	80	50	58				
	Sheet	46-70617		9.5			0.105		9.8	0.135	Bal.	85	105	50	36	102	60	
Ct-752	Wire	6.6-57033		10.25					10.8		Bal.	65	160	15	52	120	50	
	Plate	52165	2.70						9.8		Bal.	50	76	10	16	84	70	
	Sheet	52208	2.90						9.9		Bal.	40	143	102	21	180	80	
	Wire	52183	2.90						9.6		Bal.	30	60	120	51	120	90	
D-43	Plate	43-398-13	0.97						10.3		Bal.	835	63	32	930	64	20	
	Sheet	43-398-13	1.00						9.9		Bal.	1046	200	32	1100	180	10	
	Wire	43-372-1	0.88						9.7		Bal.	810	52	33		85	60	
	Sheet	95065	0.99				0.26		9.5		Bal.	960	50	26	1040	64	40	
F5-85	Plate	85D-740	0.94						10.6	28.1	Bal.	20	90	60	32	53	47	
	Sheet	85D-739	0.95						10.43	27.61	Bal.	40	40	52	12	98	50	
	Wire	85D-695	0.97						10.2	28.0	Bal.	20	40	30	24	73	40	
SCb-291	Plate	2255							10.0	9.83	Bal.	20	110	40	22	101	20	
	Sheet	1991							9.9	9.6	Bal.	12	65	76	17	110	50	
	Wire	1825							10.1	9.2	Bal.	10	67	70	12	130	50	
Ta-10W	Plate	608-758							9.90	Bal.		50	40	20	5	10	10	
	Sheet	608-758							9.90	Bal.		50	40	20	12	66	100	
	Wire	608-609																
T-111	Plate	2691		1.7					7.05	Bal.		18.5	10	26	27	34	10	
	Sheet	6-65042-Ta		2.0					8.8	Bal.		80	50	35	48	15	18	
	Wire	DX-571		2.01					8.12	Bal.		10	20	10	17	23	20	
T-222	Plate	5.510-65041		2.55					9.2	Bal.		115	50	20	119	17	11	
	Sheet	5.510-65041		2.55					9.2	Bal.		115	50	20	100	29	10	
	Wire	5.510-65041		2.55					9.2	Bal.		115	50	20	120	16	14	
W-Re W	Sheet	3.5-75002						25.6	Bal.			40	50	35	8	8	10	
	Sheet	KC-1350							Bal.						6	10	10	
	Sheet	KC-1353							Bal.						9	15	10	
Sylvania "A"	Sheet			0.51					Bal.			190	83	13				

TABLE 3. Metallurgical Data On As-Received Material

Alloy	Form	Metallurgical Condition <sup>(1)</sup>	Hardness DPH	ASTM Grain Size
AS-55	Sheet	60% Cr, Rx 1 hr/2730°F ✓	148	9
B-66	Plate	Rx 1 hr/2300°F	225	6
	Sheet	Rx 1 hr/2100°F	219	10
C129Y	Plate	25% Wr, Sr 1 hr/1800°F 75% Wr, Rx 1 hr/2400°F	218	
	Sheet	89% Cr, Rx 1 hr/2400°F	185	10
Cb-752	Plate	Rx 1 hr/2500°F	204	8
	Sheet	Rx 1 hr/2200°F (2)	205	8-9
D-43	Plate	Sr 1 hr/2200°F	202	
	Sheet	Rx 1 hr/2600°F (3)	220	5
D-43Y	Sheet	82.5% Fr, Rx 2 hrs/2400°F	150	8
FS-85	Plate	Rx	205	7
	Sheet	Rx 1 hr/2375°F	190	8
SCb-291	Plate	Rx	160	6
	Sheet	85% Cr, Rx 1 hr/2100°F	175	6
Ta-10W	Plate	Rx	197	8
	Sheet	Rx	221	6-7
T-111	Plate	Rx	223	6-7
	Sheet	96% Fr, Rx 4 hrs/2400°F	221	9
T-222	Plate	> 75% Fr, Rx 1 hr/3000°F	276	7-8
	Sheet	> 50% Cr, Rx 1 hr/3000°F	273	7-8
W-25Re	Sheet	63.8%, then cross rolled 73.1%	526	*
		Sr 1 hr/2550°F	492	
W	Sheet	82.5% Fr, Sr 1 hr/1700°F	517	*

\*Stress Relieved, Not Recrystallized

(1) Cr - cold reduction, Wr-warm reduction, Fr-final reduction, Rx-recrystallized, Sr-stress relieved. Note all sheet is recrystallized except W and W-25Re.

(2) Currently available in duplex annealed condition for slightly improved strength .

(3) Strength optimized by strain induced precipitation treatment. Penultimate anneal of 2900-3000°F prior to final optimum cold reduction and recrystallization.

## TECHNICAL APPROACH

Ductility impairment is the major area of interest in evaluating refractory metal alloy weldability. As a general rule the unalloyed base metal is very ductile but both alloying and subsequent welding cause successive losses in ductility. Hence, in developing refractory metal alloys, fabricability is traded off for strength, and success in this effort is measured in terms of achieved strength versus decreased ductility. A sensible measure of ductility, and ductility impairment occurring with welding is provided by the ductile-to-brittle transition temperature. The transition behavior is characteristic of the body centered cubic metals and is easily measured by bend testing. Hence, bend testing was emphasized in this program to evaluate weldability, follow thermal responses, and compare alloys.

## INFLUENCE OF WELDING PARAMETERS

Early observations made on refractory metal alloys indicated that welding parameter selection could greatly influence the bend ductile-brittle transition temperature. An evaluation of the effect of weld parameters on bend ductile-brittle transition temperatures seemed imperative and was established as a major welding objective. One important reason for investigating these effects was to establish a uniform method of selecting welding parameters for preparation of specimens in the successive evaluation phases of this program, i.e., the post weld anneal, tensile, and thermal stability studies. For this purpose, the parameter series was expected to provide an optimum set of weld parameters for each alloy as well as providing a broad based alloy weldability comparison.

To maintain a materials oriented perspective, the effects of variation in weld freezing rate, cooling rate, and unit weld length heat input were emphasized rather than current, speed, and voltage per se. This approach tended to vary in a qualitatively predictable manner the time-temperature relations controlling metallurgical reactions in the heat affected zone as well as its size. Similarly, these factors most significantly affect the important weld characteristics of grain and cell size, grain orientation, and solute redistribution (coring). Hence, this approach was designed to identify essential structural interactions occurring with welding

and their effect on weld properties rather than merely to evaluate welding as a method of joining these materials.

The parameter study was conducted on sheet material using automatic gas-tungsten-arc and electron beam welding. Parameter boundary conditions were selected to encompass the reasonable practical range of actual applications, and, within the limit of alloy to alloy variability, to provide sound, uniform, and defect free welds. Typical weld schedules are shown in Figures 1 and 2.

Weld freezing and cooling rates are closely associated with weld speed and clamp spacing. Hence, these were chosen as variables for both processes. Gas tungsten arc welds were run at 7.5, 15, 30, and 60 ipm with 1/4" or 3/8" clamp spacings. Electron beam welds were made at 15, 25, 50, and 100 inches per minute with 3/16 or 1/2 inch clamp spacings. The wider electron beam clamp spacing provided merely the weldment holding functions. The other clamp spacings were beneficial in restricting the heat affected zones and increasing cooling rates.

For arc welds, weld size was selected as a final parameter. Again, this selection was based on thermal considerations, size being controlled by total heat input. Different weld sizes were obtained by selecting appropriate welding currents. Weld target widths were set for all the alloys at 0.11 inch and 0.18 inch. As well as enhancing the thermal approach, this represented a practical method for comparing alloys since any given application requires a fixed weld size regardless of the alloy selected.

All arc welding variables other than welding speed, clamp spacing, and weld size (amperage) were not varied since they were considered of secondary importance both in realizing the screening objective and evaluating alloy thermal response. The influence of arc gap, electrode configuration, and shielding gas composition on weld configuration was recognized and these were held constant. Electrodes were machine ground to a fixed configuration and were extended one inch from the electrode holder with a 0.060 inch arc gap. Helium was used exclusively for shielding.

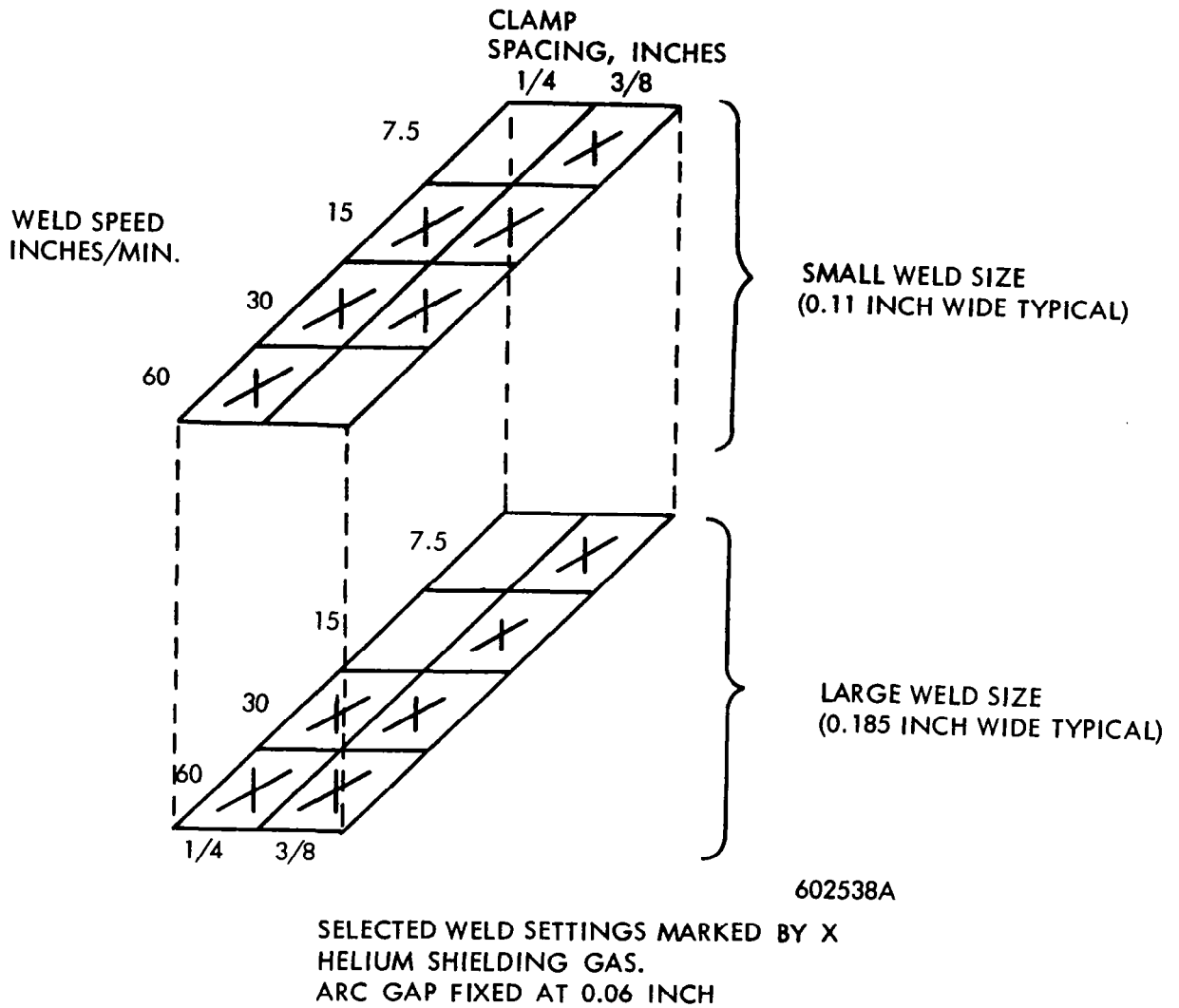
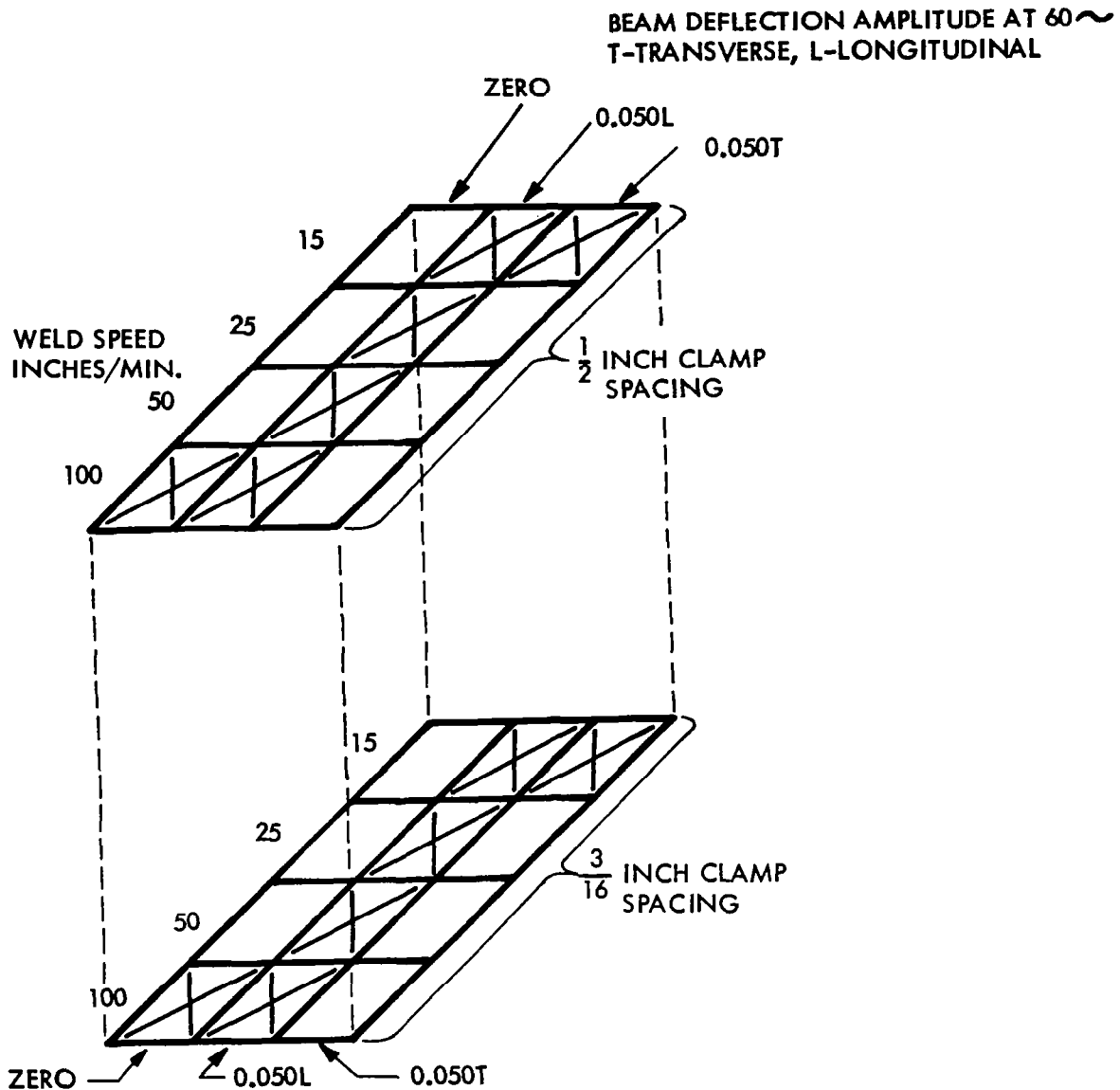


FIGURE 1 - Typical GTA Sheet Butt Weld Schedule for Welding Parameter Study



NOTES:

1. BEAM ACCELERATING VOLTAGE = 150 KV, ALL WELDS
2. BEAM CURRENT SET AT 110 % OF FULL PENETRATION POWER

FIGURE 2 - Typical EB Sheet Butt Weld Schedule

To fully realize the advantage of high voltage (150 Kv) electron beam welding, weld size, under any given set of conditions, was always minimized by focusing the electron beam to its smallest diameter (highest energy density). Beam voltage was fixed at 150 Kv because preliminary trials showed that varying voltage from 70 to 150 Kv, while using the ground rule minimum beam diameter, did not influence weld configuration. Penetration trials at various weld speeds were used to establish welding current which was set for 110% of full penetration. This provided an approximately constant weld size over the entire weld speed range for any one deflection pattern. Cyclic beam deflection is required in most applications to produce sound welds. Hence, cyclic beam deflection along with weld speed and clamp spacing were the selected electron beam variables. Sixty cycle longitudinal deflection was emphasized and generally used through the speed range. To obtain extremes of heat input, transverse deflection at the lowest speed, and "zero" deflection welding at the highest speed were also evaluated. Beam deflections of 0.025, 0.050, and 0.100 inch were used, but the 0.050 inch deflection was emphasized.

#### INFLUENCE OF SECTION SIZE

The manual plate butt welding evaluation was included in this program to ascertain the effect of section thicknesses on weldability. In general, weldability requirements tend to become more stringent with increased section thickness and the effect of welding on mechanical properties becomes exaggerated. Hence, the plate evaluation represents an important phase of this program and complements sheet welding in three ways: It measures weldability on the basis of the most flexible technique for fabricating structures; it is on the opposite end of the heat input spectrum from EB welding; and it provides an overall measure of the effect of section size on fabricability. Weld soundness, ductility, strength, and ease of welding were the criteria of the plate weldability evaluation.

## POST WELD ANNEALING

A post-weld annealing study was conducted as an integral part of the weldability study. Again, response was measured by shifts in the bend ductile-brittle transition temperature. The ultimate optimum annealing schedule selected for each alloy was evaluated by room and elevated temperature tensile testing as well as by bend testing.

## WELDING PROCEDURES AND CONTROLS

Manual and automatic gas tungsten arc welding and automatic electron beam welding were used in this study. These represent the applicable joining processes. Since refractory metals suffer an adverse ductility response if contaminated, extreme care was taken to protect them during welding. Contamination free welding is essential to assure credibility in alloy comparisons and is particularly important in the space power system application since alkali metal corrosion resistance as well as ductility are impaired. From a practical standpoint, contamination may occur during ground testing or even in the vacuum space environment during long exposures. Hence, a further advantage of minimizing contamination during fabrication is that system life is lengthened. Consequently, a considerable effort was expended to assure the adequacy of weld atmosphere controls and to improve the state-of-the-art in this area.

## GAS TUNGSTEN ARC SHEET WELDING

Arc welding was conducted in a 50 cubic foot, vacuum-purged weld chamber. This chamber could be evacuated in less than one half hour to a conventionally acceptable pressure and leak rate. However, a conventional pump down was found to result in unacceptable moisture levels in the backfilled chamber. This occurs because of moisture outgassing from internal surfaces. In this program overnight pumpdowns complemented by a heat lamp bake-out cycle of about 200°F were used to provide an acceptable vacuum purge of  $< 5 \times 10^{-6}$  torr pressure and  $< 3 \times 10^{-5}$  torr/min leak rate.\* Ultra-high purity helium was used for backfilling, providing a total active impurity level in the chamber atmosphere of about 1 ppm. During welding both oxygen and moisture were continuously monitored. Welding was discontinued when either impurity reached 5 ppm.

\* Leak rate measured over 3 minutes with chamber valved off.



Development and evaluation of the atmosphere measurement and control techniques have been described by Stoner and Lessmann<sup>(5)</sup>. The effectiveness of these procedures can be gaged from the weld chemistry data presented in Table 4. A representative sample of welds in 0.035-inch sheet was analyzed for carbon, oxygen, and nitrogen pickup. Two welds from each of six columbium alloys and three tantalum alloys were included. Random variation seemed to be associated with the values obtained and no correlation was apparent between interstitial weld pickup and atmosphere quality. The zero contamination points for carbon and nitrogen lie within the 95% confidence intervals indicating that little, if any, pickup of these elements occurred. The oxygen data display a definite bias indicating a loss of this element of between 15.6 and 39.4 ppm during welding in the high purity helium atmosphere. The sampling and analyses techniques were reasonably random so that this loss could well be real. This evaluation demonstrated that individual chemical analyses are not sufficient, and that a reasonable size statistic sample is required to assure adequacy of weld atmosphere control.

TABLE 4. Summary of Sheet Weld Chemical Surveillance

Analyzed Function, <sup>(1)(2)</sup> Change in Chemistry	Mean Change (ppm)	Standard Deviation S	95% Confidence Interval
$\Delta O = O_w - O_B$	-27.5	23.97	-39.36 to -15.64
$\Delta C = C_w - C_B$	+4.69	12.6	-1.99 to + 11.37
$\Delta N = N_w - N_B$	+6.375	20.27	-4.36 to + 17.12

(1) Subscripts: W - Weld; B - Base Metal

(2) Based on analysis of 12 Cb-base and 6 Ta-base alloy weld samples.

The sheet butt weld clampdown fixtures and traversing table are shown in Figure 3. A clamp force of approximately 100 lbs/in. is provided by this fixture. The clamp inserts are made of molybdenum and the backup bar of copper. The stationary torch is water-cooled. Welding current was provided by a three-phase direct current welder, equipped with a programmer and high frequency arc starter. Straight polarity was used exclusively. The weld set-up used is shown in Figure 4.

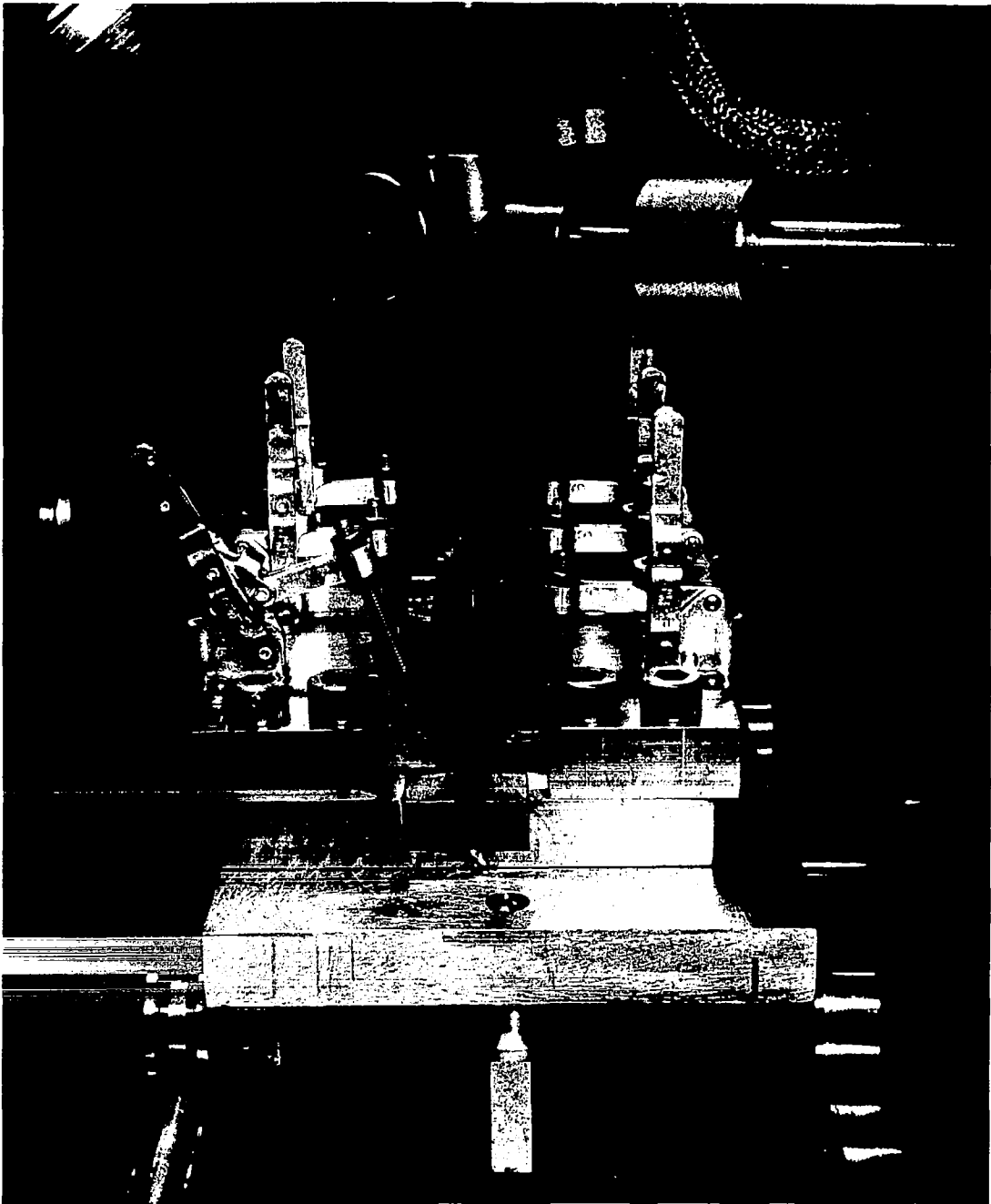


FIGURE 3 - Gas Tungsten Arc Butt Weld Tooling

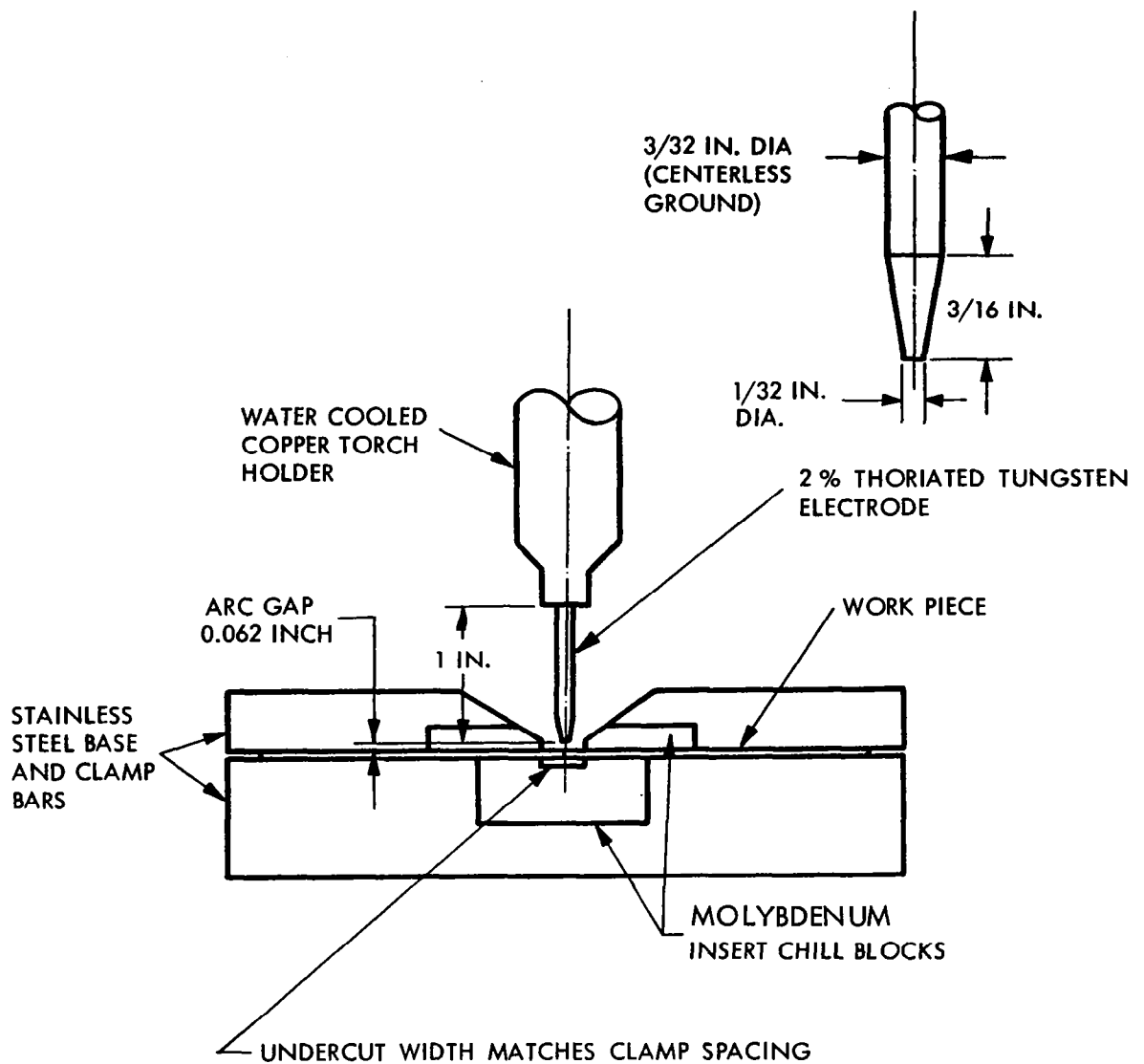


FIGURE 4 - Weld Set-Up for GTA Sheet Butt Welds

## PLATE BUTT WELDING

All plate welding was accomplished by manual helium shielded gas tungsten arc welding. The acceptable maximum chamber atmosphere moisture level was set at 10 ppm as compared with 5 ppm for sheet welding. This was a practical concession since increased outgassing of interior weld chamber surfaces occurred with the high heat input of plate welding. The shielding procedure adequacy can be gaged from the weld chemistry data, Table 5. Both base chemistry and filler wire chemistry or a combination of these were considered in ascertaining contaminant pickup levels. Oxygen increased between 7 and 12 ppm while carbon and nitrogen appear unchanged. Based on the calculated standard deviations and confidence intervals, the observed oxygen increase is probably not significant.

TABLE 5. Summary of Plate Weld Chemical Surveillance

Analyzed Function, Change in Chemistry <sup>(1)(2)</sup>	Mean Change (ppm)	Standard Deviation S	95% Confidence Interval
$\Delta O = O_w - O_B$	+12.55	29.6	-2.15 to +38.35
$\Delta O = O_w - O_{Fw}$	+6.86	30.3	-10.44 to +24.16
$\Delta O = O_w - O_{Ave(B+Fw)}$	+10.78	24.4	-1.65 to +23.21
$\Delta C = C_w - C_{Ave(B+Fw)}$	+2.33	21.45	-11.17 to +15.88
$\Delta N = N_w - N_{Ave(B+Fw)}$	+1.625	11.4	-4.32 to +7.58

O - Oxygen; N - Nitrogen; C - carbon.

(1) Subscripts: W - weld; B - base metal; Fw - filler wire.

(2) Based on analysis of 10 Cb-base and 6 Ta-base alloy weld samples.

To minimize moisture outgassing and for operator comfort during plate welding, extensive internal chamber cooling was employed. A water-cooled convection heat exchanger, a water-cooled platen, and a custom-designed water-cooled welding torch were used, Figure 5.

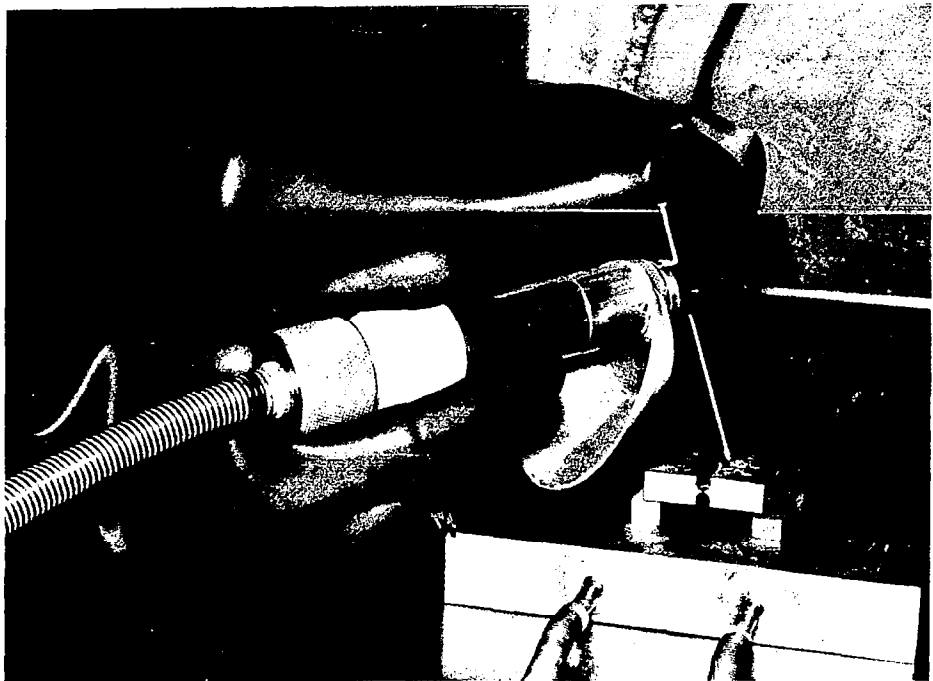
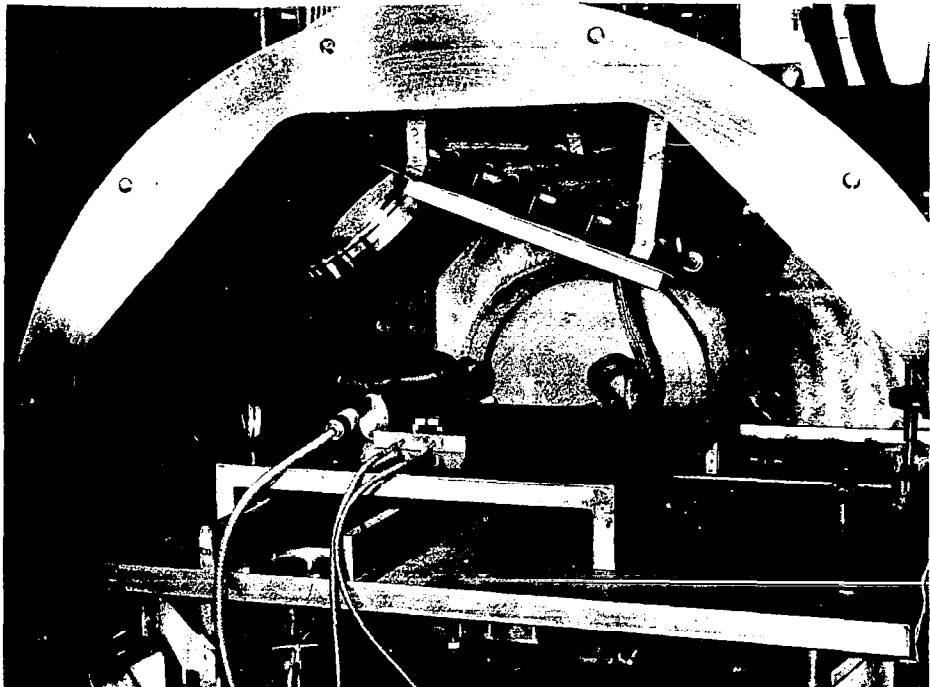


FIGURE 5 - Torch and Internal Chamber Arrangement for Manual Plate Welding

All flexible water connections on this tooling including the torch coolant lines were constructed from convoluted stainless steel tubing. Essentially zero moisture permeability was realized. The torch is equipped with a radiation shield which is required because of the increased thermal radiation of refractory metal welds.

Manual plate welding procedures for the different alloys were generally the same. All specimens were prepared with the double "U" joint configuration shown in Figure 6. This is not necessarily an optimized design but proved satisfactory for all the alloys investigated. The root of the welds were tacked together with zero joint clearance and a fusion root pass was applied from each side. Additional passes, two for the columbium base alloys and two or three for the tantalum base alloys, on each side with filler wire added manually completed the butt weld. Filler wire with an 0.082-inch diameter of the same composition as the base metal was used. Weldment flatness was controlled by alternate welding on opposite sides of the weld joint, and by introducing a camber into the joint before applying the root pass. A typical plate welding schedule is shown in Figure 7.

### ELECTRON BEAM WELDING

A 2-Kw, Model WO-2, Hamilton-Zeiss electron beam welder was used for sheet butt welding. This is a variable high voltage unit capable of 150,000 volt operation with a maximum beam current of 13.5 ma. The beam has a fine focus control (0.010 inch diameter at full power) and can be oscillated to 60 cps. A power density of 25,000 Kw per square inch can be realized.

Beam current was carefully calibrated to assure that the indicated beam power was realized at the workpiece. As with tungsten arc welding, overnight chamber pumpdowns were used with internal heat lamp bake-out. This provided pressures for welding in the low  $10^{-6}$  torr range. Aluminum holding fixtures were used for sheet butt welding. Since full beam penetration was used, a backup strip of the alloy being welded was placed in the fixture backup groove. This protected the weld underside from vapor deposition by aluminum from the fixture.

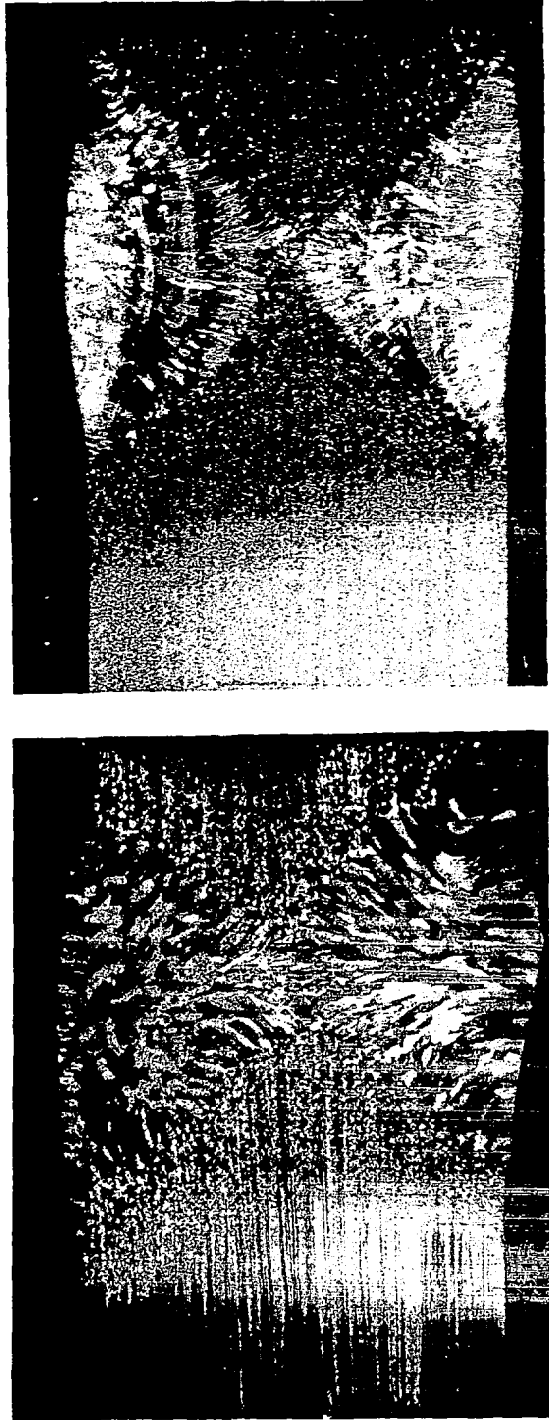
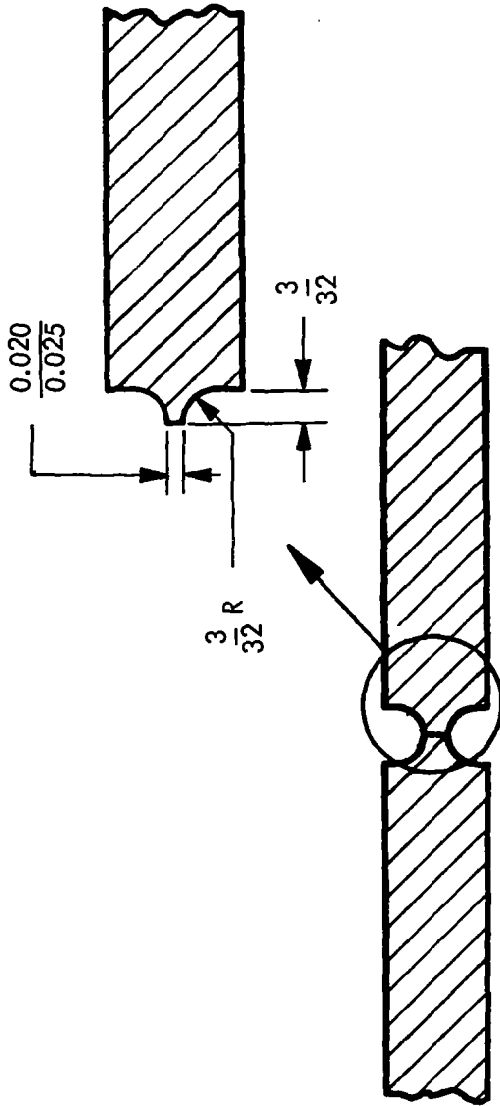


FIGURE 6 – Plate Butt Weld Joint Designs and Typical Macrosections

**WELD 321 - SCb-291 Butt Weld, 3/8 Inch Plate.**

1. Tack welded in center and at ends of joint. Positioned in clamp down fixture. 155 amperes.
2. Fusion pass on side No. 1. 300 amperes. Continuous weld from one end. One side of joint clamped, other side cantilevered.
3. Fusion pass on side No. 2. 280 amperes. Specimen supported along each edge on copper blocks. Continuous weld.
4. First filler pass on side No. 2. 300 amperes. Continuous weld.
5. First filler pass on side No. 1. 300 amperes. Continuous weld.
6. Second filler pass on side No. 2. 280 amperes. Continuous weld.
7. Second filler pass on side No. 1. 280 amperes. Continuous weld.

**FILLER WIRE REQUIREMENTS:** 2-1/2 inch of 0.082 diameter wire per inch of weld.

**FIGURE 7 - Welding Schedule for SCb-291 Butt Weld in 3/8 Inch Plate Material**



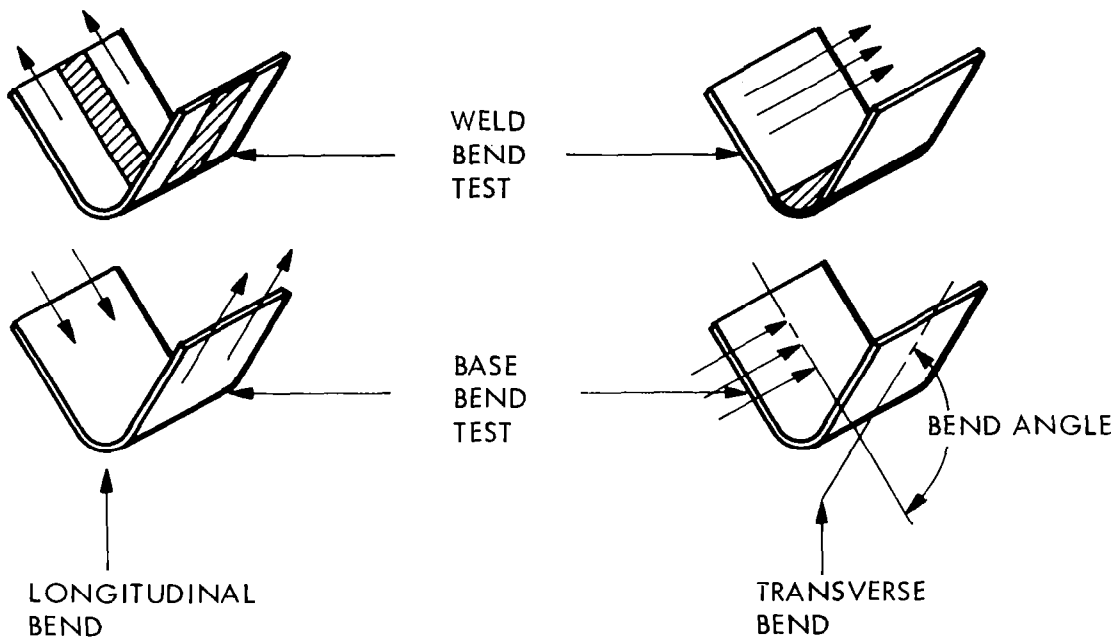
## SPECIAL TEST PROCEDURES

Sheet Bend Testing. The bend test parameters are shown in Figure 8. Note that a consistent weld and rolling direction orientation was maintained. A bend radius of  $1t$  was used almost exclusively. The bend test fixture is shown in Figure 9.

Testing procedures were fairly straightforward. Specimens were bent with as-welded surfaces with the face of the weld in tension to an angle of  $90$  to  $105^{\circ}$  after springback at a number of selected temperatures spanning the transition range. The bend ductile-to-brittle transition temperature was identified as the lowest temperature at which a  $90^{\circ}$  bend was made without cracking on the tension side of the specimens. Specimens were checked for cracks using visual and dye penetrant inspection.

The transition behavior is followed best by making a load-deflection curve during testing and, when a crack develops as indicated by a sudden load drop, stopping the test and recording this bend angle. Obviously, this represents the maximum bend for the least ductile area of the specimen. The first area where failure occurs, usually the weld or heat affected zone, is easily identified. Transverse bend specimens were canted slightly on the supports so that the bend axis was at a small angle to the weld axis. This stopped specimens from bending in a "U" shape and failing to conform to the punch radius and also produced a bending strain throughout the weld cross section. All bend test data is presented in the appendix.

Plate Bend Testing. All plate weld bend testing was done at room temperature using single point loading over a fixed test span. Each specimen was tested in three stages using successively sharper punch radii. The three punches used have radii of  $16t$ ,  $8t$ , and  $3t$ . These are used to produce successive respective bend angles of approximately  $25^{\circ}$ ,  $40^{\circ}$ , and  $140^{\circ}$ , and calculated outer fiber tensile strains of 3%, 6%, and 14%. Bend specimens were of conventional size,  $1\frac{1}{2}$  inches wide by 6 inches long. Welds were tested as welded without any mechanical surface preparation. Examples of bend-tested weldments are shown in Figure 10 while the bend test fixture is shown in Figure 11.



NOTE: ARROWS SHOW ROLLING DIRECTION

THICKNESS,  $t = 0.035$  INCH

WIDTH =  $12t$

LENGTH =  $24t$

TEST SPAN =  $15t$

PUNCH SPEED = 1 IPM

TEMPERATURE - VARIABLE

PUNCH RADIUS - VARIABLE, GENERALLY  $1t$ ,  $2t$ ,  $4t$ , or  $6t$

BEND DUCTILE TO BRITTLE TRANSITION TEMPERATURE  $\approx$   
 LOWEST TEMPERATURE FOR  $90^\circ +$  BEND WITHOUT CRACKING

FIGURE 8 - Bend Test Parameters

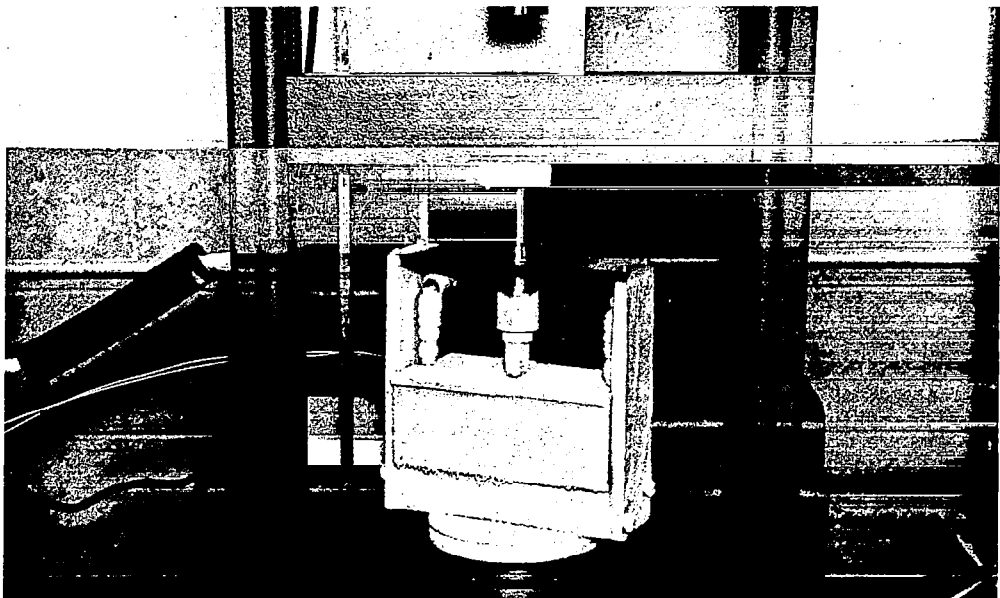
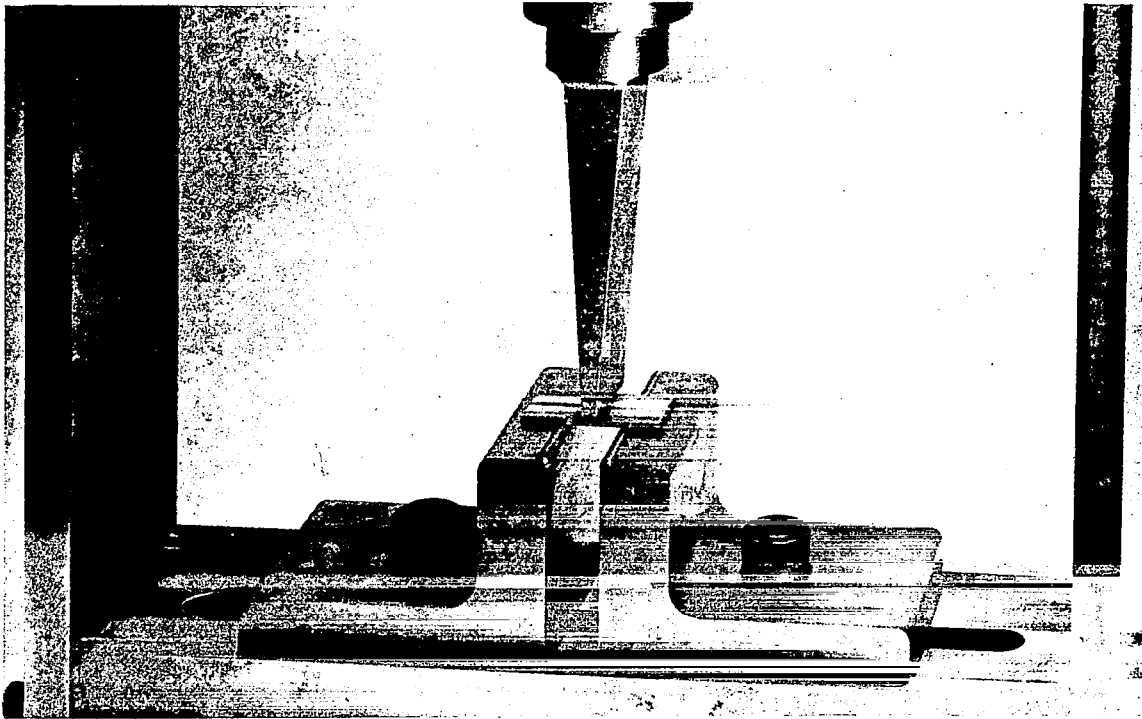


FIGURE 9 - Bend Test Fixture. Top, Open View.  
Bottom, With Liquid Nitrogen Cryostat.

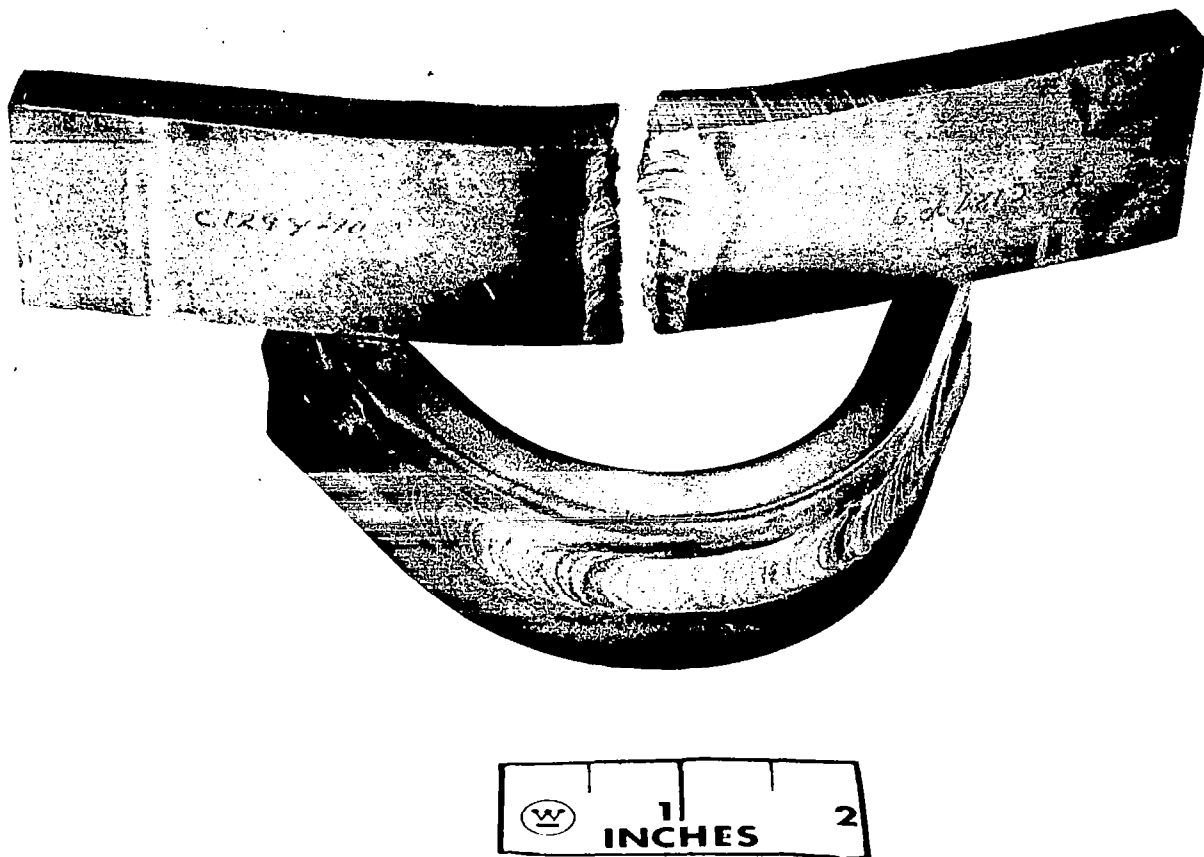


FIGURE 10 - Plate Weldments Bend Tested at Room Temperature

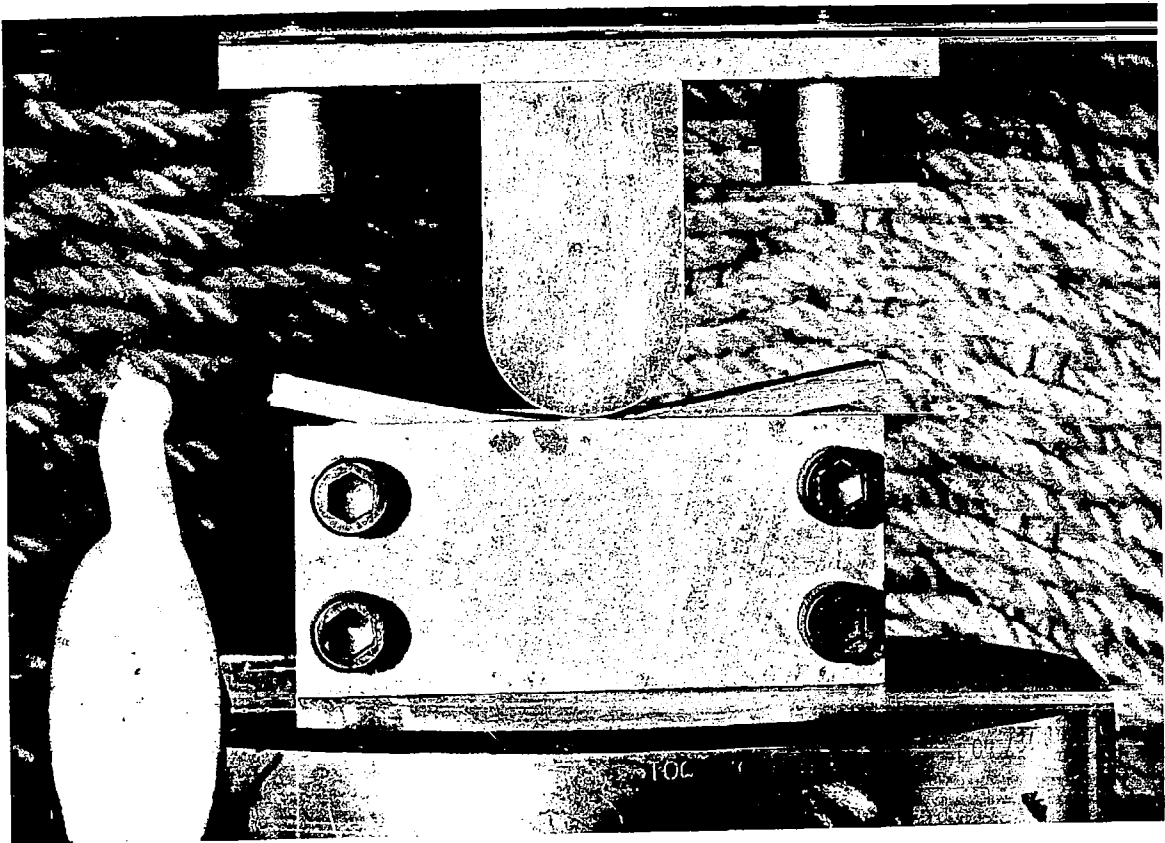


FIGURE 11 - Plate Bend Test Fixture

Tensile Testing. For room temperature tensiles a strain rate of 0.005 in/in/min was used through the 0.6% offset yield point, then 0.05 in/in/min to specimen fracture. The 0.05 in/in/min strain rate is used throughout the test at elevated temperatures. Room temperature tensile specimens had two-inch gage lengths except for longitudinal plate weld specimens which had 1-1/2 inch gage lengths. Elevated temperature tensile specimens had one inch gage lengths. The gage section of sheet tensile specimens was 0.250 inch wide with an as-rolled finish for base metal samples, and ground parallel surfaces for weld specimens. All plate specimens had machined gage sections of 0.179 inch diameter. Elevated temperature tests were run at pressures of  $10^{-6}$  torr or less with specimen gage sections wrapped in tantalum foil for additional contamination protection.

## INVENTORY AND LOGISTICS MANAGEMENT

The evaluation of the weldability and the thermal stability of eight columbium, three tantalum, and three tungsten base alloys required a very coordinated logistic system for specimen handling and identification.

Upon receiving alloys during procurement, all were coded for ease of identification and handling. Quantity (size and weight) of sheet, plate and wire were checked against purchase order requirements and customer certifications. Approximately sixty micros and chemistry samples were removed from the as-received material to determine the rolling direction, chemistry and metallurgical condition. Radiography and ultrasonics were used for evaluation of questionable as-received sheet.

Drawings were made of the as-received quantity of material and as specimens were prepared for welding it was indicated on the drawings and identified for alloy, rolling direction, and set of parameters. This identification on over 300 welds was maintained through dye-penetrant, radiography and ductile-to-brittle transition temperature bend testing. Eight bend tests (four longitudinal and four transverse to weld direction) were prepared from each weld. Approximately 2300 bend tests were prepared and tested (580 bend transition curves) maintaining weld identification and the position in the weld from where bend test samples were removed.

A post weld annealing study was conducted as an integral part of the weldability study. Both GTA and EB welding were evaluated. Approximately 120 bend transition curves were generated in this study (1000 bend samples) maintaining identification of weld parameters, type of welding, location of weld sample from original quantity, rolling direction, location of bend test specimen from each weld, and annealing temperature.

One hundred transverse tensiles were prepared from base metal sheet and GTA welded specimens using optimum weld parameters and annealing temperature. Again identification, specimen location in the original sheet, weld records and test records were maintained throughout blank and specimen preparation, welding inspection and testing. In addition, approximately 300 tensile specimens and 2600 bend specimens were prepared for inclusion in the 10,000 hour aging runs of TASK III. These were prepared approximately simultaneously with the weldability specimens and required identical logistic handling to permit maximum control and ultimately minimizing the risk of doubt in final analysis of results.

## IV. RESULTS

### RESTRAINT TESTS

Restraint tests were used for convenience in screening alloys for hot tear sensitivity and for demonstrating simple weldability. Sheet was tested using a bead-on-plate patch test, and plate using a circular groove test. Both were welded manually. Typical welded specimens are shown in Figure 12. Blank dimensions for these are shown in Figure 13. Sheet and plate specimens were inspected visually and by dye penetrant tests. Sheet specimens were also radiographed. Generally excellent weldability was demonstrated as summarized in Table 6.

The B-66 patch test had a positive dye penetrant and radiographic indication of a 1/8-inch weld start crack. This was probably a hot tear. The W-25Re alloy proved to be difficult to weld with failures occurring both by centerline cracking and heat affected zone cracking parallel to the weld. The centerline cracks seem to be hot tears whereas the heat affected zone cracks could be cleavage cracks. Unalloyed tungsten was satisfactorily welded.

No particular difficulty was encountered in welding nor were defects detected in the circular groove plate weld specimens. However, not all the alloys were available as plate, see Table 2. Specimens were welded with a fusion root pass to increase the effective weld depth before completing the test with two manual filler passes.

### DUCTILITY RESPONSE TO WELDING

Sheet Welding. Using the approach previously described, the alloys were evaluated with respect to their response to weld parameter variation. Bend ductility of butt welds, as measured by the bend ductile-brittle transition temperature (DBTT), was used to measure the effect of weld variables. The parameter study was restricted to welding 0.035-inch sheet. Twelve welding conditions were used for each welding process in studying each alloy. Approximately 580 bend transition curves, requiring 2300 bend tests were generated in this study.



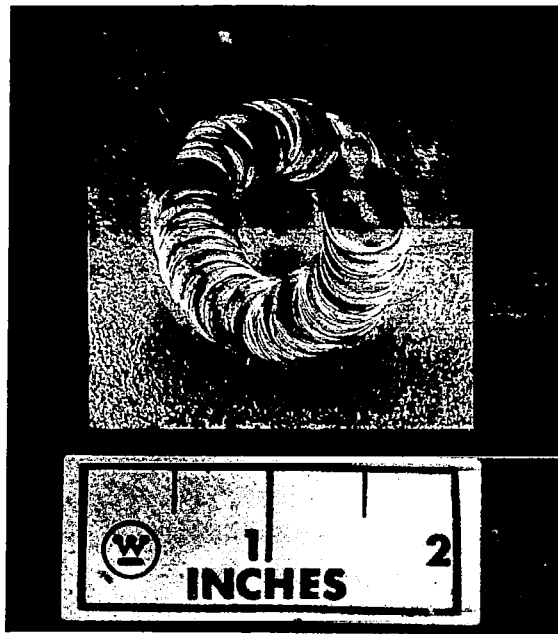
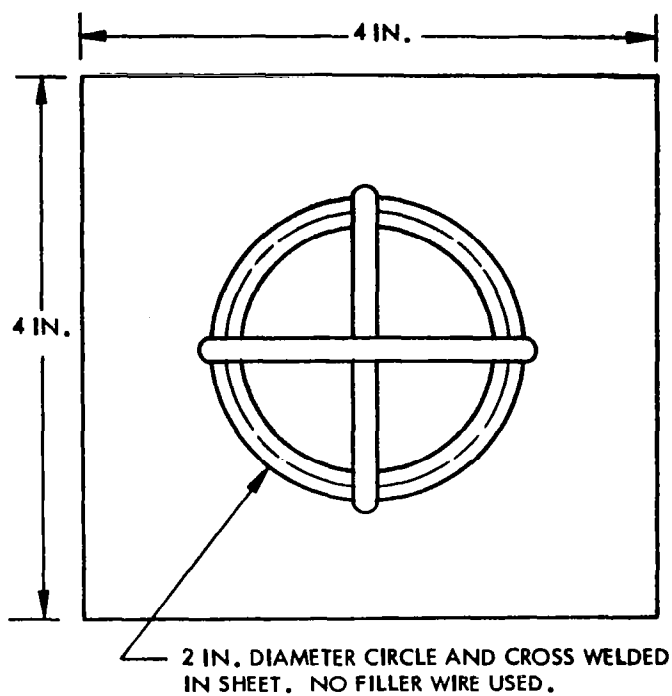
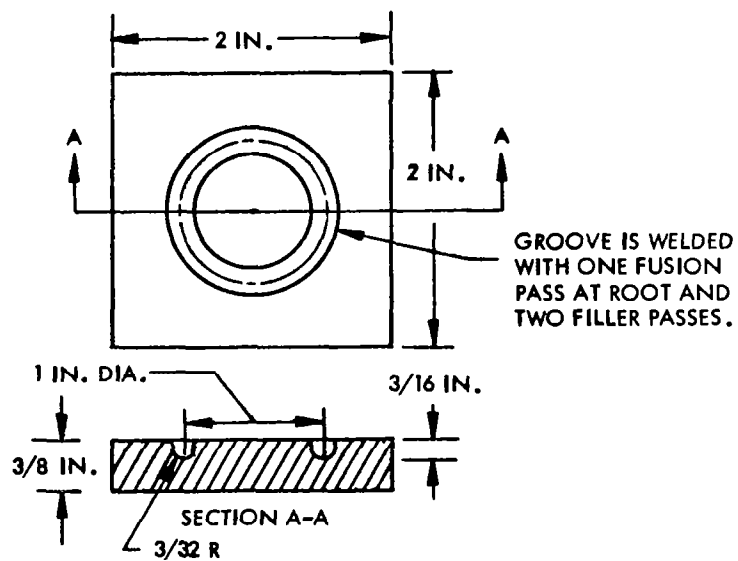


FIGURE 12 - Sheet and Plate Weld Restraint Specimens  
Top: Circular Groove Test in FS-85 Plate.  
Bottom: Bead-on-Plate Patch Test in T-111 Sheet.



(A) BEAD-ON-PLATE RESTRAINT PATCH TEST DESIGN



(B) CIRCULAR GROOVE WELD RESTRAINT TEST SPECIMEN

FIGURE 13 - Weld Restraint Test Specimens for 0.035 Inch Sheet (a), and 0.375 Inch Plate (b).

TABLE 6 - Restraint Test Summary

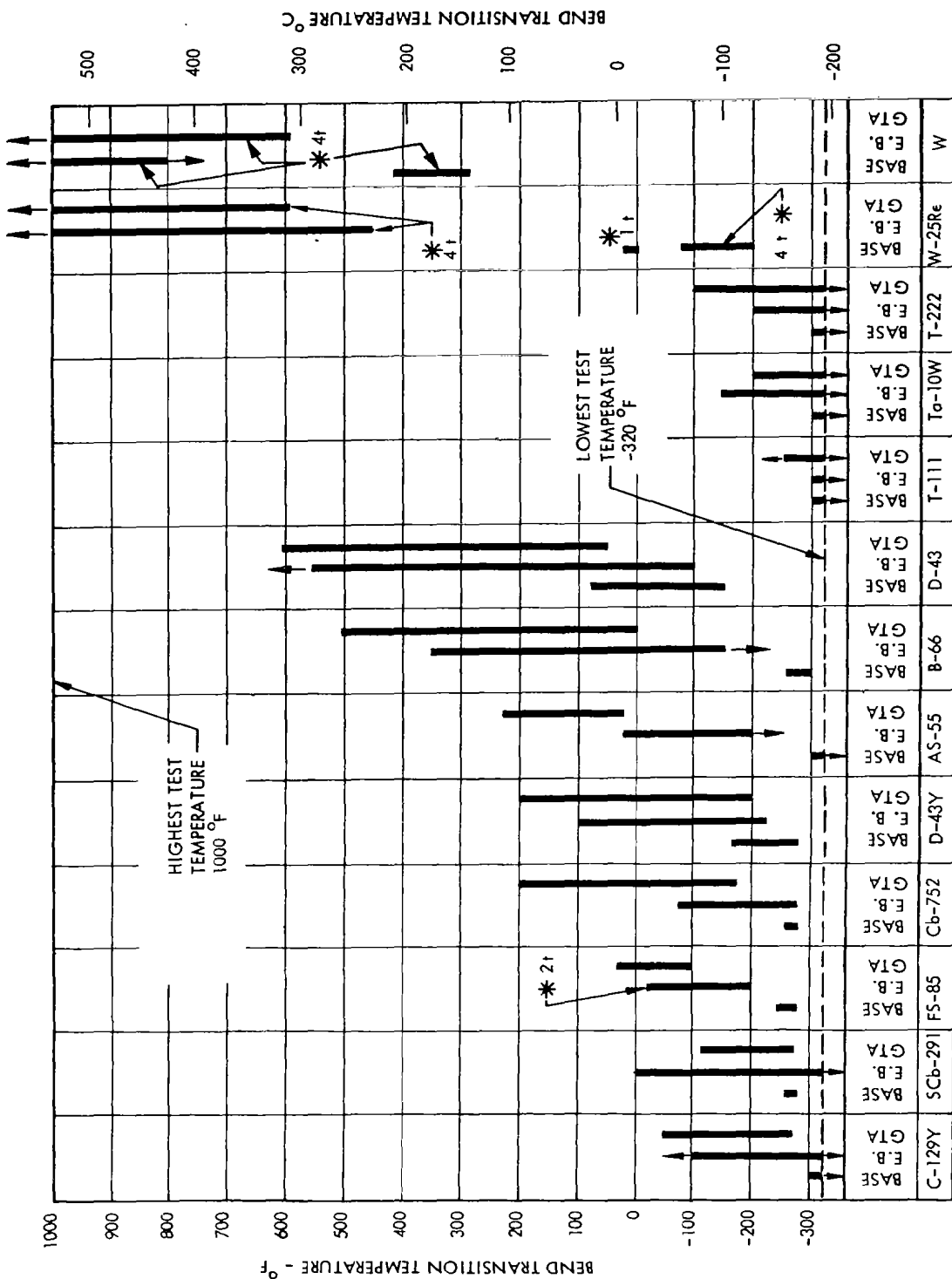
Alloy	Bead-on-Plate Patch Test (Sheet)					Circular Groove (Plate)		
	Visual	Weld Width	Dye Check	X-ray	Distortion		Visual	Dye Check
					Angle (Max)	Inches <sup>1</sup>		
AS-55	Neg.	0.24	Neg.	Negative	13°	0.75	(5)	---
B-66	Neg.	0.23	Neg.	Positive <sup>3</sup>	31°	0.63	Neg.	Neg.
C-129Y	Neg.		Neg.	Negative	30°	0.63	Neg.	Neg.
Cb-752	Neg.	0.34	Neg.	Negative	28°	0.73	Neg.	Neg.
D-43	Neg.	0.23	Neg.	Negative	32°	0.60	Neg.	Neg.
D-43Y	Neg.	0.11	Neg.	Neg.	25°	0.70	(5)	---
FS-85	Neg.	0.15	Neg.	Positive <sup>4</sup>	36°	0.76	Neg.	Neg.
SCb-291	Neg.	0.20	Neg.	Negative	32°	0.69	Neg.	Neg.
Ta-10W	Neg.	0.17	Neg.	Negative	30°	0.70	Neg.	Neg.
T-111	Neg.	0.22	Neg.	Negative	26°	0.60	Neg.	Neg.
T-222	Neg.	0.25	Neg.	Negative	18°	0.65	Neg.	Neg.

1. Closest distance between two parallel planes on opposite sides of weldment.
2. Holding one corner flat, measure lift from flat plane at diagonally opposite corner.
3. 1/8 inch starting crack identified on one leg of weld.
4. Positive x-ray indication not identified in consequent examination.
5. This alloy not evaluated as plate.

A summary of the weld parameter evaluation is shown in Figure 14. This figure shows the range, or total spread, in bend transition temperatures obtained in the weld parameter study for each alloy and process. Results of both longitudinal and transverse bend tests of every weld are included. This is a "gross effects" summary in which no allowance has been made for defected welds, except that in some cases, such as full length centerline tears, no tests could be run. Since weld defect variability is a material characteristic, this approach provides an uncluttered summary and a sensible comparison of alloys. An appreciation of alloy limitations is desirable and the data have been recast in these terms in the next section of this report.

All the tantalum alloys have excellent weld ductility and unqualified weldability. On the other hand, the tungsten alloys have poor weldability, primarily as a result of brittleness. Significant variability was demonstrated by the columbium alloys. In this group FS-85 is a stand-out because of its narrow transition range and, hence, consistent weldability coupled with particularly high creep strength as reported by Titran and Hall<sup>(7)</sup>. The solid solution alloy, SCb-291 is also very ductile, but has poor elevated temperature strength. C-129Y has the best overall ductility demonstrating the beneficial effect of yttrium but is not particularly strong in creep.

The superior weldability of the tantalum alloys is even better than is implied by the summary since the few failures in the tantalum alloys were generally ductile tears occurring at or near the 90 degree target bend angle and at the minimum test temperature,  $-320^{\circ}\text{F}$ . Columbium alloys, on the other hand, generally exhibited full section, low strain cleavage fractures at the ductile-brittle transition. However, whether cleavage or ductile tearing, the DBTT was identified as the lowest temperature where no defects were detected. Hence, the transition temperatures indicated for the tantalum alloys were not "true" transitions but rather the temperature at which a strain limitation for ductile tearing was exceeded. This difference in alloy behavior is illustrated in Figure 15.



\* - All bends 1t radius except as noted.

FIGURE 14 - Summary of Bend Test Results for Gas Tungsten Arc and Electron Beam Butt Welds in 0.035 Inch Sheet. Twelve Welding Conditions for Each Alloy and Process. Weld Tested in Both Longitudinal and Transverse Directions.

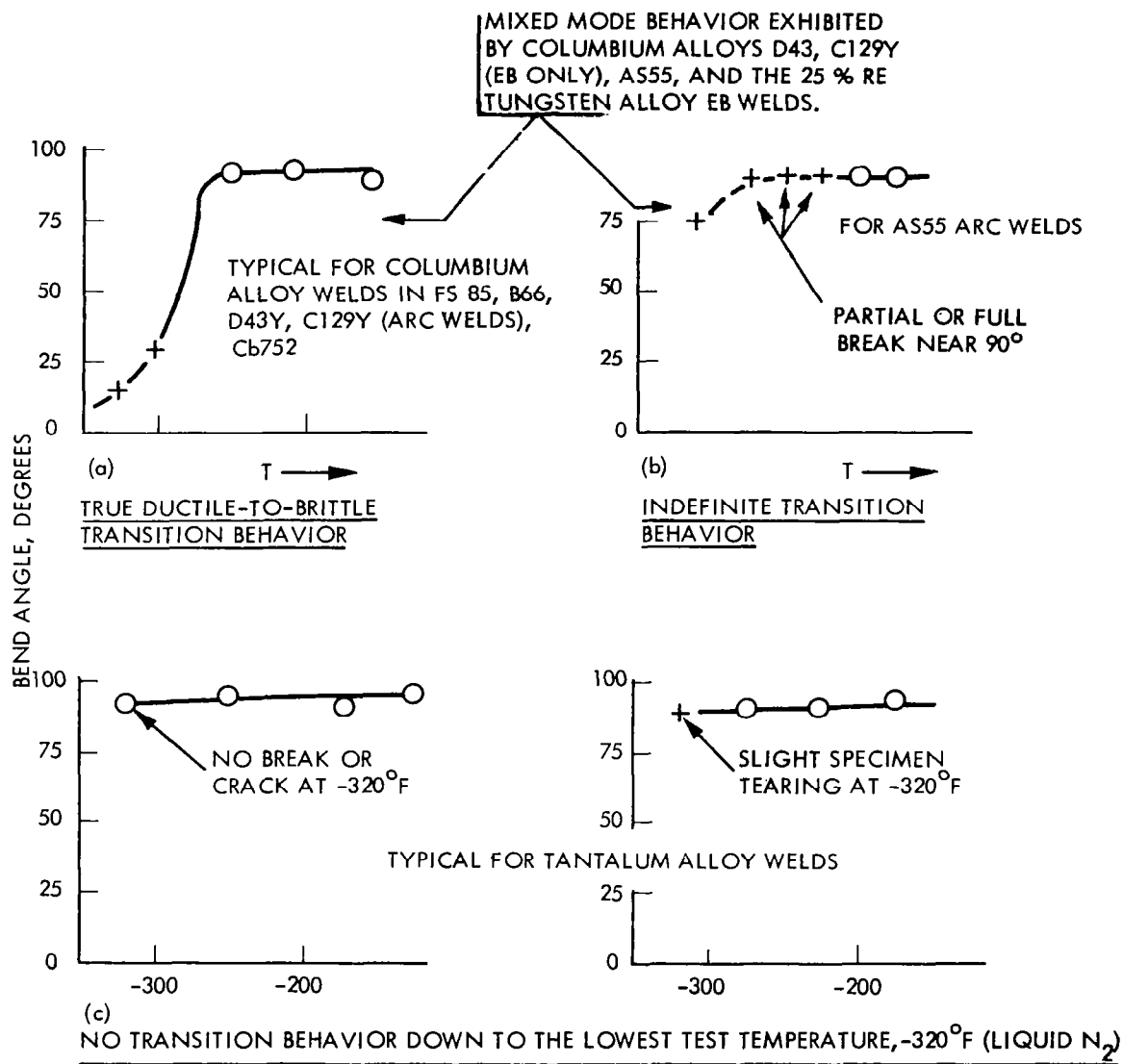


FIGURE 15 - Categorized Weld Bend Transition Behavior

Plate Welding. Because of the large size of plate weldments, and thus high material cost, the scope of this effort was more restricted than for the sheet weld evaluation. Nine alloys, including all the columbium and tantalum alloys except D-43Y and AS-55 were evaluated in the plate welding study. Approximately thirty-six feet of plate welding was required. Plates were welded by two different weld operators and evaluated primarily by bend and tensile testing in both the longitudinal and transverse directions. One post weld anneal for each alloy was also selected, based on sheet welding results. All of the alloys were successfully joined using the procedures described earlier in this report. B-66 was difficult to weld because of a hot tearing tendency which was overcome only by applying strong tack welds at each end of the weldments before making the rest of the weld. Tensile test results are presented later in this report. Room temperature bend tests are summarized in Figure 16.

To appreciate the plate weld bend test results, Figure 16, one must realize that these were run at room temperature. Loss of ductility indicates that the weld ductile-to-brittle transition temperature is above room temperature. On the other hand, sheet weld ductility responses were defined by a quantitative shift in bend transition temperature. For the more fabricable alloys, section size obviously has little effect in degrading ductility. However, with the less weldable alloys, adverse ductility responses to welding were exaggerated in plate welding. Again, the tantalum alloys display excellent ductility. Tantalum alloy failures had ductile tears whereas all columbium alloys failed by full section cleavage. SCb-291 and FS-85 are reasonably ductile and to a lesser extent C-129Y. Ductility decreases with D-43, Cb-752, and B-66. This order is much like that demonstrated in sheet welding except the relative position of D-43 has improved. B-66 welds were particularly brittle as was Cb-752. Improvement was realized in D-43 primarily through a favorable response to post weld annealing. The single post weld anneals for plate welds are listed in Table 7. It is unlikely that these are optimum anneals.

3:ND XAD Xt & CORRESPONDING  
OUTER FIBER STRAIN,  $\epsilon$

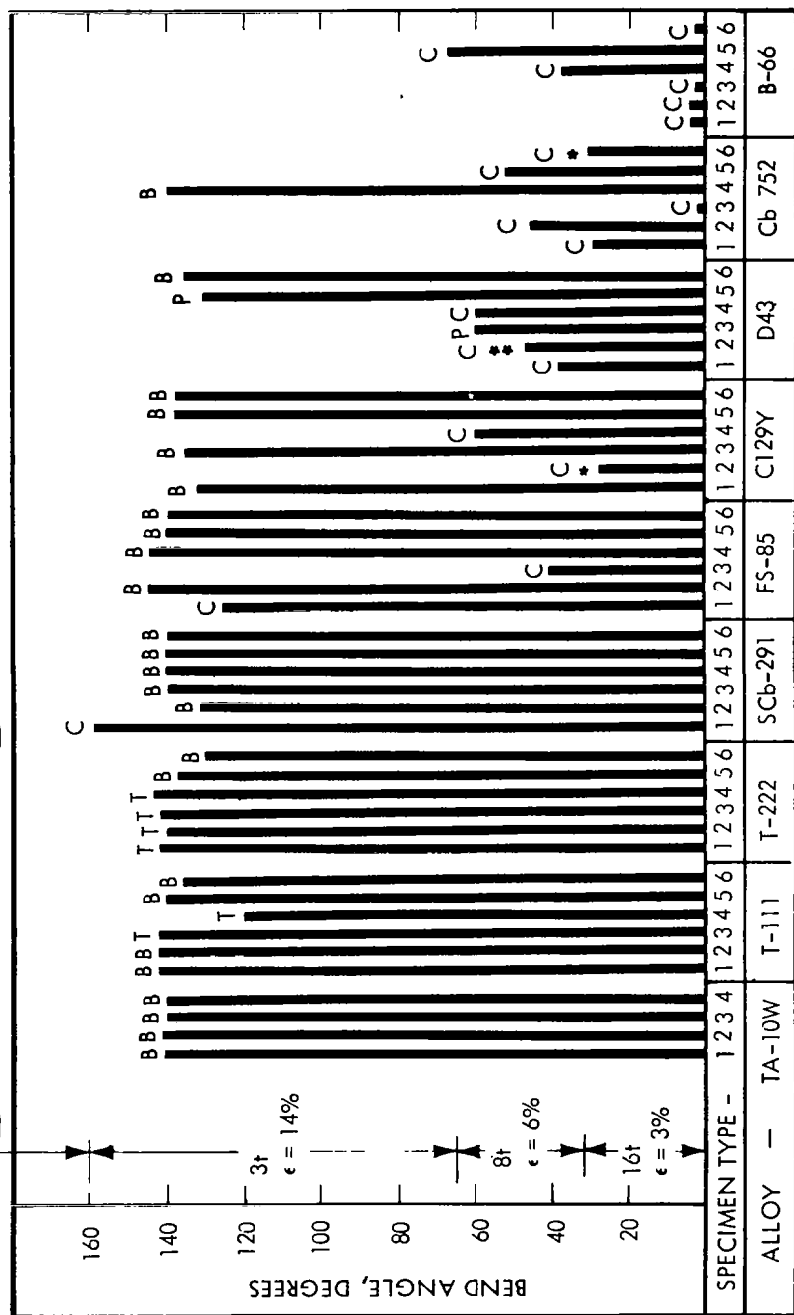


FIGURE 16 - Plate Weld Room Temperature Bend Test Summary. For Post Weld Anneals See Table 7.



TABLE 7. One Hour Post Weld Annealing Temperatures  
Used on Plate Weld Specimens

Ta-10W	None
T-111	2400°F
T-222	2400°F
B-66	1900°F
C-129Y	2400°F
Cb-752	2200°F
D-43	2400°F
FS-85	2400°F
SCb-291	1900°F

#### ALLOY WELDABILITY LIMITATIONS

An excellent measure of weldability in the conventional sense was provided in the weld "ductility response" study. The inherent flexibility in selecting weld parameters which produce sound welds can be gaged from the data summarized in Table 8.

The percent of acceptable welding conditions are listed for each alloy along with the defect source of unacceptable welds and ductility range of acceptable welds. In this table the ductility range is a "net effects" summary in that defecting welds are ignored. The relative alloy positions in this summary remain unchanged as compared with the "gross effect" summary, Figure 14.

An electron beam process limitation for most alloys at the highest welding speed, 100 ipm, was evidenced by welds having unacceptable contours. Some alloys also welded poorly at other electron beam parameter combinations. In this respect B-66 welded with difficulty presumably because vanadium tends to boil off more readily than other alloying elements.

# Mechanically Acceptable Welds Only

Alloy	Percent Parameter Combinations Producing Acceptable Welds		Bend Transition Temperature Range of Acceptable Welds		Cause(s) for Weld Rejection	
	Tungsten Arc	Electron Beam	Tungsten Arc	Electron Beam	Tungsten Arc	Electron Beam
C129Y	83	75	-250 to -100	<-320 to >-100	7	1,2
SCb-291	100	83	-275 to -125	<-320 to 0		1
FS-85	100	83	-100 to +25	-200 to -25		1
Cb-752	100	83	-175 to +100	<-320 to -75		1
D43Y	57	75	-200 to +200	-225 to +25	3,5,6	1,2
AS-55	100	83	+25 to +225	<-200 to +25		1
B-66	67	50	0 to +200	<-100 to +150	3,4	2
D43	83	83	50 to >500	-100 to +375	5	1
T-111	100	92	<-320 to >-250	<-320		1
Ta-10W	100	100	<-320 to -200	<320 to -150		1
T-222	100	83	<-320 to -100	<-320 to -200		1
W	50	See Note 9	590 to >1000	See Note 9	8	9
W-25Re	62	39	600 to >1000	450 to >1000	8,3	2,8

1. Rippled weld appearance occurring in 100 ipm welds, visual reject.
2. Coarse appearance, visual reject.
3. Hot tearing.
4. Microfissures at 60 ipm (destructive test reject).
5. Porosity.
6. Transverse cracks.
7. Shrinkage voids in 60 ipm welds.
8. Transverse and longitudinal cleavage cracks.
9. Full set of weld parameters not developed due to interference of delaminations occurring at the joint during welding.

B-66 also welded with greater difficulty in both manual and automatic arc welding due to a hot tearing tendency. This alloy is a classic example of this effect which results from an excessive freezing point depression and liquidus-solidus separation. A theoretically derived compositional correlation was demonstrated by Lessmann based on the relationship of Mo-V-Zr contents.<sup>(8)</sup> A ratio  $\frac{\text{Mo}+\text{V}}{\text{Zr}}$  greater than 10.20 is required for satisfactory weldability. The material evaluated in this program was marginal,  $R = 10.06$ , in this respect. At the highest arc welding speed B-66 showed evidence of microshrinkage, Figure 17.

Arc welds in C-129Y welded at the highest speed had gross shrinkage defects indicating a limitation in welding this material, Figure 17. D-43Y tended to hot tear along the weld centerline, have porosity, and crack (transverse) during welding. Porosity also occurred extensively in the unmodified D-43, Figure 17, but was controllable as explained later in this report by special joint preparation. All three yttrium modified alloys demonstrated a weld centerline weakness, the source of which is not apparent but is presumed to be an effect of yttrium. This occurred in D-43Y by hot tearing, in AS-55 transverse bend specimens which in several instances failed at the weld centerline at low strain along what appeared to be a single grain boundary, and in one C-129Y weld which could be torn by hand along its centerline. The C-129Y weld separated at the weld center along the boundary of a peculiar grain oriented axially in the weld direction, Figure 17. Low elongation tensile failure along this boundary at  $2400^{\circ}\text{F}$  was observed as related later in this report.

Except for hot tearing in B-66, plate welding was accomplished with relative ease with all the available alloys.

#### TUNGSTEN AND W-25Re SHEET WELDABILITY

The tungsten alloys are categorized among the refractory metal alloys by their inferior low temperature ductility. This is apparent from the bend test summary of Figure 14. Despite the handicap of poor ductility, tungsten alloys may be employed in special high temperature

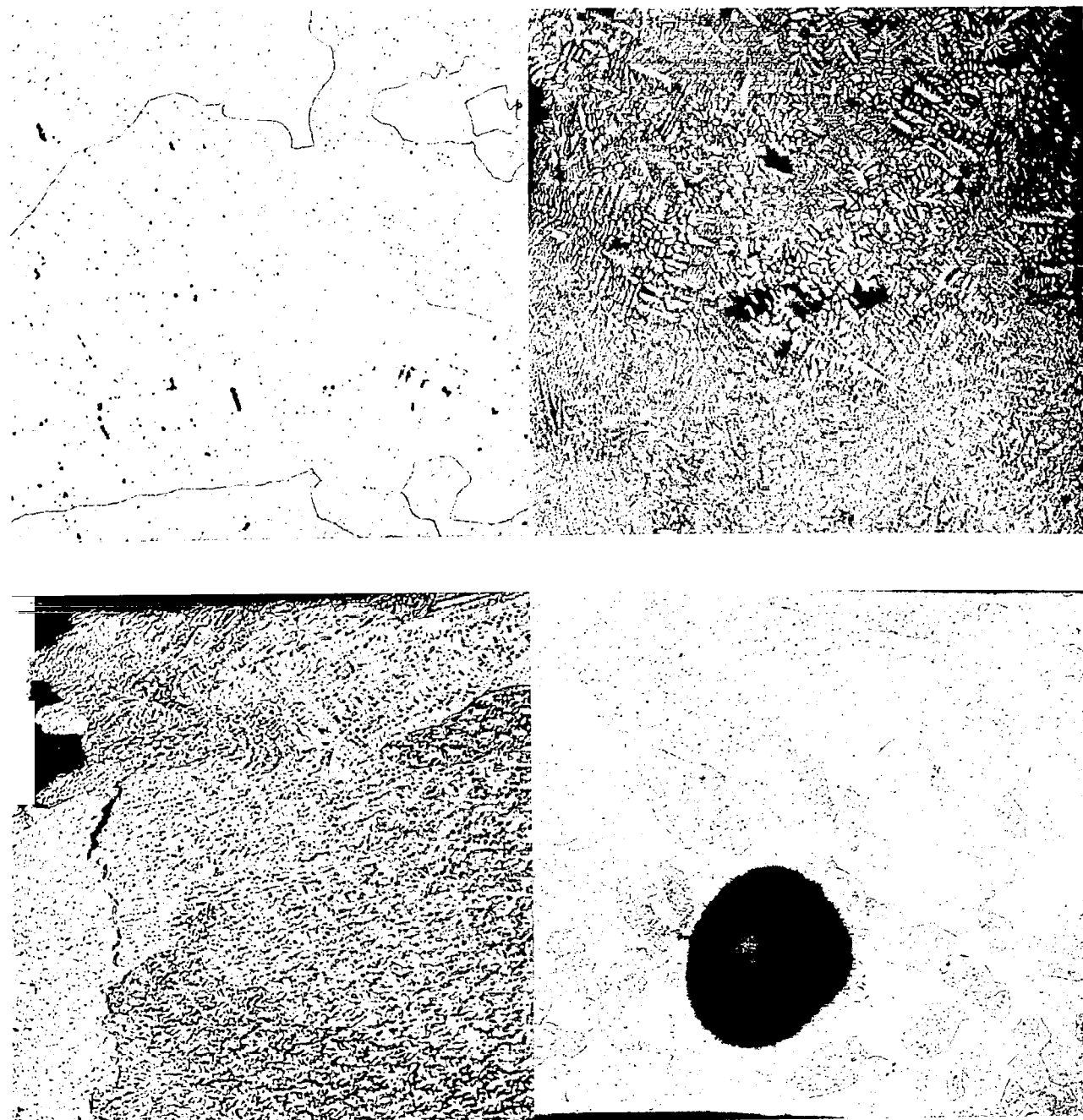


FIGURE 17 - Defected Gas Tungsten Arc Weld Microstructures for Alloys Displaying Particular Weldability Limitations. Top Left: B-66 Welded at 60 ipm Displaying Microshrinkage Voids. Top Right: Gross Centerline Shrinkage in C-129Y Welded at 60 ipm. Bottom Left: Location of Single Case of C-129Y Centerline Hot Tearing along Peculiarly Oriented Center Grain. Bottom Right: Porosity in D-43 Weld.

applications and were therefore included in this evaluation. Tungsten retains a certain degree of ductility and fabricability in the wrought and stress relieved conditions. Hence, the stress-relieved structure was selected for this study as opposed to the recrystallized condition obtained in the tantalum and columbium alloys. Also, in tungsten alloys, the strengthening effect of a cold worked structure can be appreciated at temperatures exceeding 2000°F making this structure attractive in many potential applications. The W and W-25Re sheet was converted from arc cast ingots. Tungsten alloys were evaluated as sheet only and not in plate thickness.

The effect of preheat in TIG welding was selected as an additional parameter in evaluating the tungsten alloys. Preheating was accomplished with heaters placed in the backup bar of the welding fixture. This provided a preheat of 550°F. Sample preparation for both welding and, after welding, for testing was considerably more complicated than for columbium and tantalum alloys. Specimen blanking by shearing was unsatisfactory because of edge cracking and possible delamination. Warm shearing at +600°F reduced this problem but did not eliminate it. Consequently, weld specimen blanking was accomplished by electro-discharge machining (EDM) and test specimen blanking was accomplished using an abrasive cut-off wheel. Edge finishing for butt weld specimens was accomplished by stacking and wet edge grinding prior to pickling and welding. The unalloyed tungsten and tungsten alloy weld blanks were vacuum degassed for 1 hour at 2000°F after pickling and just before welding. The pickling solution employed for tungsten and tungsten alloys consisted of 9 parts hydrofluoric acid and 1 part concentrated nitric acid.

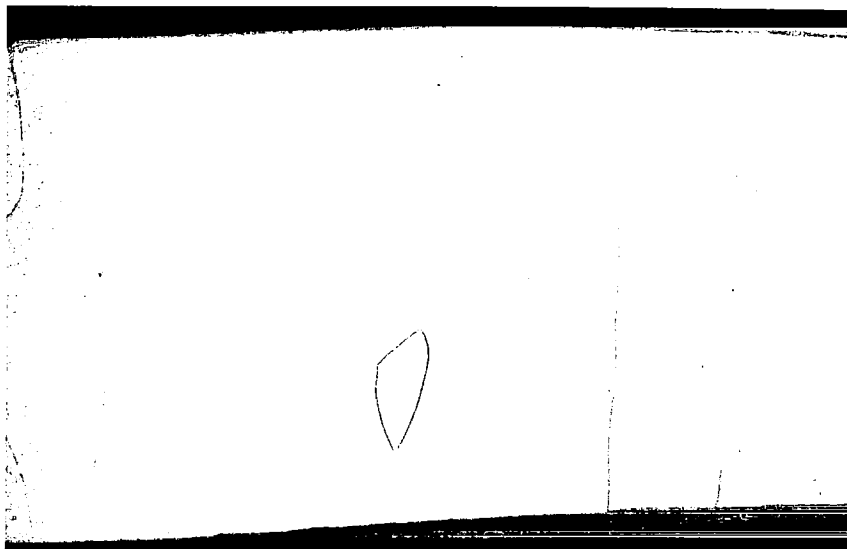
Unalloyed Tungsten. Out of 10 parameter combinations employed for GTA welding tungsten, 6 welded successfully. The other 4 contained cleavage cracks. Four out of 6 good welds were obtained using a 550°F preheat indicating that this may be beneficial. Weldability decreased with increased welding speed such that satisfactory welds were obtained at 15 ipm but not at 30 ipm. For comparison, the columbium and tantalum alloys generally were weldable to 60 ipm or faster. The manual patch test produced in tungsten proved to be defect-free even though welded without preheat. A typical gas tungsten arc weld microstructure is shown

in Figure 18. The large full section grains of the weld are largely responsible for the poor ductility of welds as compared with stress relieved base metal. The weld hardness traverses (see Appendix), indicate a weld hardness of about 375 DPH and base metal hardness (stress relieved) of about 475 DPH. A peak hardness of near 500 DPH at the base metal edge of the heat affected zone implies that an aging or solutioning response is induced in the base metal by the weld thermal cycle at the approach of recrystallization. This is most likely an interstitial effect realized as a result of low interstitial solubility in tungsten. A post weld stress relief of 1 hour at 2560°F (1400°C) proved marginal in improving weld ductility. Stress relief bend test data is included along with the as-welded data in the Appendix.

Tungsten weldability was poor in electron beam welding both as a result of brittle cleavage occurring during welding at higher speeds and because of a general underside delamination problem associated with this process. The delaminations occurred, as shown in the microstructure of Figure 19, on all welds. Cleavage cracking occurred in a number of characteristic modes as shown in Figure 20. In this figure cleavage cracks are shown for weld No. 3 (centerline crack), No. 4 (transverse), No. 7 (full section transverse, centerline, and arrested transverse), and Nos. 10 and 12 (peculiar "X" pattern arrested cleavage). The severity of weld cracking increased with welding speed. The numerous centerline defects are caused by the typical root delaminations.

W-25Re. Like unalloyed tungsten, W-25Re was welded with difficulty. Welding became increasingly difficult with higher welding speeds. Transverse arrested cracks (weld and heat affected zone only) occurred in one 15 ipm weld and in all three 30 ipm welds. One 7.5 ipm weld contained a centerline crack which may have been a hot tear. Such cracks were also observed in welding patch tests.

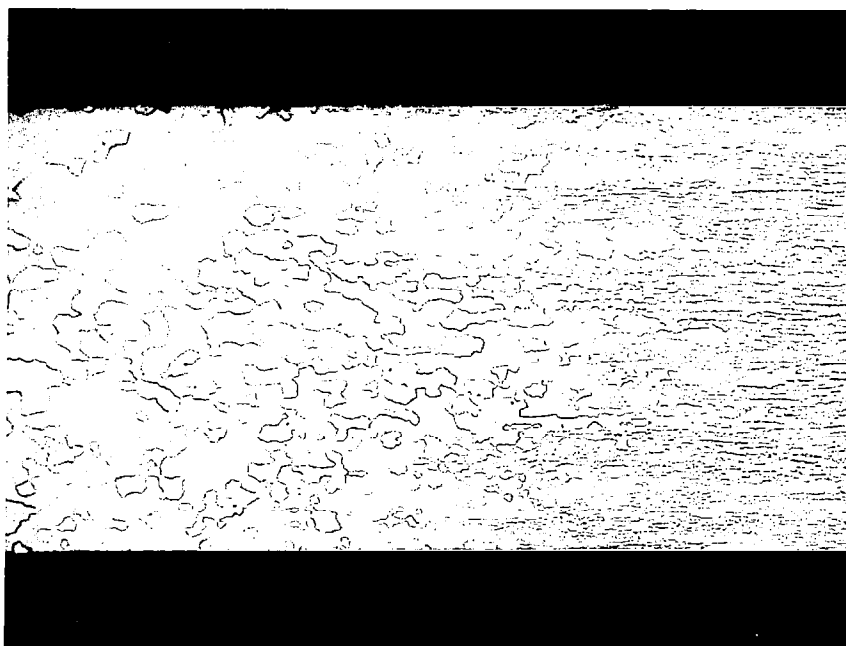
Bend specimens were cut from sound GTA welds or apparently sound sections of defective welds. The effect of weld parameters on weld ductility in this alloy is described by the summary presentation of Figure 21. The data provide a reasonably consistent trend which



13,582

Weld Structure

80X

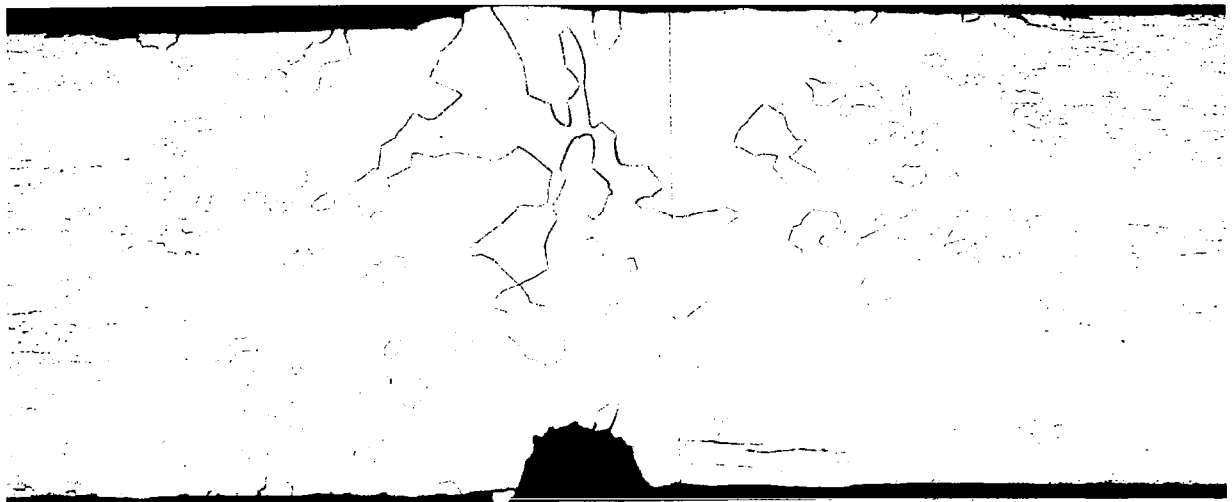


13,582 Heat Affected Zone - Base Metal Structure 80X

FIGURE 18 - GTA Weld Structure in Unalloyed Tungsten, Weld No. 1  
(Welded at 7.5 ipm without Preheat)



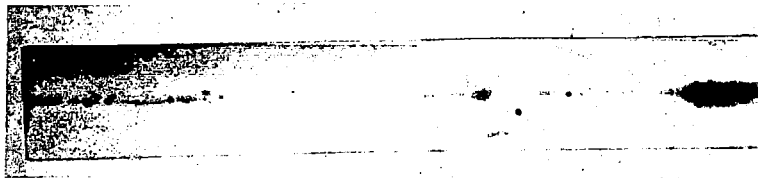
13,595    Weld No. 1    2.98 Kilojoules/inch    at 15.6 ipm    80K



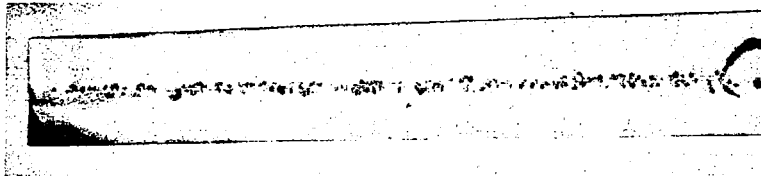
13,596    Weld No. 4    3.24 Kilojoules/inch    at 15 ipm    80X

FIGURE 19 - Typical Sections of Electron Beam Welds in Unalloyed Tungsten

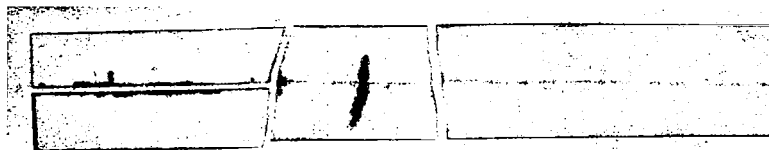




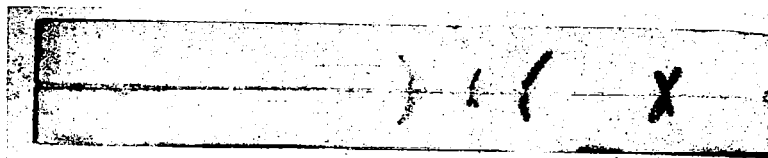
Weld No. 1  
Speed - 15 ipm  
2.98 Kilojoules/inch



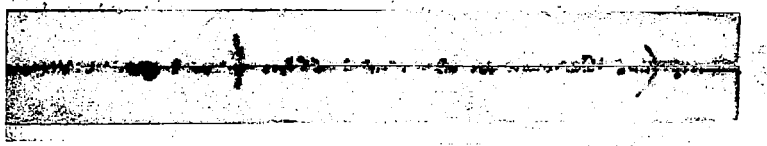
Weld No. 4  
Speed - 15 ipm  
3.24 Kilojoules/inch



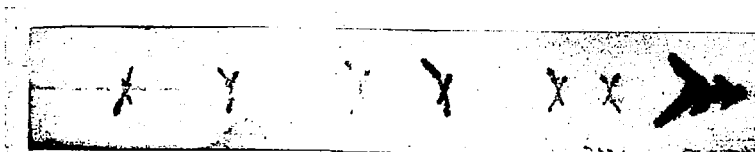
Weld No. 7  
Speed - 50 ipm  
1.19 Kilojoules/inch



Weld No. 10  
Speed - 15 ipm  
3.12 Kilojoules/inch



Weld No. 11  
Speed - 50 ipm  
1.30 Kilojoules/inch



Weld No. 12  
Speed - 100 ipm  
0.76 Kilojoules/inch

FIGURE 20 - Typical Dye-Penetrant Results of Electron Beam  
Welds in Arc Cast Unalloyed Tungsten Sheet

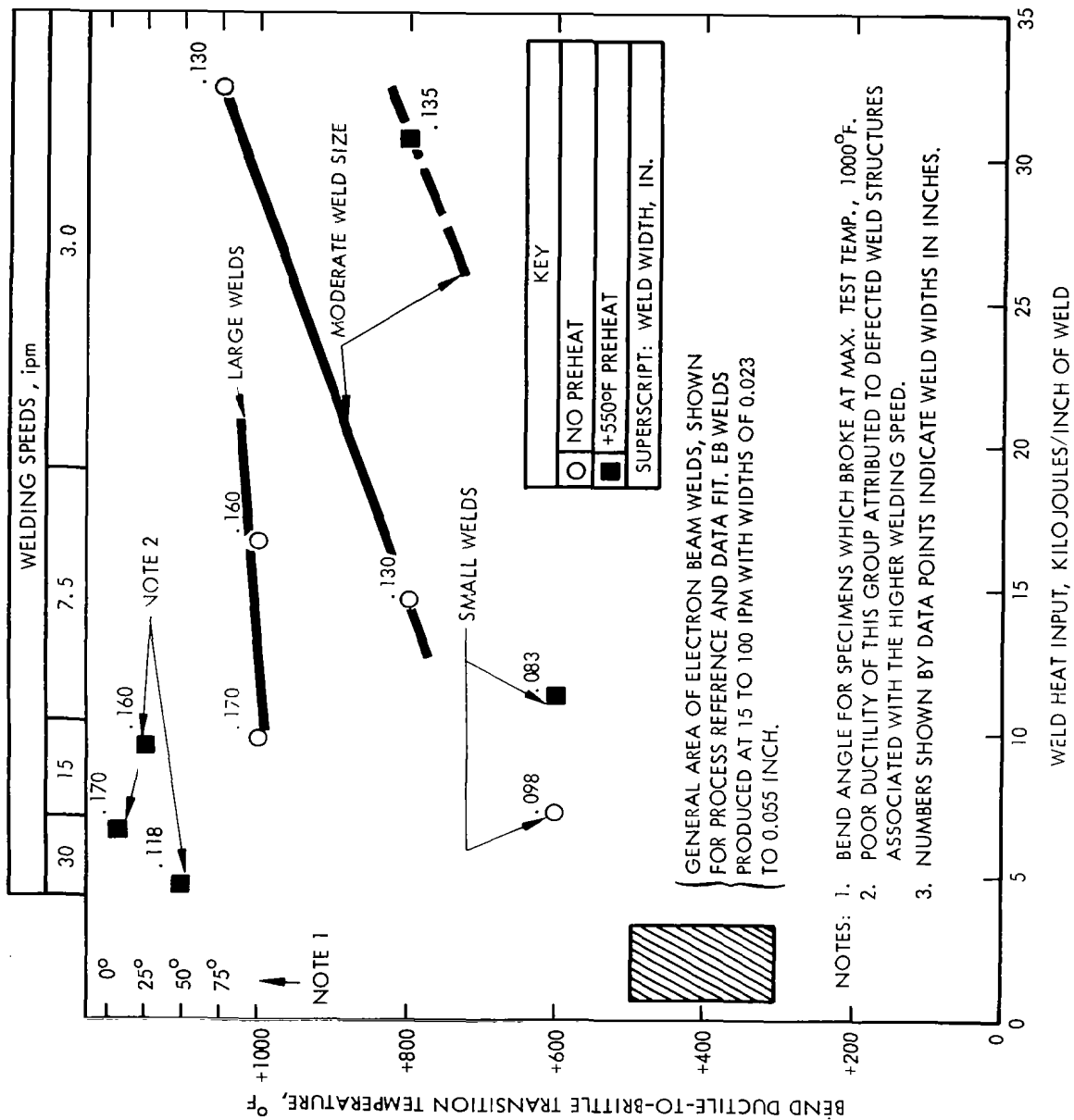


FIGURE 21 - The Effect of Weld Parameters on Ductility of Gas Tungsten Arc Welds in W-25Re Alloy Sheet

relates the dependent variables affecting weld thermal cycles (heat input per unit weld length, weld size, preheat and weld speed) to ductility. An overall trend of improved ductility with decreased unit length heat input is apparent. Decreased heat input is achieved with decreased weld size and/or higher welding speeds for any one process, or it can be further decreased, as shown, by employing the electron beam welding process. The ductility of electron beam welds demonstrates excellent correlation with the heat input trend associated with gas tungsten arc welding. The selection of welding parameters must naturally be consistent with good weldability. In this respect, an observed trend towards less weldability at higher speeds is reflected in decreased ductility in several welds which presumably results from defected structures. Preheating appears to have a beneficial effect on weld ductility but not on weldability. As with unalloyed W, a post-weld stress relief of 1 hour at 2560°F (1400°C) was only marginal in improving ductility.

An interesting ductility/weldability correlation with microstructure was observed. Weld ductility and weldability were poorer for welding conditions under which twinning occurred in the cast weld structure. This is shown in Figures 22 and 23. The preheated 7.5 ipm weld did not twin, whereas the non-preheated 7.5 ipm weld did twin and also had poorer ductility, Figure 22. Increased twinning, and less ductility, was observed in the 3 ipm, no preheat weld. Increased weld speeds, 15 and 30 ipm, even with preheat had twinned structures and less ductility, Figure 23. Variability of twinning is probably indicative of variability of weld induced residual strain since twinning is a strain associated phenomena. Hence, these results imply that the observed variability in weld ductility in this system is most likely related to the effect of weld parameters on stress distribution, as opposed to metallurgical structure.

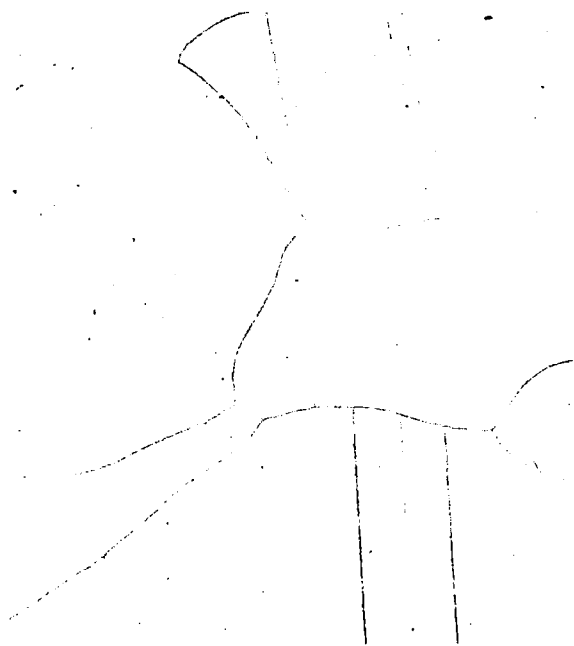
Electron beam welding of W-25Re was accomplished with comparative ease. As welded ductility was disappointing. The best ductility was obtained using slow welding speeds (less than 15 ipm) and wide clamp spacing. This again implied that residual stresses contributed significantly to ductility impairment. An improvement in bend-ductile-brittle transition temperatures of about 400°F were realized with a 2560°F/1 hr. stress relief confirming the



13,592

Weld No. 11  
3 ipm, No Preheat  
32.3 Kilojoules/inch

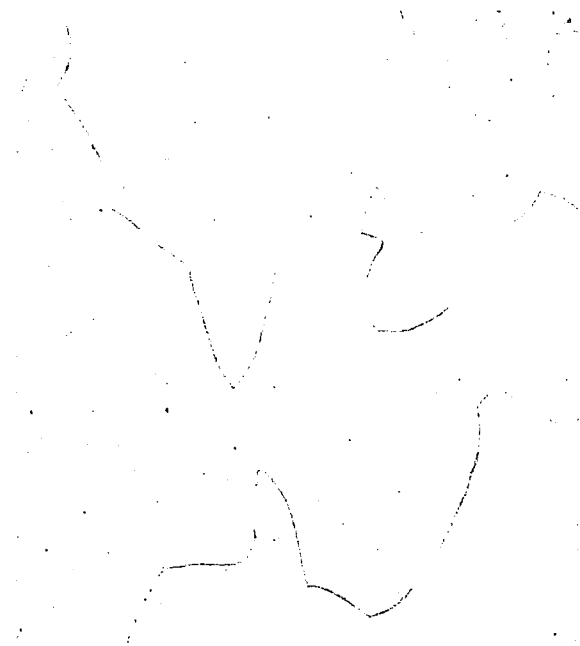
100X



13,587

Weld No. 1; 7.5 ipm  
No Preheat; 16.45 Kilojoules/inch

300X



13,589

Weld No. 4; 7.5 ipm  
Preheated; 11.29 Kilojoules/inch

300X

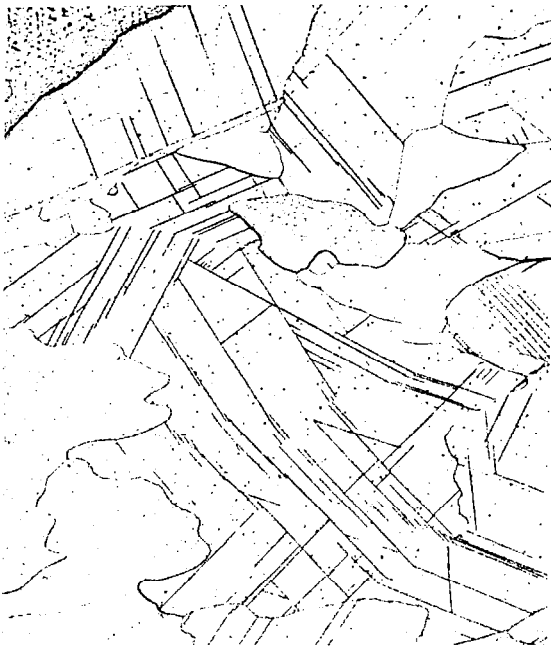
FIGURE 22 - Photomicrographs of Cast Weld Area in Gas Tungsten Arc Welded W-25Re Sheet



13,590

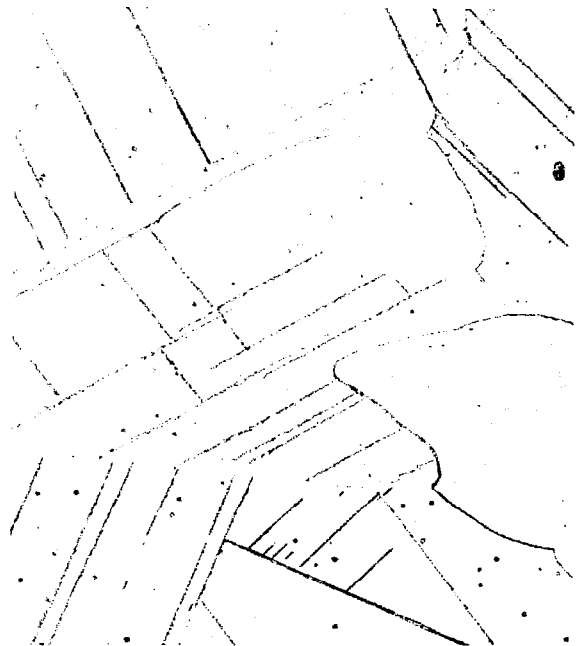
Weld No. 6; 15 ipm  
Preheated; 8.9 Kilojoules/inch

100X



13,591

100X



13,591

300X

Weld No. 9; 30 ipm; preheated; 6.28 Kilojoules/inch

FIGURE 23 - Photomicrographs of Cast Weld Area in Gas Tungsten Arc Welded W-25Re Sheet

significant influence of residual stresses. During EB welding butt joint cambering occurred causing seam spreading if tack welds were not employed. Joint spreading in W-25Re is an opposite trend to that observed in welding the tantalum and columbium alloys.

### THERMAL WELD RESPONSES IN COLUMBIUM ALLOYS

As indicated in the technical approach, the effect of welding as a variable thermal process was emphasized in the thermal response study. A summary of heat input requirements developed during this study show that a judicious selection of welding parameters was made, Figure 24. The curves in this figure are for fixed size welds. A considerable increase in efficiency is realized across the welding speed range, and the effectiveness of narrow-clamp spacing in removing heat is evident. Hence, the selected weld parameter variations could be expected to greatly influence the time-temperature dependent reactions which control metallurgical response, and therefore, mechanical properties. In this figure, electron beam welding is placed in proper overall perspective as a joining method requiring a minimum sized weld and, hence, minimum heat input. The size advantage of electron beam welds over gas tungsten arc welds is shown in Figure 25.

Welding conditions in this study were not duplicated. In a statistical sense this was most efficient both in terms of cost and total coverage. Also, this permitted investigation of a greater range of welding variables. In interpretation of data, this approach is usually less definitive with respect to any one particular effect, but more comprehensive in cross checking any one conclusion. Hence, the test data were reviewed as a continuum for proper interpretation. Columbium alloy responses were successfully evaluated while the tantalum alloys displayed excellent ductility under all welding conditions and were unresponsive within the -320°F bend test limit. Tungsten alloys had extremely poor ductility and were evaluated as previously described.

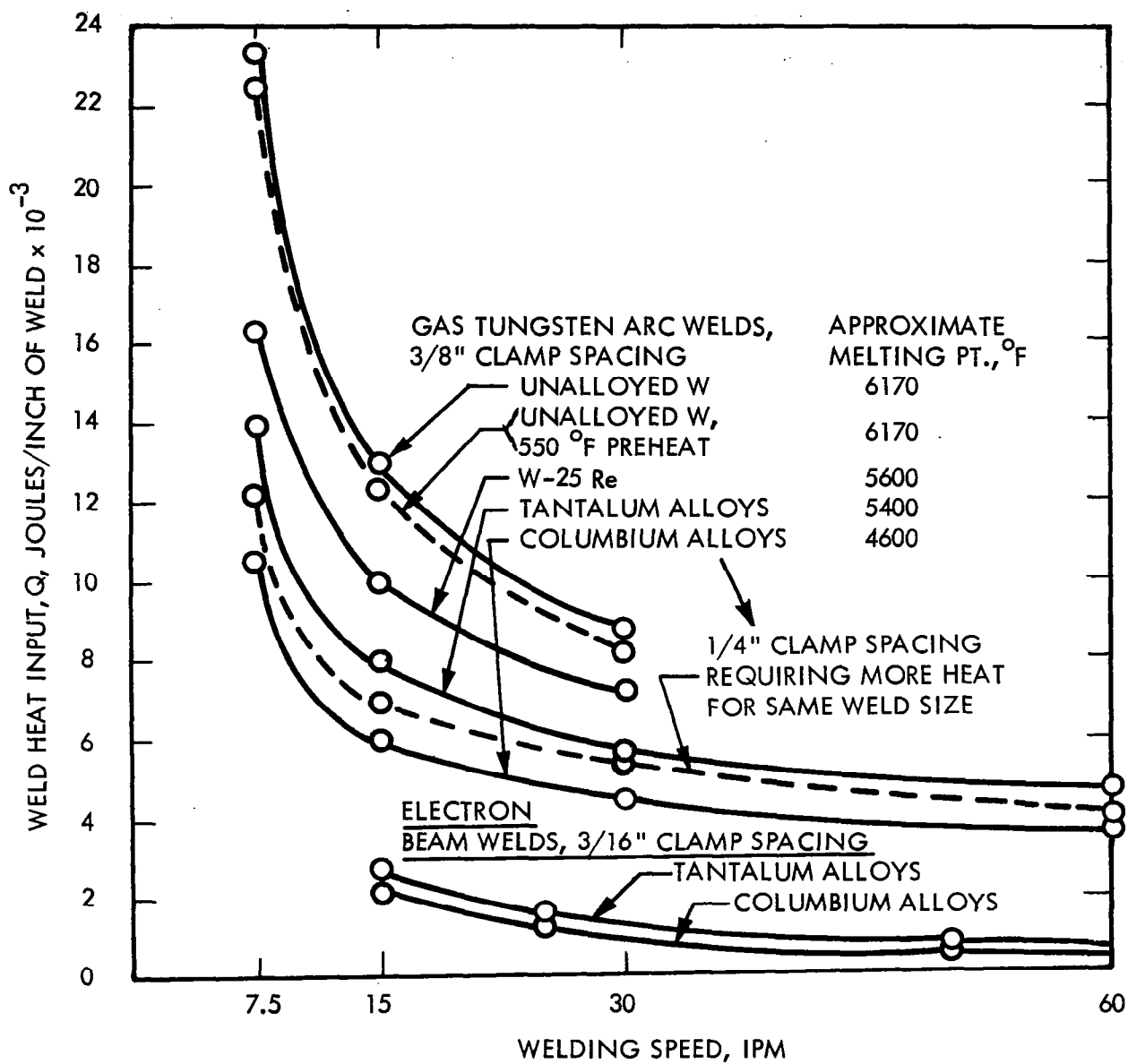
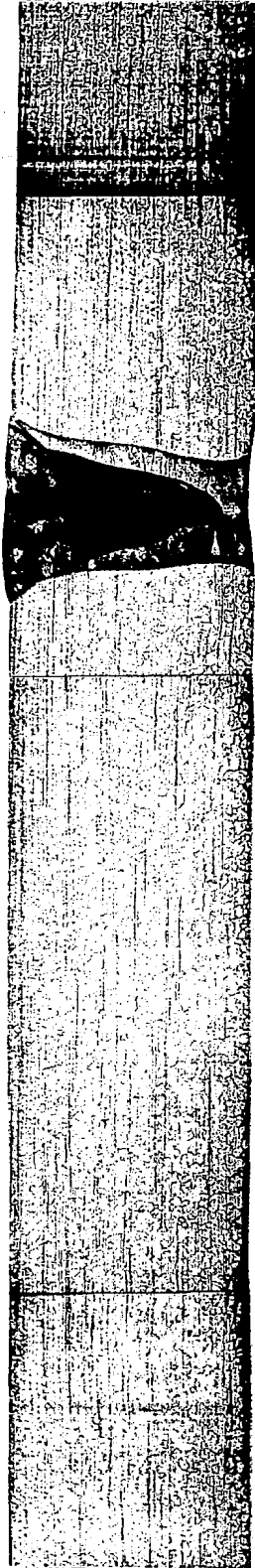


FIGURE 24 - Observed Heat Input Requirements for Welding 0.035 Inch Sheet as a Function of Welding Speed, Weld Size Constant. Typical Tungsten Arc Weld Width: 0.185 Inch. Typical Electron Beam Weld Width: 0.035 Inch



T-111



T-222

FIGURE 25 - Typical Sheet Butt Weld Configurations for Gas Tungsten Arc (top) and Electron Beam Welds



The following ground rules were used in analyzing the columbium alloy data. These were followed in the indicated sequence to minimize bias in data reduction.

1. Only sound welds were included.
2. Bend transition temperatures were interpreted in terms of true transitions, i.e., the test temperature below which ductility is severely impaired as opposed to the lowest "no defect" temperature.
3. The bend transition temperatures were rationalized for each alloy on the basis of its most ductile weld. Hence, alloys are compared in this study on the basis of their individual deviation from optimum (or change in) transition temperature.
4. Longitudinal and transverse bend transition temperatures were averaged for each weld. The effect of averaging was remarkable since independent analyses resulted in largely unreconcilable trends. This approach apparently provides strain vector averaging across the plane of weakness the orientation of which can vary considerably with welding parameters and between alloys.

Electron Beam Welds. The typical thermal response of columbium alloys to total heat input in electron beam welds is depicted by the FS-85 behavior shown in Figure 26. Total heat input over this range had little effect on ductility. In reviewing alloy behavior, different types of beam deflection patterns were observed to produce families of curves rather than a simple single response. Hence, as implied in Figure 26, an important conclusion developed, namely, that technique variations in electron beam welding must be treated as different welding processes.

The response in Figure 26 is typical except that yttrium modified alloys did not display any difference between longitudinal and transverse beam deflection as observed for FS-85. A clamp spacing effect is apparent in this figure. This may result from larger weld (or weld plus heat affected zone) width since at any one welding speed the same power input was used but larger welds were obtained with the wider clamp spacing. A chill effect was obviously realized using the narrower clamp. A weld size effects summary for all the columbium alloys confirms the tendency of larger welds to be less ductile, Figure 27.

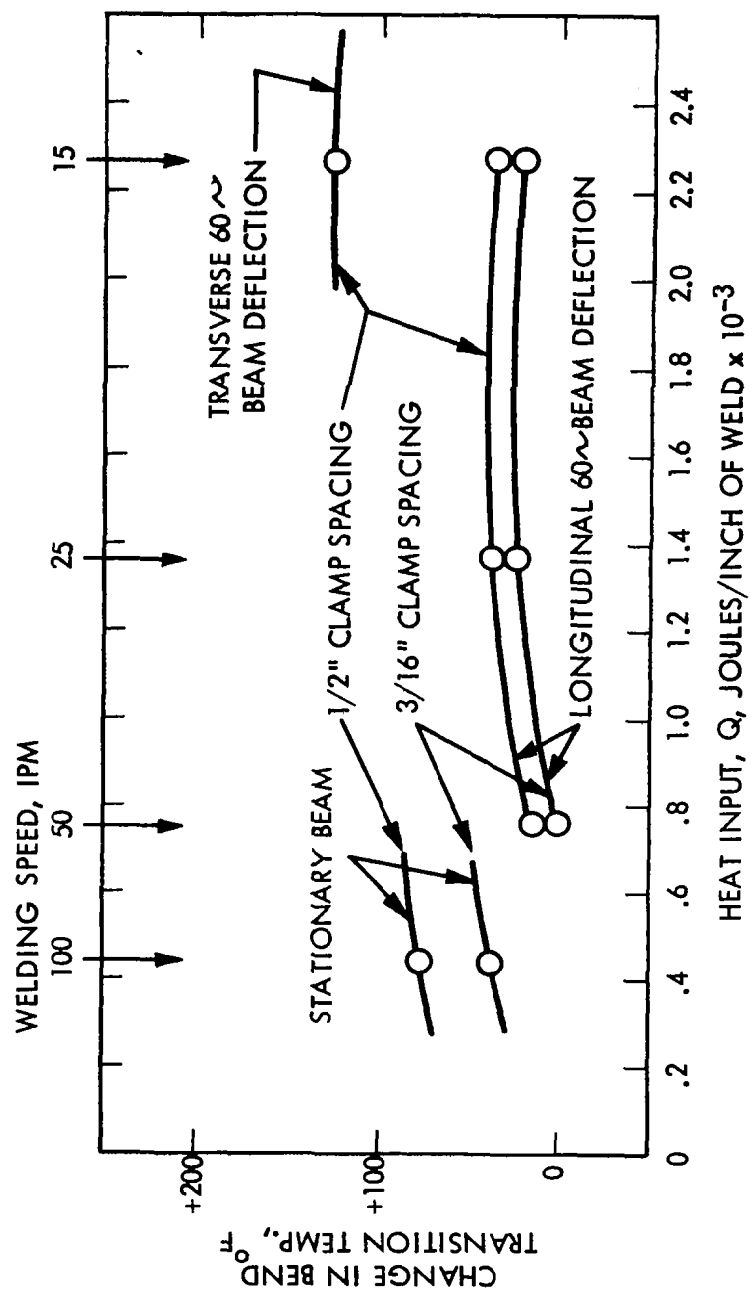


FIGURE 26 - Effect of Electron Beam Welding Variables on FS-85 Weld Ductility in 0.035 Inch Sheet

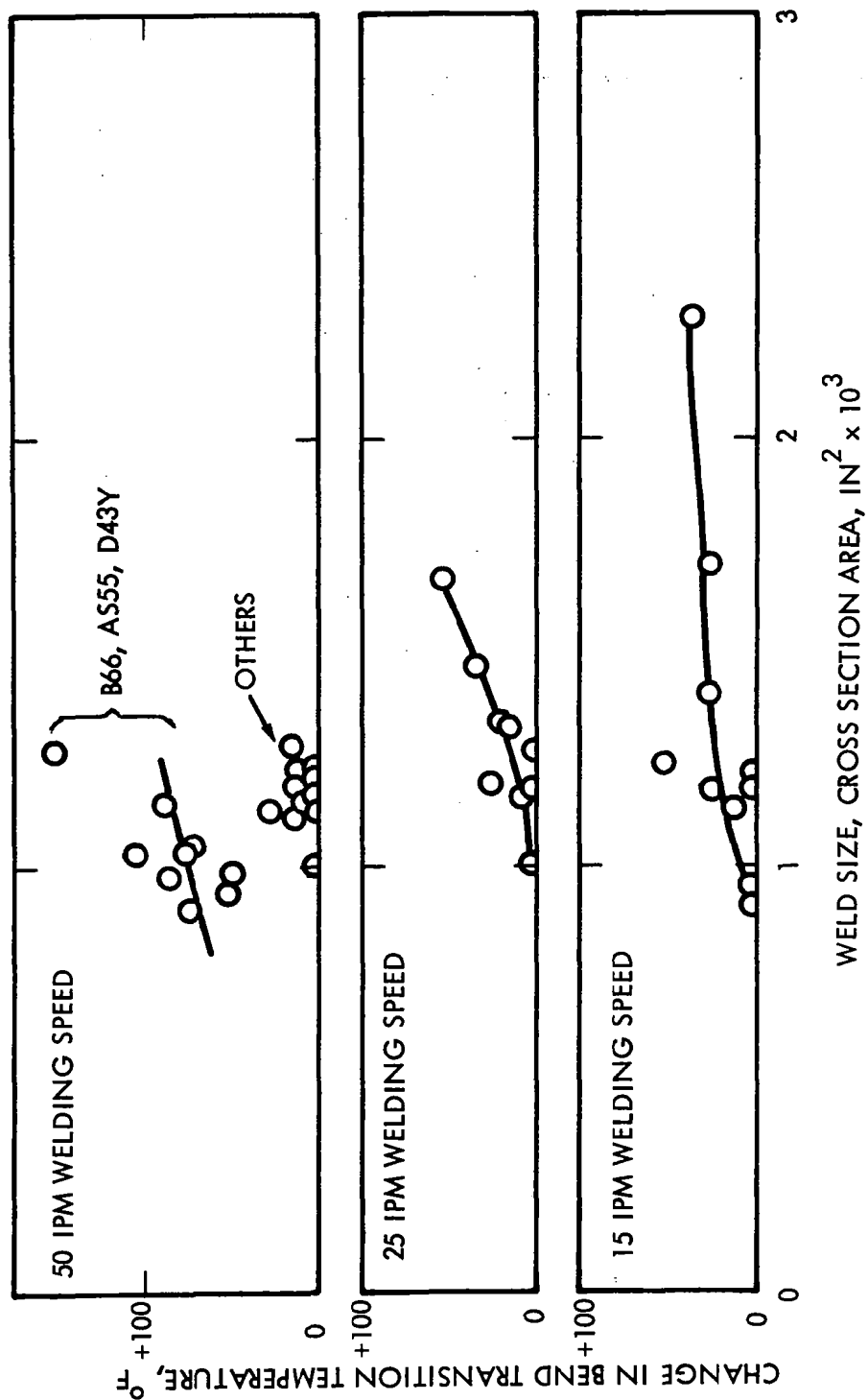


FIGURE 27 - Relationship of Weld Size to Bend Transition Temperature of Electron Beam Welds in Columbium Alloys. Data for All Columbium Alloy Welds Produced with 60 Longitudinal Deflection (Regardless of Amplitude) Included. Welding Speeds as Indicated.

However, the larger welds were made at wider clamp spacings so it isn't clear if ductility loss occurs with increased weld size, increased heat affected zone size, or a combination of both. The lower ductility of B-66, AS-55, and D-43Y at the 50 ipm welding speed probably results from microstructural defects. These were not detected in non-destructive tests but their presence can be implied from general difficulties encountered in tungsten arc welding B-66 and D-43Y at higher speeds (30 to 60 ipm).

### Gas Tungsten Arc Welds

The effect of gas tungsten arc weld parameters on columbium alloy weld ductility was rationalized by grouping the alloys as follows:

1. Solid solution strengthened alloy: SCb-291
2. Solid solution plus dispersion strengthened alloys: FS-85, Cb-752, D-43, and B-66.
3. Yttrium modified alloys: C-129Y and D-43Y (these are also solid solution plus dispersion strengthened).

AS-55 welds are not included because they displayed atypical bend transition behavior, Figure 15.

Group behavior, as reflected by changes in weld ductility, were reviewed for general effects of weld speed (freezing rate), clamp spacing (chill effect), and unit weld length heat input. Meaningful relationships which lent themselves to a significant technical interpretation were observed.

### 1. Solid Solution Alloy, SCb-291

Particular independent effects of weld speed and unit length heat input were not apparent but a pronounced and unexpected weld size effect was observed: ductility improved with increasing weld size. With the particular weld fixturing employed (fixed clamp spacing) this effect can be interpreted in a different way: ductility improved with a decrease in heat affected zone width. This approach was taken in plotting the data shown in Figure 28. Metallurgical observations in this program justify the general premise of this interpretation: i.e., weld width + heat affected zone widths = clamp spacing.

Weld size is a dependent variable determined by selections of welding power (amperage) and welding speed for any particular mechanical holding arrangement. Neither speed nor power input were independently related to ductility. Consequently, it can be reasonably inferred that heat affected zone size is a major factor influencing weld ductility.

### 2. Solid Solution Plus Dispersion Strengthened Alloys: FS-85, Cb-752, D-43, and B-66

Total heat input effects for the solid solution plus dispersion strengthened alloys are summarized in Figure 29. The two clamp spacings are plotted separately. Fitting curves for the 7.5 ipm welding speed was least successful for all the alloys. This results from a greater process sensitivity at this welding speed as indicated by the slope of the heat input curve, Figure 24.

For reference purpose, the general area of electron beam response is also shown. The electron beam and tungsten arc weld data show excellent fit with respect to a ductility threshold at a total heat input of about 3000 joules/in. of weld. Ductility is less above this energy input threshold regardless of weld speed. This is indicated by an increase in ductile-to-brittle

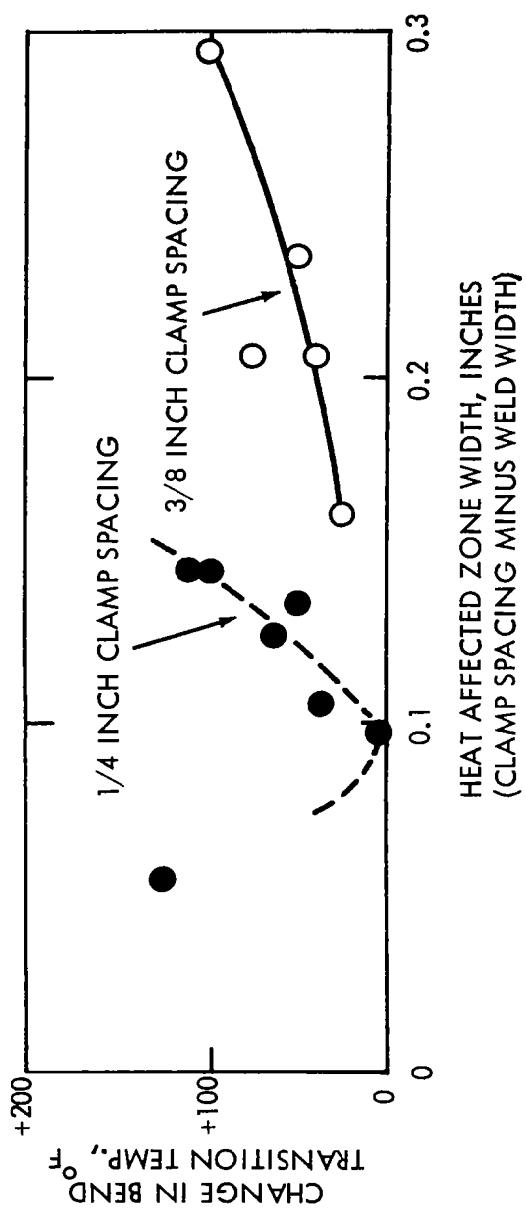


FIGURE 28 - Change in Bend Transition Temperature with Increasing Heat Affected Zone Size of Gas Tungsten Arc Welds in the Solid Solution Columbium Alloy, SCb-291

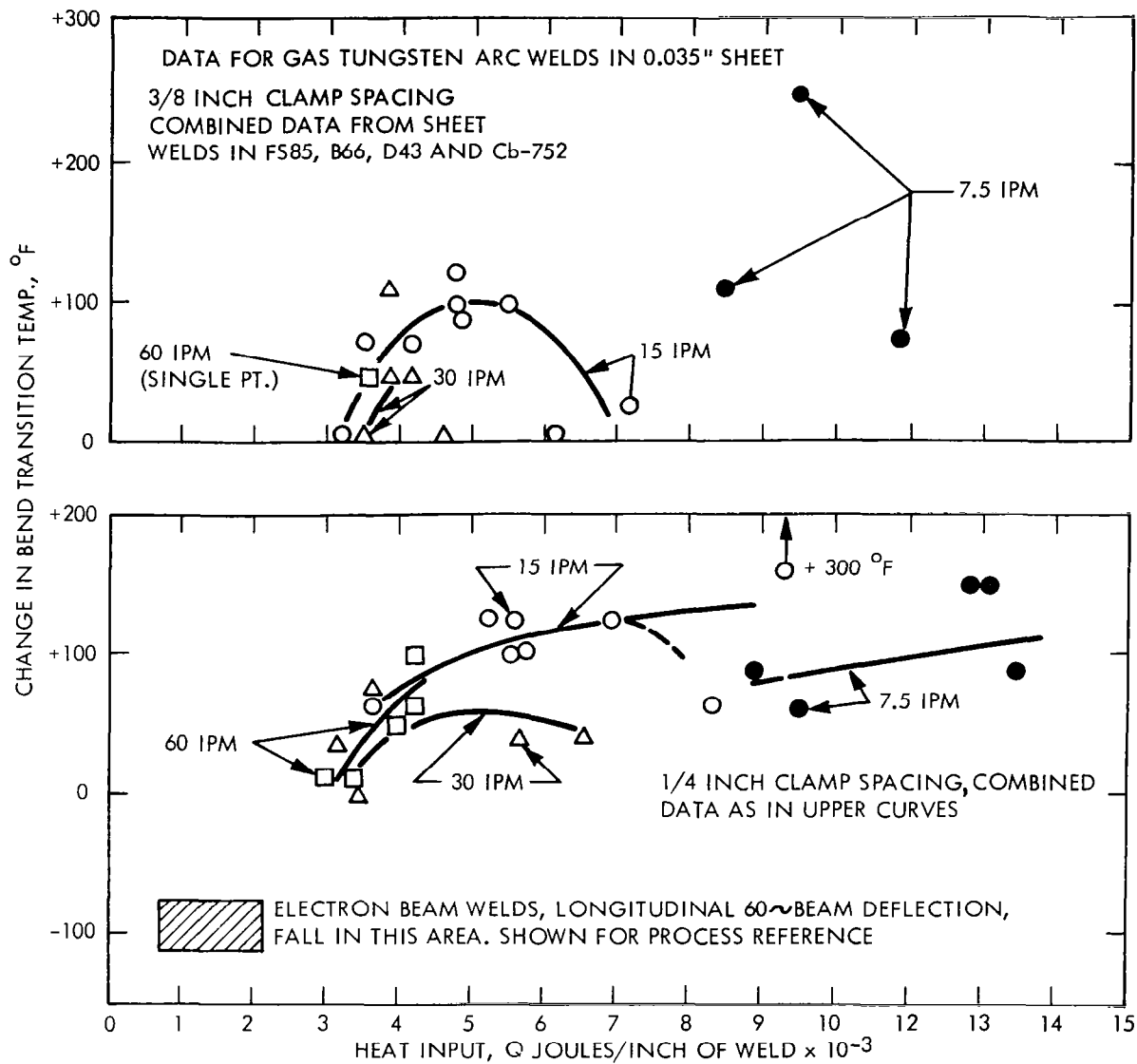


FIGURE 29 - Effect of Gas-Tungsten-Arc-Weld Heat Input on Ductility in the Solid Solution plus Dispersion (Reactive Element) Strengthened Columbium Alloys. Welding Speeds as Indicated.

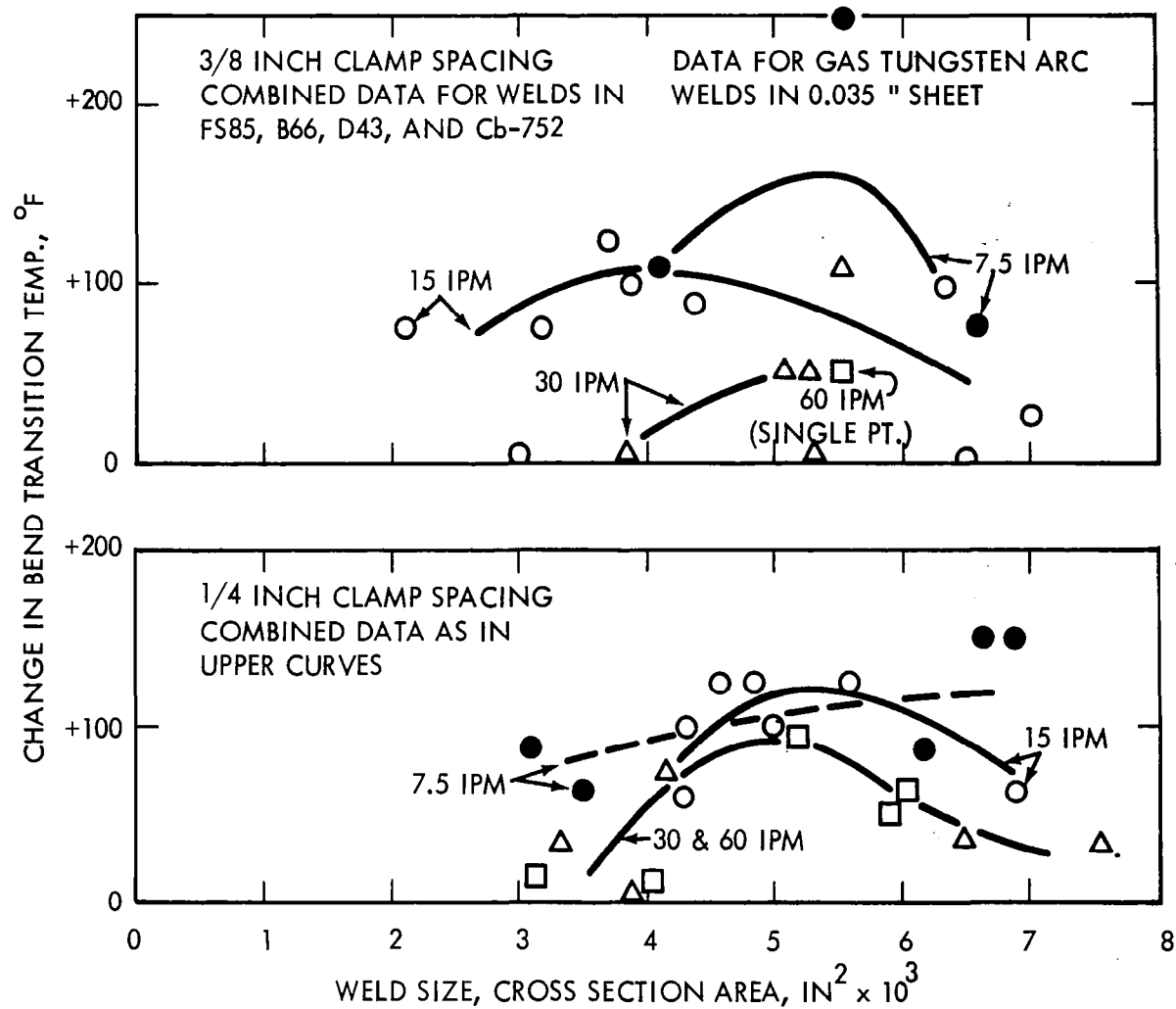


FIGURE 30 - Change in Bend Transition Temperature with Size of Gas Tungsten Arc Welds in the Solid Solution plus Dispersion Strengthened Columbium Alloys. Welding Speeds as Indicated.



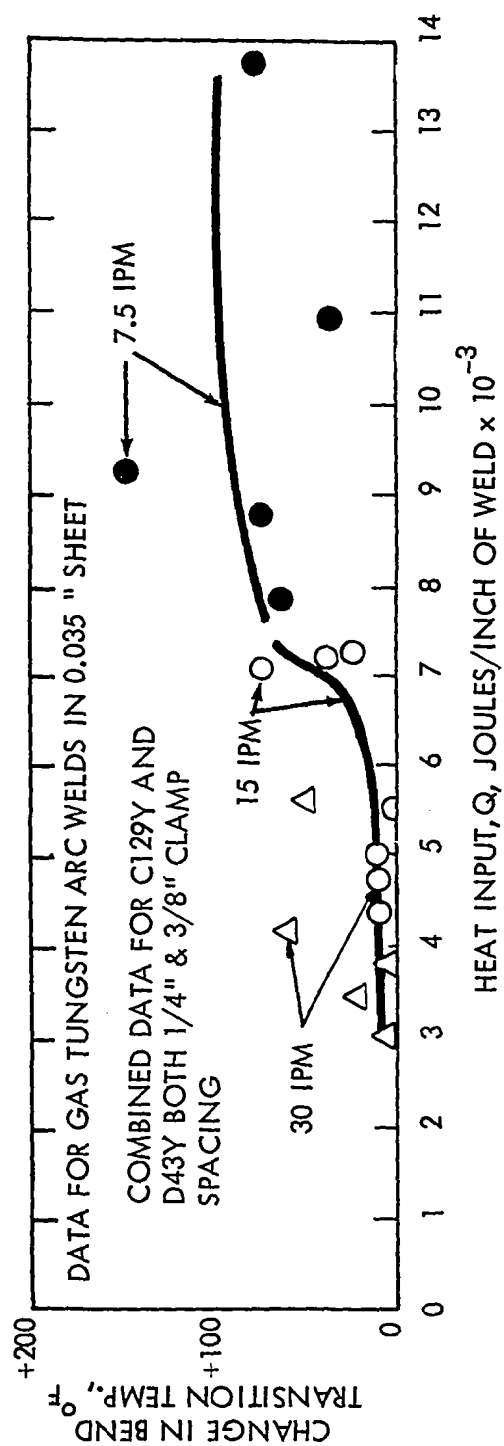


FIGURE 31 - Effect of Gas-Tungsten-Arc-Weld Heat Input on Ductility in the Yttrium Modified Alloys C-129Y and D-43Y. Welding Speeds as Indicated.

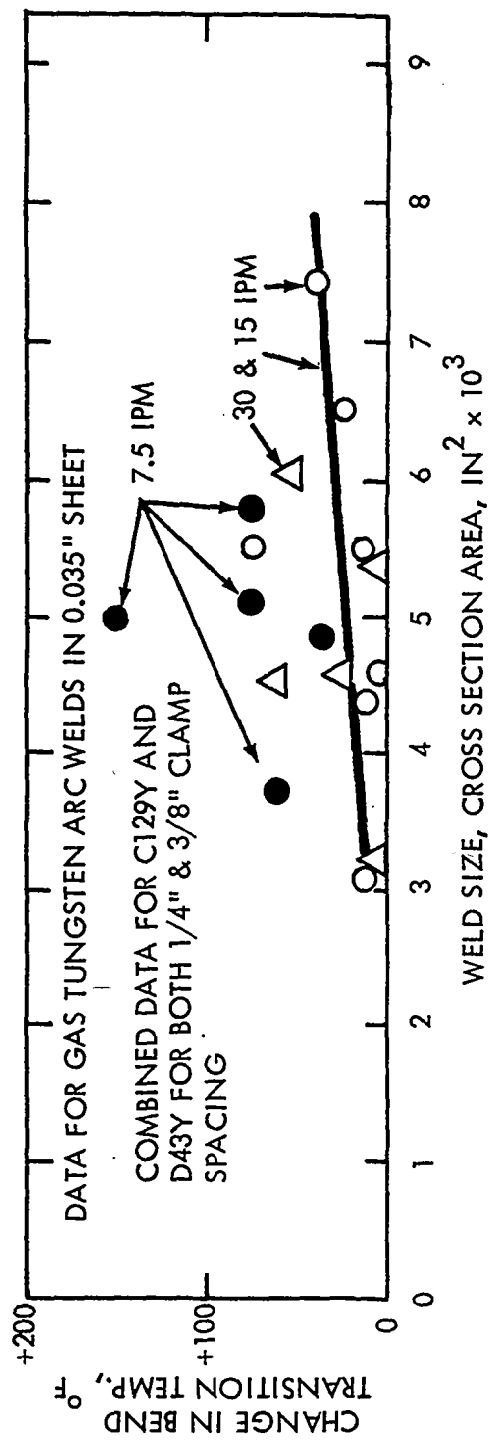


FIGURE 32 - Change in Bend Transition Temperature with Size of Gas Tungsten Arc Welds in the Yttrium Modified Alloys C-129Y and D-43Y

transition temperature. However, for any one speed, an inversion trend producing improved ductility at higher heat input is also evident. Higher heat input naturally produces larger welds. The effect of weld size on ductility, Figure 30, confirms this inversion effect. The improvement in ductility with increasing weld size for the larger welds is similar to the behavior exhibited by the solid solution alloy, SCb-291. The threshold behavior, however, represents a significant difference between these two groups.

### 3. Yttrium Modified Alloys - C-129Y and D-43Y

The yttrium modified alloy behavior is shown in Figures 31 and 32. No apparent clamp spacing effects were noted so these were not plotted separately. Ductility in this group appears to be relatively stable as compared with the other alloys. The decreased ductility of the 7.5 ipm welds appears to be a manifestation of a similar heat input threshold effect as observed for the other dispersion strengthened alloys. This threshold occurs at about 7000 joules/in. (compared with 3000 joules/in. for the second group of alloys). The threshold very nearly divides the heat input requirements for 7.5 ipm welds from that required for 15 ipm welds (compare Figure 24 and 31). Hence, in Figure 32, not much of a weld size effect is noted. Instead, the 7.5 ipm welds have poorer ductility reflecting the "threshold" heat input phenomena. In interpreting the yttrium modified alloy behavior in terms of a thermal threshold, the two least ductile of five 30 ipm welds were assumed to be of questionable quality and were ignored. This was reasonable based on increased difficulty of welding these alloys at higher speeds.

A Thermal Response Hypothesis. The weld size effect in SCb-291, the "threshold" heat input effect in the other alloys, and the ductility inversion with increasing weld size in the solid solution plus dispersion strengthened alloys all appeared significant. Interpretation of these trends provides a metallurgical appreciation of the observed weld responses. Intuitively this required a single general hypothesis. An interpretation based on probable differences in kinetics of grain growth in the heat affected zone, consequent grain size, and gross size of the heat affected area seems to satisfy the observed behavior. These factors are controlled by

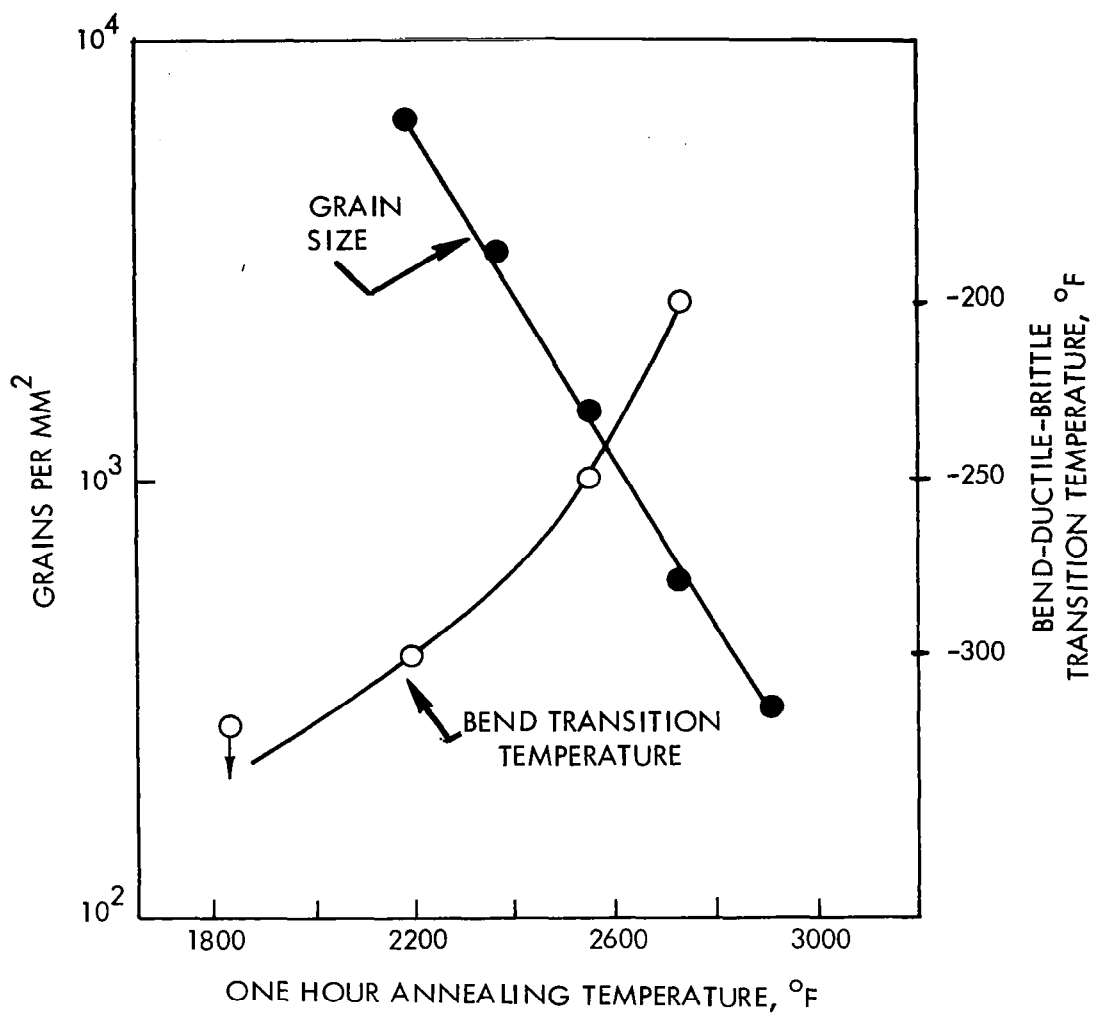


FIGURE 33 - Effect of Annealing Temperature on the Grain Size and Ductility of B-66

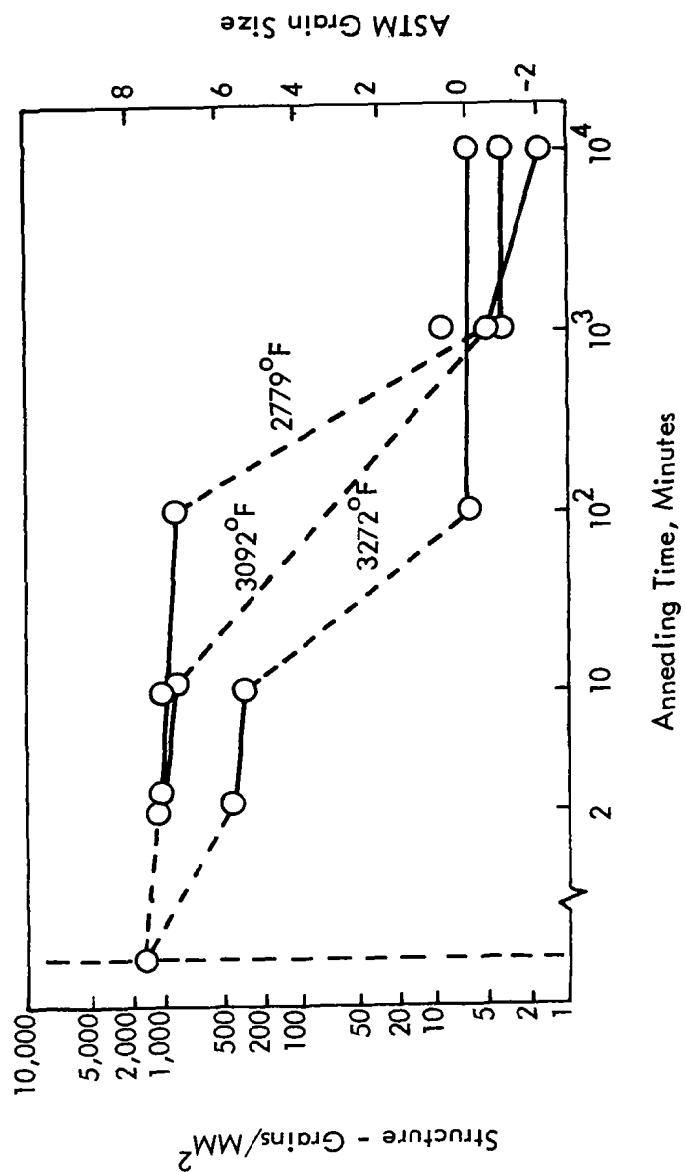


FIGURE 34 - Isothermal Discontinuous Grain Growth in Arc Cast Molybdenum (after J.H. Bechtold<sup>9</sup>)

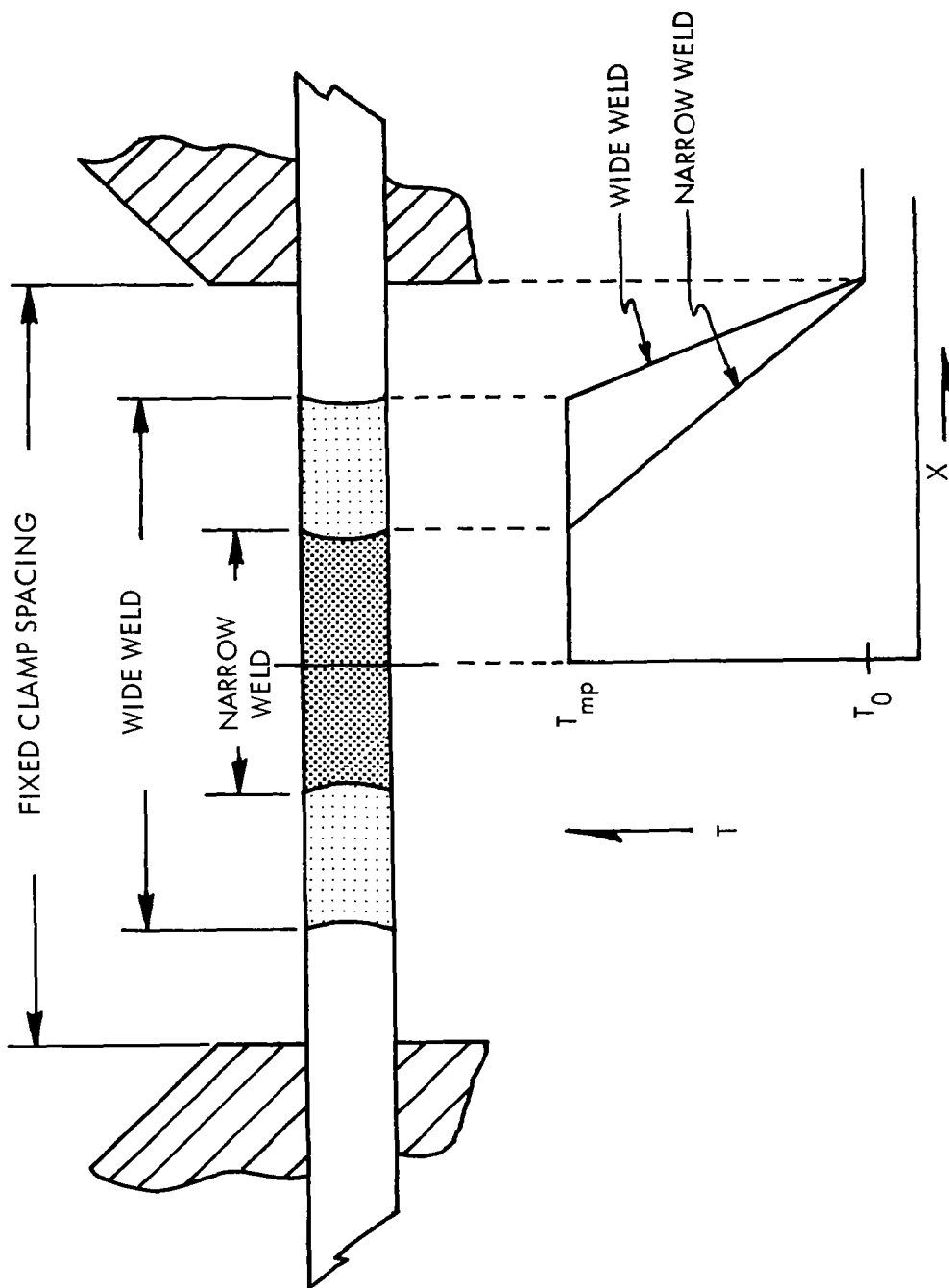


FIGURE 35 - Effect of Increased Weld Size in Reducing Heat Affected Zone Size and Increasing the Cooling Rate Through this Zone (i.e., Increased Transient Thermal Gradient During Temperature Peaking)

variation of weld induced time-temperature cycles. For this interpretation, a metallurgical appreciation of grain growth and size effects is required along with a mechanical concept of the thermal conditions during welding.

Increased grain size in refractory metal alloys generally results in an increase in ductile-to-brittle transition temperature. This is shown for B-66 in Figure 33. Hence, grain size is a reasonable indicator for following ductility responses. In solid solution alloys one would expect grain growth to be a continuous process. However, in alloys containing a dispersed second phase, grain growth may be a discontinuous process. This has been observed by Bechtold<sup>(9)</sup> in arc cast molybdenum, Figure 34. Exaggerated grain coarsening in molybdenum occurred simultaneously with the dissolution of large molybdenum carbide precipitates. This apparently caused unpinning of grain boundaries, and rapid grain coarsening. (Obviously, for this mechanism to occur the molybdenum cannot be considered strictly as "unalloyed".) The time-temperature dependence of discontinuous grain coarsening is also obvious in Figure 34.

Grain growth in the solid solution alloy, SCb-291, should be a continuous process. Hence, the continuous improved ductility occurring with decreased heat affected zone size, Figure 28, is a reasonable grain size effect. A mechanical concept for heat affected zone development is depicted in oversimplified form in Figure 35. A rough approximation of the maximum transient thermal gradients in the heat affected zones of small and large welds are shown. For larger welds the thermal gradient through the heat affected zone is larger and the width of this zone is smaller. Hence, heat affected zone size is decreased, with increasing weld size. Further, the cooling rate for large welds is faster resulting in less grain growth. The net result is a depression of heat affected zone development, and improved ductility, with increased weld size using fixed clamp spacing.

Using the same general line of reasoning a rationale<sup>1</sup> can also be developed for the threshold power input effect observed for the dispersion strengthened alloys. As indicated in the alloy discussion, strengthening in alloys containing reactive elements is achieved in part through the formation of stable precipitates. These are based on zirconium or hafnium reactions with residual interstitials, primarily oxygen and carbon. These precipitates enhance strength and stabilize grain size. A reasonable possibility of discontinuous grain growth as observed for molybdenum, Figure 34, exists in these systems. Hence, the threshold behavior represents a requirement for a critical heat input for dissolution of stable precipitates above which grain growth occurs rapidly. Metallurgical observations of structure and hardness in these systems support this position. Also, a distinguishing characteristic of electron beam welds is their significantly smaller heat affected zone or complete absence of grain growth in the heat affected zone. This is shown for FS-85 in Figure 36. This observation clearly fits the "threshold" concept as it applies to the observed behavior in Figure 29. This also agrees with a previous interpretation by Lessmann<sup>(8)</sup> attributing the difference in electron beam and tungsten-arc weld ductility to differences in heat affected zone development.

The behavior of the yttrium modified alloys lends further general support to this line of reasoning. Improved fabricability in alloys containing yttrium is generally attributed to grain refinement and stabilization caused by the presence of highly stable yttrium compound precipitates. The shift in "thermal" threshold from 3000 joules/in. for the yttrium-free alloys to 7000 joules/in for the yttrium modified alloys reflects increased grain stability.

Summary: Basic ductility of welds in columbium alloys is less than that of base metal. Variable degradation of ductility occurs depending on the selection of welding parameters. This variability depends primarily on the weld thermal cycles as measured by their influence on the heat affected zone. In this respect, thermal and mechanical factors combine to modulate or depress heat affected zone development. Differences between alloys seem to be related to probable differences in the kinetics of grain growth mechanisms. Although these considerations lend themselves to a rationalization of the observed data, grain size, per se, is probably not so important as the factors which influence grain growth (also substructure or cell size) phenomena. Hence, grain growth as used in this context is a



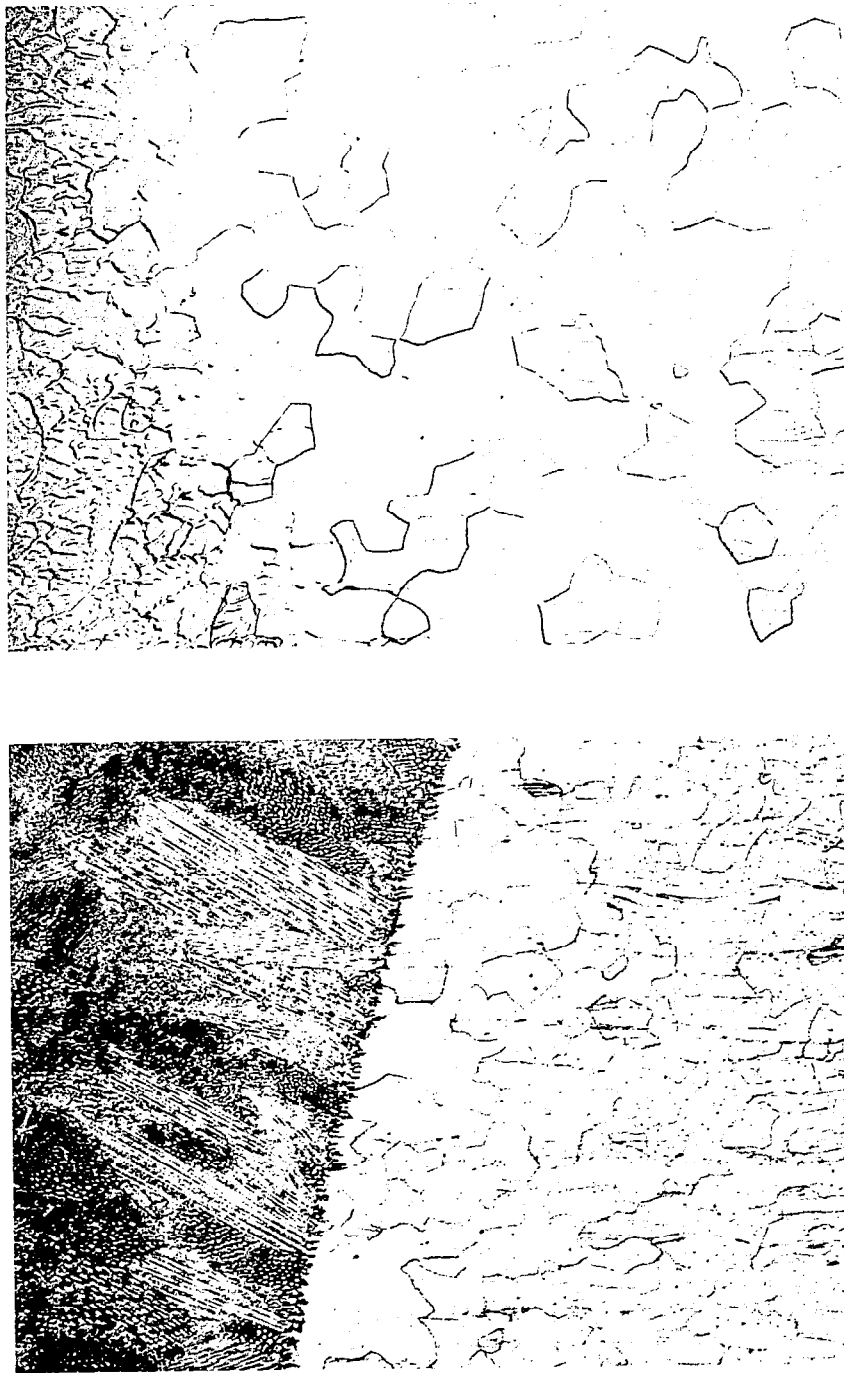


FIGURE 36 - Interface of Gas Tungsten Arc Weld (top) and Electron Beam Weld (bottom) in FS-85, showing Thermal Effects of Higher Arc Weld Heat Input: Increased Weld Cell Size, Heat Affected Zone Grain Growth, Heat Affected Zone Size, and Dissolution of Fine Precipitates Along Grain Structure in the Heat Affected Zone

metallurgical indicator. Metallographic observations demonstrate that grain boundaries at weld interfaces cross the interface. Hence, the influences of grain size or the factors reflected through grain growth are not confined to the heat affected zone but are also carried over into the weld. This is important since the bend data were rationalized on the basis of heat affected zone development while fractures frequently appeared to initiate in the cast weld structure. Just below the bend transition temperature, cracks usually propagated through both welds and heat affected zone with frequent arrests in the base metal. Hence, the time-temperature hypothesis based on heat affected zone development seems also to influence, perhaps indirectly, the ductility of the cast weld structure. This interplay of properties between cast metal and adjacent thermally disturbed base metal deserves further investigation as a general area of welding technology.

#### WELD POROSITY AND EDGE PREPARATION

An inspection of 30 welds of each alloy prepared for thermal stability studies indicated that a porosity problem existed in tungsten-arc butt welds made from sheared and pickled blanks of 0.035-inch sheet. Inspection results showing a comparison of alloy porosity sensitivity are summarized in Table 9. In this check severe porosity was found in D43 (D43Y) and moderate porosity (2-3 pores/in.) in C-129Y, Cb-752, and B-66. No porosity was noted in Ta-10W and only minor amounts in T-111, T-222, FS-85 and SCb-291.

Since this problem was of a variable but general nature, joint preparation and welding techniques were implicated. Further, the alloy-to-alloy variability indicated that porosity formation is also dependent on differences in innate alloy characteristics. The alloy differences are not readily defined, and could not be within the scope of this program. To circumvent this limitation, the most sensitive alloy, D-43, was employed to investigate this problem. This approach appeared rational since it was assumed that a solution to porosity in the worst alloy would be fully applicable to the others, and the worst alloy would provide the best indicator for process development.

The relative importance of joint preparation and welding procedures was easily determined by

TABLE 9. Gas Tungsten Arc Weld Porosity Count

Alloy	Pores/in. <sup>(1)</sup>
Ta -10W	0
T-222	0.034
T-111	0.051
FS85	0.092
SCb291	0.83
C129Y	2.0
B66	2.6
Cb752	2.9
D43	8.4
D43Y	8.0

(1) Based on approximately 15 feet of weld using optimum weld parameters based on bend ductility, except D-43Y for which the weld parameter series count is shown.

producing bead-on-plate welds. A check using D-43, D-43Y, C-129Y, Cb-752, and SCb-291 showed that bead-on plate welds contained no porosity. This demonstrated that butt joint preparation, not welding procedure, was the source of porosity.

Mechanical and chemical edge preparations were evaluated using D-43 sheet. These tests are summarized in the flow chart of Figure 37 while the respective pickling and rinsing procedures are listed in Table 10. The results, as determined by a porosity count are also shown in Figure 37.

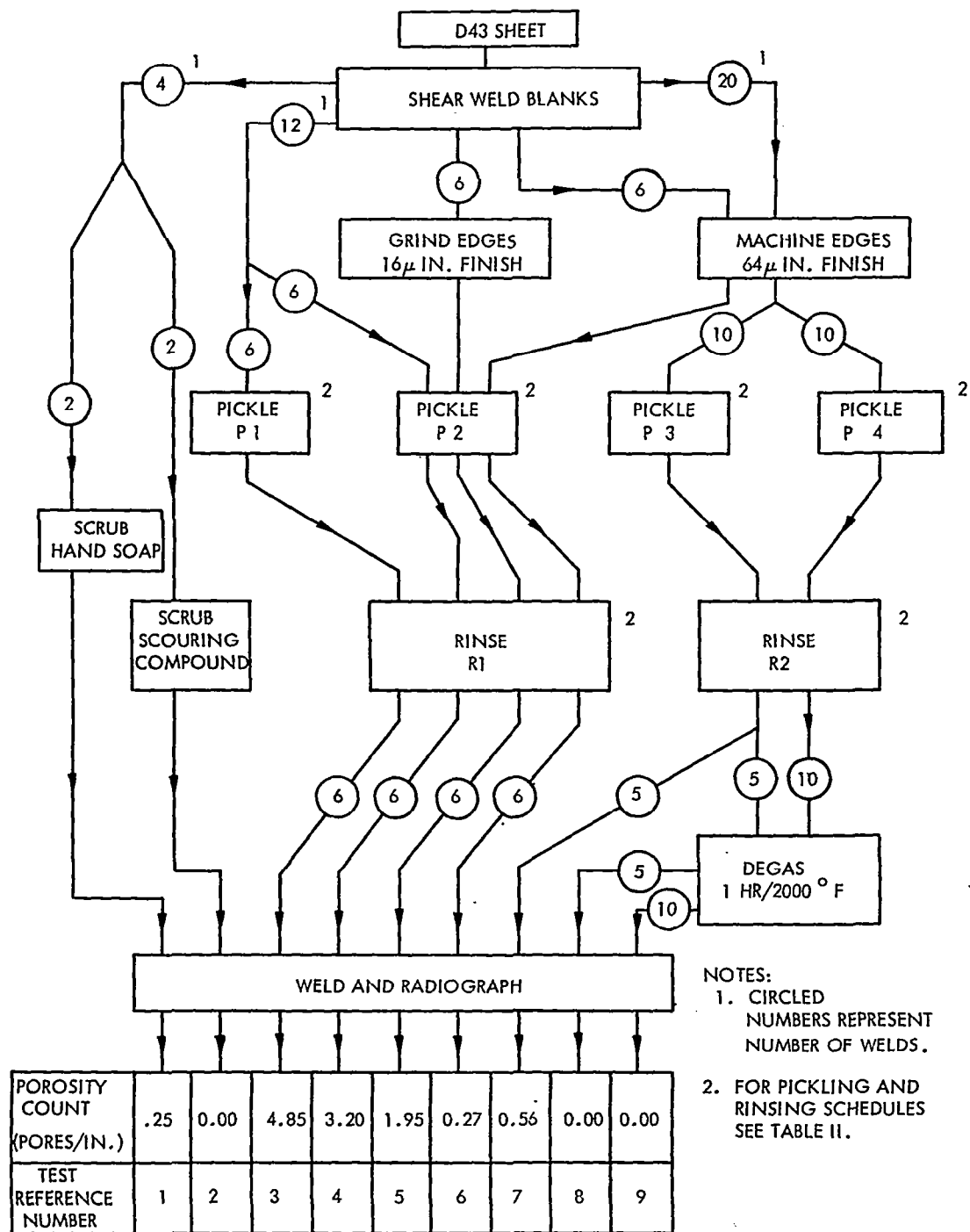


FIGURE 37 - Process Flow Diagram for Weld Porosity Evaluation of D-43

TABLE 10. Pickling and Rinsing Schedules for Weld Porosity Evaluation (See Figure 23)

	<u>Pickling Solution, v/o</u>
P1	25% $H_2NO_3$ , 25% HF, $H_2O$ balance
P2	20% $H_2NO_3$ , 15% HF, 10% $H_2SO_4$ , $H_2O$ balance
P3	25% $H_2NO_3$ , 8% HF, 25% $H_2SO_4$ , $H_2O$ balance
P4	25% $H_2NO_3$ , 15% HF, 25% $H_2SO_4$ , $H_2O$ balance
	<u>Rinsing Schedules</u>
R1	<ol style="list-style-type: none"> <li>1. Fast transfer from pickle bath to rinse</li> <li>2. 30-second boiling distilled water</li> <li>3. 1-minute flowing cold water rinse</li> <li>4. 5-minute boiling distilled water</li> <li>5. Ethyl alcohol rinse</li> <li>6. Hot air flash dry</li> </ol>
R2	<ol style="list-style-type: none"> <li>1. Fast transfer from pickle bath to rinse</li> <li>2. 10-minute rinse in cold flowing tap water</li> <li>3. 3-minute rinse in boiling distilled water</li> <li>4. Ethyl alcohol rinse</li> <li>5. Hot air flash dry</li> </ol>

Test number 4 (see Figure 37) represents the normal shear-pickle-rinse-weld sequence employed in the early phases of this program. The improvement in porosity over the thermal stability welds (3.2 per inch versus 8.4 per inch, see Table 9) probably resulted from greater care in rinsing. Interestingly, unpickled specimens, tests 1 and 2, using only sheared and scrubbed edges nearly eliminates porosity. Hence, pickling is essential for the formation of

porosity. Edge grinding, test 5, resulted in a measurable decrease in porosity. Machined edges, test 6, proved to be better than ground edges and reduced porosity to a level where it could well be overlooked in routine inspection. Among the pickling solutions those containing sulfuric acid proved superior. The rinsing procedures proved to be about equal. Porosity in pickled samples was eliminated only by vacuum baking prior to welding, tests 8 and 9.

The following conclusions were made based on this series of tests:

1. The direct cause of porosity was not identified but porosity appears to result from the degassing during welding of a pickling residue (or adsorbed hydrogen) from the surfaces of the joint interface.
2. Mechanical preparation is important to the extent of minimizing the joint interface surface area.
3. The difference between alloys probably also reflects a difference in joint interface area. The more fabricable alloys had less porosity in welds produced on sheared blanks. Apparently the more fabricable alloys had less edge tearing from shearing and, hence, less edge area and less porosity. With the exception of C-129Y, bend transition temperatures increase with increasing porosity sensitivity. Hence, porosity as measured in these tests, like bend ductility, is a measure of alloy fabricability.
4. For D-43, vacuum degassing of components following pickling and prior to welding is required to prevent porosity. The less sensitive alloys, particularly T-111, T-222, FS-85, Ta-10W, and SCb-291 should not require vacuum degassing while for the intermediate alloys Cb-752, B-66, and C-129Y, degassing is probably desirable.
5. Pickling solutions containing sulfuric acid proved advantageous. This indicates that fluoride residues, whose removal is enhanced by including sulfuric acid in the pickling solution, are at least partially responsible for the occurrence of porosity.

The results of these experiments provide guidelines for the edge preparation of these alloys. Naturally, specific refinements are probably required to optimize these procedures for any particular alloy. As demonstrated with D-43, optimization of joint preparation in the most

severe case requires vacuum degassing. This strongly implicates hydrogen as the source of weld porosity. Atomic hydrogen tends to be absorbed during pickling and, because of its low solubility at elevated temperatures, is released as gaseous hydrogen producing porosity. Hydrogen evolution observed by Stoner and Lessmann<sup>(12)</sup> during vacuum annealing of pickled refractory metals lends support to this conclusion. Pickling and welding did not result in a detectable hydrogen contamination. Ten welds were chemically analyzed and found to be essentially free of hydrogen. The highest value was 1.6 ppm while eight values were less than 1 ppm.

As a cross-check on the effect of edge preparation and welding procedures on weld ductility, bead-on-plate welds were made using parameters previously employed for butt welding and were bend tested. These tests indicated that edge preparation had no significant effect on ductility.

## POST WELD ANNEALING

The effect of post weld annealing on the weld ductility of the various alloys is shown for GTA welds in Figure 38 and for EB welds in Figure 39. Approximately 120 bend transition curves are summarized in these figures. This comparison of alloy behavior is based on longitudinal bend transition temperatures. Similar results were obtained for transverse bend testing and are therefore not shown. Broken curves are shown below the lowest annealing temperatures since annealing response in this range was not determined.

The 1 hour post weld annealing temperatures were selected in the stress relief-recrystallization range. Hence, the columbium alloys were annealed at 1900, 2200, and 2400°F, while the tantalum alloys were annealed at 2400, 2700, and 3000°F. Welding parameters which produced the lowest DBTT, as determined in the weld parameter study, were used in preparing welds for this evaluation. The selected weld parameters are listed in Table 11 along with the most beneficial post weld anneals identified in this study.

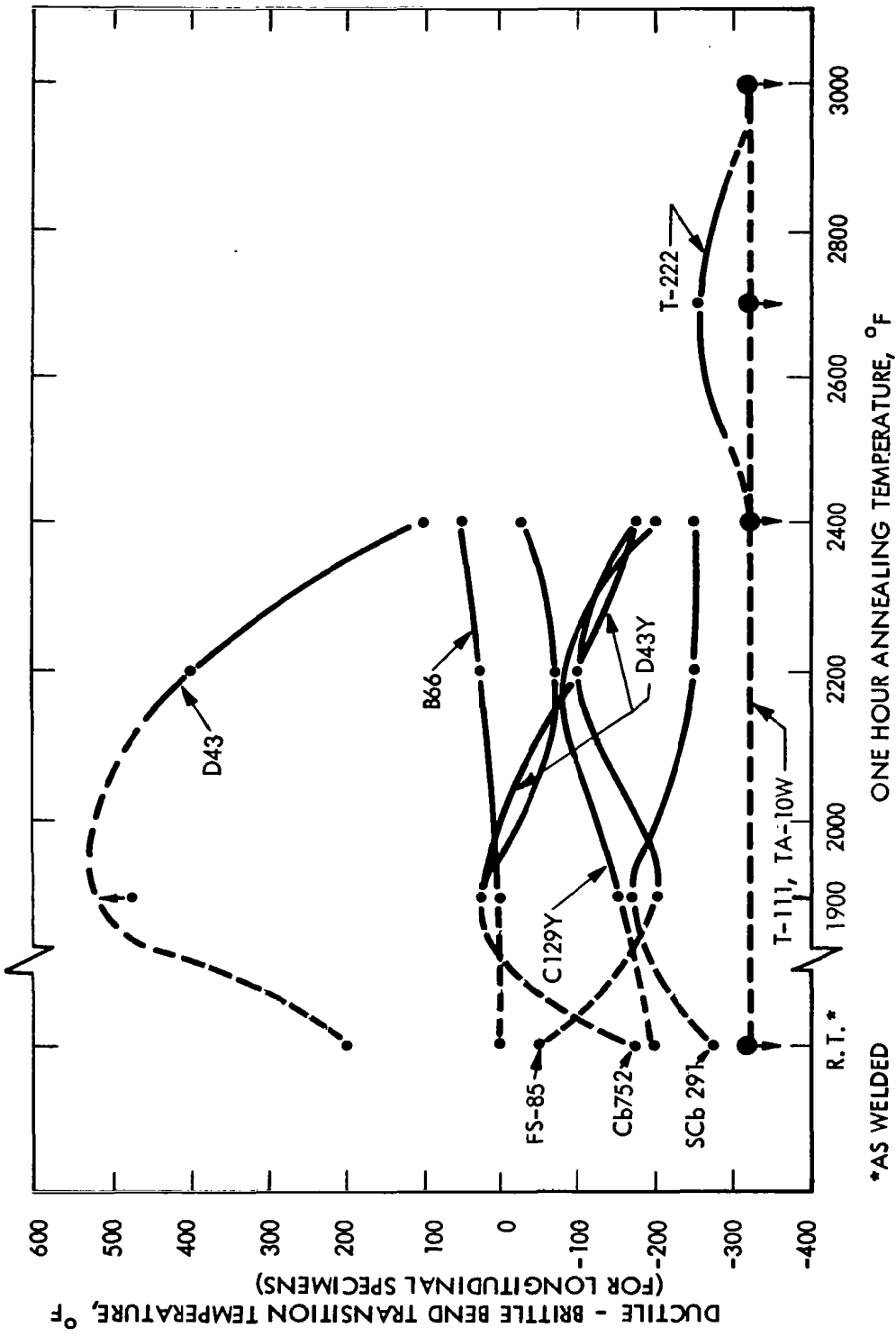


FIGURE 38 - Summary Showing the Effect of Annealing on GTA Weld Bend Ductility



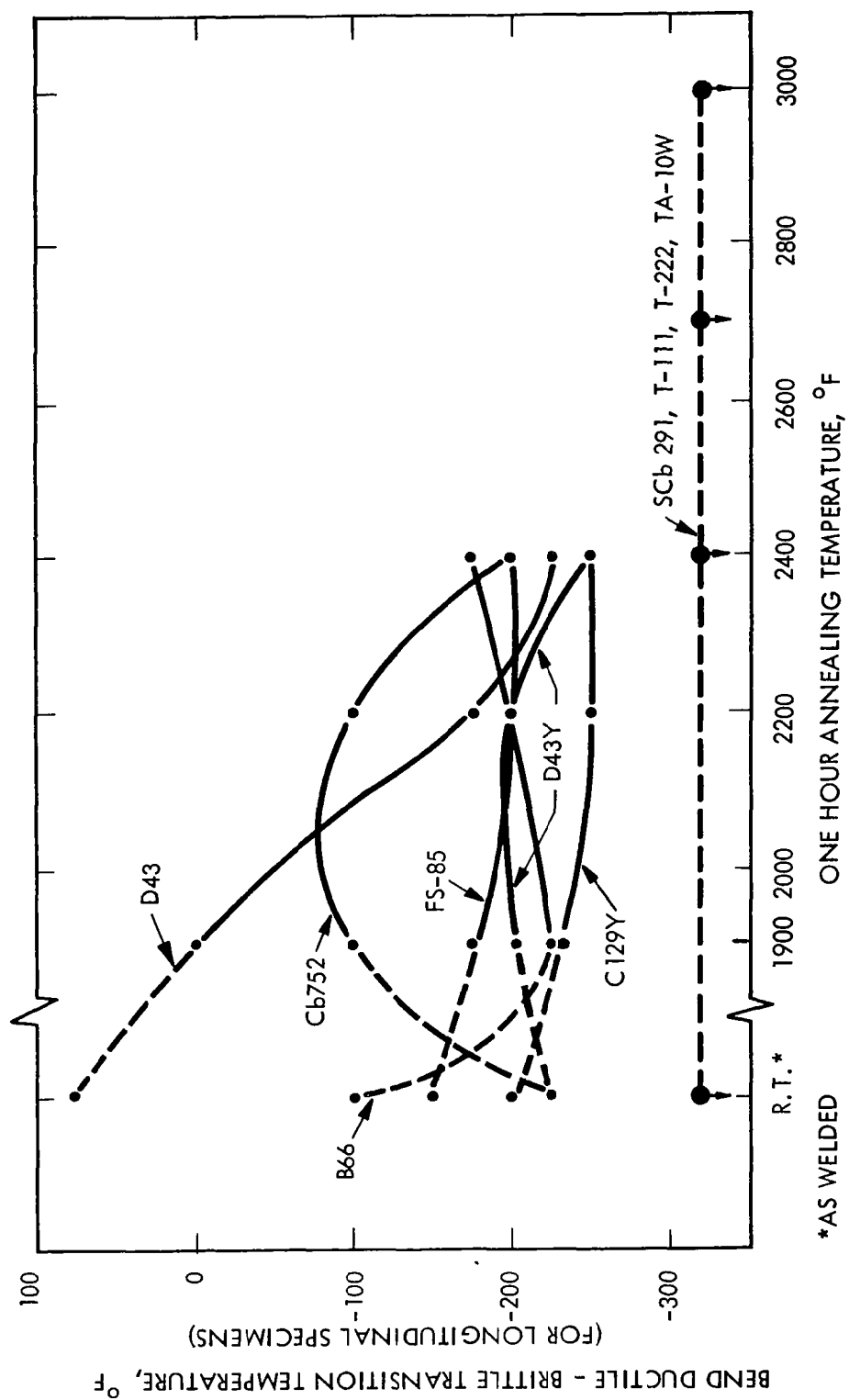


FIGURE 39 - Summary Showing the Effect of Annealing on EB Weld Bend Ductility

TABLE 11 - Optimized Weld Conditions for 0.035 Inch Sheet

Alloy	Process	Parameters (1)	One Hour Post Weld Anneal Temp., °F	Weld Width Top/Bottom (inches)	BDBTT, °F(2)	
					Long. Bends	Trans. Bends
Ta-10W	GTA	7.5-1/4-118	None	.190/.180	<-320	<-320
	EB	15-1/2-4.5	None	.049/.034	<-320	<-320
T-111	GTA	15-3/8-115	2400°F	.195/.189	<-320	<-320
	EB	15-1/2-3.8	2400°F	.038/.027	<-320	<-320
T-222	GTA	30-1/4-190	2400°F	.180/.159	<-320	<-320
	EB	15-1/2-3.8	2400°F	.039/.026	<-320	<-320
B-66	GTA	15-3/8-86	None	.190/.180	0	+75
	EB	25-3/16-3.2	1900°F	.036/.024	-225	-175
C-129Y	GTA	30-3/8-110	2400°F	.180/.130	-200	-225
	EB	50-1/2-4.1	2200°F	.040/.026	-250	-250
Cb-752	GTA	30-3/8-87	2200°F	.129/.090	-75	0
	EB	15-3/16-3.3	2400°F	.036/.017	-200	-200
D-43	GTA	30-3/8-114	2400°F	.159/.143	+100	0 <sup>(3)</sup>
	EB	50-1/2-4.4	2400°F	.040/.027	-225	-225
D-43Y	GTA	15-3/8-83	2400°F	.165/.150	-175	-250
	EB	50-1/2-4.0	2400°F	.036/.022	-250	<-300
FS-85	GTA	15-3/8-90	2400°F	.204/.195	-175	-175
	EB	50-3/16-4.4	2200°F	.038/.026	-200	-200
SCb-291	GTA	15-1/4-83	2200°F	.160/.150	-275	-275
	EB	50-1/2-4.4	None	.038/.027	<-320	-250

(1) For GTA Welds: Speed (ipm) - Clamp Spacing (in.) - Amperes  
 For EB Welds: Speed (ipm) - Clamp Spacing (in.) - Milliamperes  
 (All EB welds with 60~, 0.050 inch longitudinal deflection and  
 150 KV beam voltage)

(2) BDBTT ≈ Bend Ductile Brittle Transition Temperature at 1t Bend Radius Except  
 FS-85 EB Welds at 2t Bend Radius.

(3) Probable Value (Determined Value <-125°F)

Measurable responses to post weld annealing were noted for all the columbium alloys. GTA welds in D-43, Cb-752, C-129Y and SCb-291 appear to experience an age-overage response with increasing annealing temperature. All these tend to lose ductility at the lower annealing temperatures and recover at the higher temperature. D-43 demonstrated the most severe aging response. Interestingly, the yttrium modified material, D-43Y, merely improved in ductility with increased annealing temperature to the extent of nearly recovering base metal ductility after 1 hour at 2400°F. FS-85 GTA welds had a double aging response improving in ductility at 1900°F, aging at 2200°F and overaging at 2400°F. A similar response for FS-85 welds was previously observed.<sup>(13)</sup> B-66 GTA welds showed a 50°F increase in the DBTT which probably resulted primarily from grain growth. GTA welded tantalum alloys, except T-222 annealed at 2700°F, did not respond to aging with any apparent change in ductility.

Electron beam welds in columbium alloys did not generally display the age-overage response characteristic of the GTA welds. In this group, Figure 39, only Cb-752 had a marked age-overage response while D-43Y had a slight aging response. The other columbium alloys have improved annealed weld ductility while the tantalum alloys and SCb-291 EB welds were ductile below -320°F for all conditions.

## TENSILE EVALUATION

Tensile testing was used as a weldability screening tool to compare the tantalum and columbium alloys. In order of decreasing importance, this evaluation was based on joint efficiency, fracture mode, and strength. Joint efficiency is most tenable, providing a simple comparison of base and weld metal. Fracture behavior provides a qualitative comparison and an intuitive measure of performance in long life applications. Tensile strength was considered least important since it does not correlate with creep strength accurately enough to be used in alloy selection or system design. However, it does provide a means of categorizing alloys. All tensile specimens were prepared using optimum welding and post weld annealing schedules, Tables 7 and 11.

Joint Efficiencies. Excellent joint efficiencies were obtained through 2400°F as is apparent in Figures 40 and 41. Hence, all alloys satisfied the basic screening objective of this study. The joint efficiencies obtained are true metallurgical comparisons since weld contour effects were eliminated by grinding weld specimen surfaces.

Tensile Strength. Tensile strength provides an indication of the effectiveness of the strengthening mechanisms employed in these systems. Interestingly, there is not much variability in room temperature strength, Figure 40 and Table 12. This reflects a fabricability limitation since increased room temperature strength is usually achieved with a decrease in fabricability.

These materials were designed for high temperature strength which is summarized in Figures 41, 42, and 43. A tantalum alloy superiority in both strength and stability (rate of change of strength with increasing temperature) is apparent. Within alloy groups, alloys containing a reactive element (Zr or Hf) are stronger. Carbide strengthening proved particularly beneficial for D-43. Most of the columbium alloys lose uniqueness at 2400°F as demonstrated by a convergence of tensile strengths.

Tensile properties compared well with generally reported data. D-43 was about 6000 psi stronger than expected indicating a fairly optimum metallurgical condition was achieved in this strain-induced precipitation-hardened alloy. T-222 was weaker than expected probably because of a post weld anneal induced reaction similar to a 16 hour at 2000°F effect observed by Ammon, Filippi, and Harrod.<sup>(1)</sup> Cb-752 strength is perhaps 4000 psi less at 2000°F than obtainable through optimum duplex anneal processing.<sup>(10)</sup> Data for Ta-10W and SCb-291 were available only for stress-relieved material which is stronger than re-crystallized material.

The tendency for weld yield strengths to equal or exceed base yield strengths, Figure 42, reflects the fact that straining in transverse weld tests generally does not occur uniformly throughout the gage section. Hence, one cannot infer that true weld yield strengths greater than base metal strengths were realized. Similarly, a comparison of tensile elongation

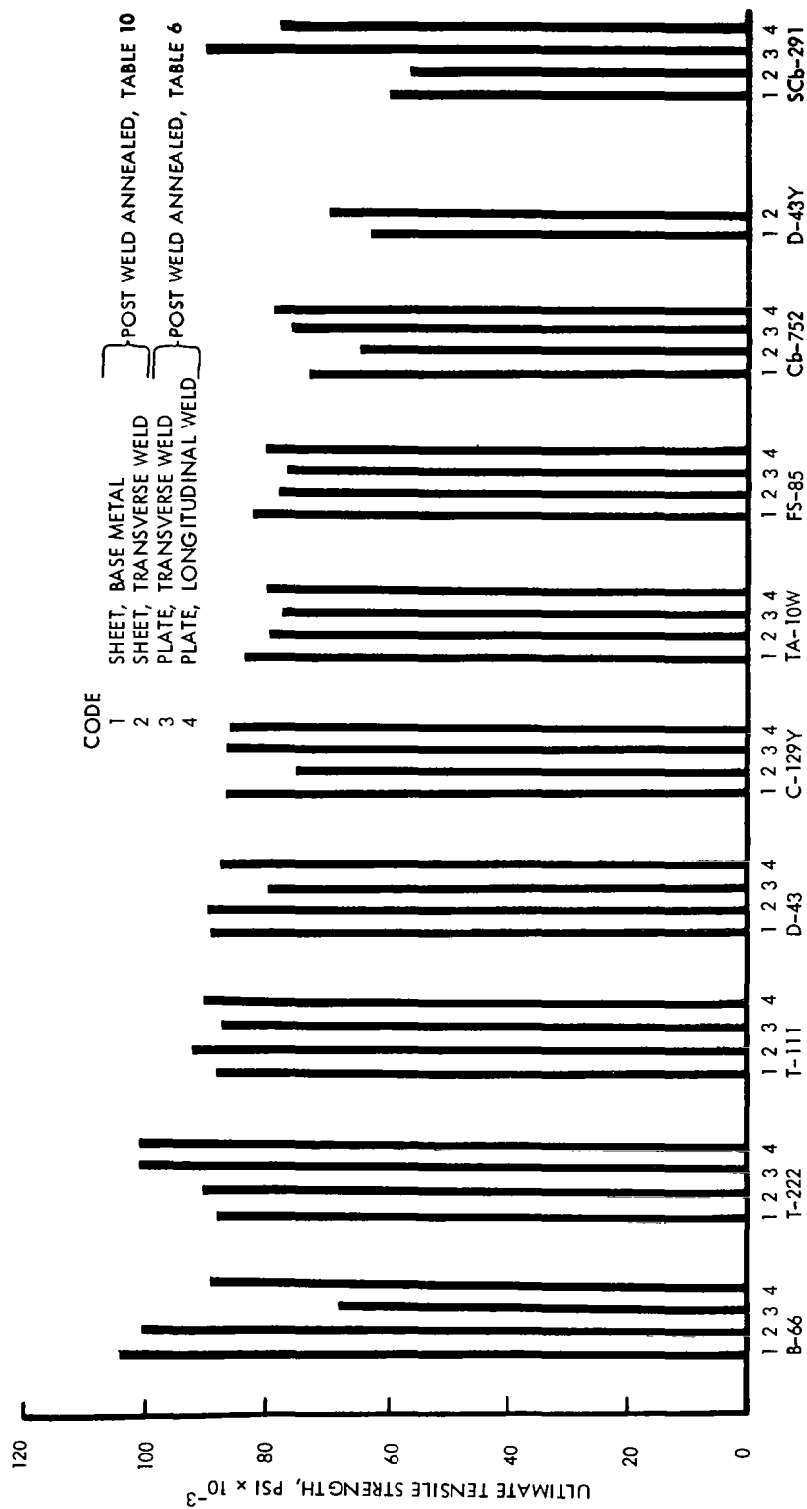


FIGURE 40 - Room Temperature Tensile Strength

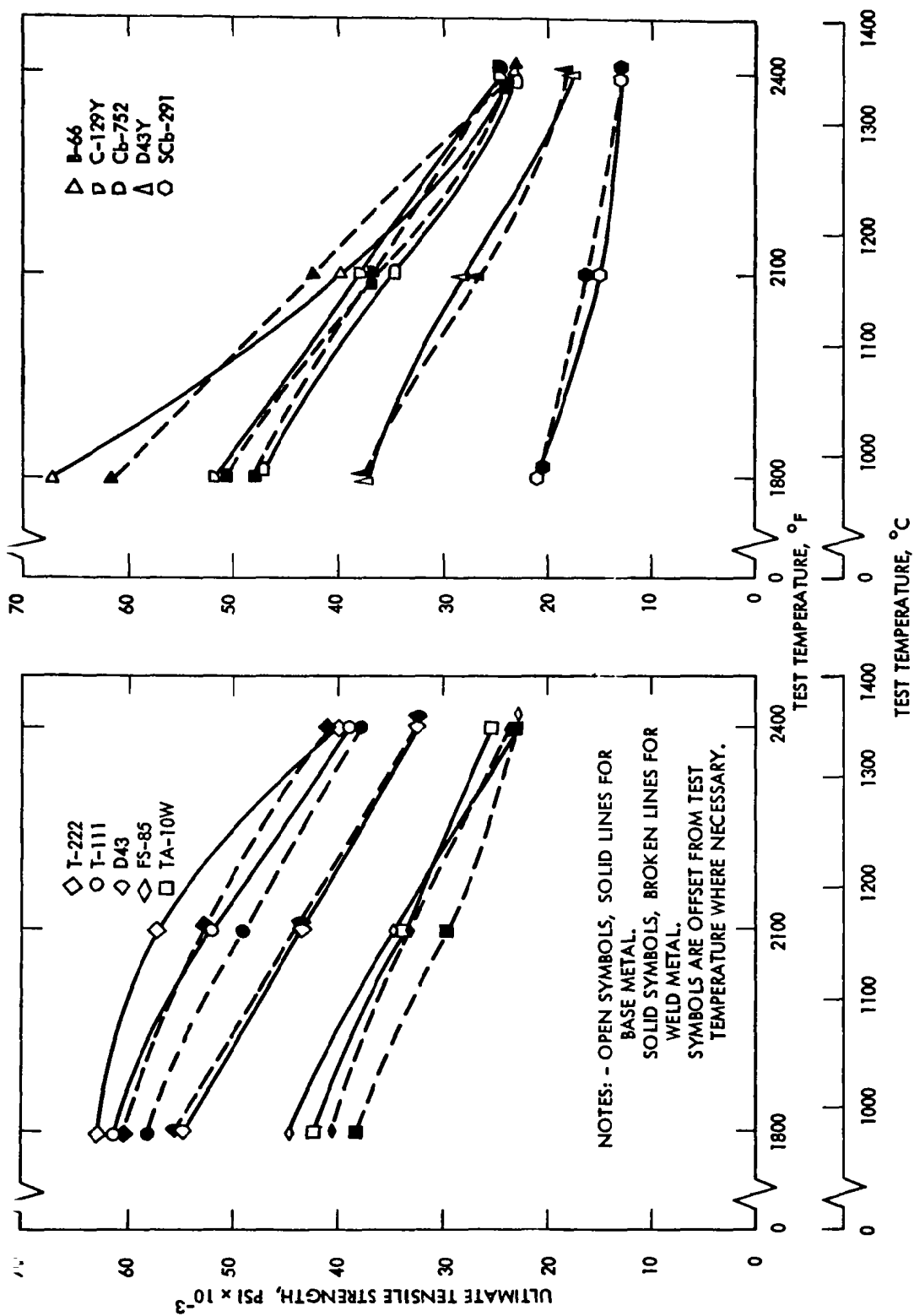


FIGURE 41 - Elevated Temperature Tensile Strength of Annealed Base Metal and Arc Welds.  
 Optimum Welding and Annealing Schedules Used, See Table 11.

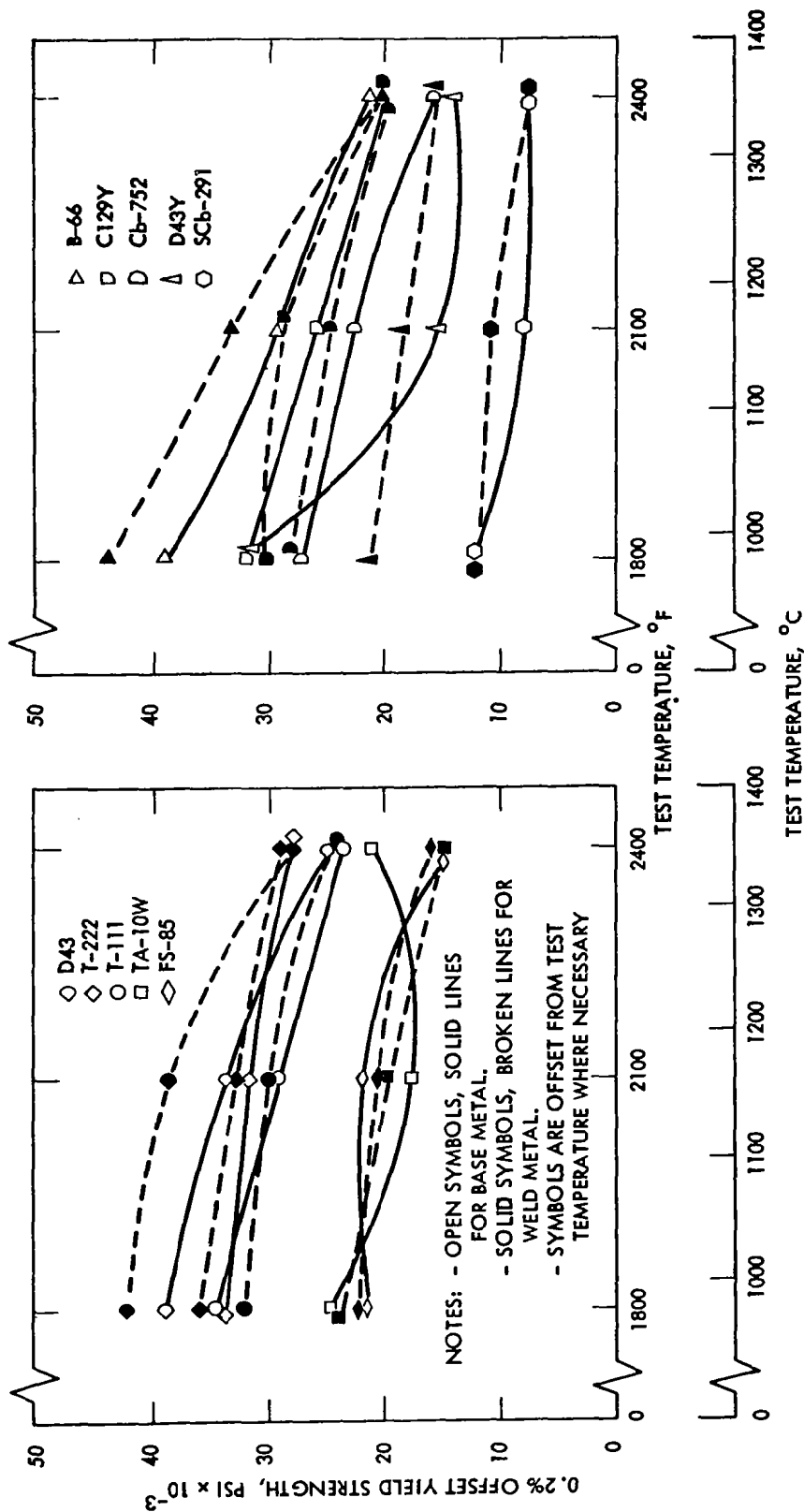


FIGURE 42 - Elevated Temperature Yield Strength of Annealed Base Metal and Arc Welds  
Optimum Welding and Annealing Schedules Used, See Table 11.

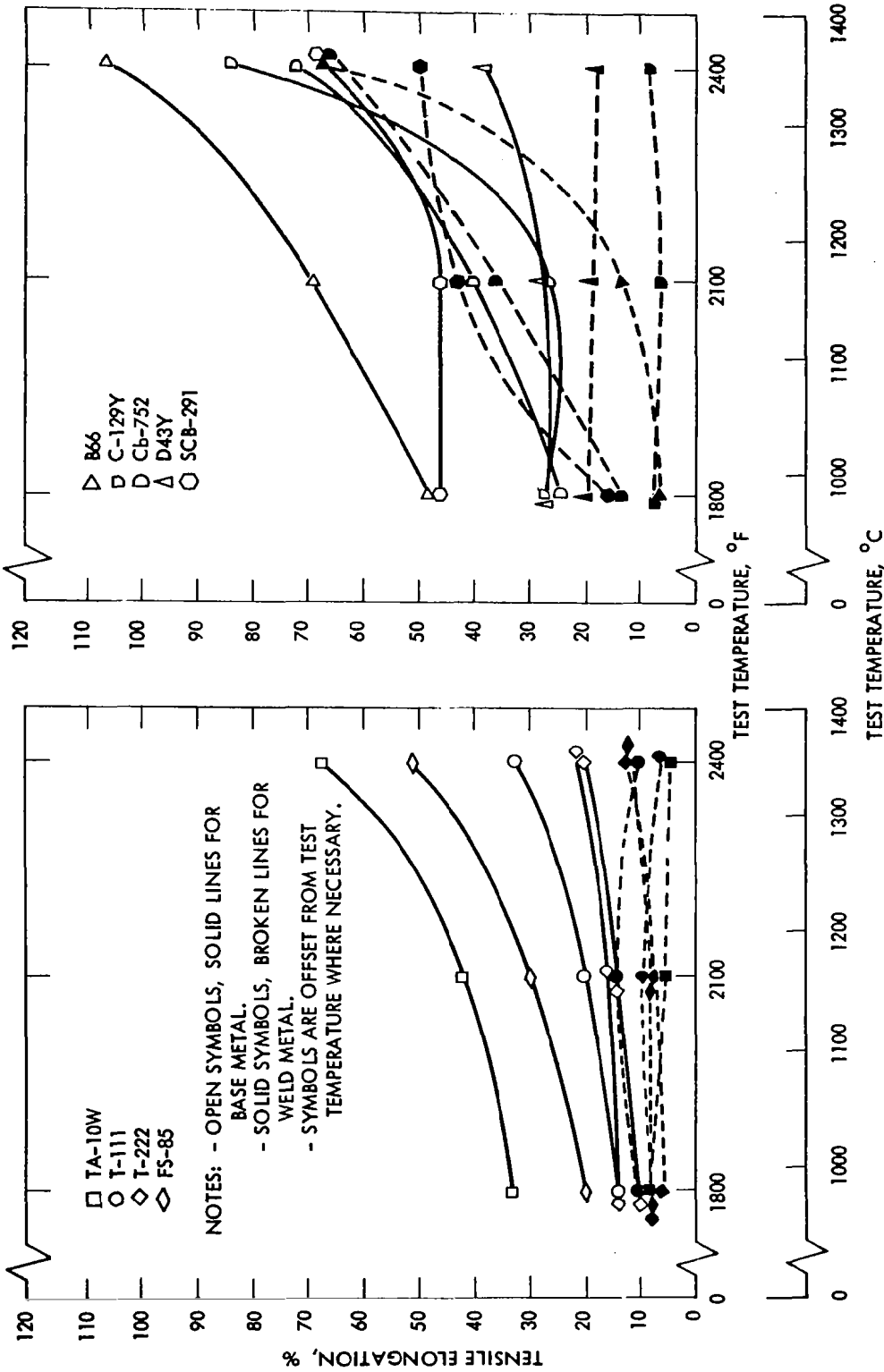


FIGURE 43 - Elevated Temperature Tensile Elongation of Annealed Base Metal and Arc Welds.  
Optimum Welding and Annealing Schedules Used, See Table 11.



TABLE 12 - Room Temperature Tensile Properties for Welded Plate

Alloy	Type	1 Hr. Post Weld Anneal Temp. (°F)	0.2% Offset Yield Pt. psi x 10 <sup>-3</sup>	Ultimate Stress psi x 10 <sup>-3</sup>	R.A. (%)	Elongation (%)	Fracture Location
T-111	Trans.	2400	73.70	86.99	76.0	17.4	Weld
T-111	Long.	2400	76.20	89.85	64.7	22.3	--
Ta-10W	Trans.	None	61.16	77.71	82.2	21.9	Weld
Ta-10W	Long.	None	65.85	81.30	70.0	24.3	--
T-222	Trans.	2400	88.21	101.01	74.4	18.7	Weld
T-222	Long.	2400	87.99	100.74	68.3	21.9	--
B-66	Trans.	1900	(1)	68.36	0.0	0.0	Weld
B-66	Long.	1900	77.79	88.81	2.6	6.6	--
D-43	Trans.	2400	59.40	79.74	70.7	5.2	Weld
D-43	Long.	2400	54.86	88.22	28.7	17.4	--
FS-85	Trans.	2400	60.21	76.72	9.7	9.4	Weld
FS-85	Long.	2400	61.81	79.82	66.6	21.0	--
Cb-752	Trans.	2200	56.32	75.90	79.7	24.9	Base
Cb-752	Long.	2200	61.00	79.30	46.2	20.7	--
SCb-291	Trans.	1900	47.03	62.70	88.9	22.5	Weld
SCb-291	Long.	1900	46.86	62.47	77.5	21.2	--
C-129Y	Trans.	2400	70.07	87.38	16.9	12.7	Weld
C-129Y	Long.	2400	68.10	86.90	44.7	22.0	--

(1) Brittle Fracture

behavior, Figure 43, is not meaningful except when interpreted in terms of fracture mode as is done below.

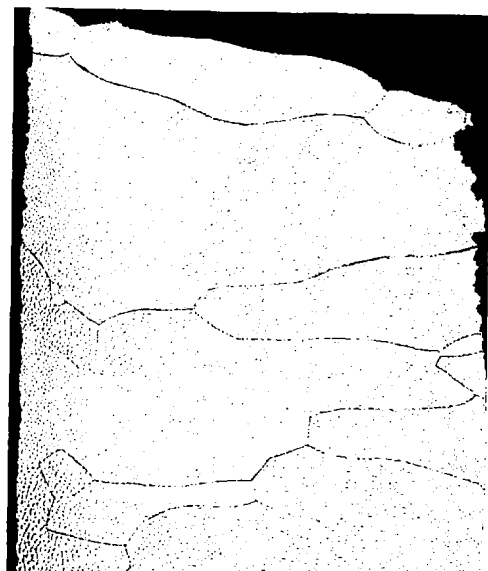
Tensile Deformation and Fracture. Transverse sheet weld specimens generally failed in the welds except for D-43Y, which failed only in base metal, and the alloys B-66, Cb-752, and 5Cb-291 which had base failures at 2100°F and 2400°F.

At room temperature failures occurred by ductile shear although welds in the stronger columbium alloys, particularly in B-66, and to some extent D-43 and FS-85, had partial cleavage fractures. As a total exception, the B-66 plate welds failed by brittle cleavage.

The ductile shear fracture behavior persists for all alloys to 1800°F. Between 1800°F and 2400°F a transition in fracture mode occurs. Significant differences in alloy fracture behavior occur in this transition region. These differences can be interpreted in terms of the effect of grain size (as a measure of unit volume grain boundary area), structural stability (recrystallization), and relative matrix-grain boundary strengths. For high temperature application, the role of grain boundaries in deformation and fracture is particularly important as has been indicated by Begley and Godshall.<sup>(11)</sup>

Alloys were categorized in three groups based on the observed elevated temperature transition behavior. This approach provided a further insight into the effectiveness of the strengthening processes operative in these alloys. These groups are discussed below in an intuitive order of decreasing effectiveness for long life application.

The first category is comprised of the tantalum based alloys and the stronger columbium alloys, FS-85 and D-43. These alloys had well balanced matrix and grain boundary strength throughout the test temperature range. Base metal specimens failed primarily by ductile shear. Weld specimens failed in the welds by ductile shear through 1800°F but by grain boundary separation at 2400°F. Weld grain size and orientation were most important in 2400°F fracture behavior, Figure 44. The solid solution alloy Ta-10W, having the largest weld grain size, is seen to have failed at low total strain in wide grain boundaries spanning nearly the entire specimen



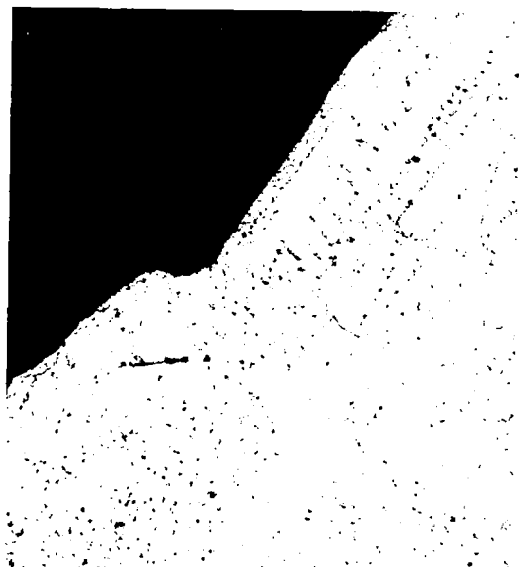
Ta-10W

80X



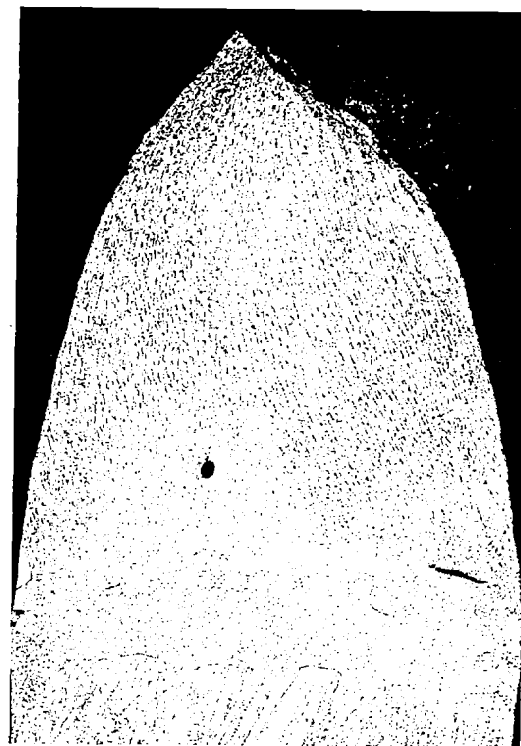
T-111

100X



D-43

200X



T-222

80X

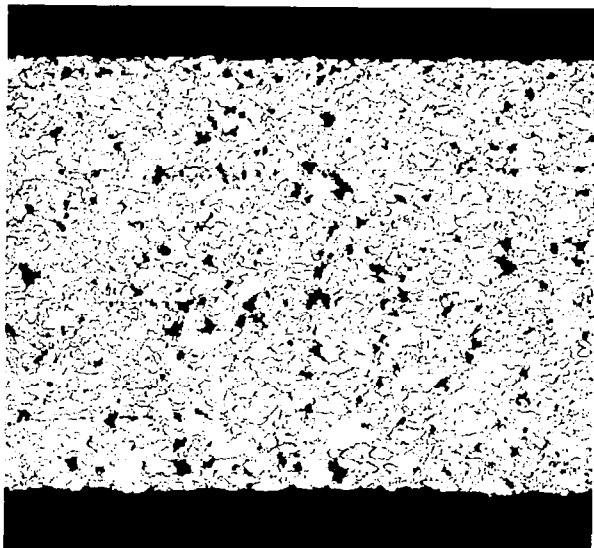
Tensile  
Direction

FIGURE 44 - Fracture Characteristics of Typical Welds in Tantalum Alloys and the Highest Strength Columbium Alloys ( e.g. FS-85 and D-43 ). Lower Right: Typical 2100°F Ductile Shear Fracture. Others: Failure by Grain Boundary Sliding at 2400°F. ( All Base Metal Specimens Failed by Ductile

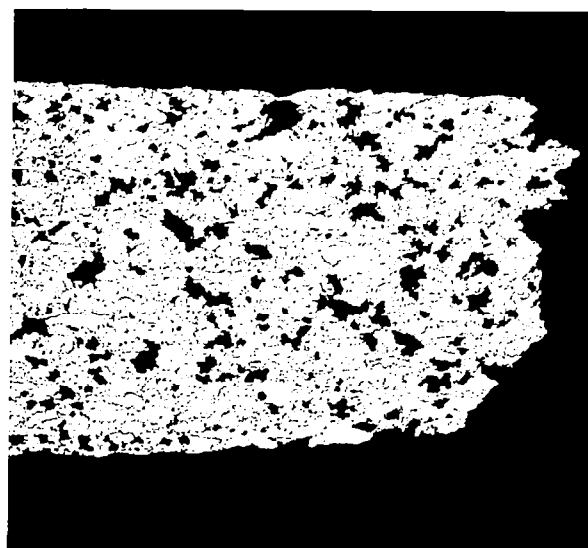
thickness. The large grain size of Ta-10W welds probably results from a narrow freezing range and single phase structure since this is typical of that observed in unalloyed refractory metals. The other alloys failed largely in grain boundaries oriented in the direction of maximum resolved shear stress as shown clearly for D-43. Because of the orientation preference, fracture location was often near the weld edge where grain boundary orientations were favorable. The localized yielding in weld failures accounts for the low weld elongations. The disparity between base and weld elongation which tends to increase with temperature results from the weld transition to grain boundary failures.

The second category is comprised of the yttrium modified alloys C-129Y and D-43Y. These were characterized by a poorer balance of grain boundary versus matrix strength and a stable, more refined grain size. Grain boundaries are relatively weak in yttrium containing alloys. The failure mode shifted rapidly with increasing test temperature from ductile shear to grain boundary sliding. Extensive bulk grain boundary separation occurred at higher temperatures in the fine grained base metal. This resulted in a very large and rapidly increasing total elongation. Considerably less elongation was noted for welds presumably because of localized yielding and increased grain sizes in the C-129Y specimens which failed in the weld, and presumably because of the localized base metal failures occurring in D-43Y. Typical failure modes for these are evident in the structures shown in Figure 45.

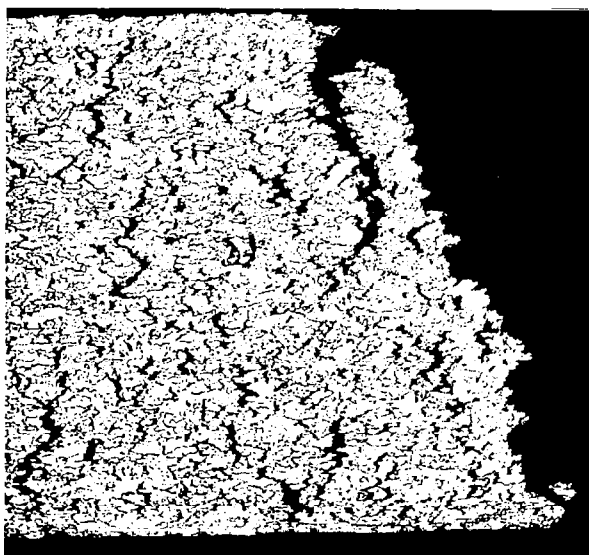
The third category is comprised of those alloys which have less stable grain structures and tend to recrystallize during elevated temperature testing. Because of the resultant grain boundary mobility these do not display a pronounced shift to grain boundary fracture at 2400°F. They fail primarily in the base metal with very little flow resistance in either matrix or grain boundaries as evidenced by high elongation. The columbium alloys B-66, Cb-752, and SCb-291 fall in this category. Fracture structures are shown in Figure 46. The B-66 failure is somewhat mixed-mode displaying grain boundary separation.



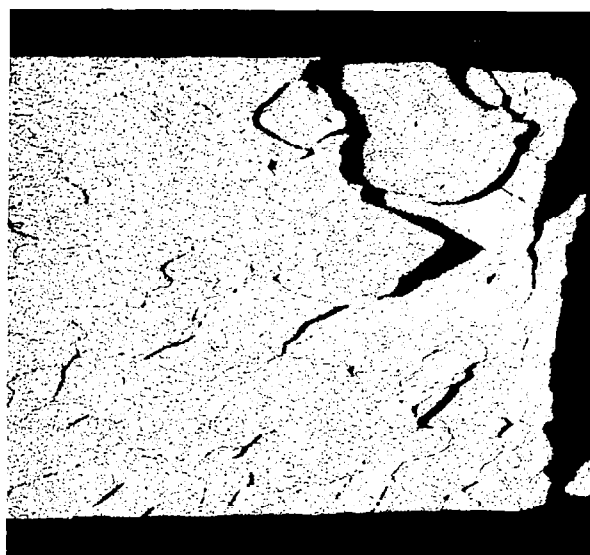
C-129Y Base Metal General Area at 100X



C-129Y Base Metal Fracture at 100X



C-129Y Weld Fracture at 80X



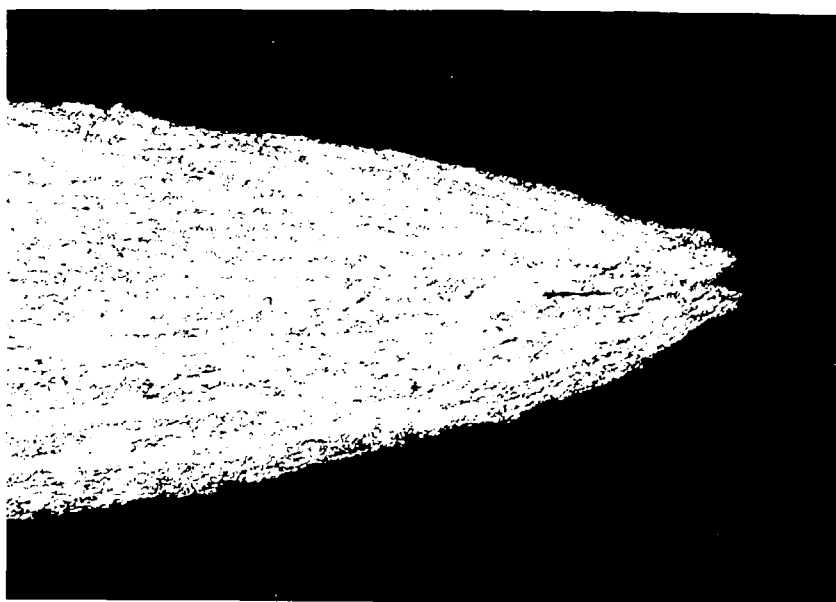
D-43Y Base Metal Fracture at 100X

FIGURE 45 - Fracture Characteristics of Yttrium Modified Alloys Tensile Tested at 2400°F. Fracture by Grain Boundary Separation. (D-43Y Weld Specimens Failed in the Base Metal Without any Indication of Incipient Weld Failures.)



B-66

200X



Cb-752

200X

FIGURE 46 - Base Metal Fractures for B-66 (top) and Cb-752 (bottom) Tensile Tested at 2400°F

## REFERENCES

1. R. L. Ammon, A. Filippi, D. L. Harrod, "Pilot Production and Evaluation of Tantalum Alloy Sheet", Summary Phase Report, Part III, WANL-PR-M-014, Westinghouse Astronuclear Laboratory, August 15, 1965.
2. F. Ostermann and F. Bollenrath, "On the Precipitation Behavior of Niobium Alloy D-43," Paper No. 22, 6th Plansee Seminar, 1968 (June), Vol. 1 Preprints.
3. A. Taylor, W. M. Hickam, and N. J. Doyle, "Solid Solubility Limits of Y and Sc in the Elements W, Ta, Mo, Nb and Cr", February 1965, Contract AF 33(616)-8315, Westinghouse Research Laboratories.
4. C. E. Carlson and E. J. Delgrosso, "Utilization of Yttrium in Gettering Oxygen and Nitrogen in Columbium Base Materials", Pratt and Whitney Aircraft, Contract AT(30-1)2789, PWAC-441, June 24, 1965.
5. D. R. Stoner and G. G. Lessmann, "Measurement and Control of Weld Chamber Atmospheres" Welding Journal Research Supplement, 44(8), 337-S to 346-S, August 1965.
6. G. G. Lessmann and D. R. Stoner, "Welding Refractory Metal Alloys for Space Power System Applications", Ninth National SAMPE Symposium on Joining of Materials for Aerospace Systems, November 15-17, 1965. Westinghouse Astronuclear Laboratory, WANL-SP-009.
7. R. H. Titran and R. W. Hall, "Ultrahigh-Vacuum Creep Behavior of Columbium and Tantalum Alloys at 2000°F and 2200°F for Times Greater than 1000 Hours", NASA TM-X-52130, 1965.
8. G. G. Lessmann, "Welding Evaluation of Experimental Columbium Alloys", The Welding Journal Research Supplement, Vol. 29 (3) March 1964.
9. J. H. Bechtold, Trans. Amer. Soc. Metals 46 (1954) 1449.
10. J. G. Bewley, "Strengthening of Columbium Alloy Cb-752 by Duplex-Annealing Process", Stellite Division, Union Carbide Corporation, 1965.
11. R. T. Begley, J. Godshall, "Some Observations on the Role of Grain Boundaries in High Temperature Deformation and Fracture of Refractory Metals", presented at the AIME Symposium on the Physical Metallurgy of Refractory Metals, French Lick, Indiana, Oct. 3-5, 1965. Westinghouse Astronuclear Laboratory, WANL-SP-012, January 15, 1966.
12. D. R. Stoner and G. G. Lessmann, "Operation of a  $10^{-10}$  Torr Vacuum Heat Treating Furnace in Routine Processing", WANL-SP-010. Presented at the 8th Annual Conference on Vacuum Metallurgy, January 21-23, 1965, New York.
13. R.A. Nadler, "Processing and Evaluation of Pre-Production Quantities of Columbium Alloy Sheet," Final Report, Bureau of Naval Weapons, Contract N600(19)-59546, Westinghouse Electric Corporation, Materials Manufacturing Division, January 20, 1964.

## APPENDIX, PROGRAM DATA COMPILATION

### LIST OF FIGURES AND TABLES

<u>Figure No.</u>	<u>Table No.</u>	<u>Title</u>	<u>Page</u>
A1	--	Key for Presentation of Bend Test Data	106
		<u>T-111 PROGRAM TEST DATA</u>	
A2	--	As-Received Microstructure of T-111	107
--	A1	T-111 Sheet GTA Butt Weld Record	108
A3	--	Bend Test Results for T-111 GTA Welds	109
A4	--	Bend Test Results for T-111 GTA Welds	110
--	A2	T-111 Sheet EB Butt Weld Record	111
A5	--	Bend Test Results for T-111 EB Welds	112
A6	--	Bend Test Results for T-111 EB Welds	113
A7	--	Effect of Post-Weld Annealing on T-111 Sheet Weld Ductility	114
A8	--	Hardness Traverses, T-111 GTA Sheet Butt Welds	115
A9	--	T-111 As-Welded Microstructure for GTA Sheet Butt Welds	116
A10	--	T-111 As-Welded Microstructure for GTA Sheet Butt Welds	117
A11	--	Post-Weld Annealed T-111 GTA Sheet Butt Weld Microstructure	118
A12	--	T-111 EB Sheet Butt Weld Microstructure	119
A13	--	T-111 Plate Weld, As-Welded	120
A14	--	T-111 Plate Weld, Annealed One Hour at 2400°F	121
		<u>T-222 PROGRAM TEST DATA</u>	
A15	--	As-Received Microstructure of T-222	122
--	A3	T-222 Sheet GTA Butt Weld Record	123
A16	--	Bent Test Results for T-222 GTA Welds	124



<u>Figure No.</u>	<u>Table No.</u>	<u>Title</u>	<u>Page</u>
A17	--	Bent Test Results for T-222 GTA Welds	125
--	A4	T-222 Sheet EB Butt Weld Record	126
A18	--	Bend Test Results for T-222 EB Welds	127
A19	--	Bend Test Results for T-222 EB Welds	128
A20	--	Effect of Post-Weld Annealing on T-222 Weld Ductility	129
A21	--	Hardness Traverses, T-222 GTA Sheet Butt Welds	130
A22	--	T-222 As-Welded Sheet Butt Weld Microstructure	131
A23	--	Post-Weld Annealed T-222 GTA Weld Microstructure	132
A24	--	Post-Weld Annealed T-222 EB Weld Microstructure	133
A25	--	Post-Weld Annealed T-222 EB Weld Microstructure	134
A26	--	T-222 Plate Weld Hardness Traverse	135
A27	--	T-222 Plate Weld Annealed One Hour at 2400°F	136

#### Ta-10W PROGRAM TEST DATA

A28	--	As-Received Microstructure of Ta-10W	137
--	A5	Ta-10W Sheet, GTA Butt Weld Record	138
A29	--	Bend Test Results for Ta-10W GTA Welds	139
A30	--	Bend Test Results for Ta-10W GTA Welds	140
--	A6	Ta-10W Sheet EB Butt Weld Record	141
A31	--	Bend Test Results for Ta-10W EB Welds	142
A32	--	Bend Test Results for Ta-10W EB Welds	143
A33	--	Effect of Post-Weld Annealing on Ta-10W Sheet Weld Ductility	144
A34	--	Hardness Traverses in Ta-10W GTA Sheet Butt Welds	145

<u>Figure No.</u>	<u>Table No.</u>	<u>Title</u>	<u>Page</u>
A35	--	Ta-10W Sheet Weld Microstructure	146
A36	--	Post-Weld Annealed Ta-10W Weld Microstructure	147
A37	--	Ta-10W Weldability Qualification Tests	148
A38	--	Ta-10W Plate Weld Hardness Traverse	149
<u>FS-85 PROGRAM TEST DATA</u>			
A39	--	As-Received Microstructure of FS-85	150
A40	--	FS-85 Sheet Base Metal Bend Test Results	151
--	A7	FS-85 Sheet, GTA Butt Weld Record	152
A41	--	Bend Test Results for FS-85 GTA Welds	153
A42	--	Bend Test Results for FS-85 GTA Welds	154
--	A8	FS-85 Sheet, EB Butt Weld Record	155
A43	--	Bend Test Results for FS-85 EB Welds	156
A44	--	Bend Test Results for FS-85 EB Welds	157
A45	--	Effect of Post-Weld Annealing on FS-85 Weld Ductility	158
A46	--	Hardness Traverses of FS-85 Sheet GTA Butt Welds	159
A47	--	FS-85 GTA Sheet Weld Microstructure	160
A48	--	FS-85 GTA Sheet Weld Microstructure	161
A49	--	FS-85 Plate Weld Macrosection	162
A50	--	FS-85 Plate Weld Bend Specimens	163
A51	--	FS-85 Welded Plate Microstructure	164
A52	--	FS-85 Plate Weld Hardness Traverse	165
A53	--	FS-85 Plate Weld Hardness Traverse	166

<u>Figure No.</u>	<u>Table No.</u>	<u>Title</u>	<u>Page</u>
<u>AS-55 PROGRAM TEST DATA</u>			
A54	--	As-Received Microstructure of AS-55 Sheet	167
--	A9	AS-55 Sheet GTA Weld Record	168
A55	--	Bend Test Results for AS-55 GTA Welds	169
A56	--	Bend Test Results for AS-55 GTA Welds	170
--	A10	AS-55 Sheet, EB Weld Record	171
A57	--	Bend Test Results for AS-55 EB Welds	172
A58	--	Bend Test Results for AS-55 EB Welds	173
A59	--	AS-55 Sheet Butt Weld	174
A60	--	AS-55 GTA Sheet Weld Microstructure	175
A61	--	Hardness Traverses of AS-55 GTA Sheet Butt Welds	176
<u>B-66 PROGRAM TEST DATA</u>			
A62	--	As-Received Microstructure of B-66	177
A63	--	B-66 Base Metal Bend Test Results	178
--	A11	B-66 Sheet, GTA Butt Weld Record	179
A64	--	Bend Test Results for B-66 GTA Welds	180
A65	--	Bend Test Results for B-66 GTA Welds	181
--	A12	B-66 Sheet EB Butt Weld Record	182
A66	--	Bend Test Results for B-66 EB Welds	183
A67	--	Bend Test Results for B-66 EB Welds	184
A68	--	Effect of Post-Weld Annealing on B-66 Sheet Weld Ductility	185
A69	--	Hardness Traverse, B-66 GTA Sheet Butt Weld	186

<u>Figure No.</u>	<u>Table No.</u>	<u>Title</u>	<u>Page</u>
A70	--	B-66 Sheet Butt Weld Microstructure	187
A71	--	B-66 Plate Weld Microstructure	188
A72	--	B-66 Plate Weld Hardness Traverse	189
A73	--	B-66 Plate Weld Hardness Traverse	190
A74	--	B-66 Plate Weld Bend Specimens	191
 <u>C-129Y PROGRAM TEST DATA</u>			
A75	--	As-Received Microstructure of C-129Y	192
--	A13	C-129Y Sheet GTA Butt Weld Record	193
A76	--	Bend Test Results for C-129Y GTA Welds	194
A77	--	Bend Test Results for C-129Y GTA Welds	195
--	A14	C-129Y Sheet EB Butt Weld Record	196
A78	--	Bend Test Results for C-129Y EB Welds	197
A79	--	Bend Test Results for C-129Y EB Welds	198
A80	--	Effect of Post-Weld Annealing on C-129Y Sheet Weld Ductility	199
A81	--	Hardness Traverses on C-129Y GTA Sheet Butt Welds	200
A82	--	C-129Y Sheet Butt Weld Microstructure	201
A83	--	C-129Y Plate Weld Hardness Traverses	202
A84	--	C-129Y Plate Weld Hardness Traverses	203
A85	--	C-129Y Plate Weld Bend Specimens	204
 <u>Cb-752 PROGRAM TEST DATA</u>			
A86	--	As-Received Microstructure of Cb-752	205

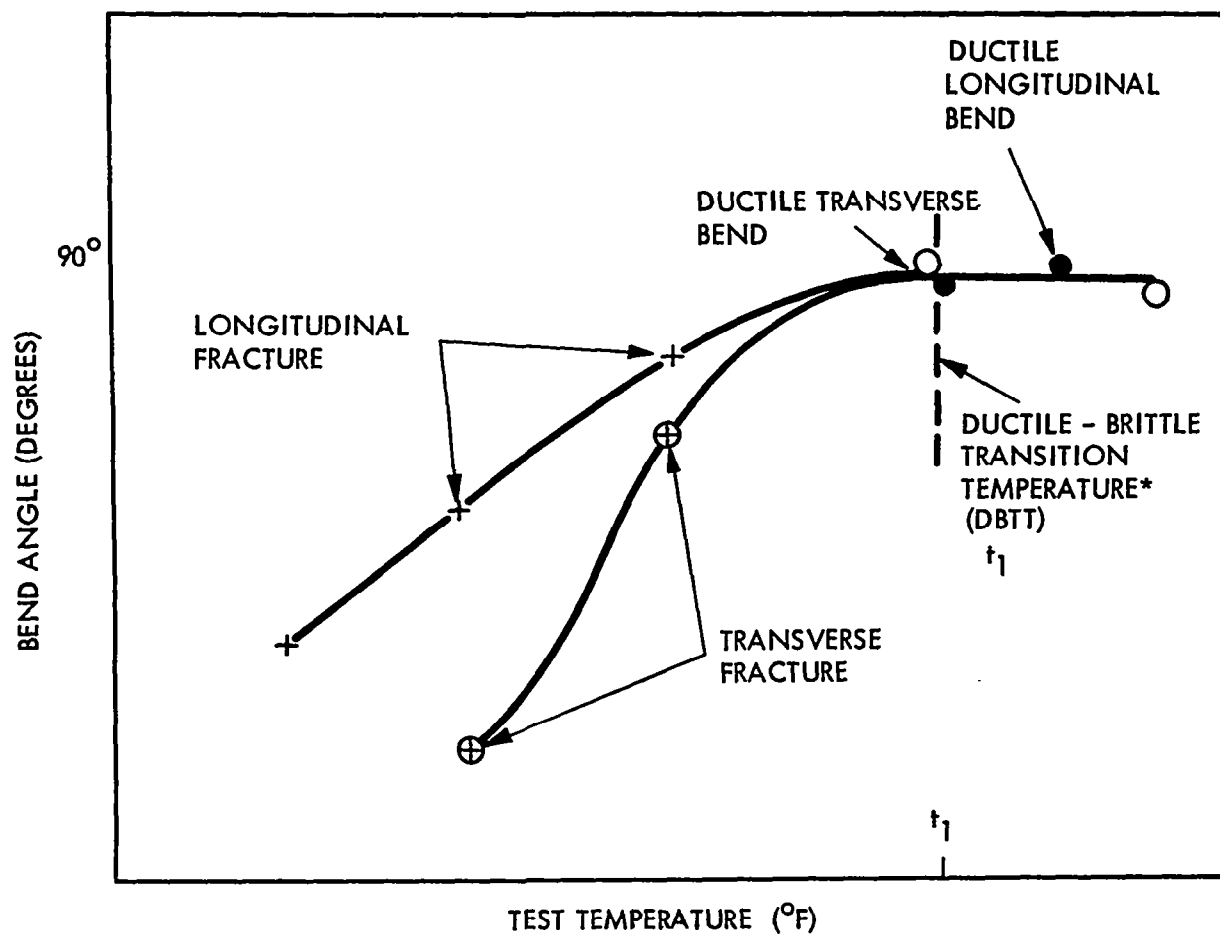
<u>Figure No.</u>	<u>Table No.</u>	<u>Title</u>	<u>Page</u>
A87	--	Cb-752 Base Metal Bend Test Results	206
--	A15	Cb-752 Sheet GTA Weld Record	207
A88	--	Bend Test Results for Cb-752 GTA Welds	208
A89	--	Bend Test Results for Cb-752 GTA Welds	209
--	A16	Cb-752 Sheet EB Weld Record	210
A90	--	Bend Test Results for Cb-752 EB Welds	211
A91	--	Bend Test Results for Cb-752 EB Welds	212
A92	--	Effect of Post-Weld Annealing on Cb-752 Weld Ductility	213
A93	--	Hardness Traverses, Cb-752 GTA Sheet Butt Welds	214
A94	--	Cb-752 EB Weld No. 11	215
A95	--	Cb-752 GTA Sheet Weld Microstructure	216
A96	--	Cb-752 GTA Sheet Weld Microstructure	217
A97	--	Plate Weld Microstructure of Cb-752	218
A98	--	Plate Weld Hardness Traverses of Cb-752	219
A99	--	Plate Weld Hardness Traverses of Cb-752	220
A100	--	Plate Weld Bend Specimens of Cb-752	221
 <u>D-43 PROGRAM TEST DATA</u>			
A101	--	As-Received Microstructure of D-43	222
A102	--	D-43 Base Metal Bend Test Results	223
--	A17	D-43 Sheet GTA Weld Record	224
A103	--	Bend Test Results of D-43 GTA Welds	225
A104	--	Bend Test Results of D-43 GTA Welds	226
--	A18	D-43 Sheet EB Weld Record	227
A105	--	Bend Test Results of D-43 EB Welds	228

<u>Figure No.</u>	<u>Table No.</u>	<u>Title</u>	<u>Page</u>
A106	--	Bend Test Results of D-43 EB Welds	229
A107	--	Effect of Post Weld Annealing on D-43 Weld Ductility	230
A108	--	Hardness Traverses, D-43 GTA Sheet Butt Welds	231
A109	--	Weld Microstructure in D-43 GTA Sheet Butt Welds	232
A110	--	D-43 Welded Plate, Weld Microstructure	233
A111	--	D-43 Weld Plate, Hardness Traverses	234
A112	--	D-43 Welded Plate Hardness Traverses	235
A113	--	D-43 Plate Weld Bend Specimens	236
<u>D-43Y PROGRAM TEST DATA</u>			
A114	--	As-Received Microstructure of D-43Y Sheet	237
A115	--	D-43Y Base Metal Bend Test Results	238
--	A19	D-43Y Sheet. GTA Weld Record	239
A116	--	Bend Test Results of D-43Y GTA Welds	240
A117	--	Bend Test Results of D-43Y GTA Welds	241
--	A20	D-43Y Sheet. EB Weld Record	242
A118	--	Bend Test Results of D-43Y EB Welds	243
A119	--	Bend Test Results of D-43Y EB Welds	244
A120	--	Effect of Post Weld Annealing on D-43Y Weld Ductility	245
A121	--	Hardness Traverses, D-43Y GTA Sheet Butt Welds	246
A122	--	D-43Y GTA Sheet Weld Microstructure	247
A123	--	D-43Y GTA Sheet Butt Weld Microstructure Annealed One Hour at 2400°F	248

<u>Figure No.</u>	<u>Table No.</u>	<u>Title</u>	<u>Page</u>
<u>SCb-291 PROGRAM TEST DATA</u>			
A124	--	As-Received Microstructure of SCb-291	249
A125	--	SCb-291 Base Metal Bend Test Results	250
--	A21	SCb-291 Sheet. GTA Butt Weld Record	251
A126	--	Bend Test Results for SCb-291 GTA Welds	252
A127	--	Bend Test Results for SCb-291 GTA Welds	253
--	A22	SCb-291 Sheet. EB Butt Weld Record	254
A128	--	Bend Test Results for SCb-291 EB Welds	255
A129	--	Bend Test Results for SCb-291 EB Welds	256
A130	--	Effect of Post Weld Annealing on SCb-291 Weld Ductility	257
A131	--	Hardness Traverses, SCb-291 GTA Sheet Butt Welds	258
A132	--	SCb-291 EB Sheet Butt Weld Microstructure	259
A133	--	SCb-291 Welded Plate Hardness Traverses	260
A134	--	SCb-291 Welded Plate Hardness Traverses	261
A135	--	SCb-291 Welded Plate Bend Specimens	262
<u>UNALLOYED ARC CAST TUNGSTEN, PROGRAM TEST DATA</u>			
--	A23	Unalloyed Arc Cast Tungsten Sheet, GTA Weld Record	263
A136	--	Bend Test Results for Base Metal and GTA Welds in Unalloyed Arc Cast Tungsten	264
A137	--	Typical GTA Welds in Unalloyed Arc Cast Tungsten	265
A138	--	Hardness Traverses for GTA Welds in Unalloyed Arc Cast Tungsten	266
--	A24	Unalloyed Arc Cast Tungsten Sheet, EB Weld Record	267
A139	--	Bend Test Results for EB Welded Unalloyed Arc Cast Tungsten	268

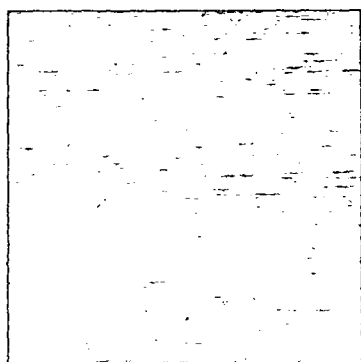
<u>Figure No.</u>	<u>Table No.</u>	<u>Title</u>	<u>Page</u>
<u>ARC CAST W-25Re, PROGRAM TEST DATA</u>			
A140	--	Base Metal Bend Test Results for W-25Re	269
--	A25	W-25Re Sheet. GTA Weld Record	270
A141	--	GTA Welds in W-25Re	271
A142	--	Bend Test Results for W-25Re GTA Welds	272
A143	--	Bend Test Results for W-25Re GTA Welds	273
A144	--	Hardness Traverses of GTA Welds in W-25Re	274
--	A26	Electron Beam Welding Parameters for W-25Re	275
A145	--	Bend Test Results for W-25Re EB Welds	276
A146	--	Bend Test Results for W-25Re EB Welds	277
A147	--	Bend Test Results for W-25Re EB Welds, Stress Relieved One Hour at 2560°F	278
A148	--	Bend Test Results for W-25Re EB Welds, Stress Relieved One Hour at 2560°F	279
A149	--	W-25Re EB Weld and Base Metal Microstructure	280
<u>SYLVANIA "A" PROGRAM TEST DATA</u>			
--	A27	Sylvania "A" Sheet, GTA Weld Record	281
A150	--	Sylvania "A" GTA Welds	282
A151	--	Sylvania "A" GTA Bead-on-Plate Patch Test	283





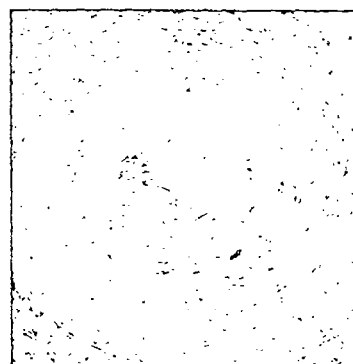
\*TEMPERATURE OF LAST DUCTILE BEND AS CHECKED BY DYE PENETRANT EXAMINATION

FIGURE A1 - Key for Presentation of Bend Test Data



8383

0.082 Wire

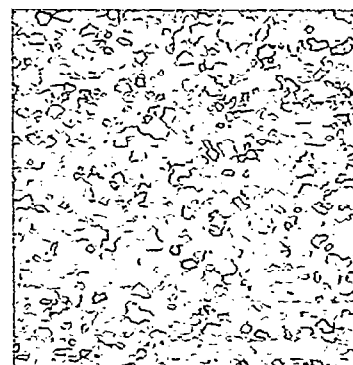


8384



7731

0.035 Sheet

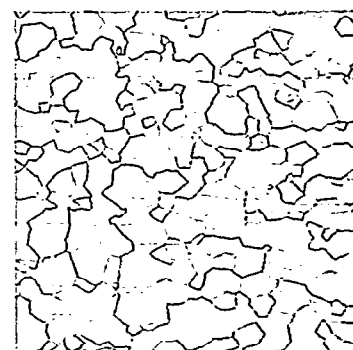


7732



2975

0.375 Plate



2796

Longitudinal

Transverse

FIGURE A2 - As-Received Microstructure of T-111, 100X

TABLE A1 - T-111 Sheet. GTA Butt Weld Record

Weld No.	Clamp Spacing (Inch)	Speed (ipm)	Current Amperes	Weld Width Top/Bottom (Inch)	Q Joules/Inch	Atmosphere Monitor Readings			Comments	
						O <sub>2</sub> (1) ppm	O <sub>2</sub> (2) ppm	H <sub>2</sub> O (3) ppm	Visual & Dye Penetrant	Radiography
1	3/8	7.5	70	0.123/0.066	9520	1.5	3.0	0.5	Negative	Negative
2	3/8	7.5	90	0.165/0.150	11880	---	3.0	0.6	Negative	Negative
3	3/8	15.0	115	0.195/0.189	8500	---	3.0	0.7	Negative	Negative
4	3/8	15.0	85	0.135/0.084	5780	---	3.6	0.9	Negative	Negative
5	1/4	15.0	90	0.120/0.060	6120	---	4.4	0.9	Negative	Negative
6	1/4	15.0	165	0.210/0.210	11870	---	4.4	0.9	Negative	Negative
7	1/4	30.0	200	0.189/0.180	7600	---	4.4	1.1	Negative	Negative
8	1/4	30.0	125	0.120/0.045	4120	---	4.4	1.1	Negative	Negative
9	3/8	30.0	126	0.150/0.105	4160	3.0	4.0	1.5	Negative	Negative
10	3/8	30.0	185	0.240/0.225	6660	0.5	4.0	1.6	Negative	Negative
11	3/8	60.0	220	0.165/0.138	4180	1.0	3.2	2.5	Negative	Negative
12	3/8	60.0	165	0.117/0.030	2880	1.0	3.2	2.3	Lack of	Penetration

- (1) Westinghouse Oxygen Gage  
 (2) Lockwood & McLorie Oxygen Gage  
 (3) CEC Moisture Monitor

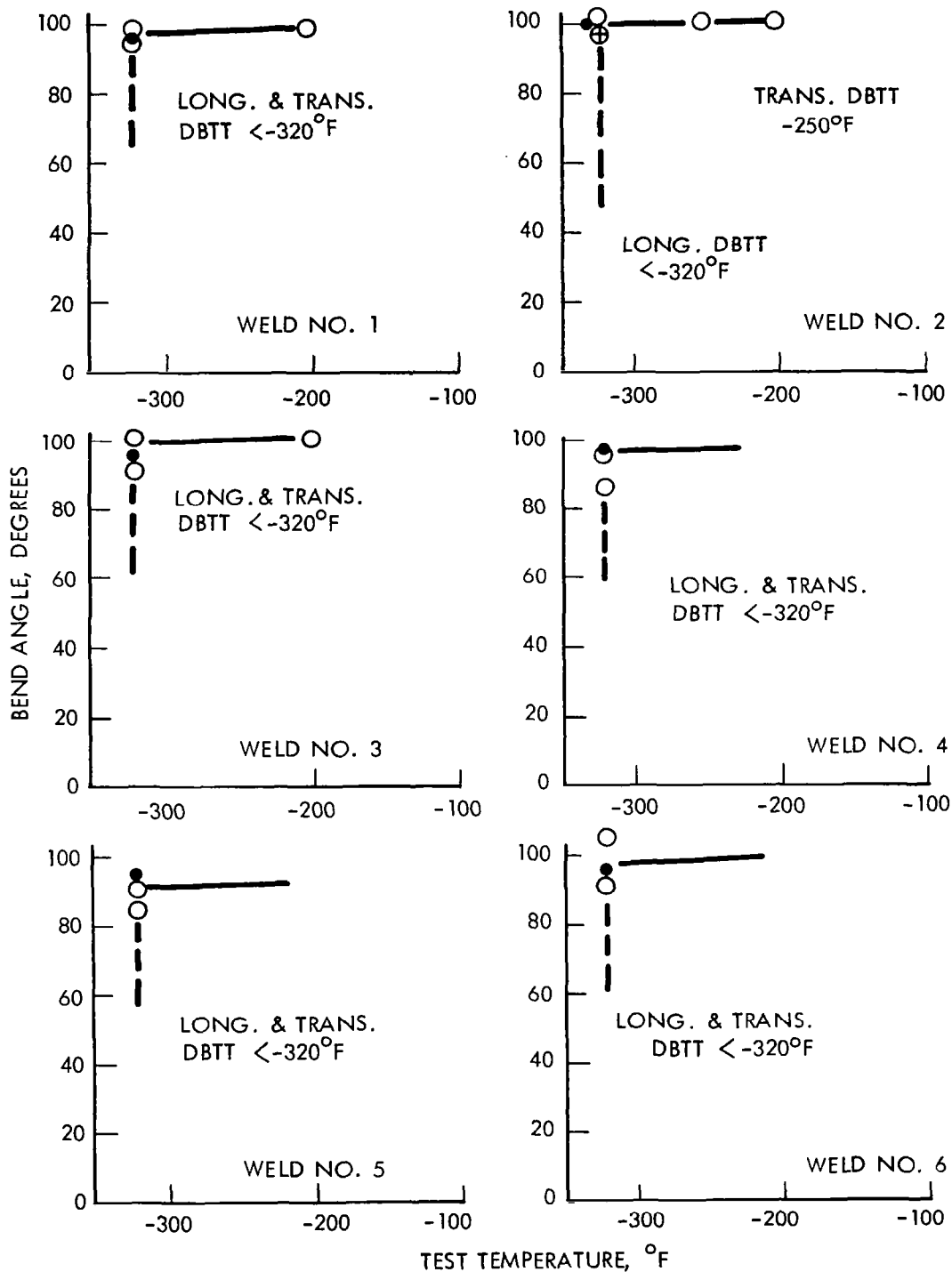


FIGURE A3 - Bend Test Results for T-111 GTA Welds  
1† Bend Radius

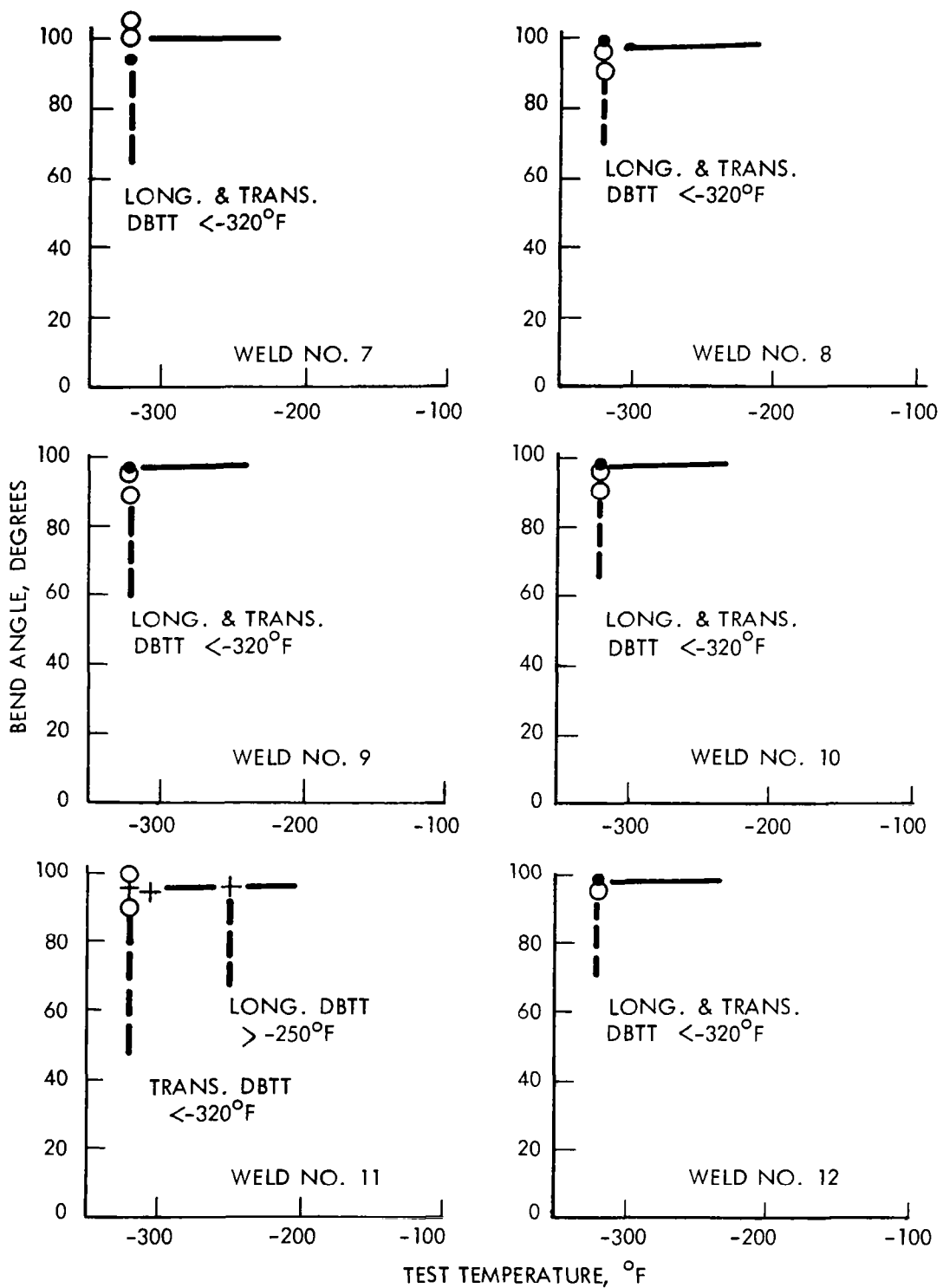


FIGURE A4 - Bend Test Results for T-111 GTA Welds  
1t Bend Radius

TABLE A2 - T-111 Sheet. EB Butt Weld Record

Weld No.	Speed (ipm)	Deflection <sup>1</sup> (Inches)	Current (ma)	Chill Spacing (Inches)	Power (watts)	Watt-Sec. per inch Q	Weld Bead Width (Inches)		Vacuum torr	Ave. Weld Bead Width
							Top	Bottom		
1	15	Zero	3.6	.094	540	2160	.035	.022	$2 \times 10^{-6}$	.028
2	15	L - .050	4.2	.094	630	2520	.041	.029	$2 \times 10^{-6}$	.035
3	15	T - .050	4.2	.094	630	2520	----	----	$2 \times 10^{-6}$	
4	15	L - .050	3.0	.250	570	2280	.038	.027	$2 \times 10^{-6}$	.032
5	25	L - .050	4.2	.094	630	1510	.038		(2)	.032
6	50	L - .025	4.8	.094	720	865	.031	.022	$2.5 \times 10^{-6}$	.026
7	50	L - .050	5.0	.094	750	900	.032	.020	$2.5 \times 10^{-6}$	.026
8	50	L - .100	5.6	.094	840	1000	.029	.019	$2.5 \times 10^{-6}$	.025
9	100	L - .050	5.8	.094	870	521	.025	.018	$2.5 \times 10^{-6}$	.022
10	25	L - .050	4.0	.250	600	1440	.036	.025	$2.5 \times 10^{-6}$	.030
11	50	L - .050	4.6	.250	690	830	.034	.018	$2.5 \times 10^{-6}$	.026
12	100	L - .050	5.6	.250	840	504	.026	.018	$2.5 \times 10^{-6}$	.022

All welds made at 150 KV.

1. L. is longitudinal

T. is transverse

(2) Pressure not recorded.

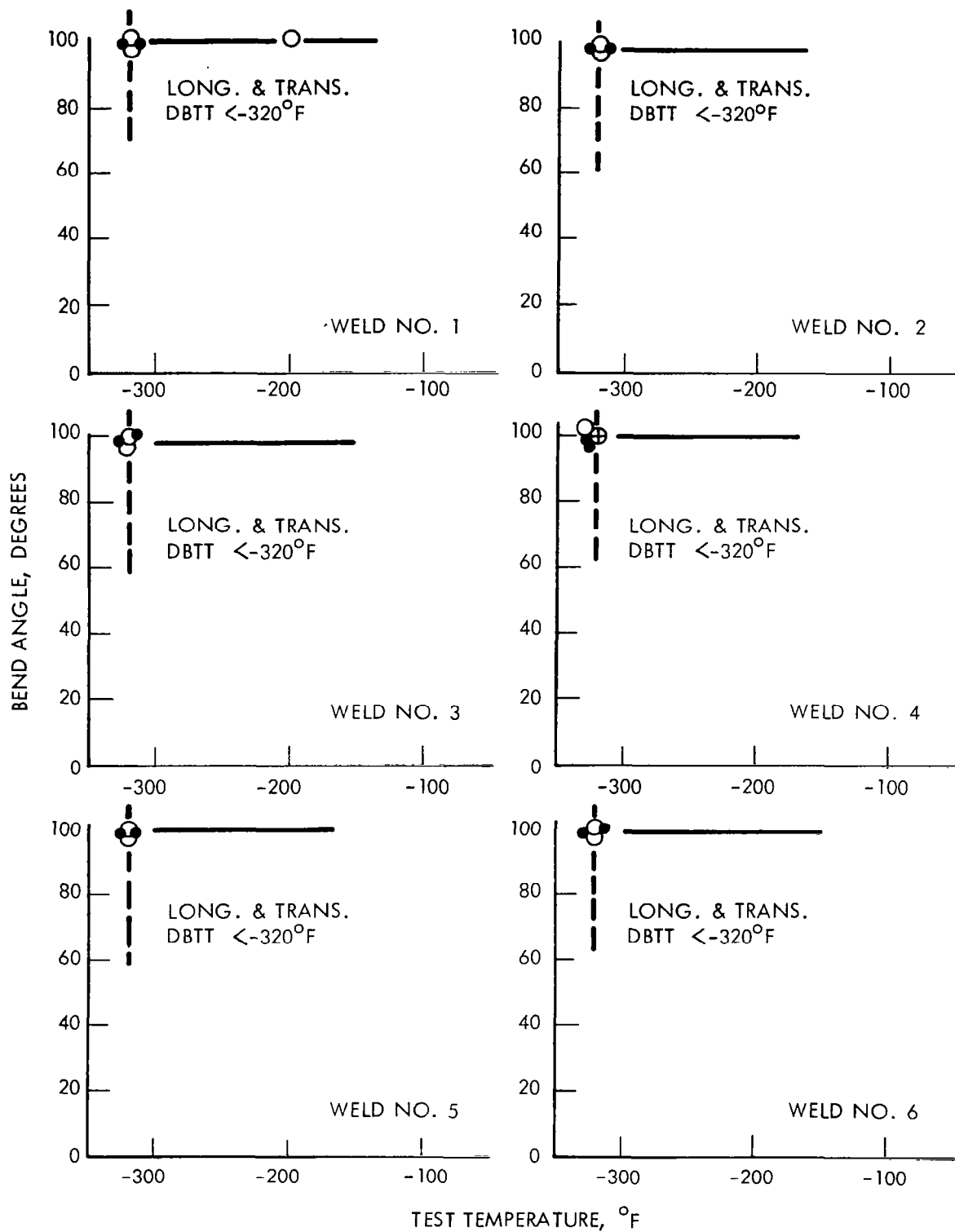


FIGURE A5 - Bend Test Results for T-111 EB Welds  
1t Bend Radius

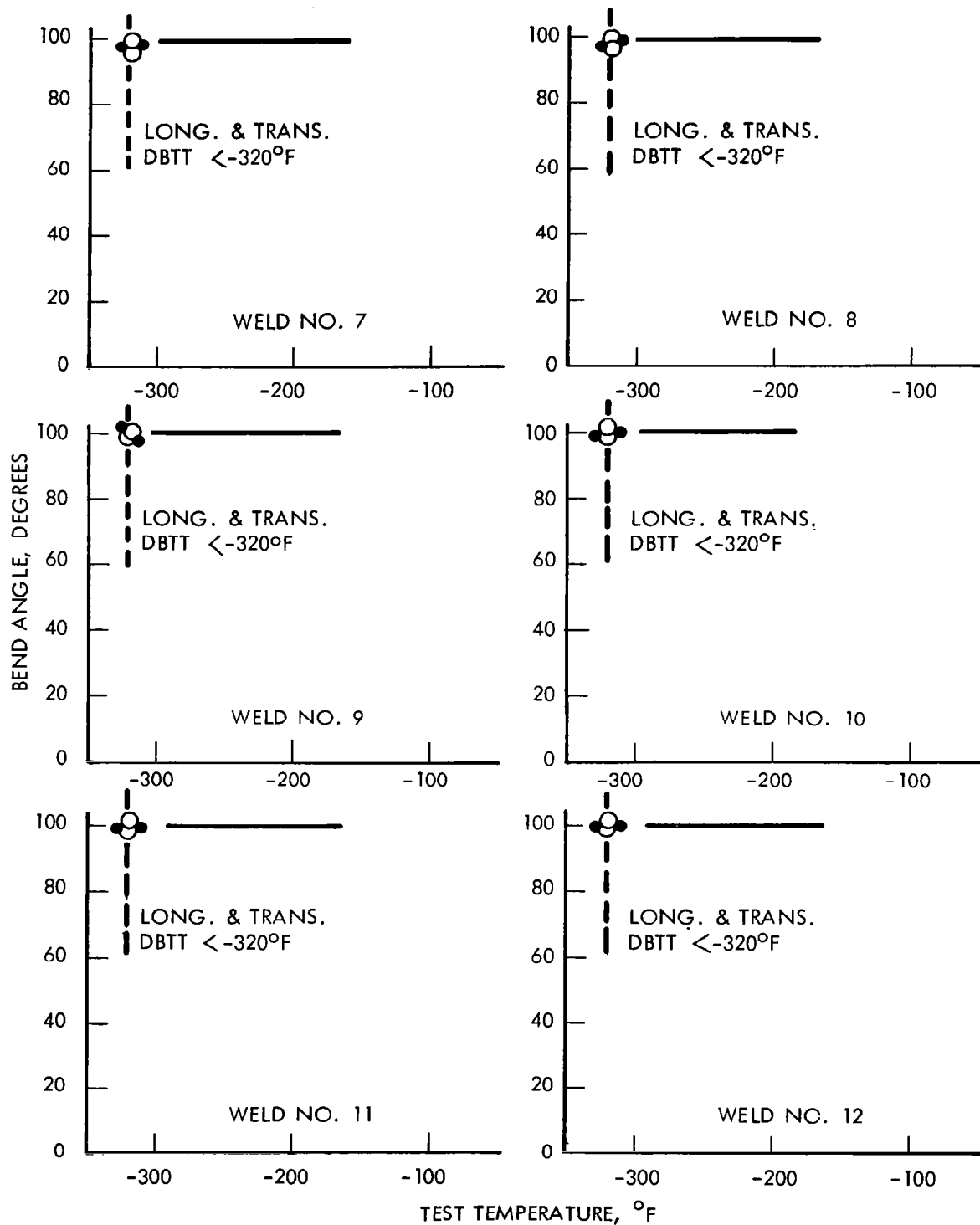


FIGURE A6 - Bend Test Results for T-111 EB Welds  
1t Bend Radius



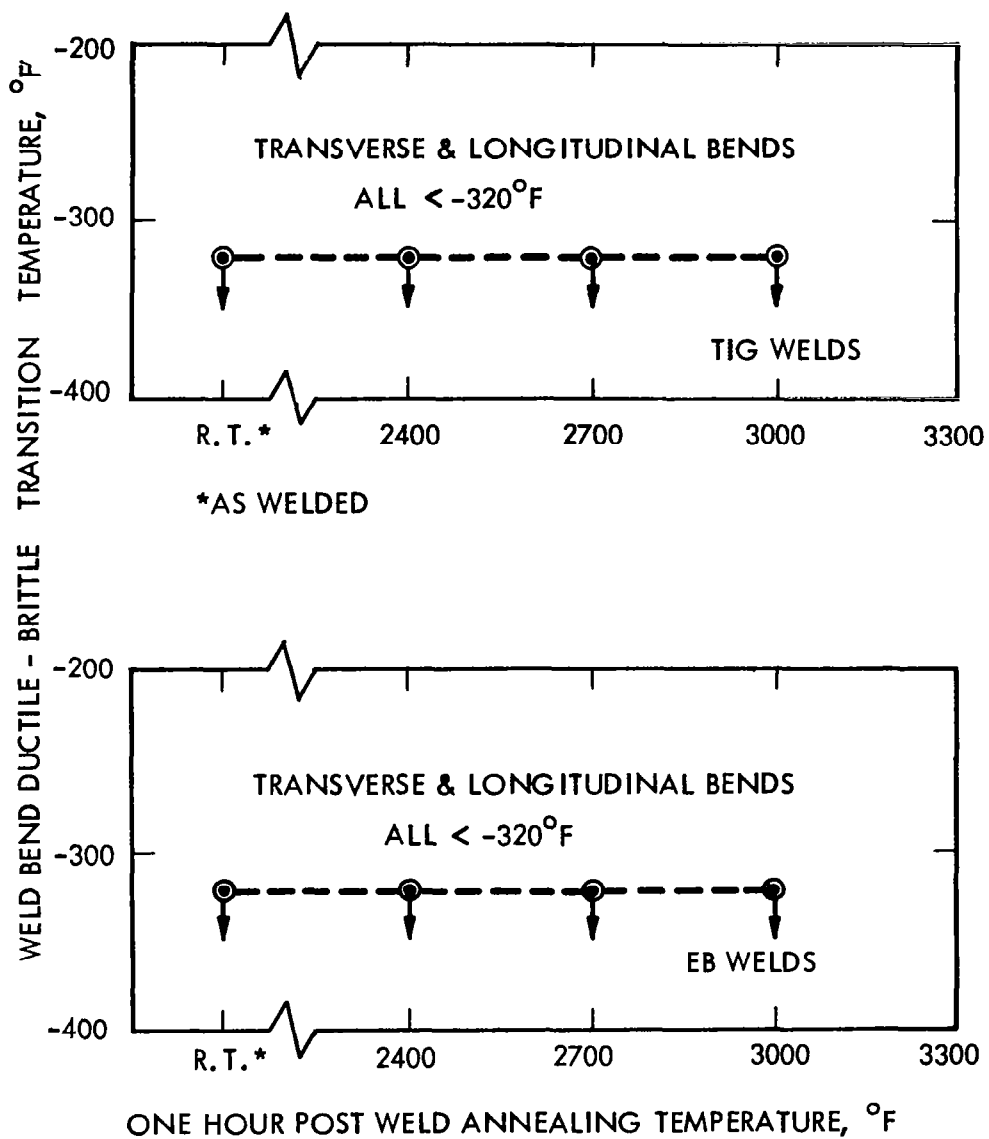


FIGURE A7 - Effect of Post-Weld Annealing on T-111 Sheet Weld Ductility

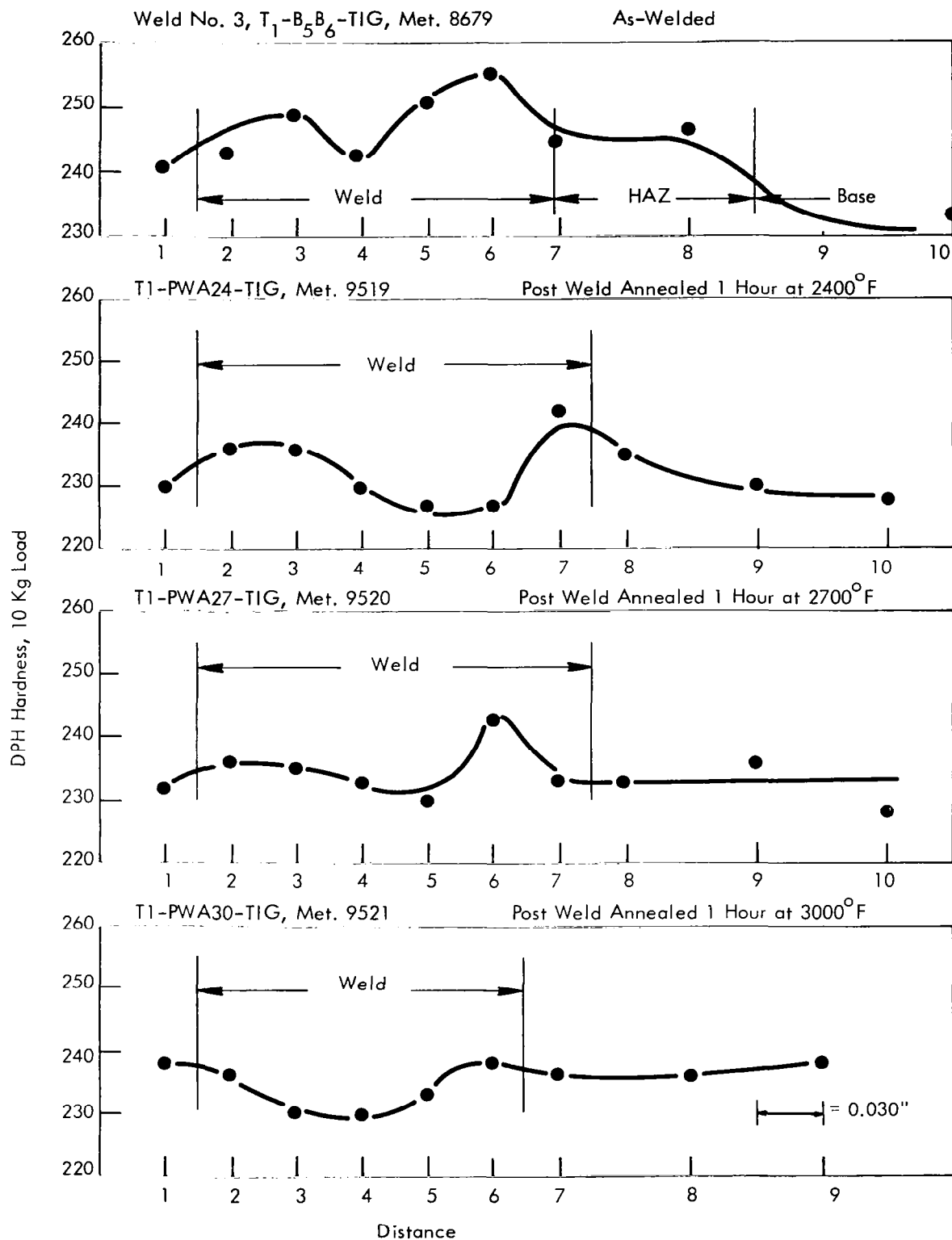
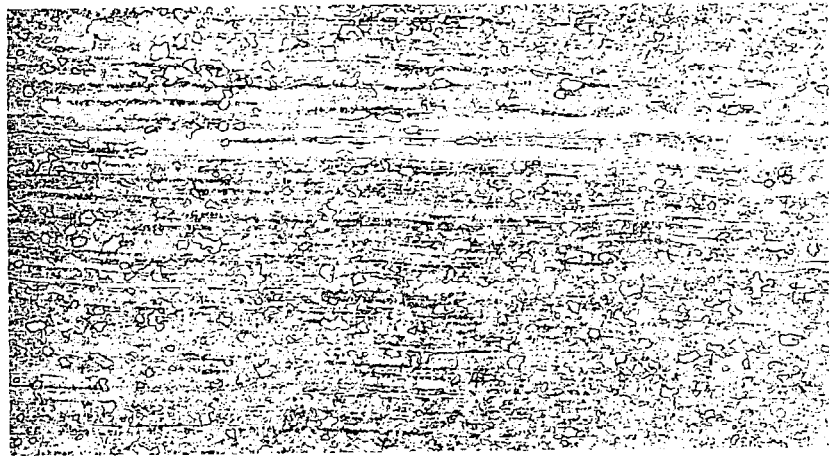


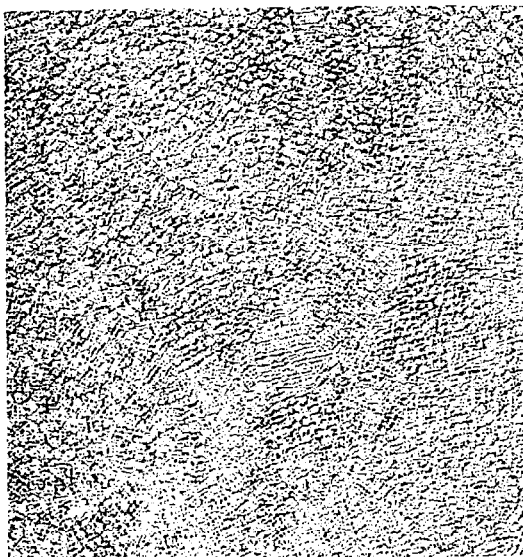
FIGURE A8 - Hardness Traverses, T-111 GTA Sheet Butt Welds



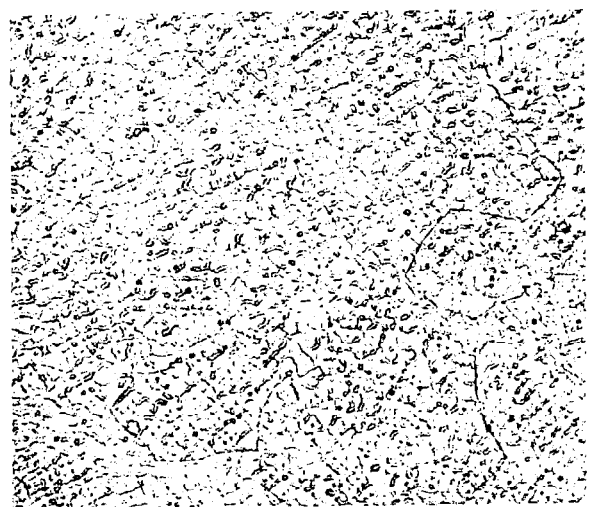
Weld Edge 100X



Area Between Base and HAZ 100X

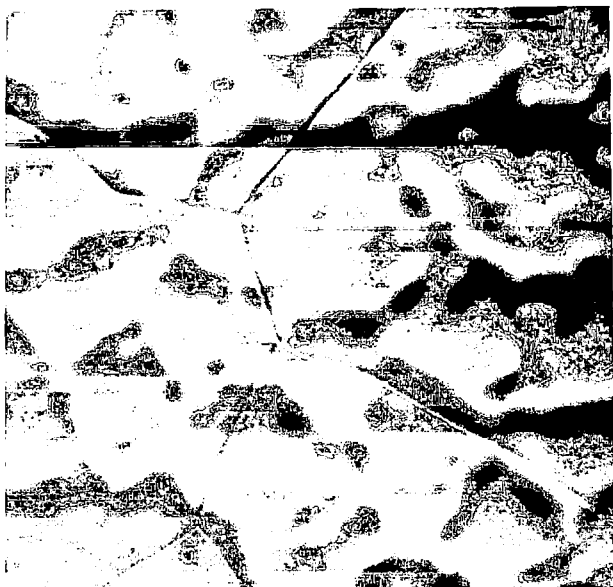


Weld Center 100X



Weld Center 200X

FIGURE A9 - T-111 As-Welded Microstructures for Sheet GTA Butt Weld No. 3  
(Met. 8679)



Weld Center



HAZ (Near Weld)

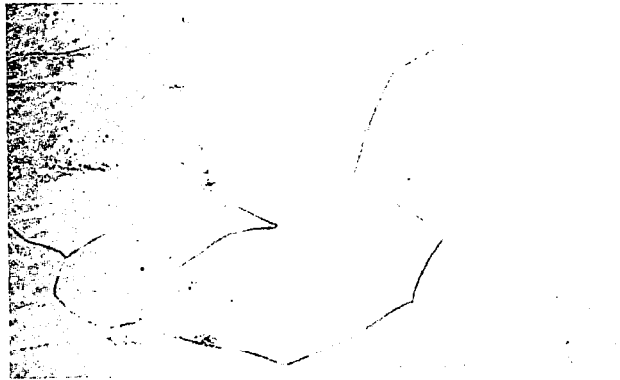


Base Metal

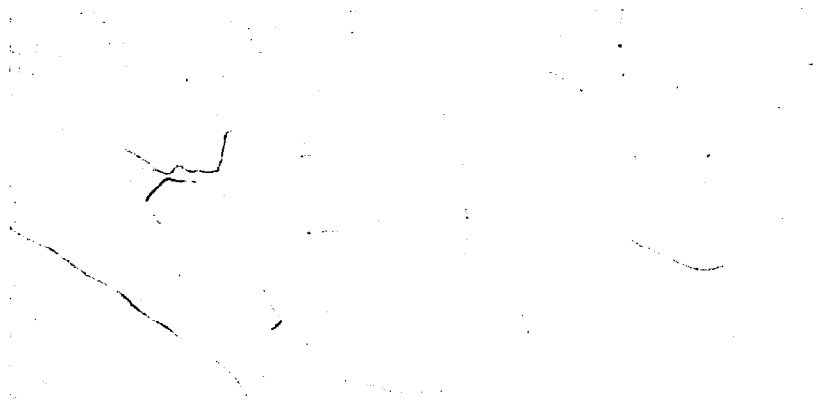


Base-HAZ Area

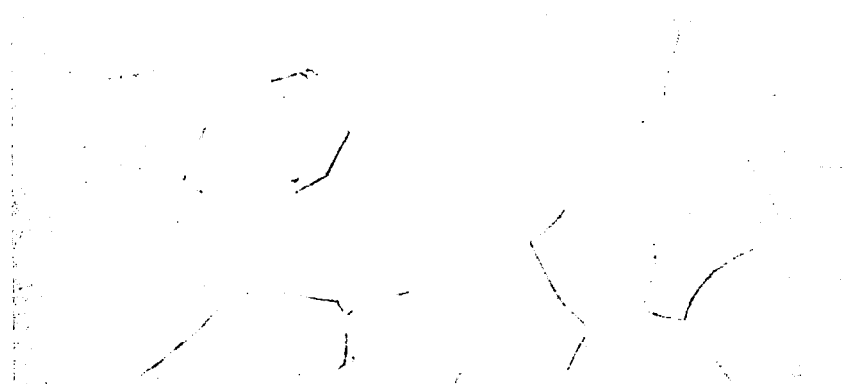
FIGURE A10 - T-111 As-Welded Microstructure for GTA Sheet Butt Welds, at 1500X  
(Met. 16697)



Post Weld Annealed One Hour at 2400°F  
(Met. 9519)

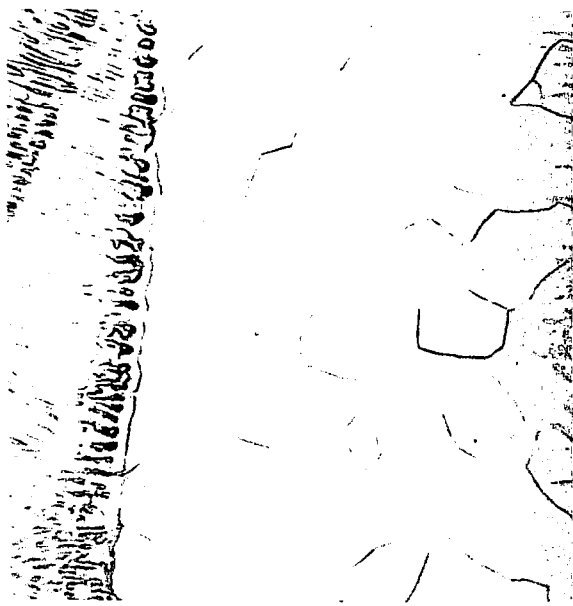


Post Weld Annealed One Hour at 2700°F  
(Met. 9520)



Post Weld Annealed One Hour at 3000°F  
(Met. 9521)

FIGURE A11 - Post Weld Annealed T-111 GTA Sheet Butt Weld Microstructure,  
All 400X at Weld Interface

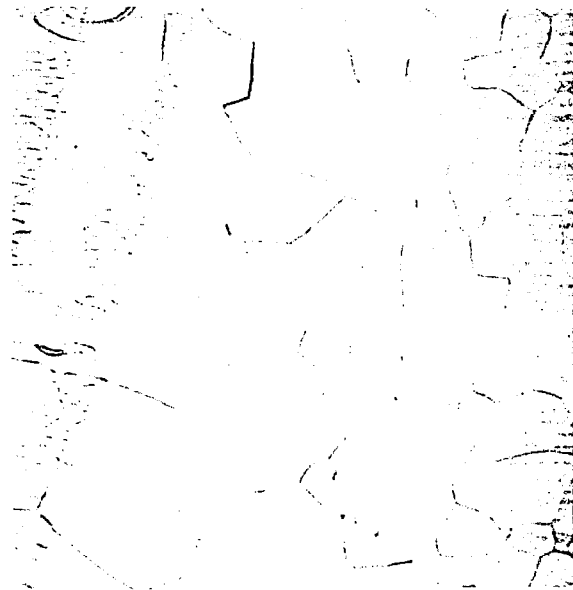


As-Welded

Met. 9174-6



Post Weld Annealed 1 Hr. at 2400°F  
Met. 9522



Post Weld Annealed 1 Hr. at 2700°F  
Met. 9523



Post Weld Annealed 1 Hr. at 3000°F  
Met. 9524

FIGURE A12 - T-111 EB Sheet Butt Weld Microstructure  
(Weld Interface, all at 400X)

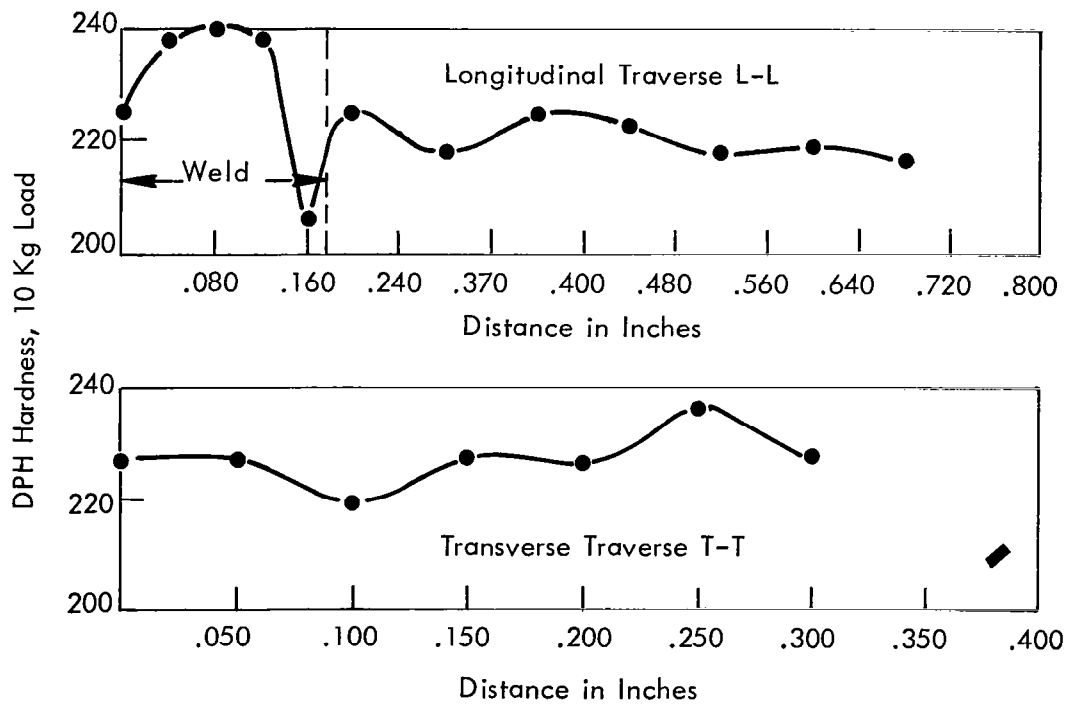
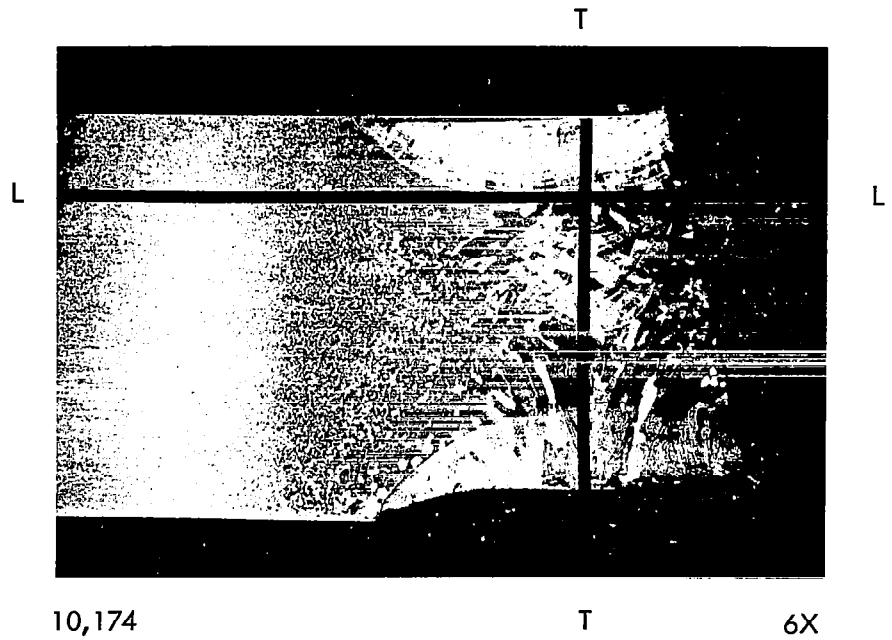


FIGURE A13 - T-111 Plate Weld, As-Welded

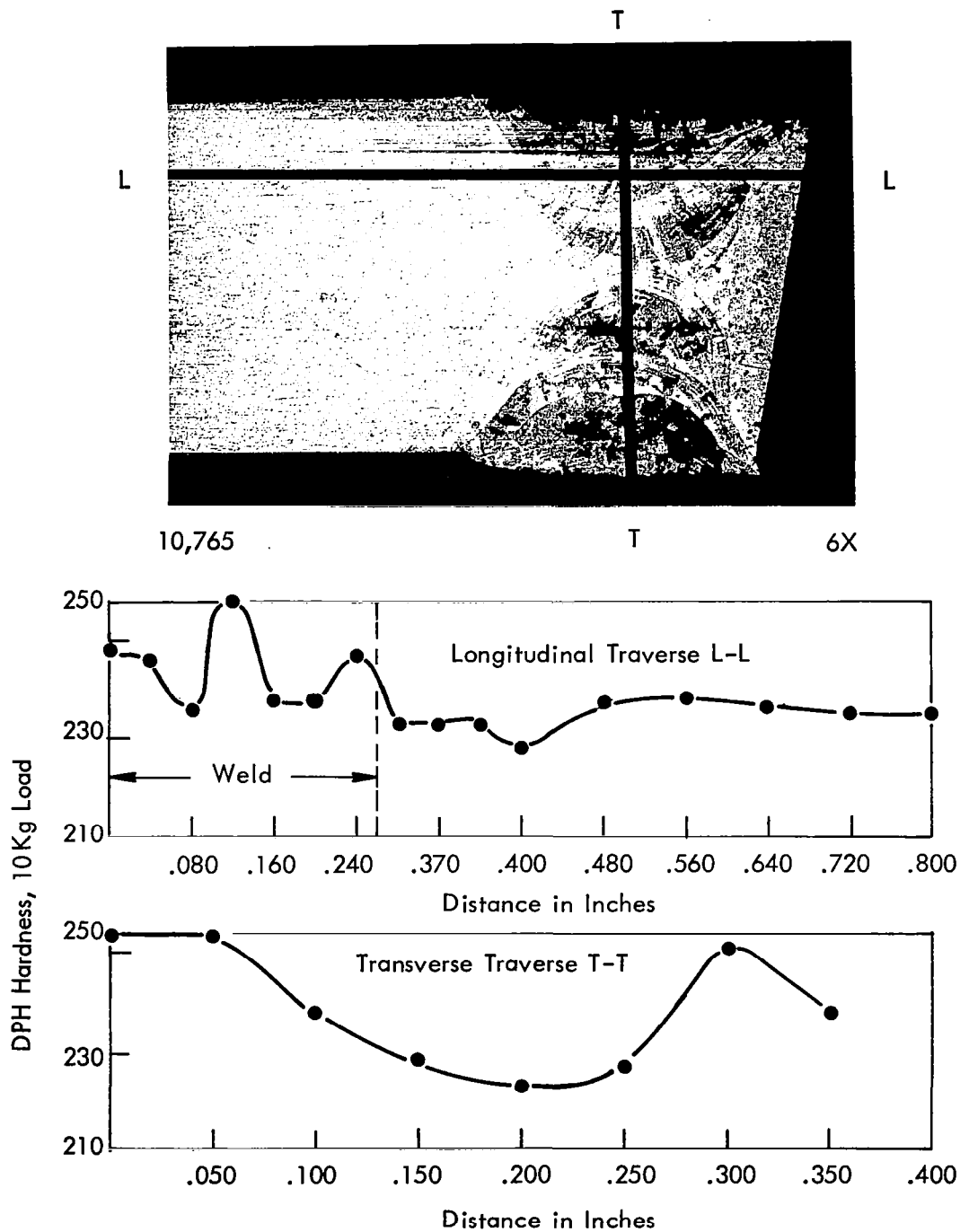
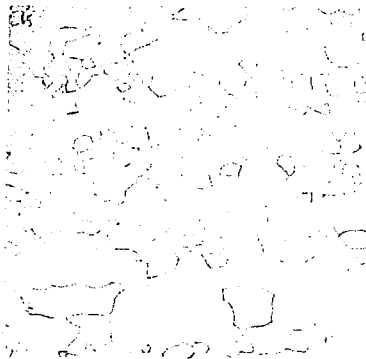


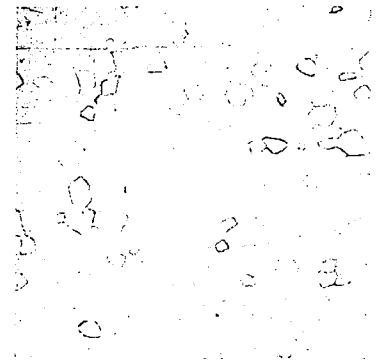
FIGURE A14 - T-111 Plate Weld, Annealed One Hour at 2400°F



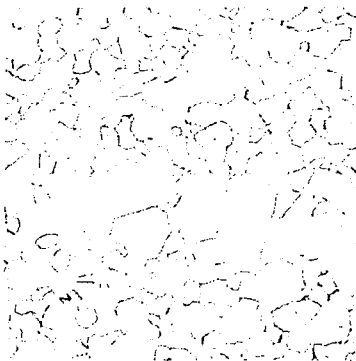


8385

0.035 Sheet



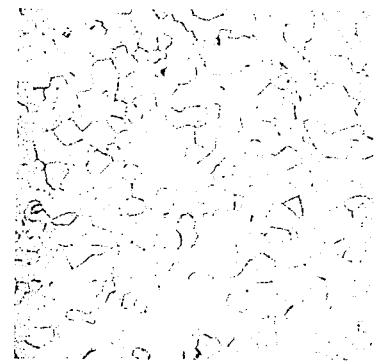
8386



8387

0.375 Plate

Longitudinal



8388

Transverse

FIGURE A15 - As-Received Microstructure of T-222, 100X

TABLE A3 - T-222 Sheet. GTA Butt Weld Record

Weld No.	Clamp Spacing (Inch)	Speed (ipm)	Current Amperes	Weld Width Top/Bottom (Inch)	Q Joules/Inch	Atmosphere Monitor Readings			Comments	
						O <sub>2</sub> (1) ppm	O <sub>2</sub> (2) ppm	H <sub>2</sub> O(3) ppm	Visual & Dye Penetrant	Radiography
1	3/8	7.5	75	0.141/0.096	10200	---	1.5	0.3	Negative	Porosity
2	3/8	7.5	95	0.182/0.174	13300	---	1.6	0.4	Negative	Negative
3	3/8	15.0	110	0.195/0.171	7480	---	1.6	0.5	Negative	Porosity
4	3/8	15.0	85	0.144/0.105	5780	---	1.6	0.6	Negative	Porosity
5	1/4	15.0	95	0.120/0.072	6460	---	1.8	0.7	Negative	Porosity
6	1/4	15.0	150	0.195/0.190	10800	---	1.9	0.8	Negative	Porosity
7	1/4	30.0	190	0.180/0.159	6830	---	1.8	1.0	Negative	Negative
8	1/4	30.0	133	0.129/0.069	4530	---	1.7	1.2	Negative	Negative
9	3/8	30.0	120	0.135/0.070	4080	---	2.2	2.0	Negative	Negative
10	3/8	30.0	170	0.210/0.189	6120	---	2.4	2.1	Negative	Negative
11	3/8	60.0	220	0.174/0.150	4180	---	2.4	2.3	Negative	Negative
12	3/8	60.0	170	0.120/0.015	3060	---	2.5	2.4	Negative	Negative

(1) Westinghouse Oxygen Gage

(2) Lockwood &amp; McLorie Oxygen Gage

(3) CEC Moisture Monitor

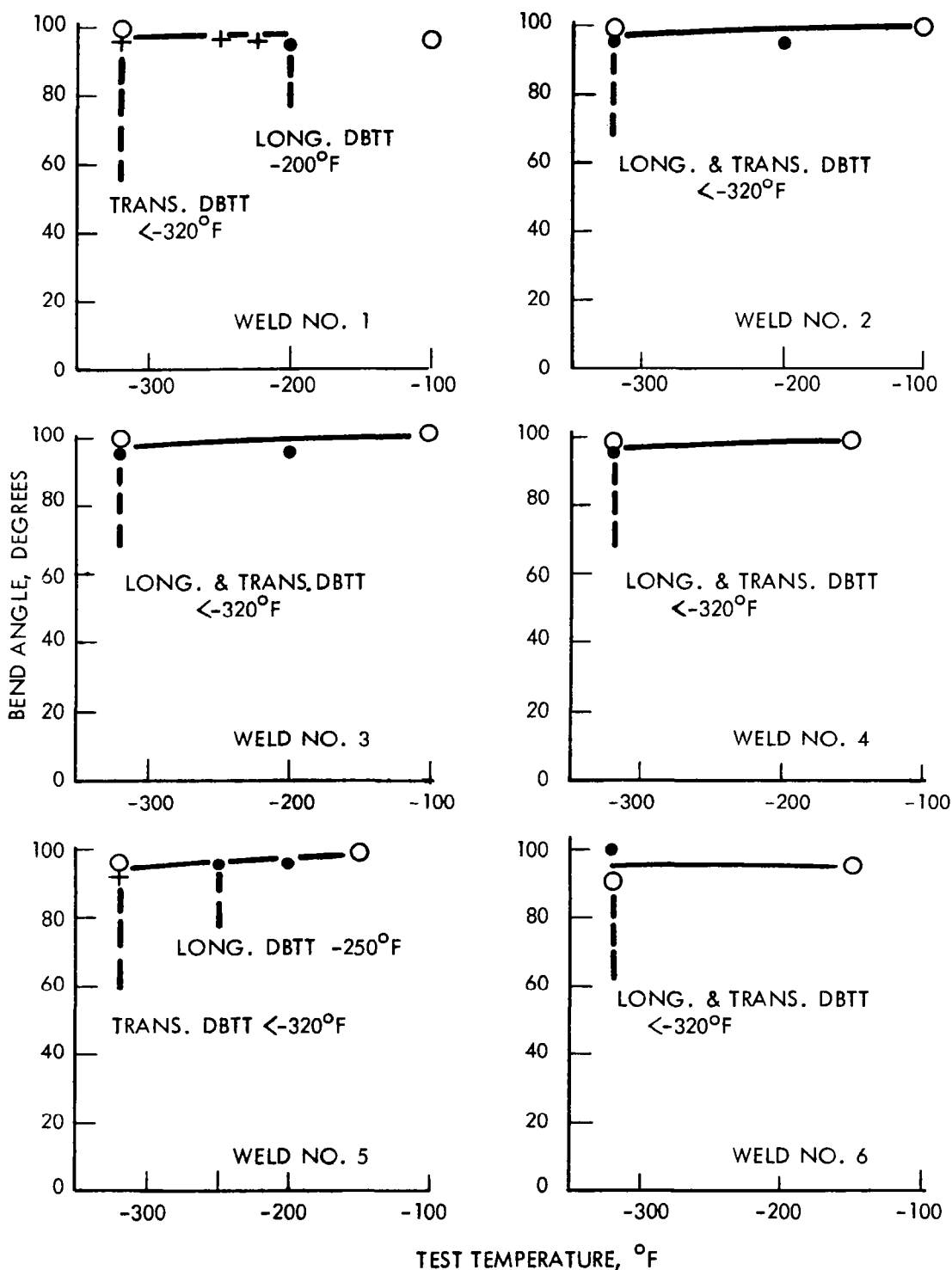


FIGURE A16 - Bend Test Results for T-222 GTA Welds  
1t Bend Radius

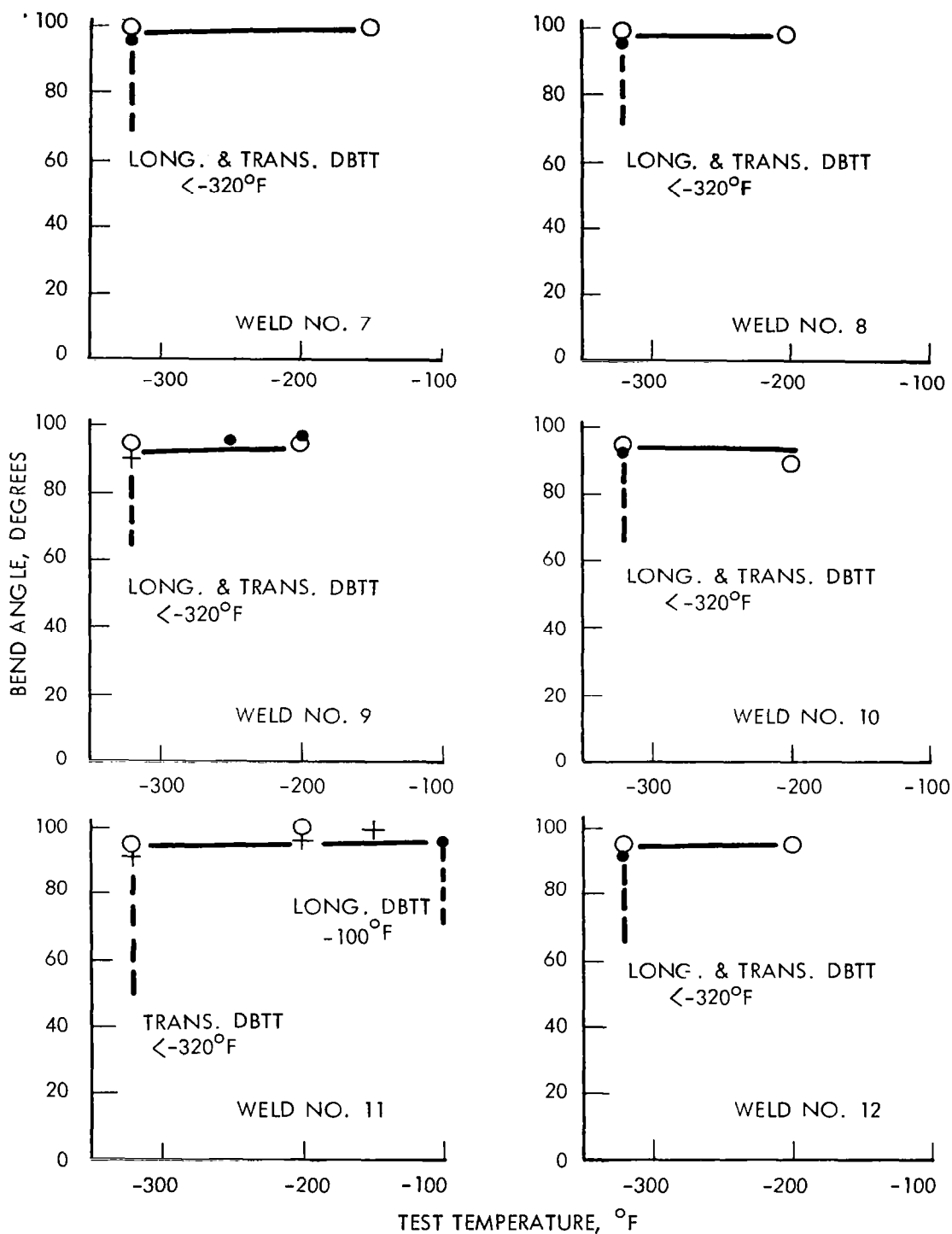


FIGURE A17 - Bend Test Results for T-222 GTA Welds  
1t Bend Radius

TABLE A4 - T-222 Sheet. EB Butt Weld Record

Weld No.	Speed (ipm)	Deflection <sup>1</sup> (Inches)	Current (ma)	Chill Spacing (Inches)	Power (watts)	Watt-Sec. per inch Q	Weld Bead Width (Inches)		Vacuum torr	Ave. Weld Bead Width
							Top	Bottom		
1	15	Zero	3.6	.094	540	2160	.033	.024	$2.4 \times 10^{-6}$	28
2	15	L - .050	4.2	.094	630	2520	.036	.022	$2.4 \times 10^{-6}$	29
3	15	T - .050	4.2	.094	630	2520	.065	.060	$2.4 \times 10^{-6}$	62
4	25	L - .050	4.2	.094	630	1510	.034	.022	$2.4 \times 10^{-6}$	28
5	15	L - .050	3.8	.250	570	2280	.039	.026	$2.4 \times 10^{-6}$	32
6	25	L - .050	4.0	.250	600	1440	.036	.023	$2.4 \times 10^{-6}$	30
7	50	L - .050	4.6	.250	690	830	.031	.018	$2.4 \times 10^{-6}$	24
8	100	L - .050	5.6	.250	840	505	.027	.019	$3.0 \times 10^{-6}$	23
9	50	Zero	4.6	.094	690	830	.027	.020	$3.0 \times 10^{-6}$	24
10	50	L - .025	4.8	.094	720	865	.031	.022	$3.0 \times 10^{-6}$	26
11	50	L - .050	5.0	.094	750	900	.031	.019	$3.0 \times 10^{-6}$	25
12	100	L - .050	5.8	.094	870	522	.031	.020	$3.0 \times 10^{-6}$	26

All welds made at 150 KV.

1. L is longitudinal

T is transverse

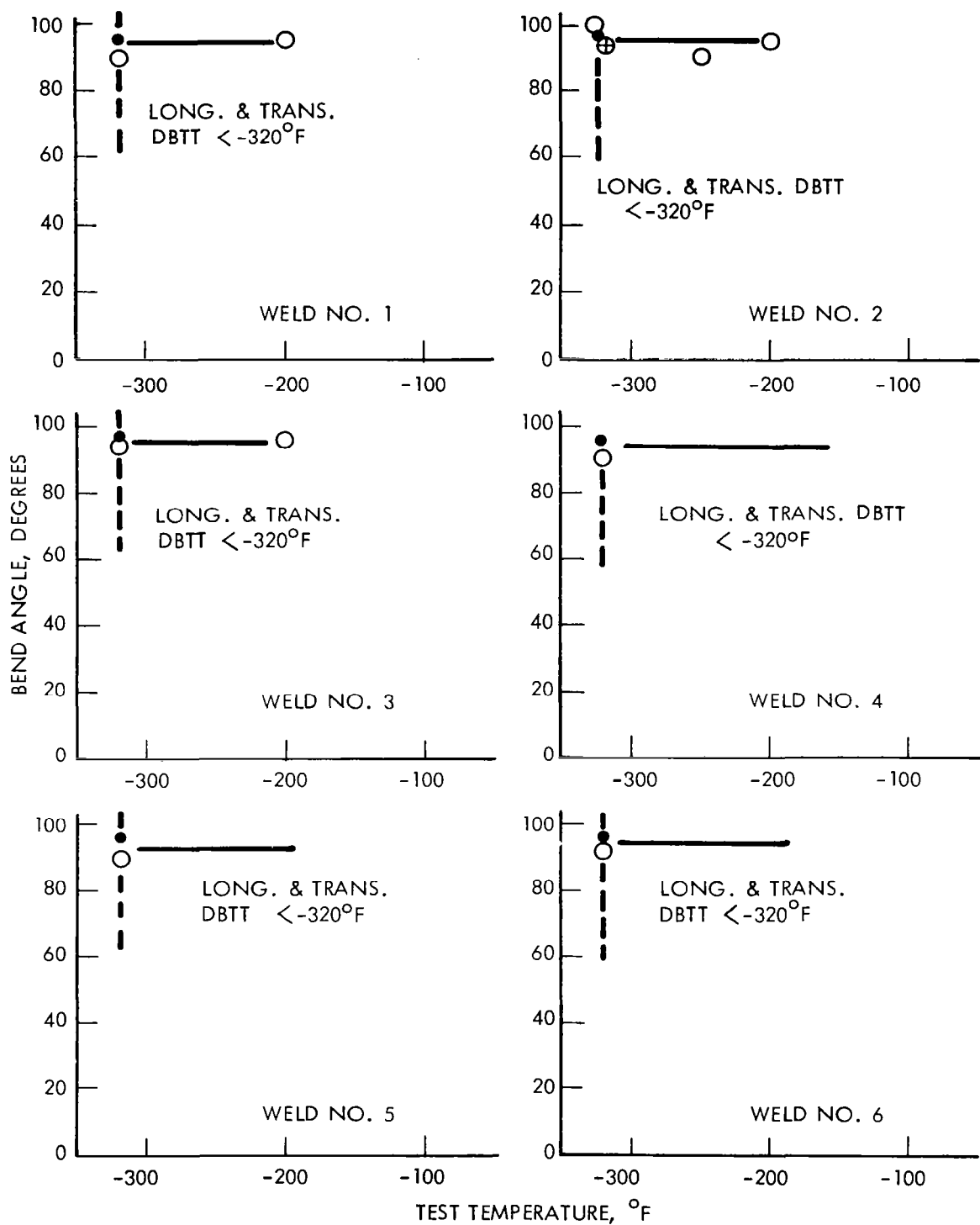


FIGURE A18 - Bend Test Results for T-222 EB Welds  
1½ Bend Radius

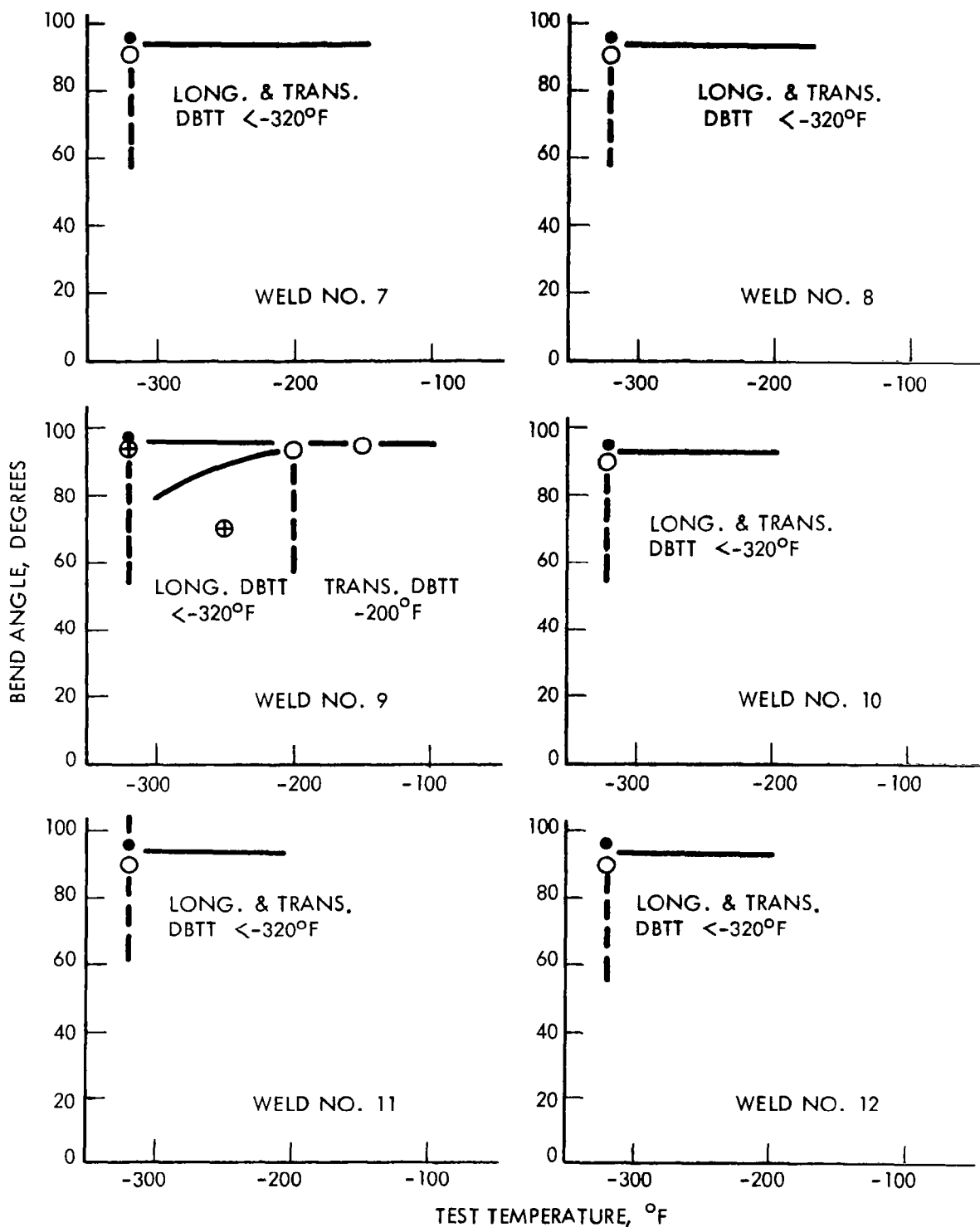


FIGURE A19 - Bend Test Results for T-222 EB Welds  
1t Bend Radius

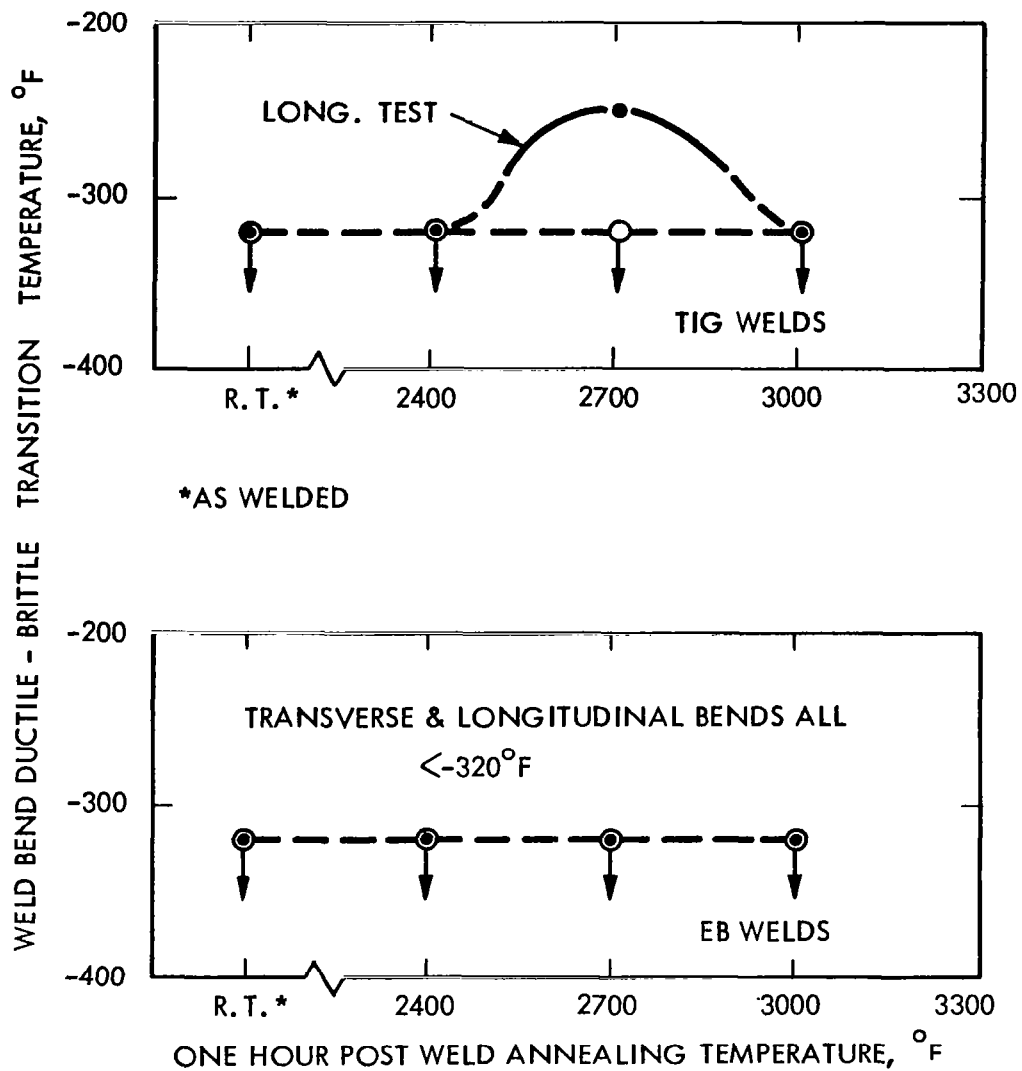


FIGURE A20 - Effect of Post Weld Annealing on T-222 Weld Ductility



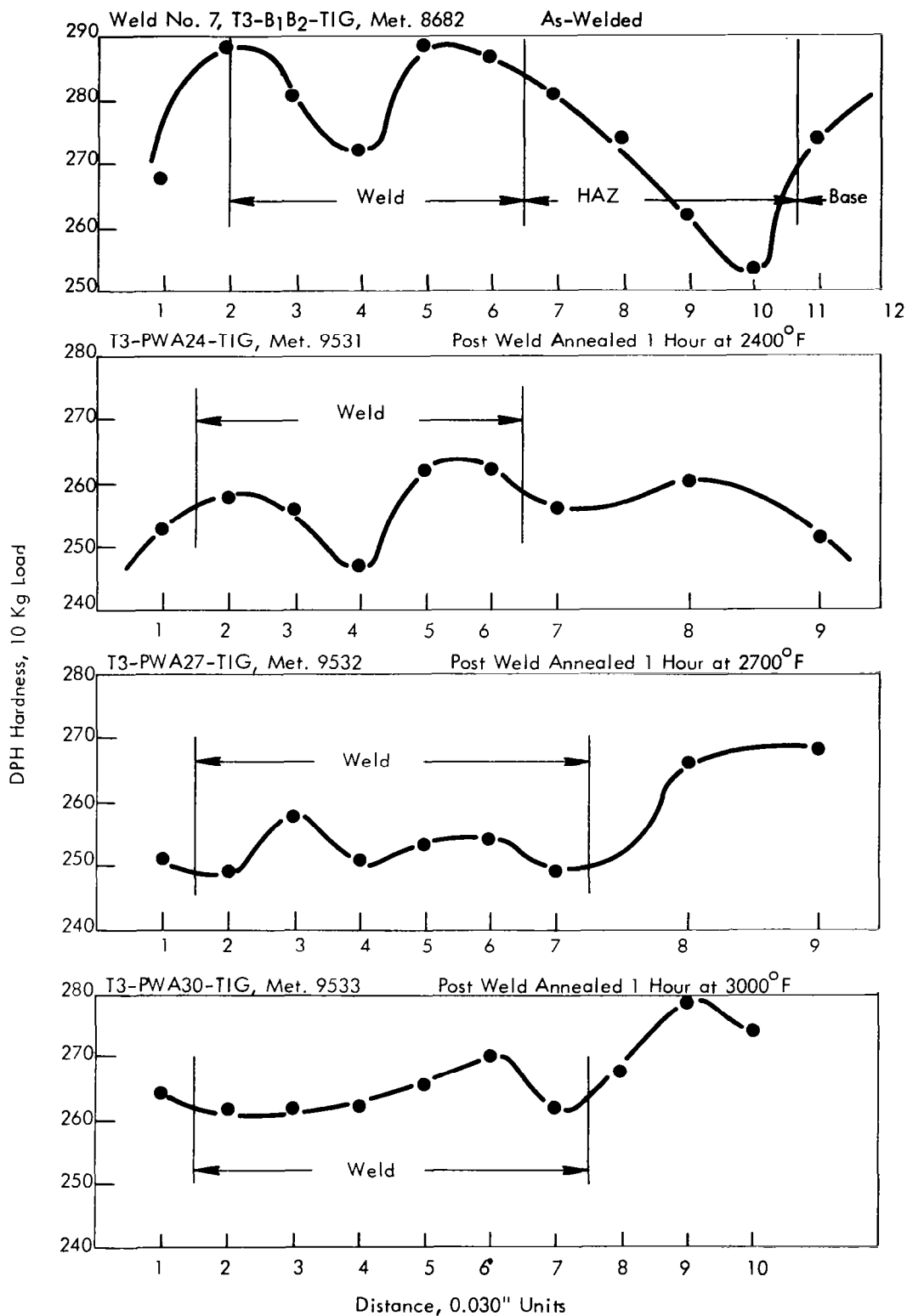
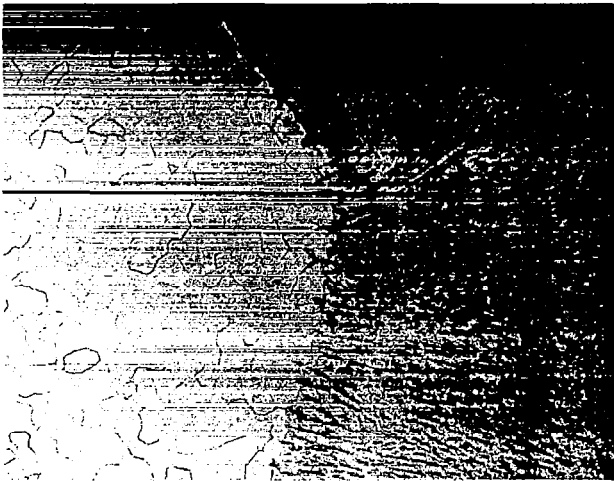
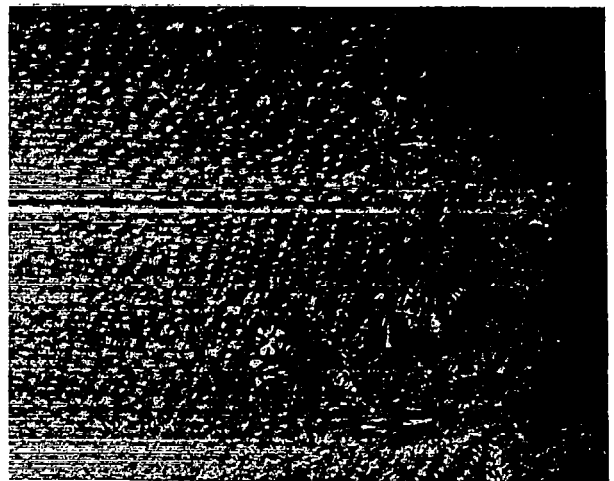


FIGURE A21 - Hardness Traverses, T-222 GTA Sheet Butt Welds



Weld Edge

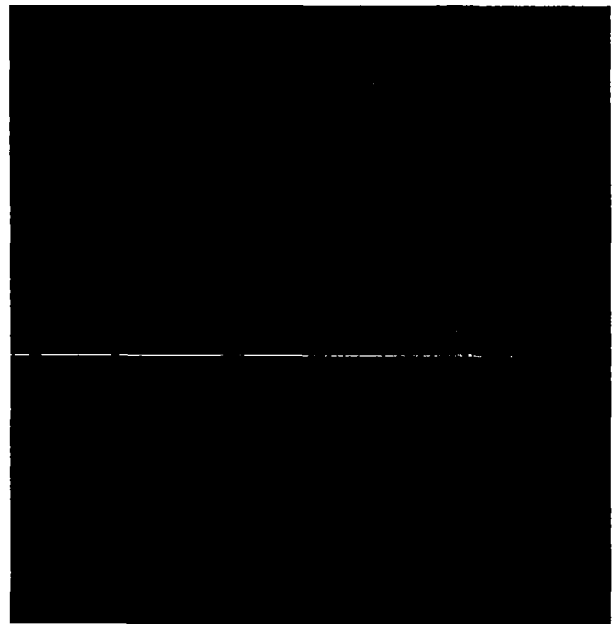


Weld Center

GTA Weld No. 7 Met. 8682 100X



80X

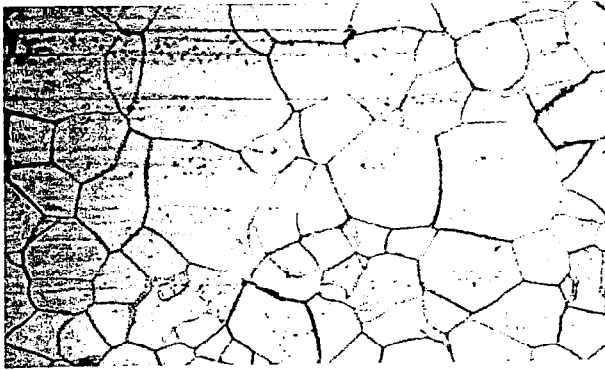


Weld Edge

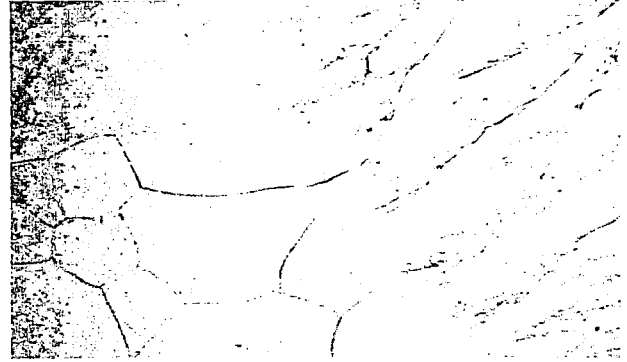
400X

EB Weld No. 5 Met. 9177-4

FIGURE A22 - T-222 As-Welded Sheet Butt Weld Microstructure

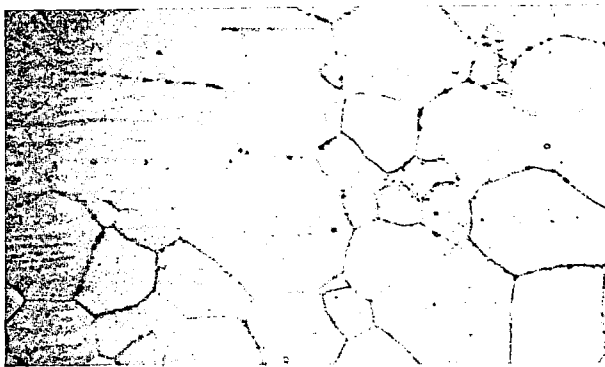


Base

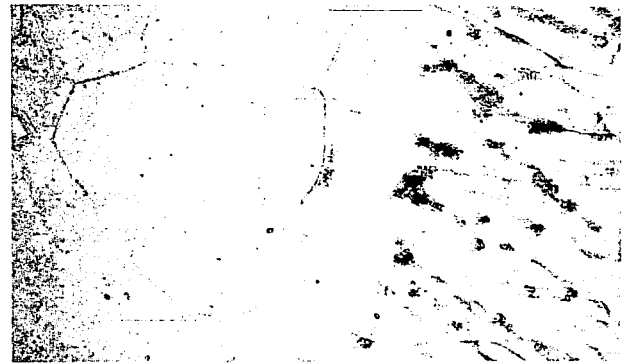


Weld Edge

Annealed One Hour at 2400°F. Met. 9531, 500X

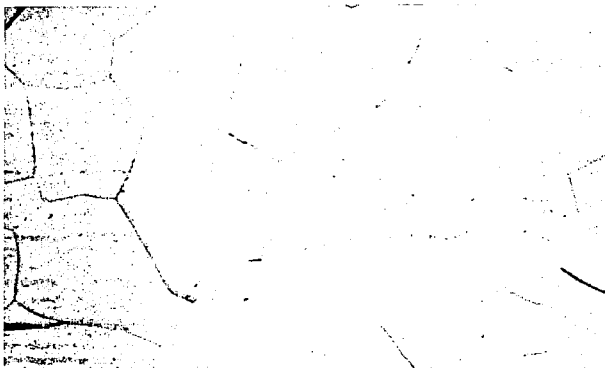


Base



Weld Edge

Annealed One Hour at 2700°F. Met. 9532, 500X



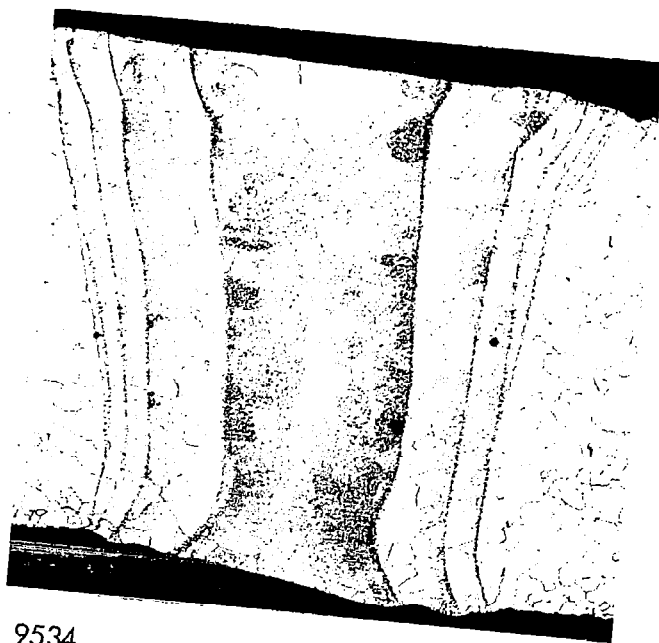
Base



Weld Edge

Annealed One Hour at 3000°F. Met. 9533, 500X

FIGURE A23 - Post Weld Annealed T-222 GTA Weld Microstructure

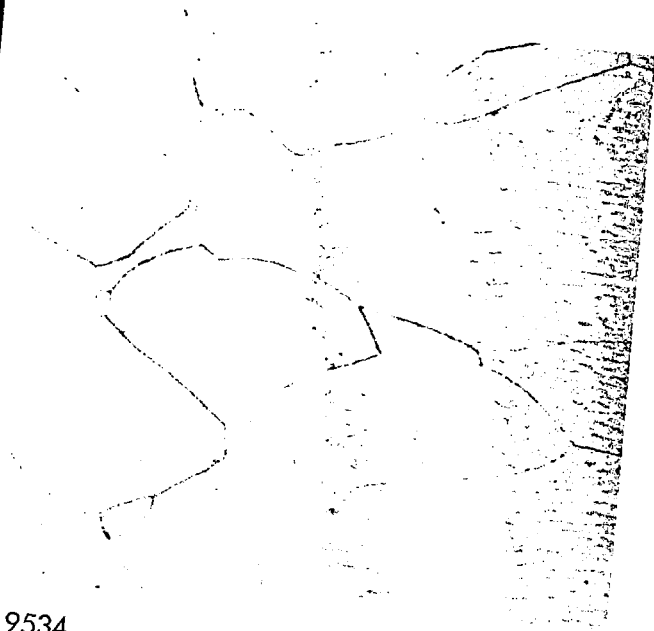


9534

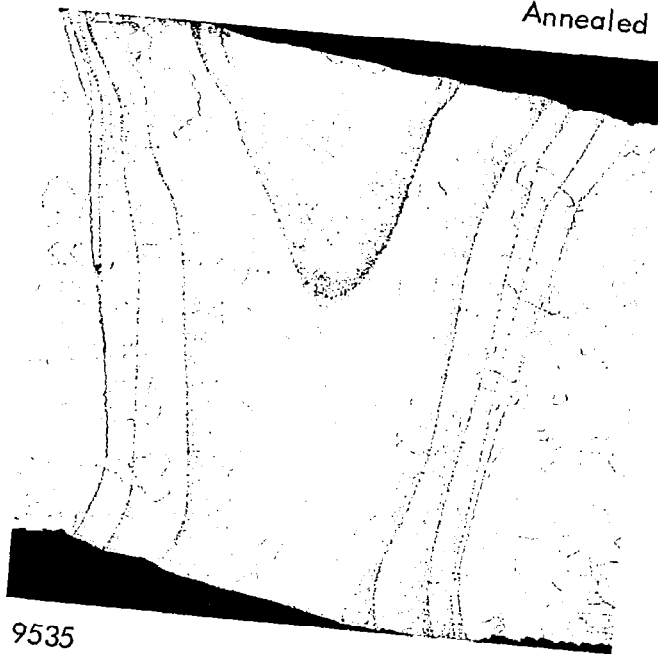
80X

9534

Annealed One Hour at 2400°F



500X

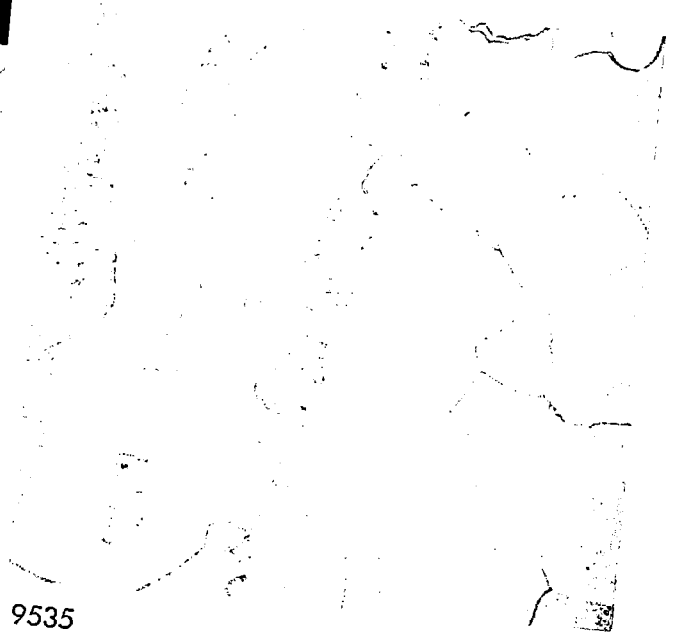


9535

80X

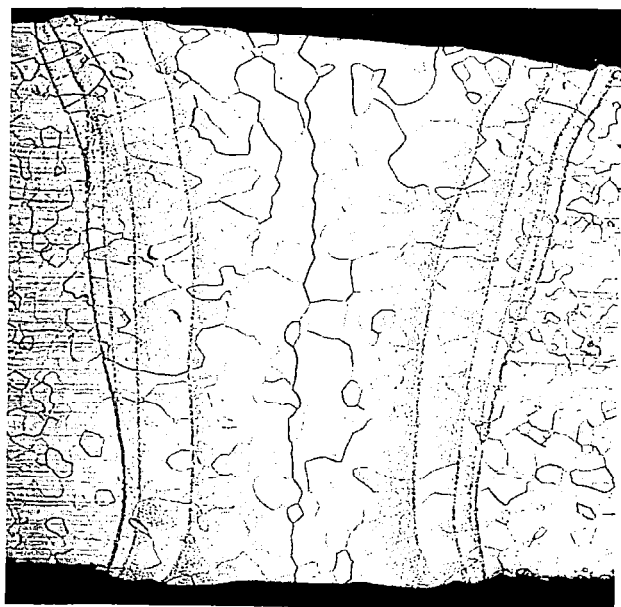
9535

Annealed One Hour at 2700°F



500X

FIGURE A24 - Post Weld Annealed T-222 EB Weld Microstructure



9536

80X



9536

500X

FIGURE A25 - Post Weld Annealed T-222 EB Weld Microstructure

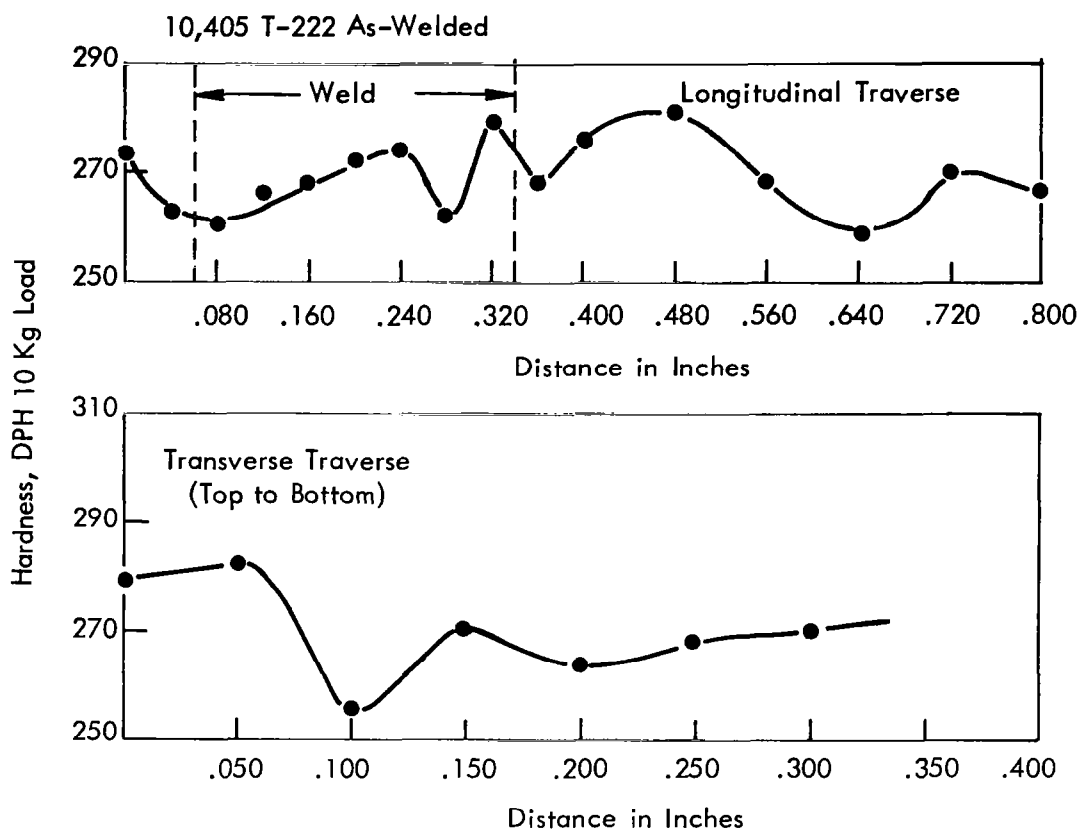


FIGURE A26 - T-222 Plate Weld Hardness Traverses

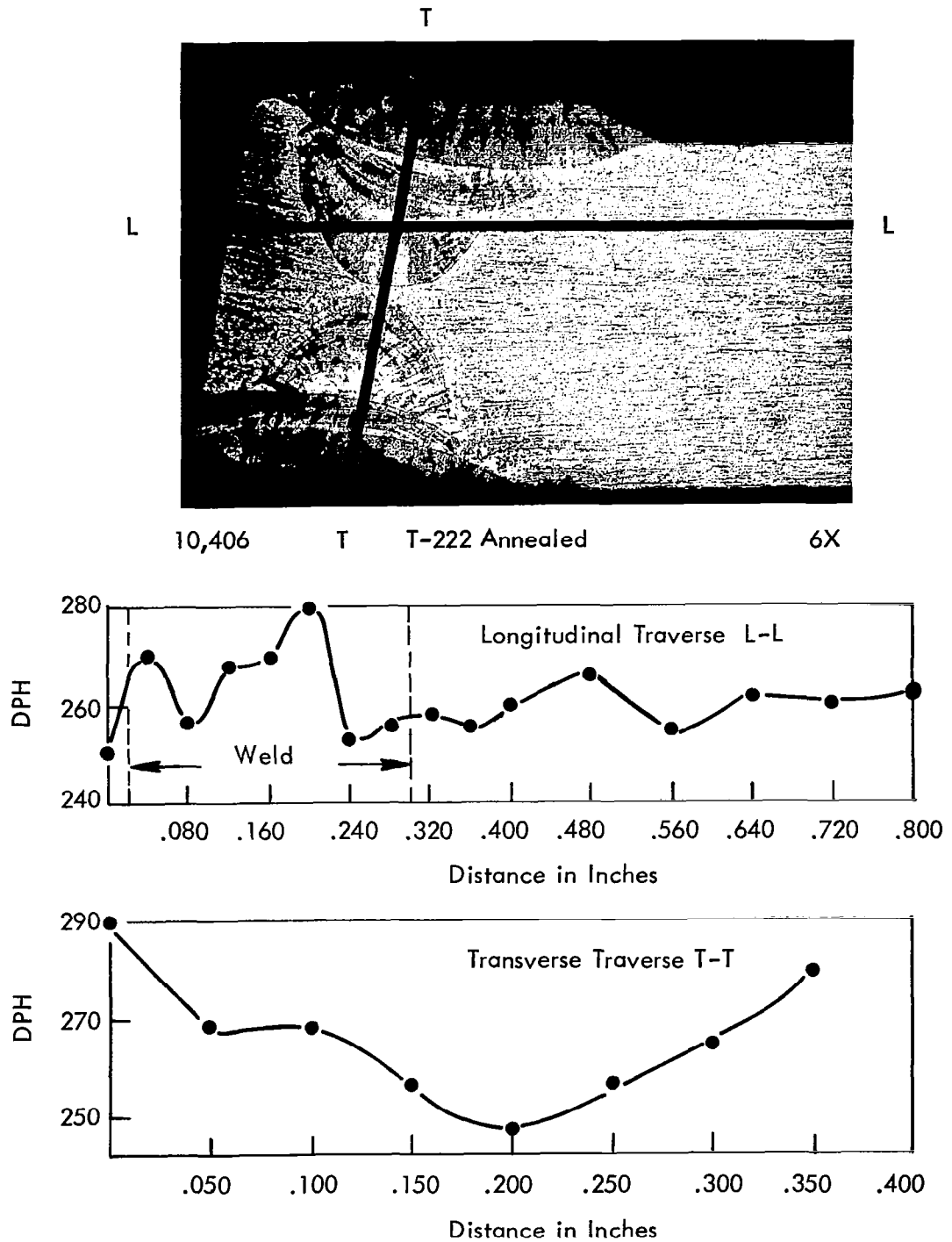
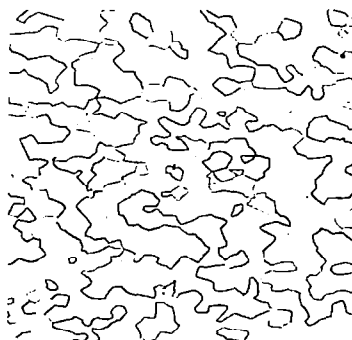
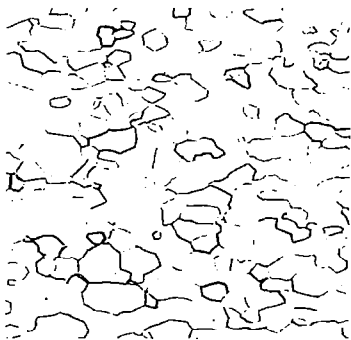


FIGURE A27 - T-222 Plate Weld Annealed One Hour at 2400°F

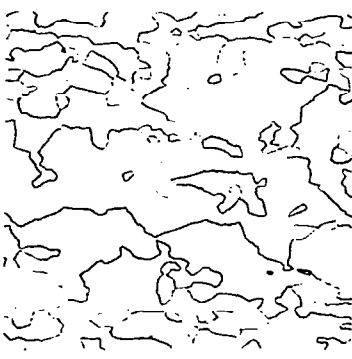
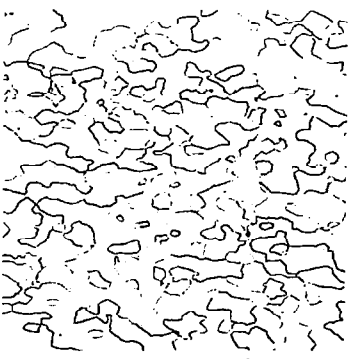
0.082"  
Wire



0.035"  
Sheet



0.375"  
Plate



Longitudinal

Transverse

FIGURE A28 - As-Received Microstructure of Ta-10W, 100X



TABLE A5 - T<sub>a</sub>-10W Sheet. GTA Butt Weld Record

Weld No.	Clamp Spacing (inch)	Speed (ipm)	Current Amperes	Weld Width Top/Bottom (inch)	Q Joules/Inch	Atmosphere Monitor Readings			Comments	
						O <sub>2</sub> (1) ppm	O <sub>2</sub> (2) ppm	H <sub>2</sub> O (3) ppm	Visual Inspection	Dye Check
1	3/8	15	115	0.180/0.180	7,800	--	3.5	3.0	Negative	Negative
2	3/4	15	90	0.160/0.150	6,110	--	3.5	4.5	Negative	Negative
3	1/4	15	90	0.135/0.080	6,110	4.5	4.6	2.3	Negative	Negative
4	1/4	30	126	0.125/0.075	4,295	5.0	3.6	2.6	Edge Flash (4)	Negative
5	1/4	7.5	80	0.120/0.082	11,500	--	2.4	0.4	Negative	Negative
6	1/4	7.5	73	0.190/0.180	17,450	5.0	4.0	4.8	Negative	Negative
7	3/8	7.5	118	0.165/0.144	12,910	--	2.6	5.2	Negative	Negative
8	1/4	15	167	0.195/0.189	13,350	--	2.7	0.3	Negative	Negative
9	1/4	30	215	0.1195/0.189	8,160	--	1.7	3.3	Negative	Negative
10	1/4	60	255	0.165/0.150	5,350	1.5	3.4	0.2	Negative	Negative
11	3/8	60	230	0.165/0.150	4,370	1.5	3.6	1.1	Negative	Negative
12	1/4	60	215	0.150/0.096	4,080	1.5	3.7	1.2	Negative	Negative

(1) Westinghouse Oxygen Gage  
(2) Lockwood & McLorie Oxygen Gage

(3) CEC Moisture Monitor  
(4) Instantaneous Arcing to Weld Clamp Down

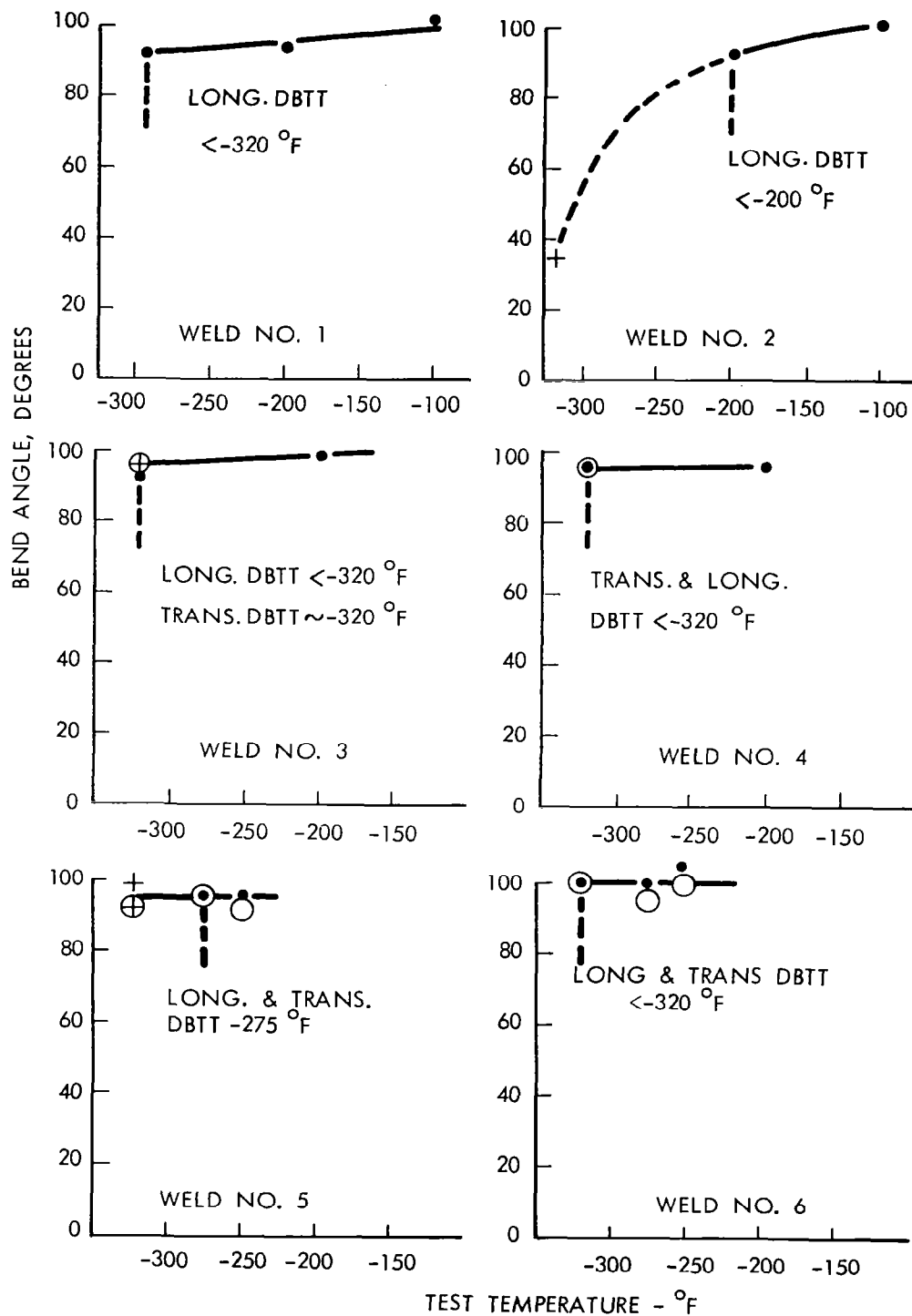


FIGURE A29 - Bend Test Results for Ta-10W GTA Welds  
1t Bend Radius

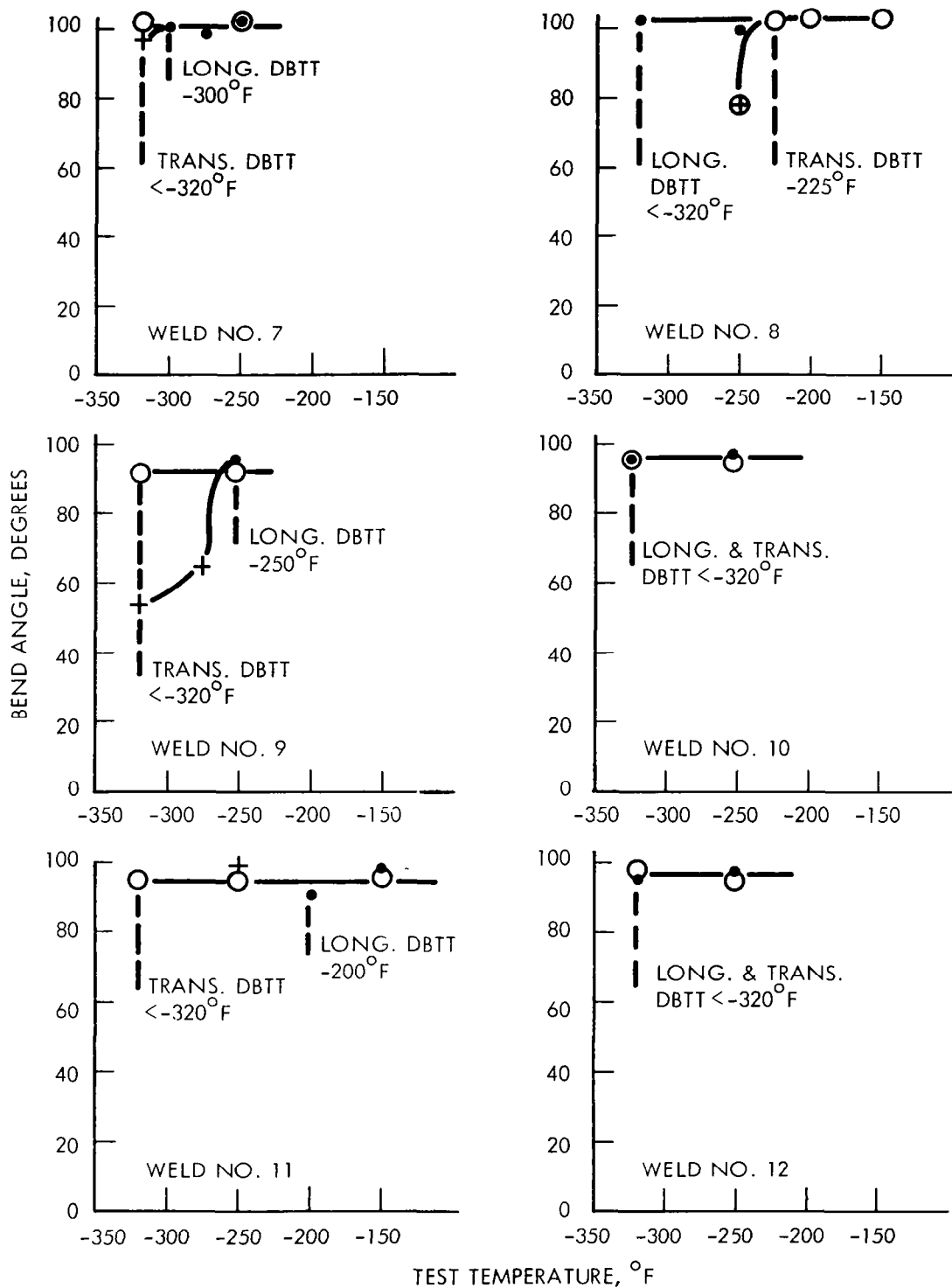


FIGURE A30 - Bend Test Results for Ta-10W GTA Welds  
1t Bend Radius

TABLE A6 - Ta-10W Sheet. EB Butt Weld Record

Weld No.	Speed (ipm)	Deflection <sup>1</sup> (inches)	Current (ma)	Chill Spacing (inches)	Power (watts)	Watt-Sec. per inch	Weld Bead Width (inches)		Vacuum <sup>2</sup> (Torr)
							Top	Bottom	
1	100		6.6	0.250	900	540	0.030	0.015	$9 \times 10^{-6}$
2	100	L-0.050"	8.2	→	1130	680	0.025	0.020	$9 \times 10^{-6}$
3	50	L-0.050"	5.0		750	900	0.055	0.040	$1.9 \times 10^{-6}$
4	25	L-0.050"	5.0		750	1800	0.060	0.055	$1.4 \times 10^{-6}$
5	15	L-0.050"	4.5	0.250	675	2700	0.065	0.050	$1.4 \times 10^{-6}$
6	15	T-0.050"	4.4		600	2400	0.070	0.060	$2 \times 10^{-5}$
7	100		6.6	0.094	900	540	0.020	0.010	$1 \times 10^{-5}$
8	100	L-0.050"	8.2	→	1130	680	0.030	0.030	$1 \times 10^{-5}$
9	50	L-0.050"	5.5		825	990	0.040	0.020	$1 \times 10^{-5}$
10	25	L-0.050"	5.5		825	1980	0.048	0.025	$8 \times 10^{-6}$
11	15	L-0.050"	5.5	0.094	825	3300	0.040	0.032	$5 \times 10^{-6}$
12	15	T-0.050"	4.9		740	2960	0.070	0.062	$5 \times 10^{-6}$

1. L is longitudinal  
T is transverse  
See Figure 14

2. Current evacuation practice provides pressures of  $1.5 \times 10^{-6}$  Torr

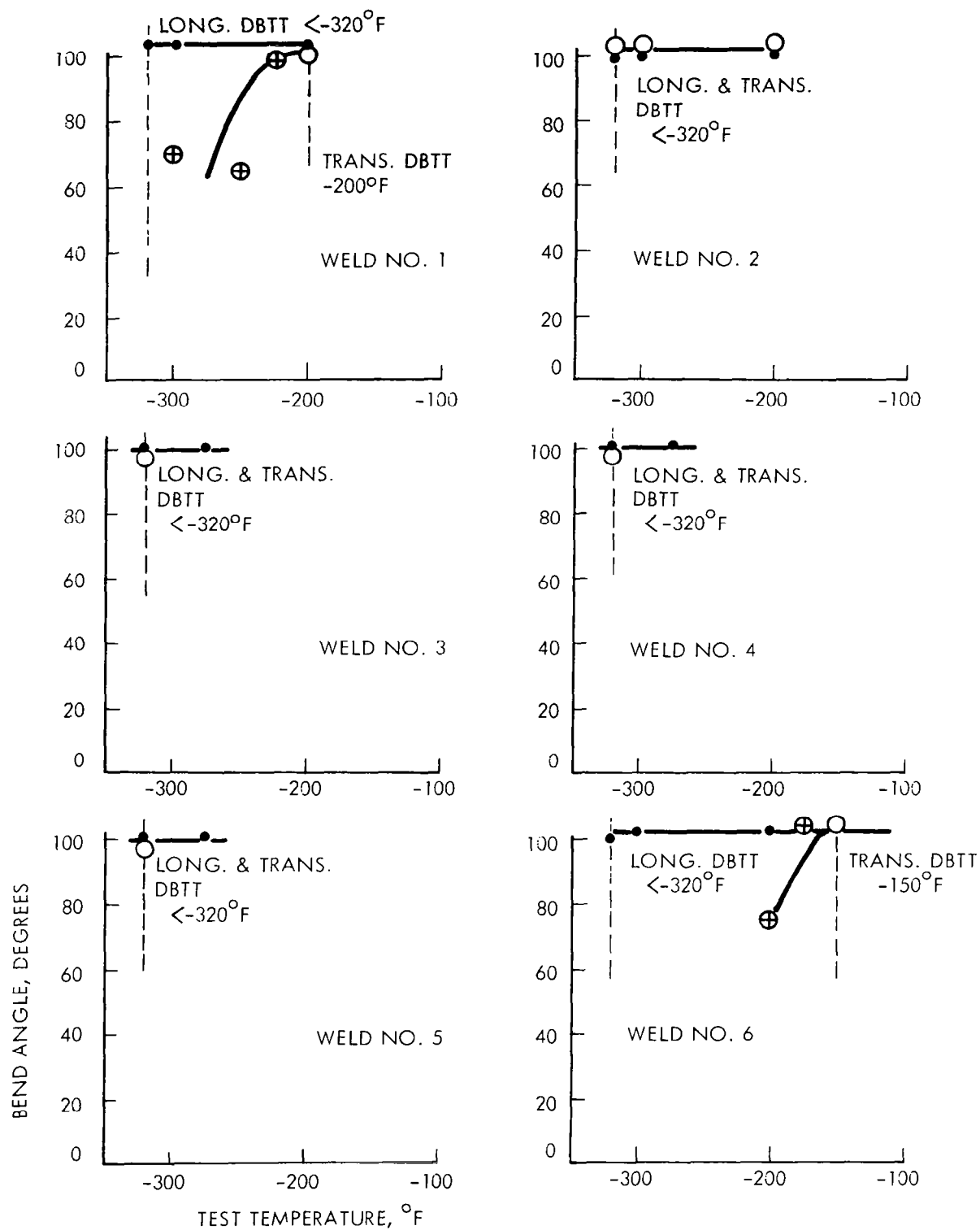


FIGURE A31 - Bend Test Results for Ta-10W EB Welds  
1t Bend Radius

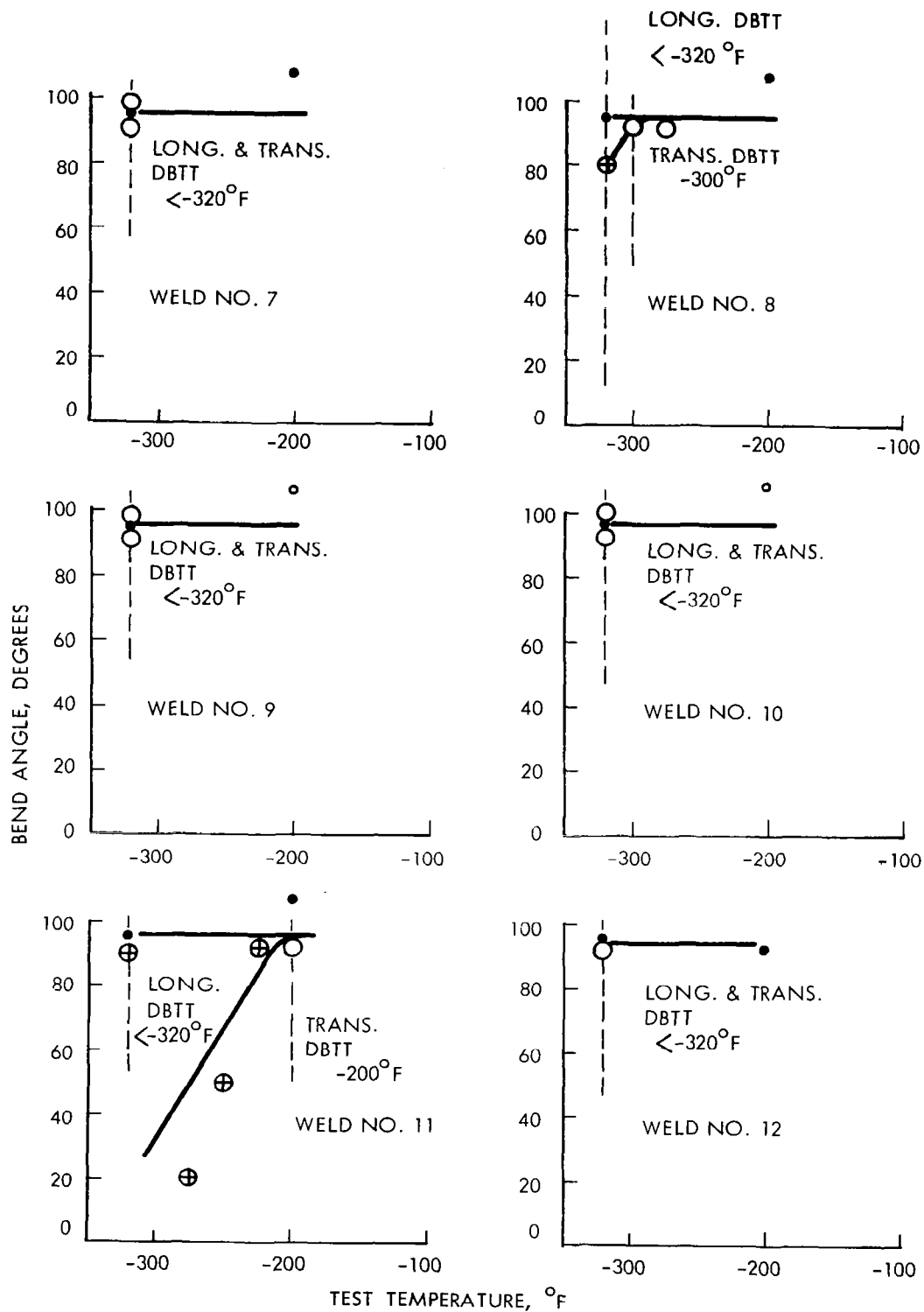


FIGURE A32 - Bend Test Results for Ta-10W EB Welds  
1t Bend Radius

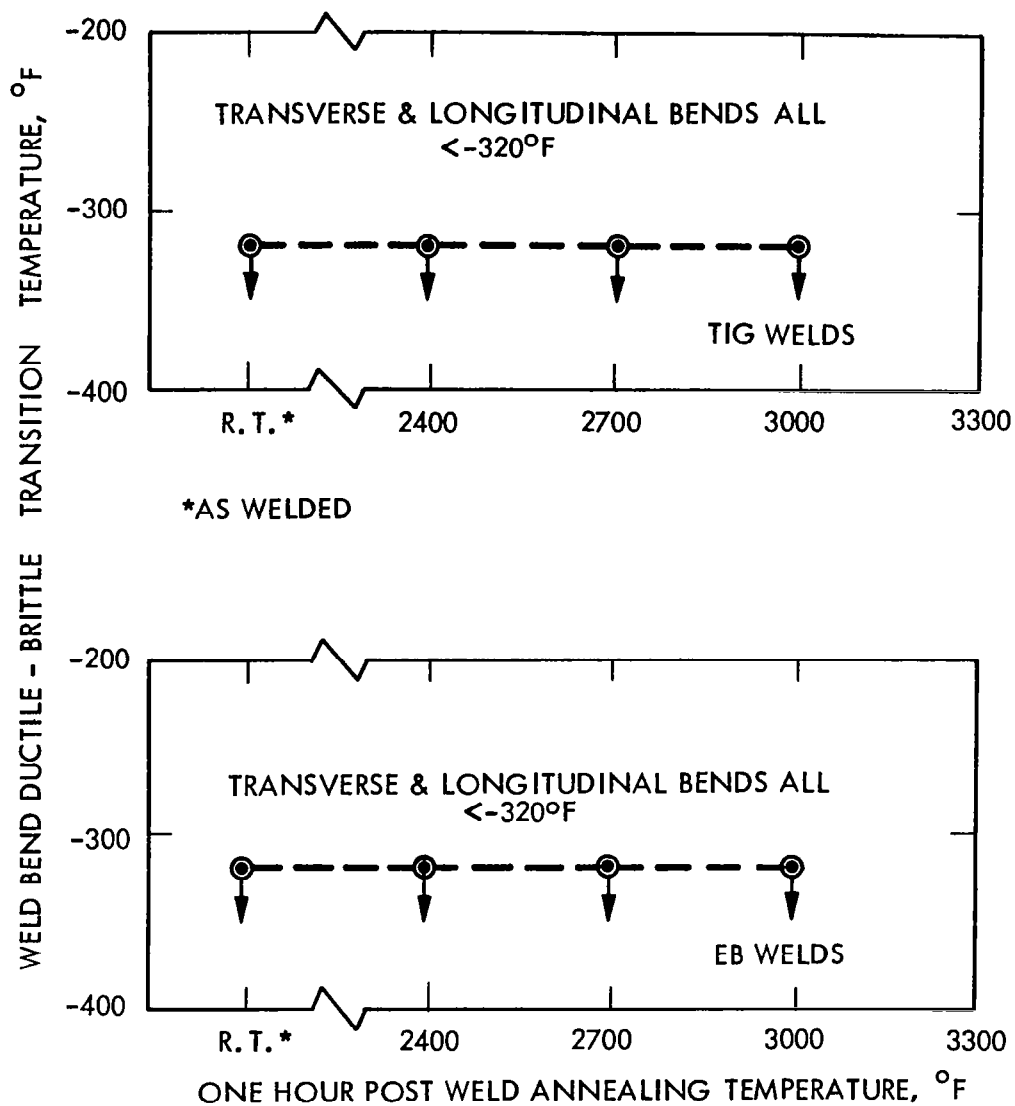


FIGURE A33 - Effect of Post Weld Annealing on Ta-10W Weld Ductility

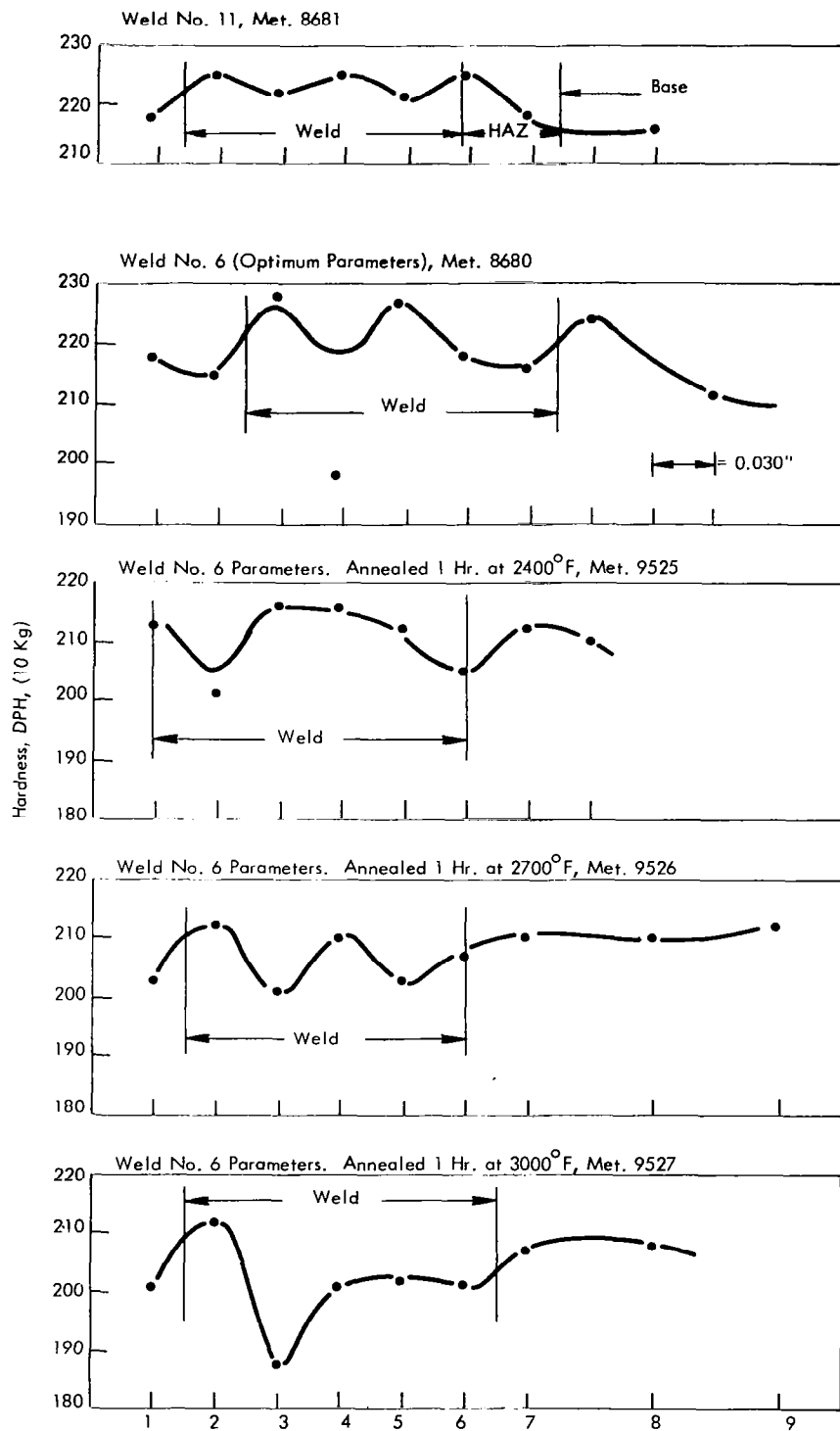
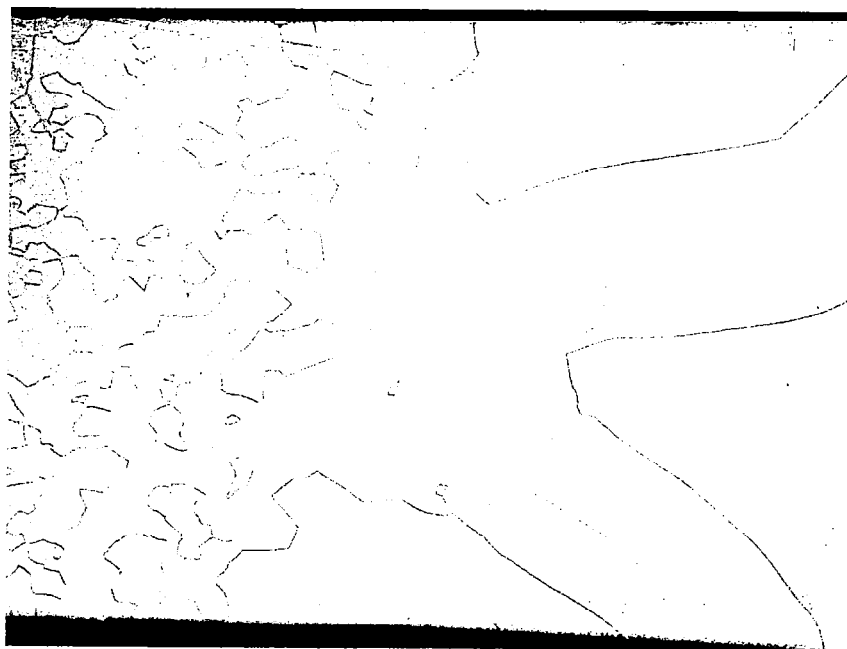


FIGURE A34 - Hardness Traverses in Ta-10W GTA Welds

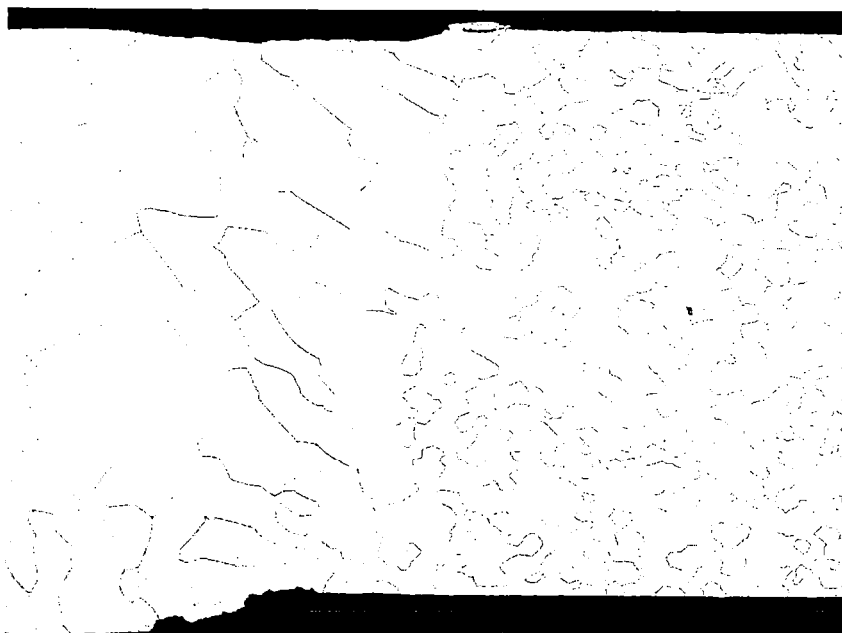




8680

GTA Weld No. 6

100X

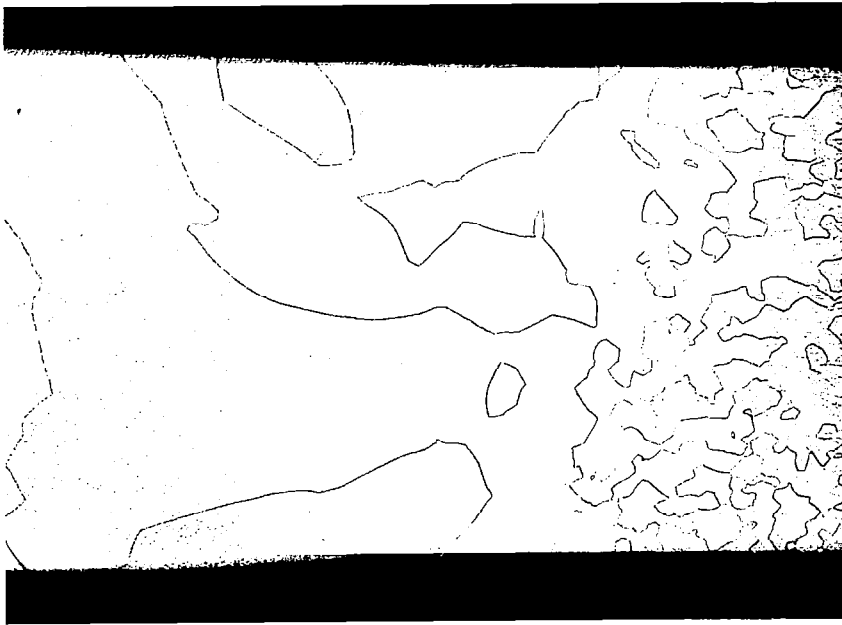


9176-1

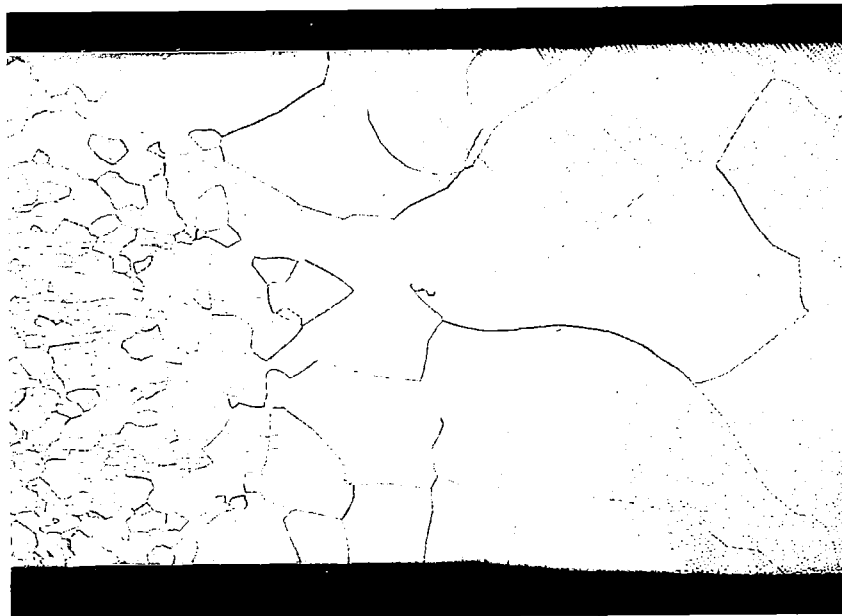
EB Weld No. 6

80X

FIGURE A35 - Ta-10W Sheet Weld Microstructure at Weld Edge  
(Clean Structured Weld Typical of Both GTA & EB Welds)



9525      Annealed One Hour at 2400°F      80X

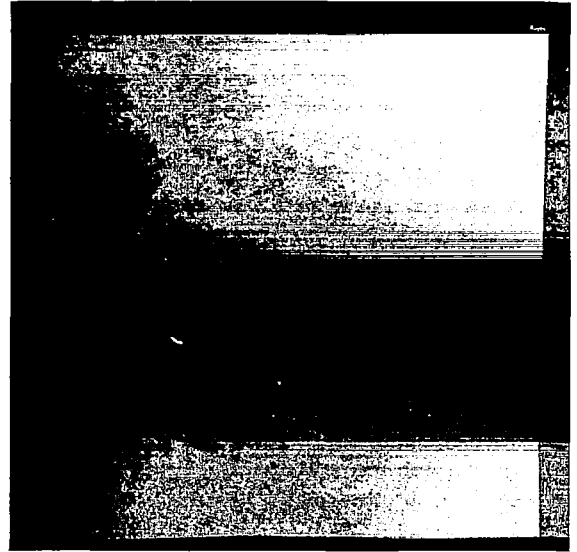


9527      Annealed One Hour at 3000°F      80X

FIGURE A36 - Post Weld Annealed Ta-10W Weld Microstructure at Weld Edge,  
GTA Weld No. 6 Parameters

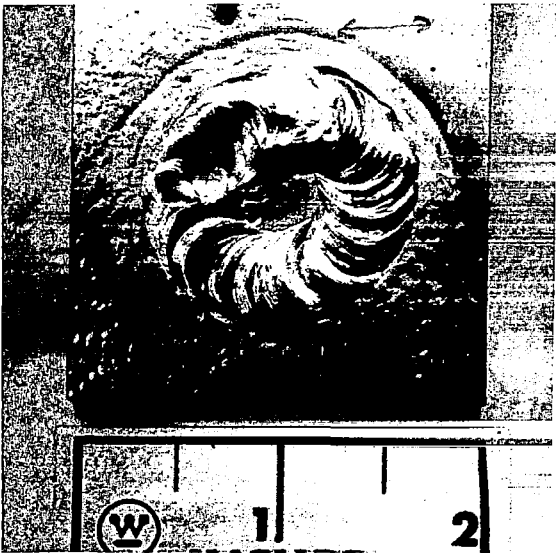


As-Welded Patch Test 43650

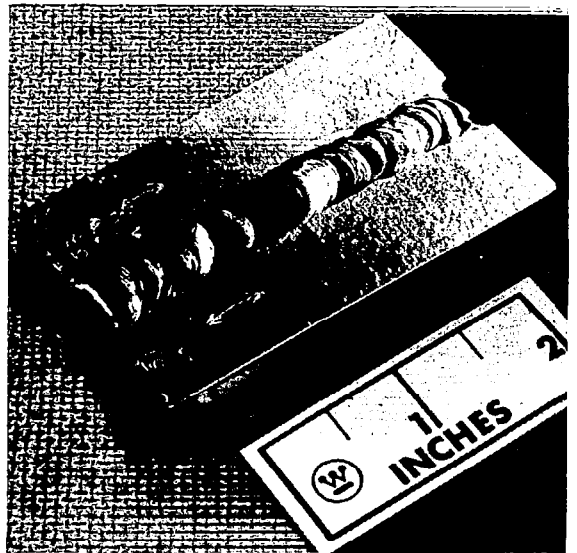


Dye Penetrant Inspected 43650

0.035 Sheet



Welded Circular Groove 43650



Butt Weld Specimen 126-3

0.375 Plate

FIGURE A37 - Ta-10W Weldability Qualification Tests

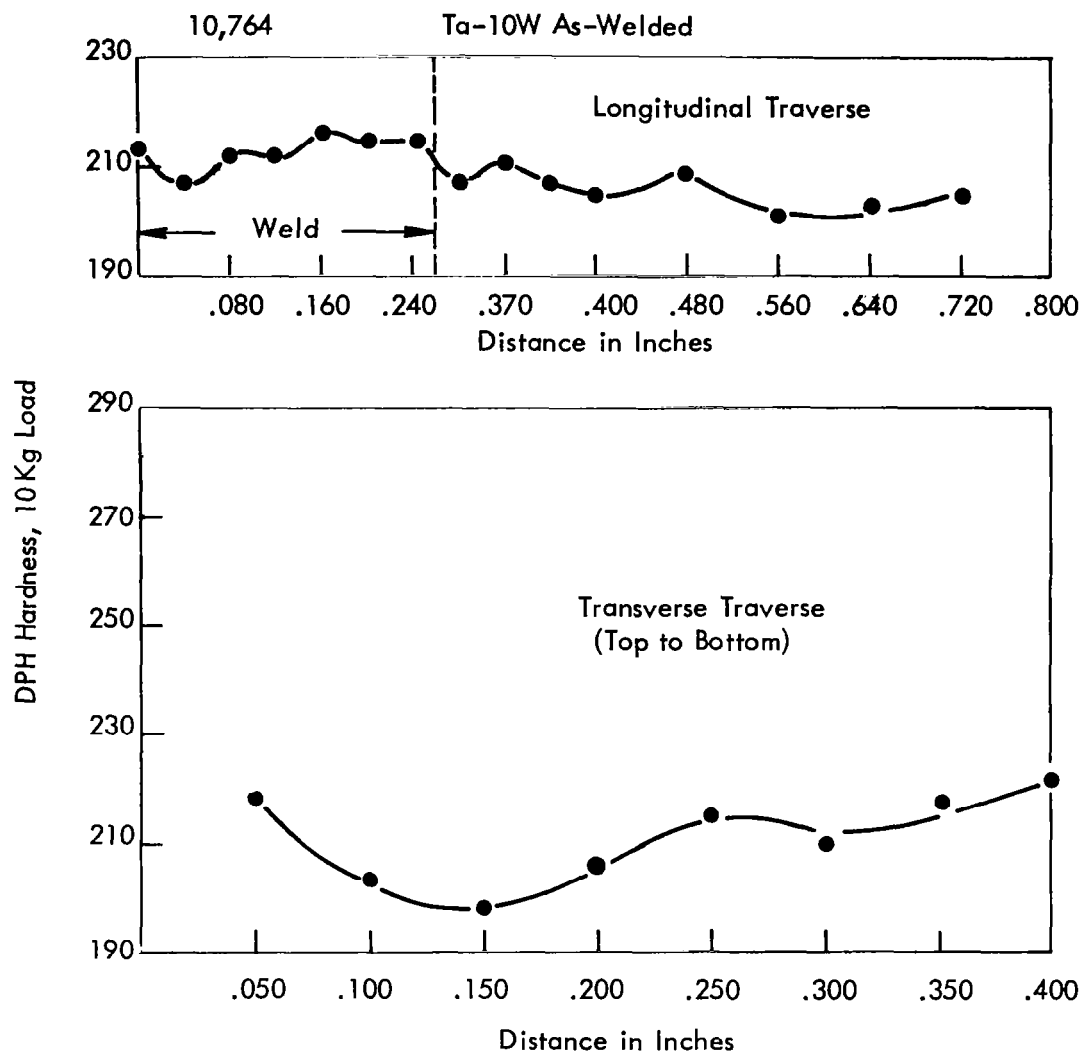
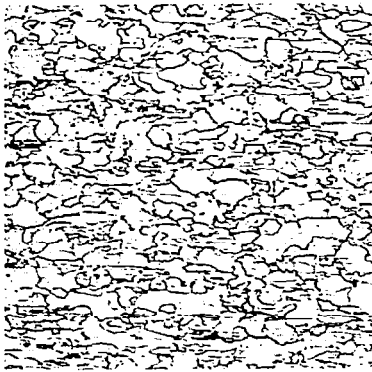
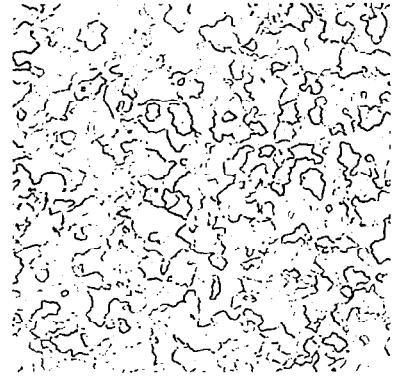


FIGURE A38 - Ta-10W Plate Weld Hardness Traverses

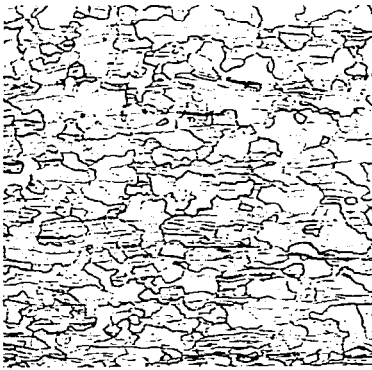


3742

0.082" Wire

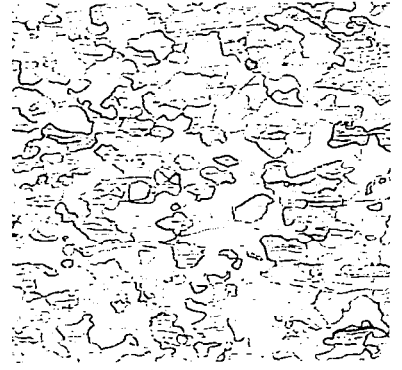


3743

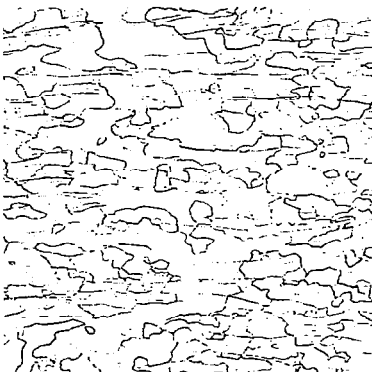


3740

0.035" Sheet



3741



5370

0.375" Plate

Longitudinal



5371

Transverse

FIGURE A39 - As-Received Microstructure of FS-85 100X

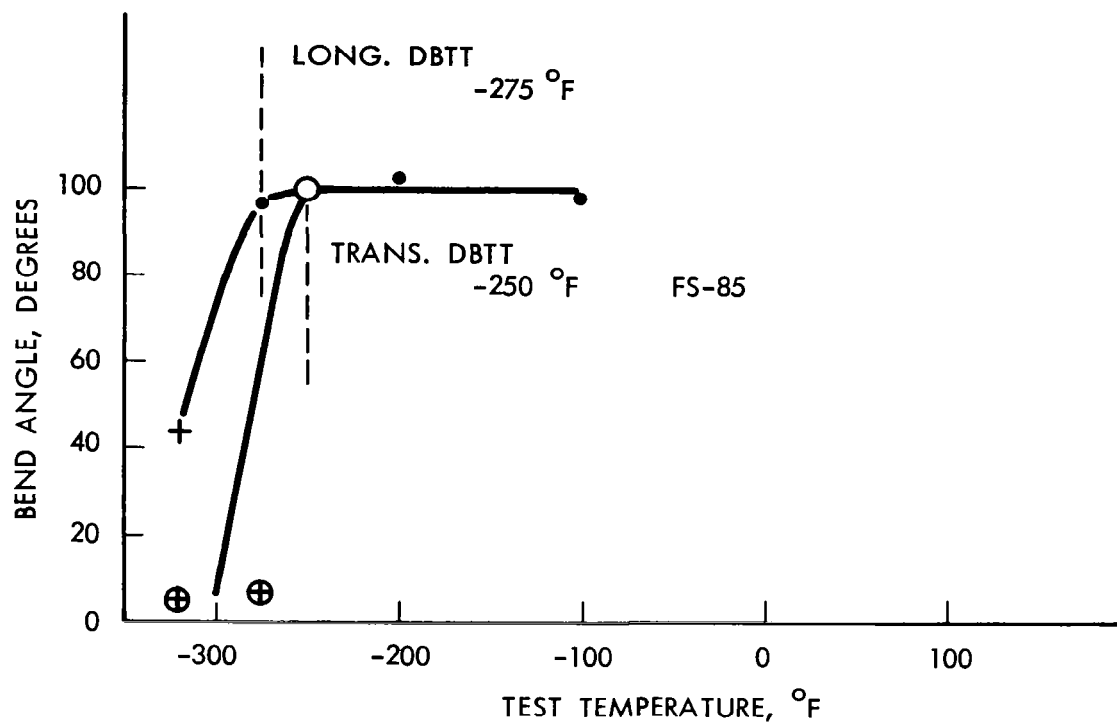


FIGURE A40 - FS-85 Sheet Base Metal Bend Test Results

TABLE A7 - FS-85 Sheet. GTA Butt Weld Record

Weld No.	Clamp Spacing (inch)	Speed (ipm)	Current Amperes	Weld Width Top/Bottom (inch)	Joules/Inch Q	Atmosphere Monitor Readings			Comments	
						O <sub>2</sub> (1) ppm	O <sub>2</sub> (2) ppm	H <sub>2</sub> O (3) ppm	Visual Inspection	Dye Check
1	3/8	15	70	0.14/0.11	4,770	4.5	--	1.8	Negative	Negative
2	3/8	30	110	0.17/0.15	3,730	4.5	--	1.9	Negative	1/16" HAZ Crack
3	1/4	15	85	0.15/0.135	5,800	4.0	6.2	0.5	Edge Flash (4)	Negative
4	1/4	30	104	0.135/0.110	3,540	4.5	5.5	0.6	Edge Flash (4)	Negative
5	1/4	7.5	64	0.120/0.080	9,460	3.0	4.0	1.7	Negative	Negative
6	3/8	7.5	75	0.190/0.190	10,800	3.5	4.6	1.9	Negative	Negative
7	3/8	15	95	0.204/0.195	7,030	2.2	4.6	2.5	Negative	Negative
8	3/8	30	85	0.11/0.060	3,140	2.3	4.6	2.7	Negative	Negative
9	1/4	30	169	0.216/0.216	6,410	1.0	3.4	2.5	Negative	Negative
10	1/4	60	155	0.117/0.060	3,865	0.5	3.2	3.2	Negative	Negative
11	1/4	60	210	0.17/0.17	3,880	1.4	--	1.4	Negative	Negative
12	3/8	60	185	0.168/0.15	3,420	--	2.3	0.3	Negative	Negative

(1) Westinghouse Oxygen Gage

(2) Lockwood &amp; McLorie Oxygen Gage

(3) CEC Moisture Monitor

(4) Instantaneous Arcing to Weld Clamp Down

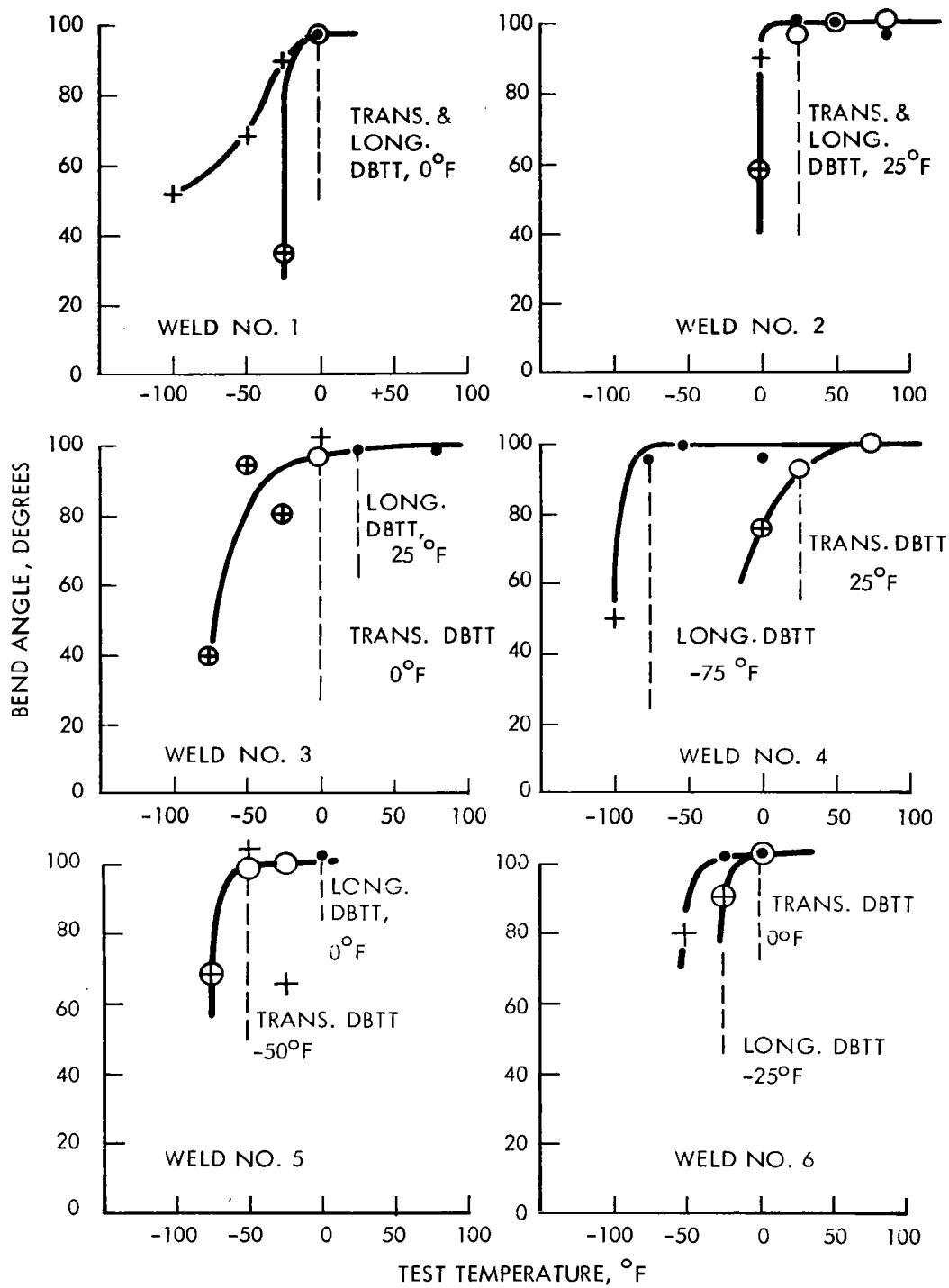


FIGURE A41 - Bend Test Results for FS-85 GTA Welds  
2t Bend Radius



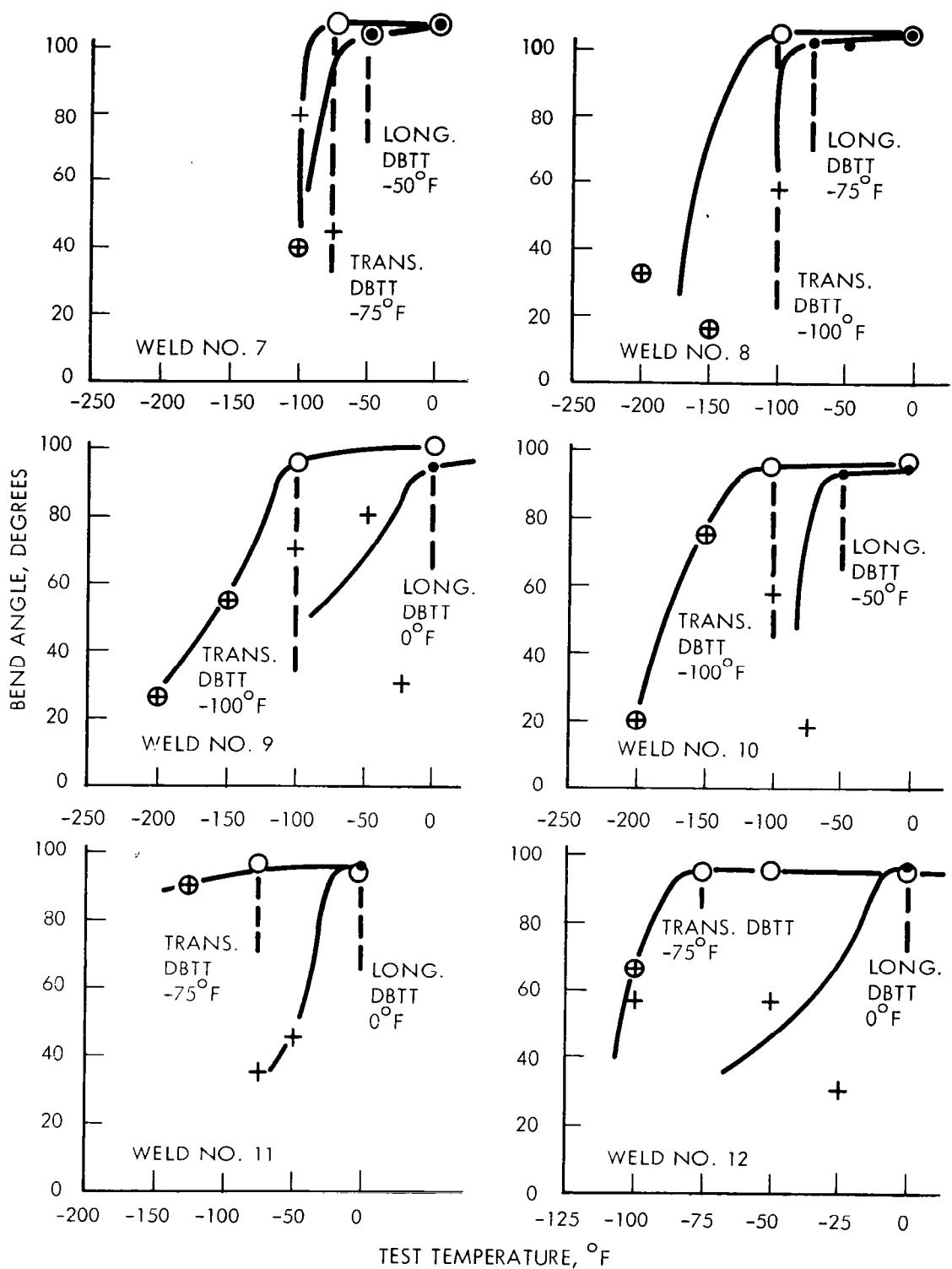





FIGURE A42 - Bend Test Results for FS-85 GTA Welds

TABLE A8 - FS-85 Sheet. EB Butt Weld Record

Weld No.	Speed (ipm)	Deflection <sup>1</sup> (inches)	Current (ma)	Chill Spacing (inches)	Power (watts)	Watt-Sec. per inch	Weld Bead Width (inches)		Vacuum <sup>2</sup> (Torr)
							Top	Bottom	
1	100		5.0	0.250	750	450	0.027	0.020	$6 \times 10^{-6}$
2	100	L-0.050"	5.5		825	495	0.038	0.027	$6 \times 10^{-6}$
3	50	L-0.050"	4.4		660	790	0.045	0.027	$6 \times 10^{-6}$
4	25	L-0.050"	3.8		570	1370	0.047	0.037	$6 \times 10^{-6}$
5	15	L-0.050"	3.8		570	2280	0.049	0.040	$6 \times 10^{-6}$
6	15	T-0.050"	3.8		570	2280	0.070	0.060	$6 \times 10^{-6}$
7	100		5.0		750	450	0.027	0.020	$6 \times 10^{-6}$
8	100	L-0.050"	5.5		825	495	0.036	0.025	$6 \times 10^{-6}$
9	50	L-0.050"	4.4		660	790	0.038	0.026	$6 \times 10^{-6}$
10	25	L-0.050"	3.8		570	1370	0.040	0.027	$6 \times 10^{-6}$
11	15	L-0.050"	3.8		570	2280	0.038	0.027	$6 \times 10^{-6}$
12	15	T-0.050"	3.8		570	2280	0.060	0.050	$6 \times 10^{-6}$

1. L is longitudinal All Welds Made at 150 KV, Optical Focusing

T is transverse

See Figure 14

2. Current evacuation practice provides pressures of  $1.5 \times 10^{-6}$  Torr

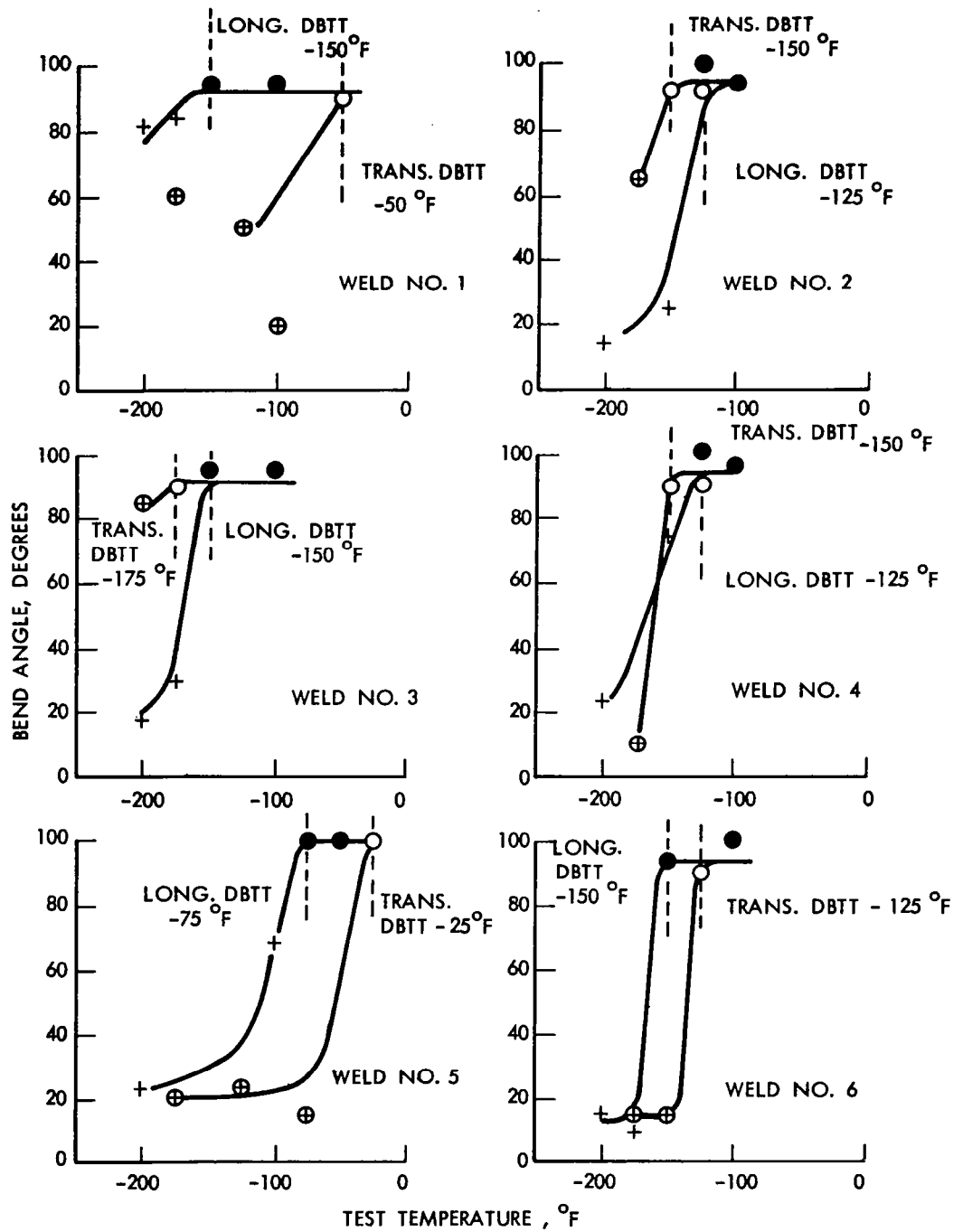


FIGURE A43 - Bend Test Results for FS-85 EB Welds

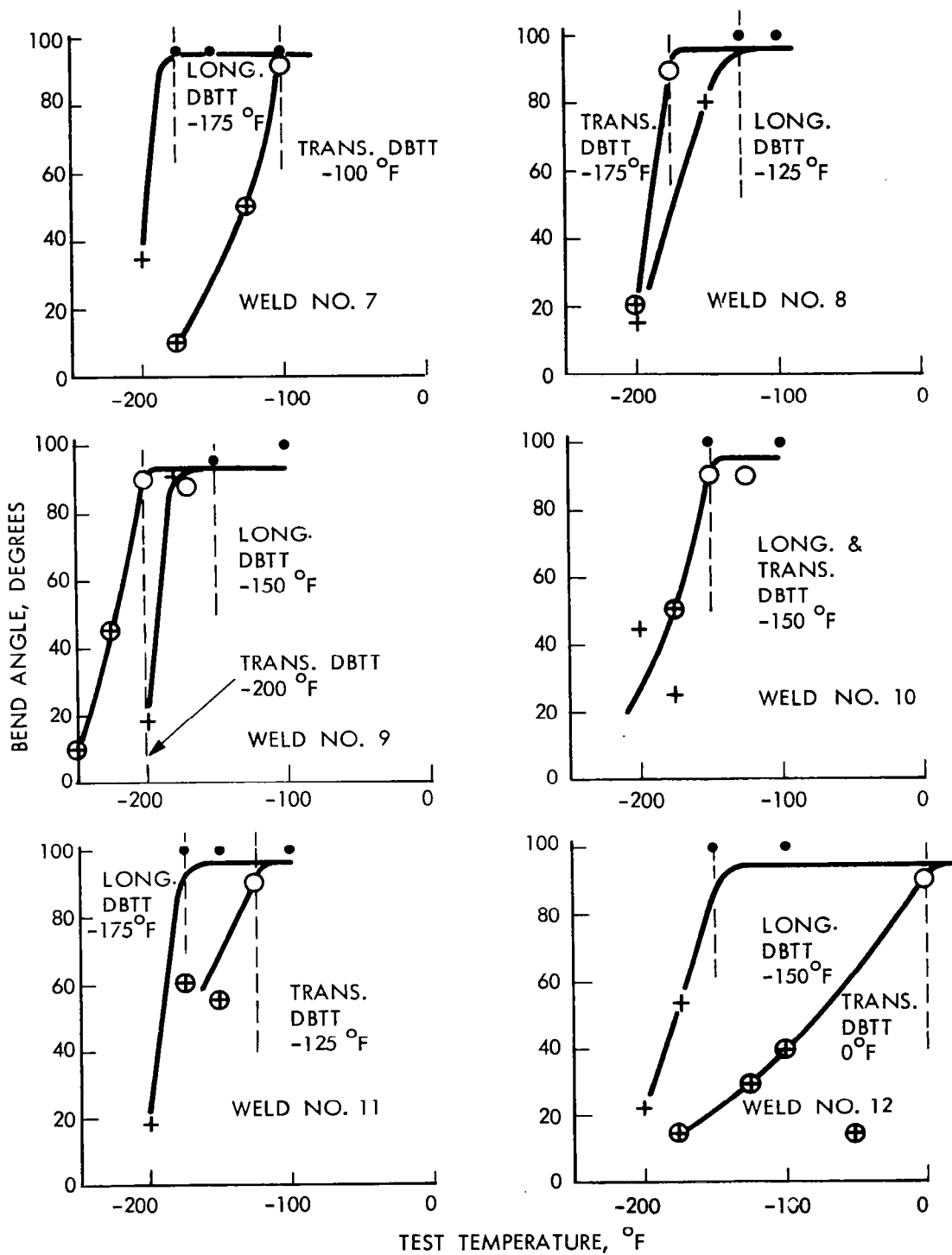


FIGURE A44 - Bend Test Results for FS-85 EB Welds

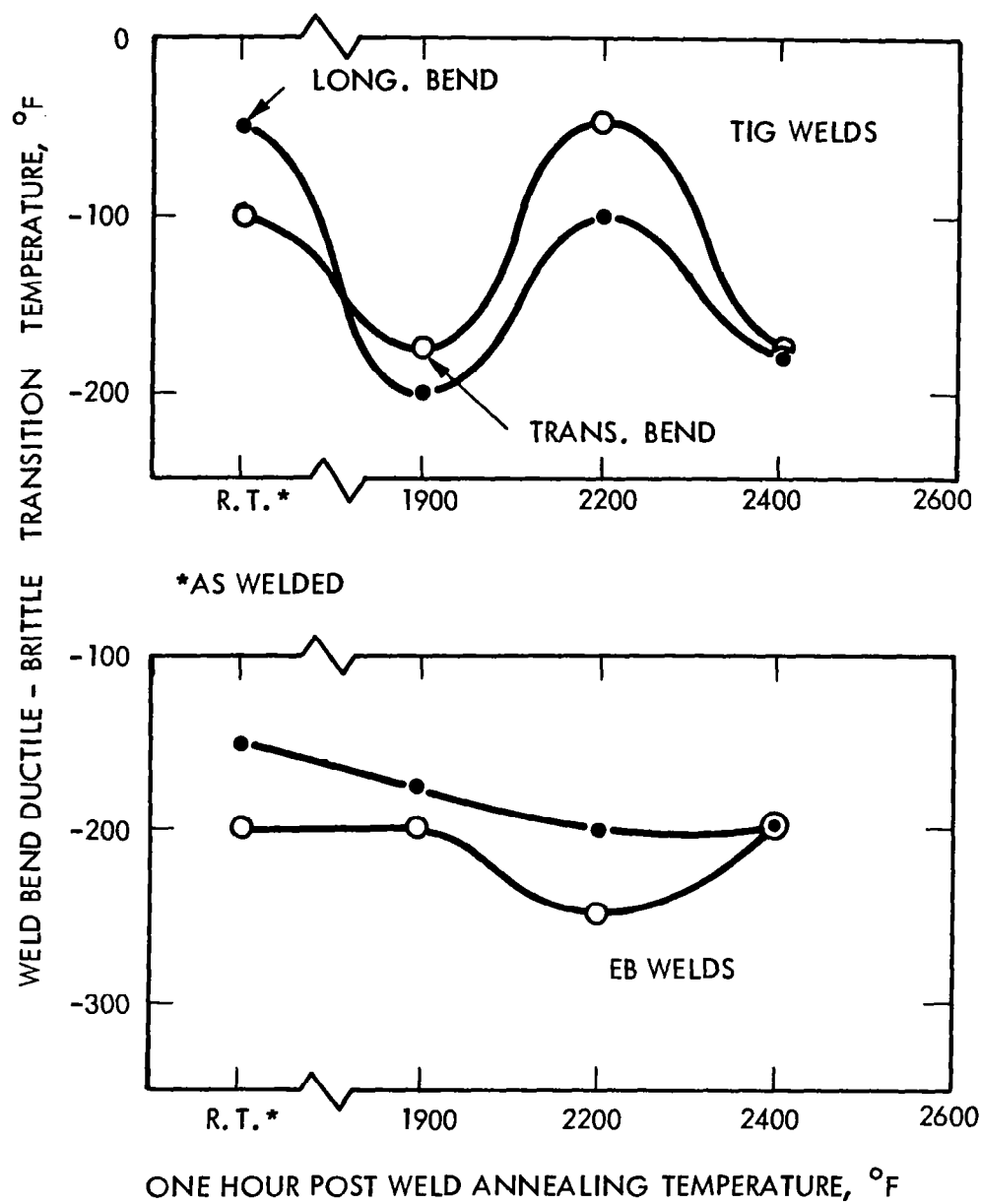


FIGURE A45 - Effect of Post-Weld Annealing on FS-85 Weld Ductility

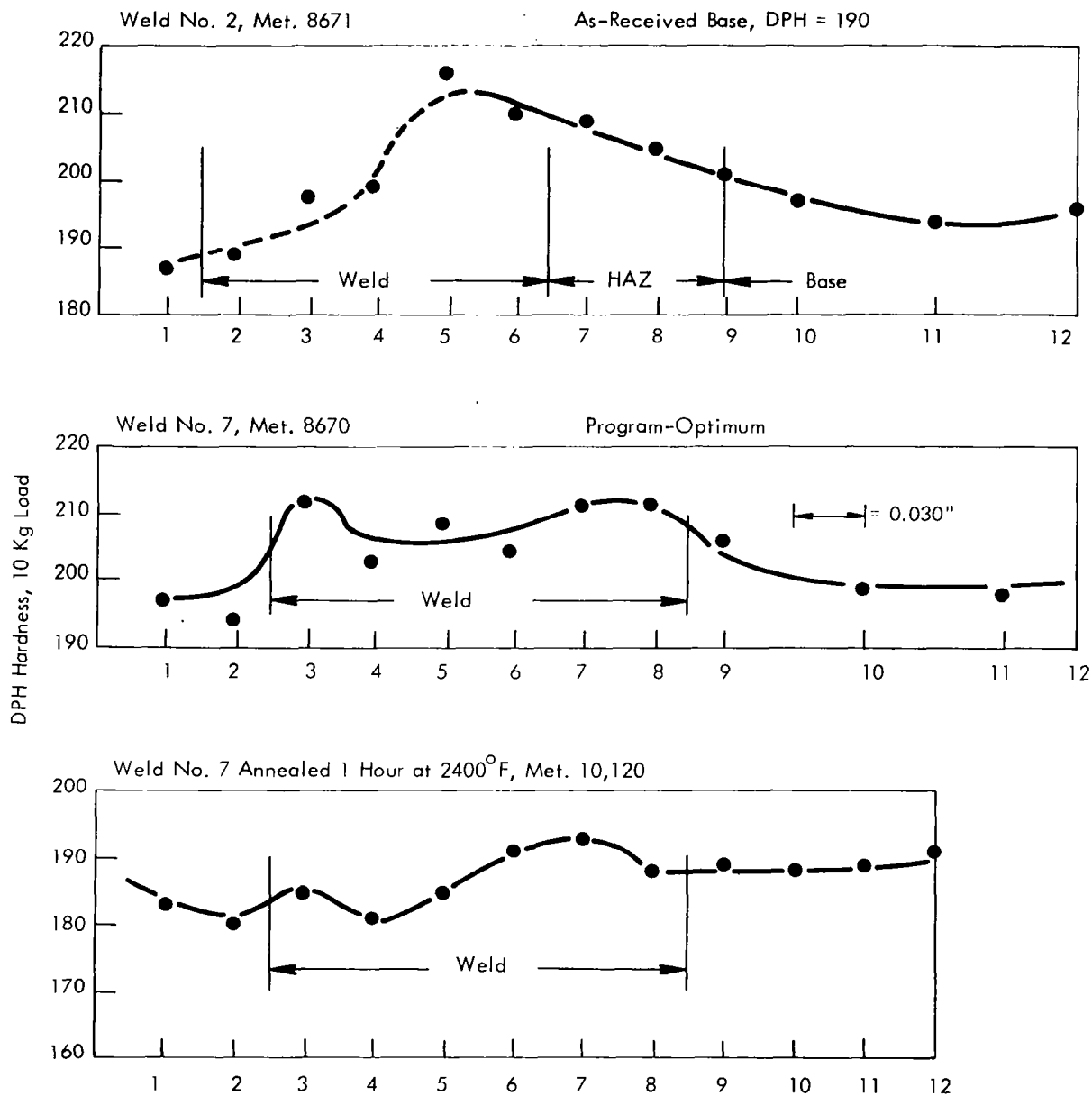


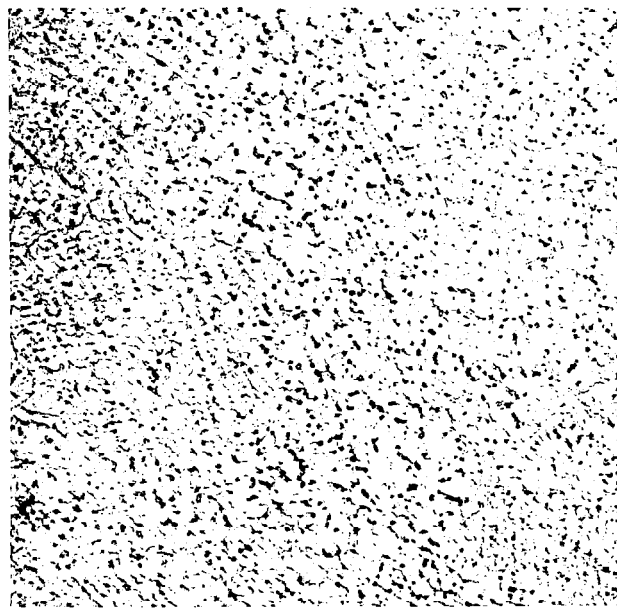
FIGURE A46 - Hardness Traverses of FS-85 Sheet GTA Butt Welds  
(183 & 183 DPH for Annealed EB Weld)



8670

Weld

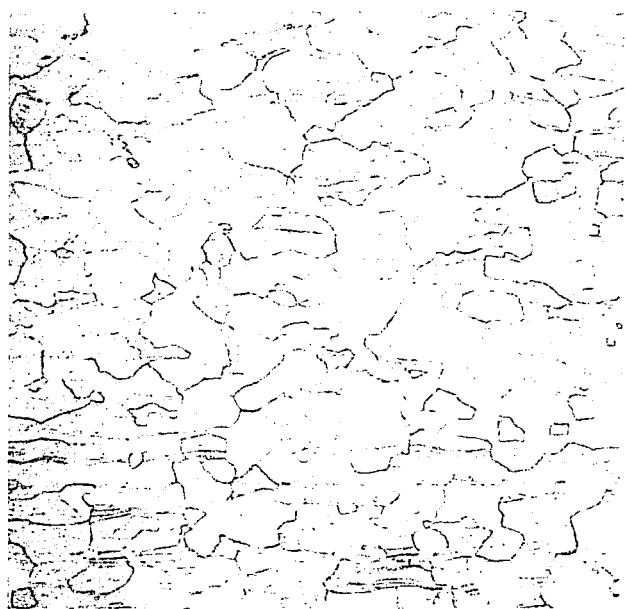
200X



10,120

Weld

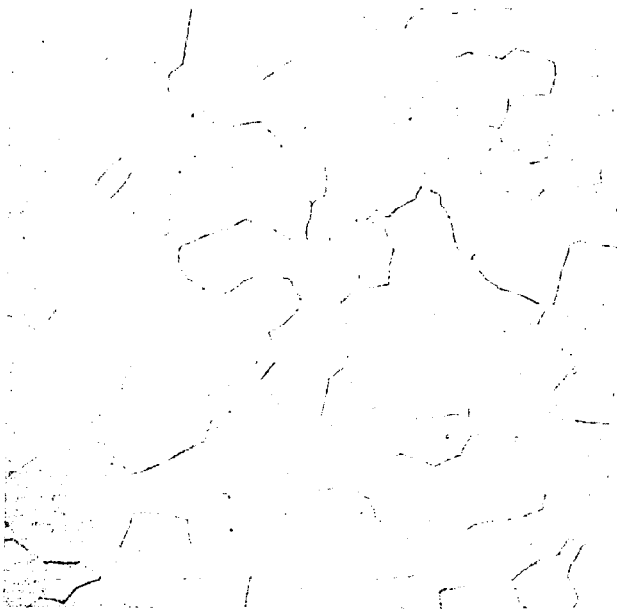
200X



8670

Base

200X

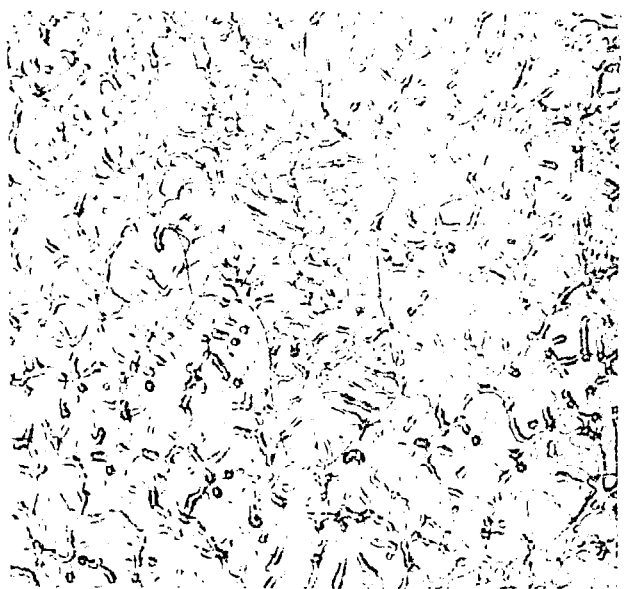


10,120

HAZ

200X

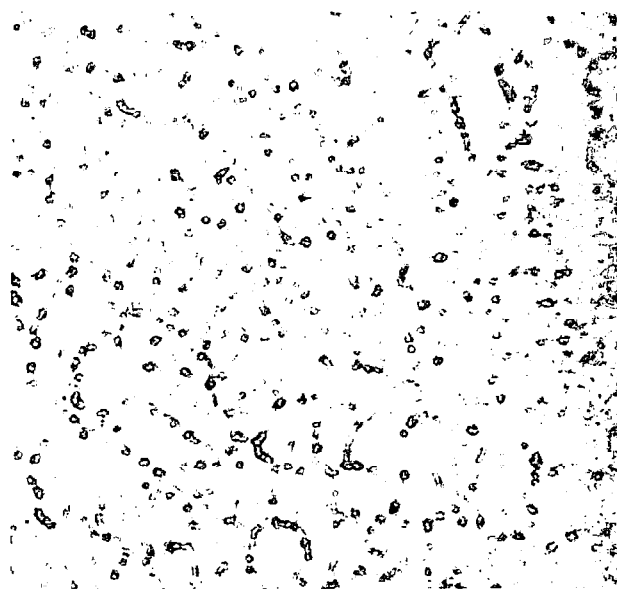
FIGURE A47 - FS-85 GTA Sheet Weld Microstructure. As-Welded, Left. Annealed 1 Hour at 2400°F, Right. Clean, Largely Single Phase Throughout.



10,118

Weld

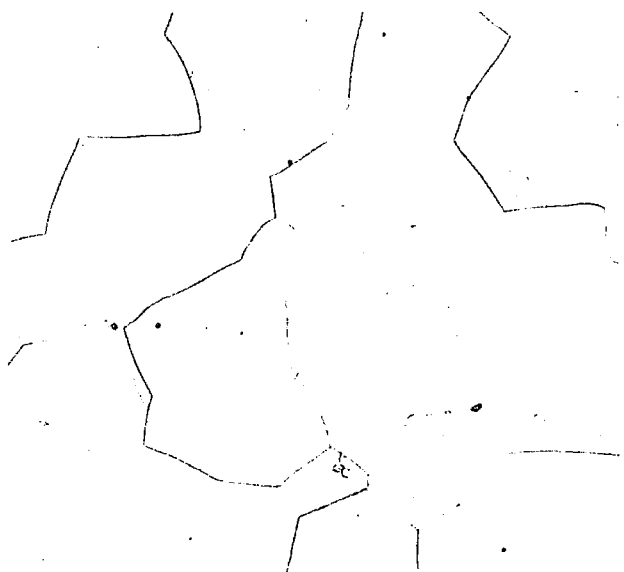
400X



10,119

Weld

400X



10,118

HAZ

400X



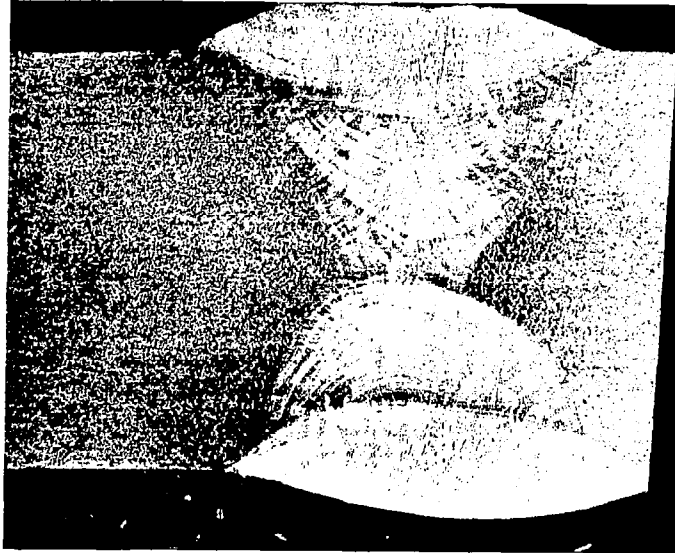
10,119

HAZ

200X

FIGURE A48 - FS-85 GTA Sheet Weld Microstructure. Annealed 1 Hour at 1900°F, Left. Annealed 1 Hour at 2200°F, Right.



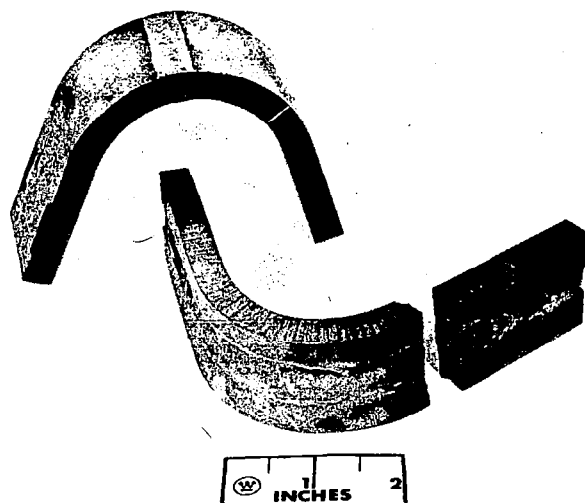


10,181

6X

FS-85

FIGURE A49 - FS-85 Plate Weld Macrosection



FS-85

427-6

125° Longitudinal Bend  
145° Transverse Bend

FIGURE A50 - FS-85 Plate Weld Bend Specimens

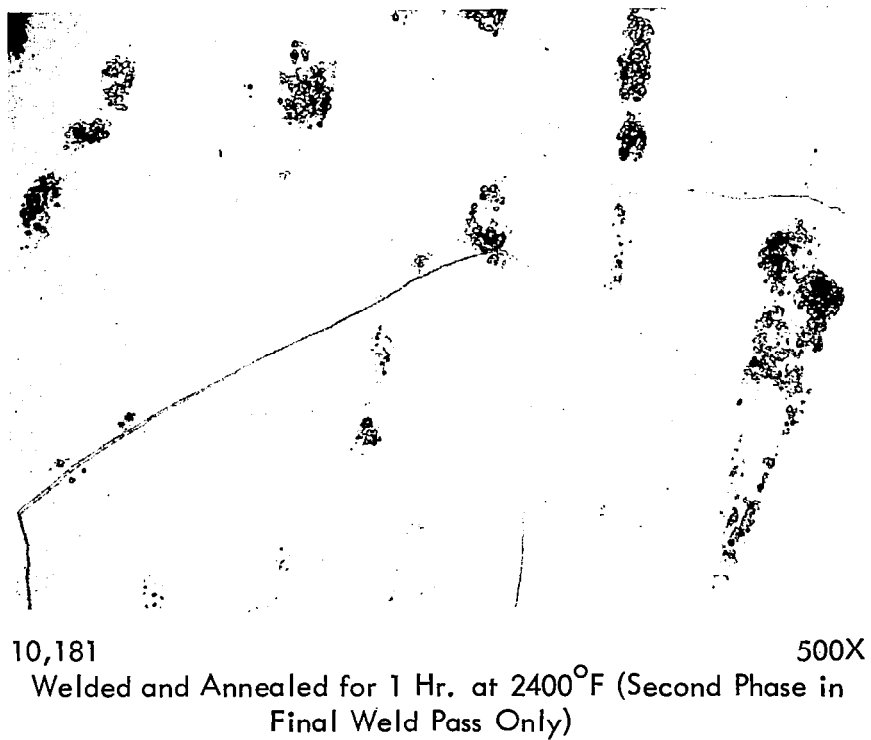
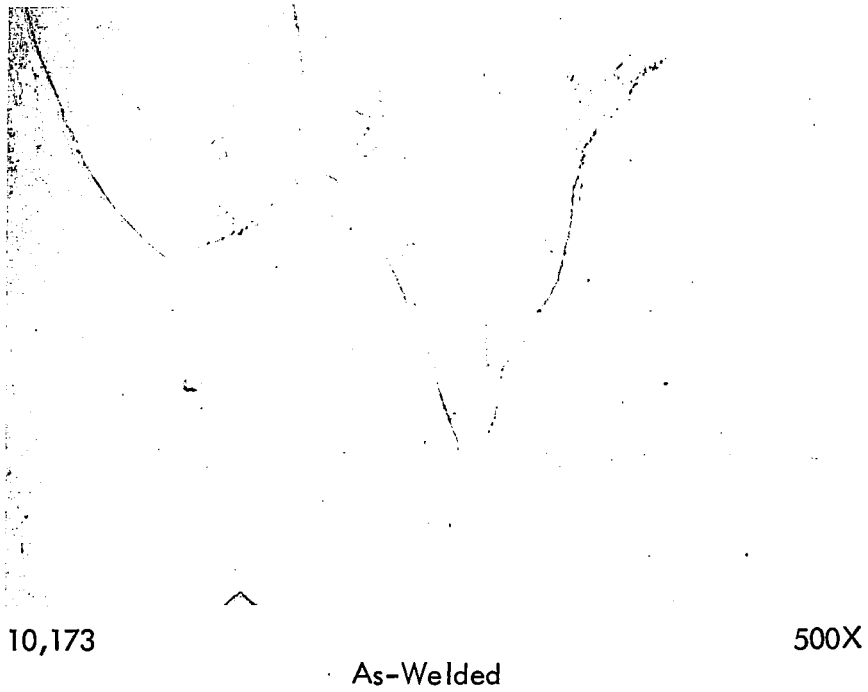


FIGURE A51 - FS-85 Welded Plate Microstructure

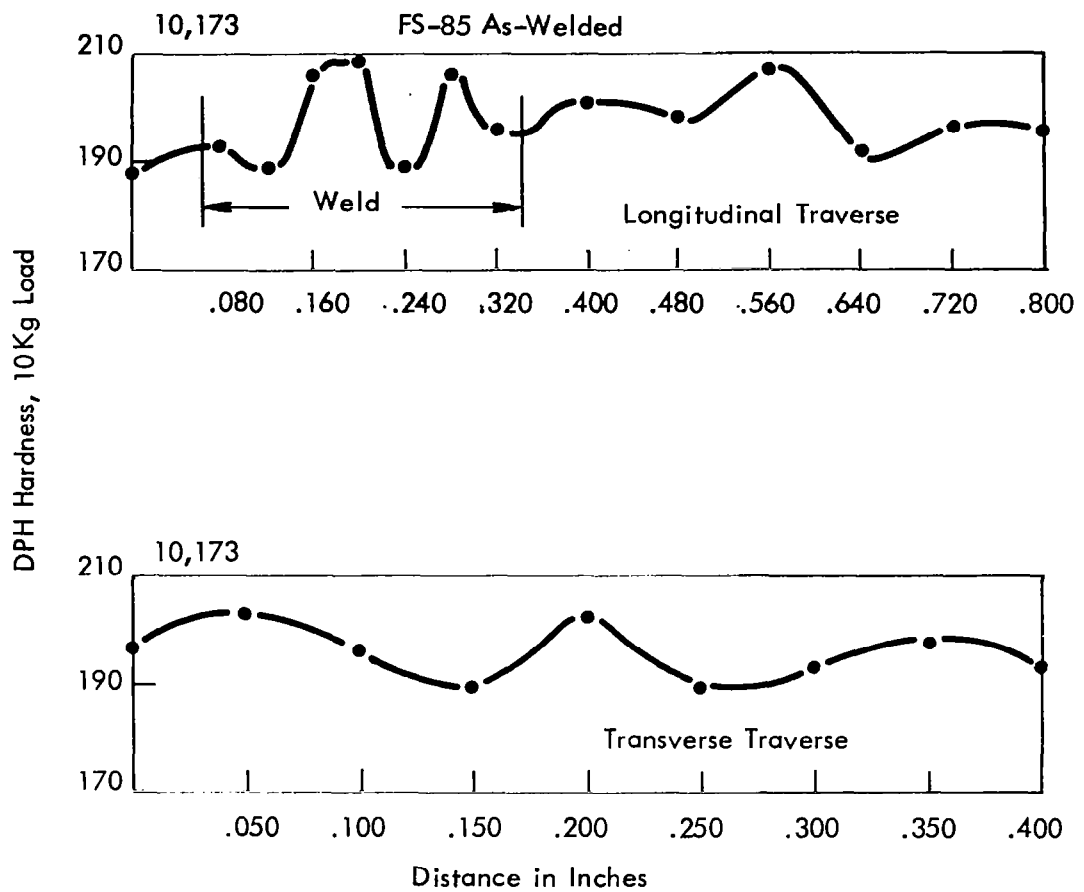


FIGURE A52 - FS-85 Plate Weld Hardness Traverse

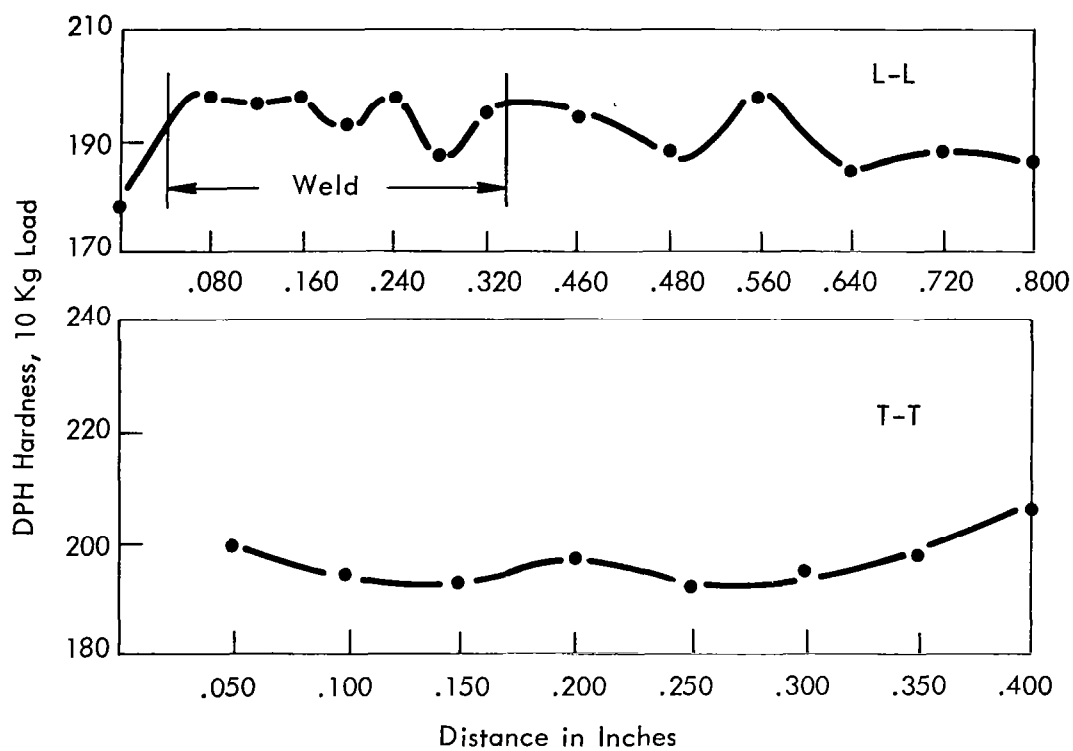
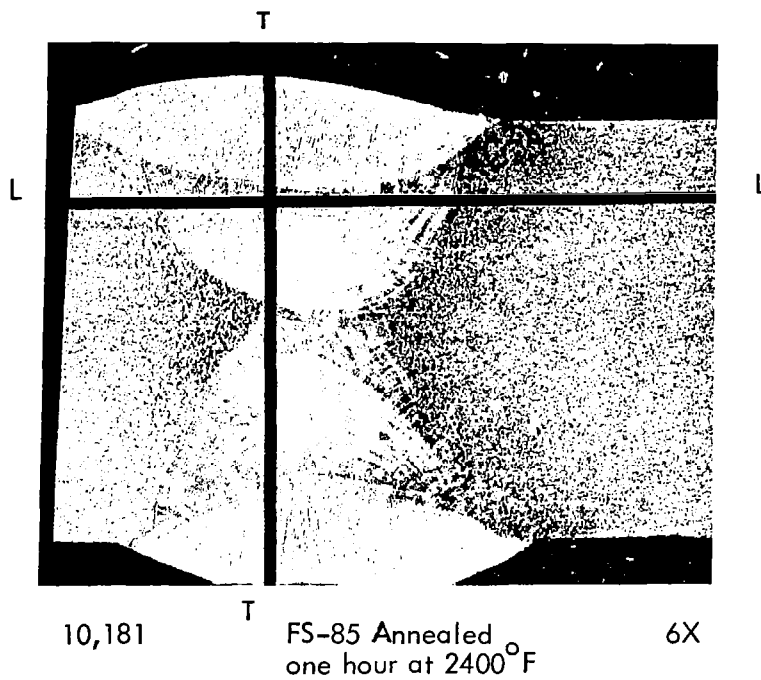
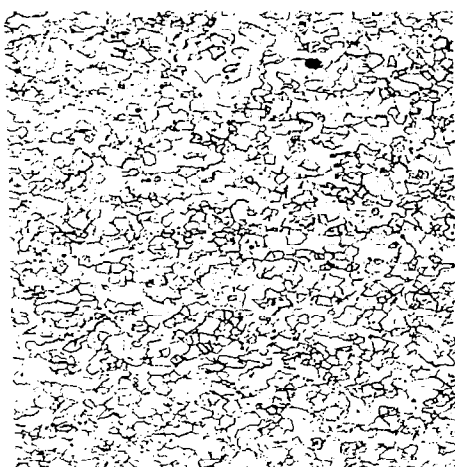


FIGURE A53 - FS-85 Plate Weld Hardness Traverse



100X

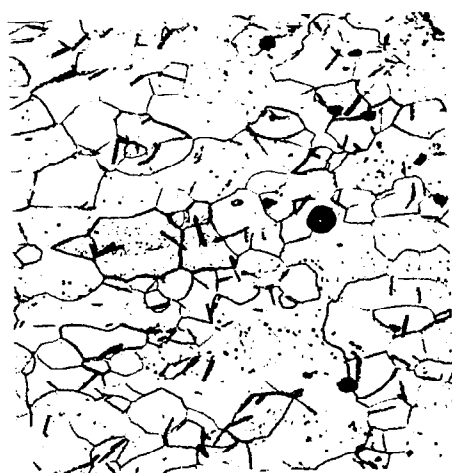
6856

.035 Sheet



100X

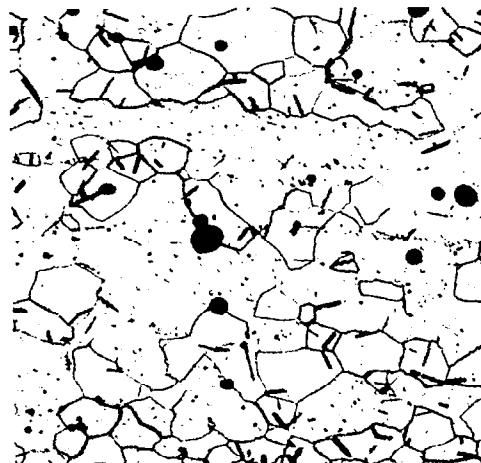
6857



400X

6856

.035 Sheet



400X

6857

Longitudinal

Transverse

FIGURE A54 - As-Received Microstructure of AS-55 Sheet

TABLE A9 - AS-55 Sheet. GTA Butt Weld Record

Weld No.	Clamp Spacing (Inch)	Speed (ipm)	Current Amperes	Weld Width Top/Bottom (Inch)	Q Joules/Inch	Atmosphere Monitor Readings			Comments	
						O <sub>2</sub> (1) ppm	O <sub>2</sub> (2) ppm	H <sub>2</sub> O(3) ppm	Visual Inspection	Dye Check
1	1/4	7.5	57	0.099/0.075	6380	0.7	1.0	0.4	Negative	Negative
2	1/4	7.5	80	0.150/0.135	8950	---	1.1	0.6	Negative	Negative
3	1/4	1.5	95	0.165/0.150	5700	0.5	2.0	0.9	Negative	Negative
4	3/8	15.0	81	0.180/0.150	5190	1.4	2.0	0.7	Negative	Negative
5	1/4	15.0	69	0.108/0.069	3860	0.5	1.5	0.8	Negative	Negative
6	3/8	15.0	62	0.132/0.069	3720	1.9	2.0	0.9	Negative	Negative
7	1/4	30.0	90	0.132/0.045	2700	0.8	2.2	1.0	Negative	Negative
8	3/8	30.0	85	0.120/0.048	2720	3.0	1.5	1.5	Negative	Negative
9	1/4	30.0	149	0.192/0.174	5070	---	2.3	1.1	Negative	Negative
10	3/8	30.0	120	0.165/0.138	4080	3.0	1.7	1.8	Negative	Negative
11	3/8	60.0	151	0.159/0.090	2565	1.3	2.5	1.2	Negative	Negative
12									Burn	Through

- (1) Westinghouse Oxygen Gage  
(2) Lockwood & McLorie Oxygen Gage  
(3) CEC Moisture Monitor

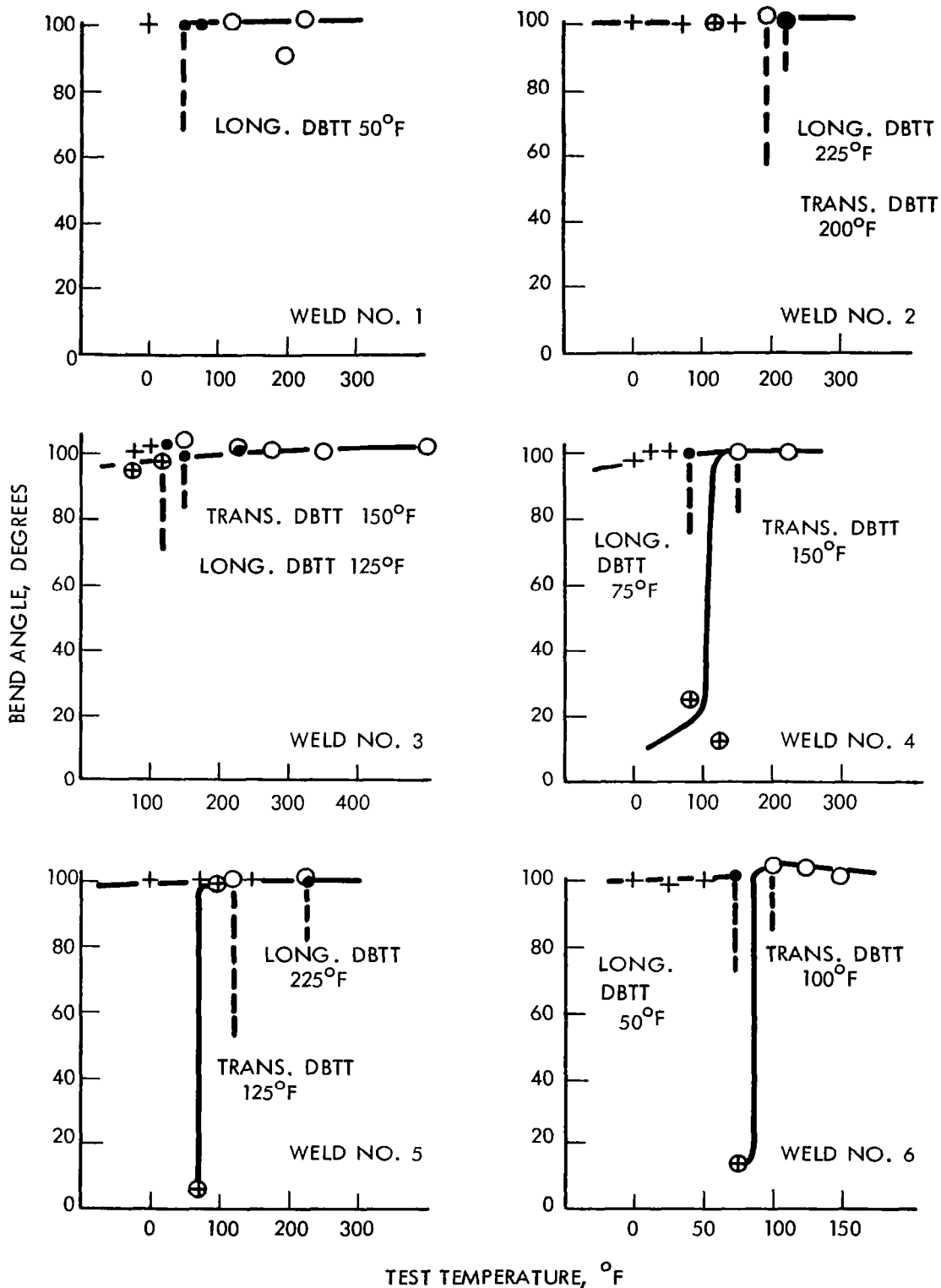


FIGURE A55 - Bend Test Results for AS-55 GTA Welds  
1½ Bend Radius



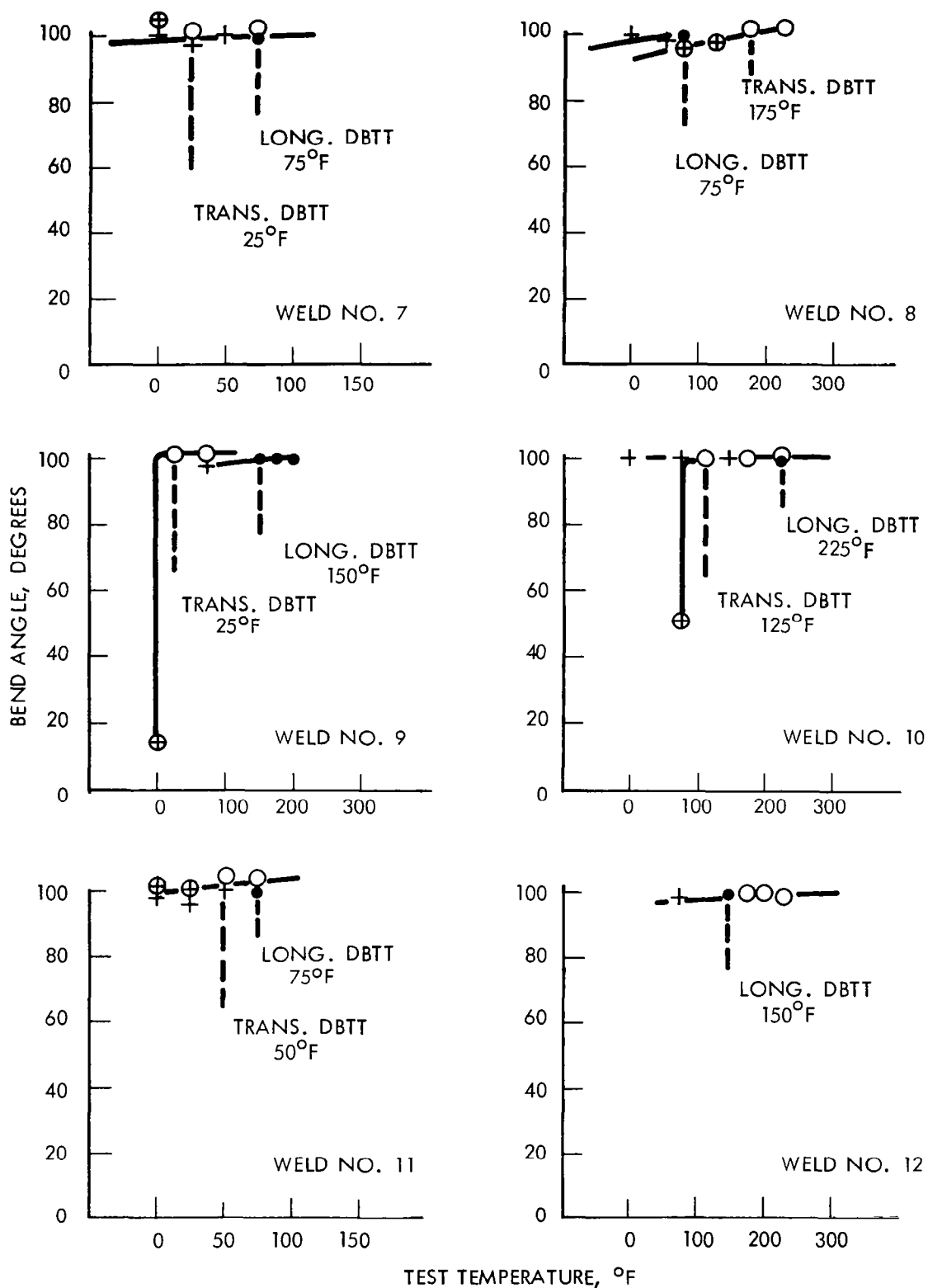


FIGURE A56 - Bend Test Results for AS-55 GTA Welds  
1t Bend Radius

TABLE A10 - AS-55 Sheet. EB Butt Weld Record

Weld No.	Speed (ipm)	Deflection <sup>1</sup> (Inches)	Current (ma)	Chill Spacing (Inches)	Power (watts)	Watt-Sec. per inch	Weld Bead Width (Inches)		Vacuum torr
							Top	Bottom	
1	15	Zero	2.8	.094	420	1680	.027	.023	$3.6 \times 10^{-6}$
2	15	L - .050	3.4	.094	510	2040	.044	.023	$3.6 \times 10^{-6}$
3	15	T - .050	3.4	.094	510	2040	.062	.057	$3.6 \times 10^{-6}$
4	25	L - .050	3.6	.094	540	1300	.045	.027	$3.6 \times 10^{-6}$
5	15	L - .050	3.1	.250	465	1860	.044	.031	$3.6 \times 10^{-6}$
6	25	L - .050	3.3	.250	495	1190	.040	.027	$3.6 \times 10^{-6}$
7	50	L - .050	3.7	.250	555	667	.033	.020	$3.6 \times 10^{-6}$
8	100	L - .050	4.9	.250	735	440	.033	.020	$3.6 \times 10^{-6}$
9	50	Zero	3.8	.094	570	684	.025	.018	$3.0 \times 10^{-6}$
10	50	L - .025	4.1	.094	615	740	.034	.021	$3.0 \times 10^{-6}$
11	50	L - .050	4.1	.094	615	740	.036	.022	$3.0 \times 10^{-6}$
12	100	L - .050	5.4	.094	810	485	.030	.020	$3.0 \times 10^{-6}$

All welds made at 150 KV.

1. L. is longitudinal

T. is transverse

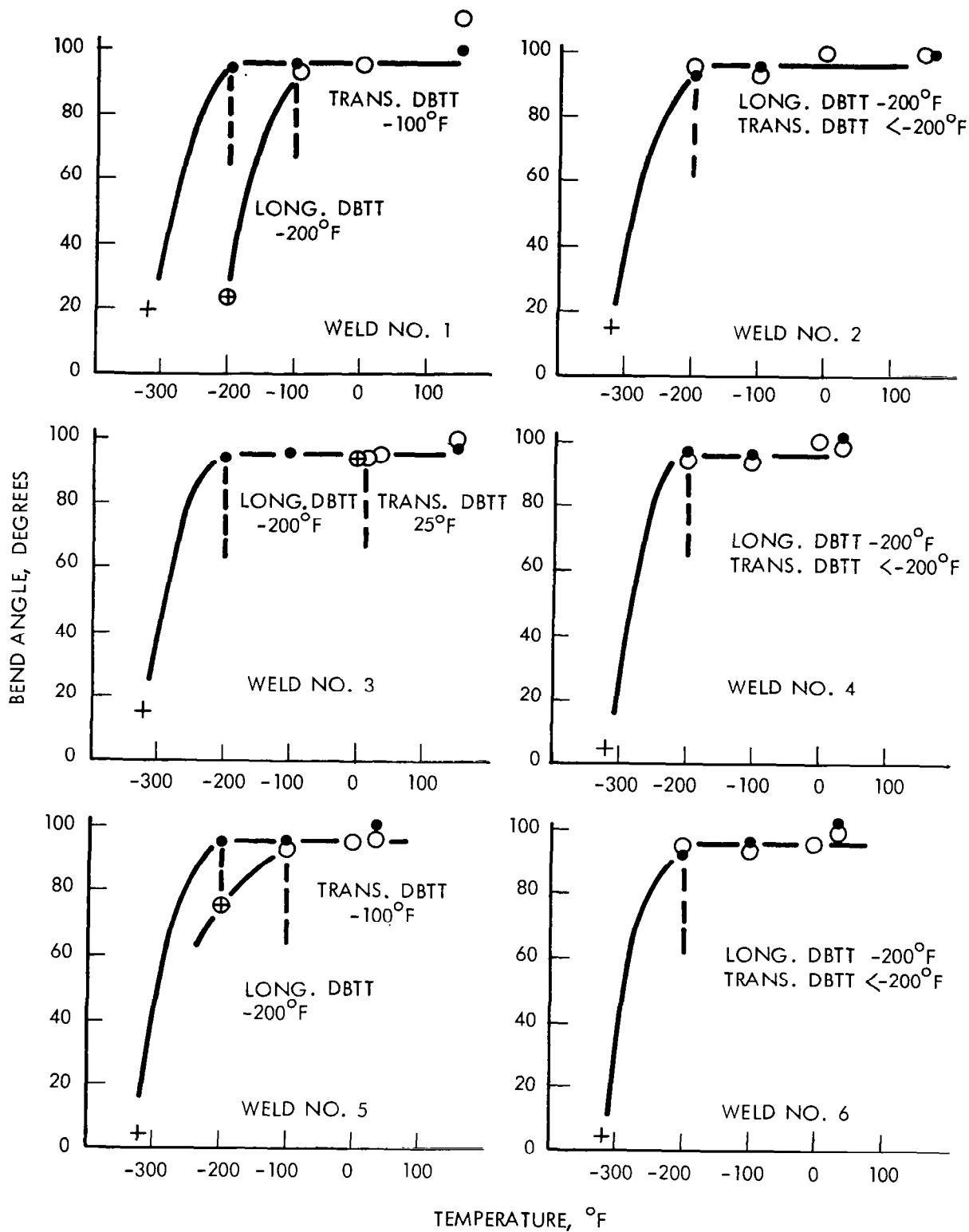


FIGURE A57 - Bend Test Results for AS-55 EB Welds  
1½ Bend Radius

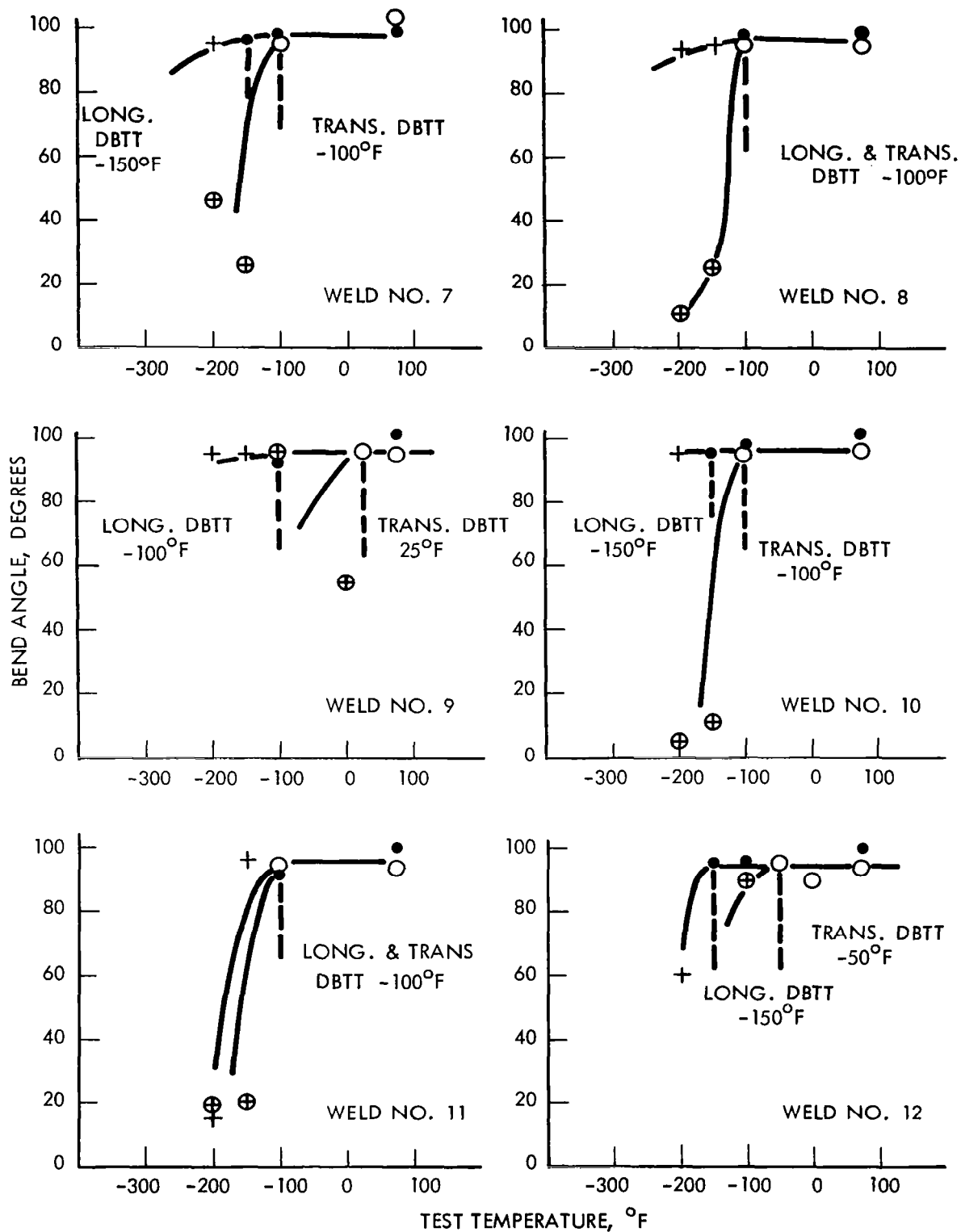


FIGURE A58 - Bend Test Results for AS-55 EB Welds  
1t Bend Radius

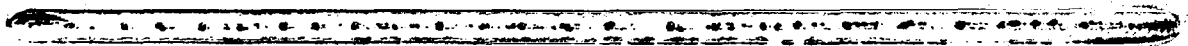
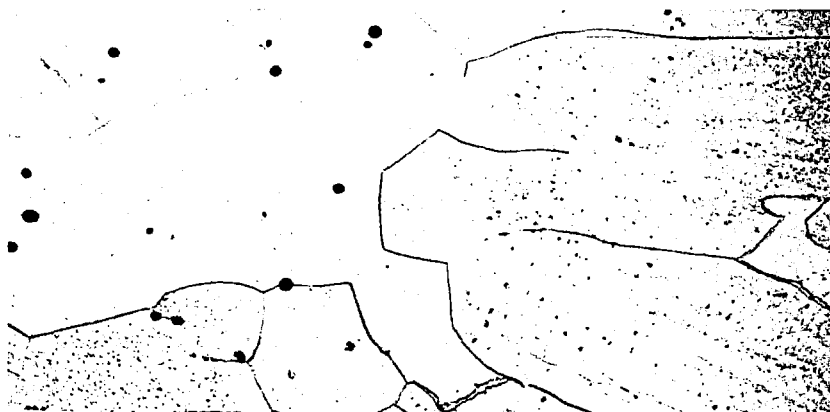


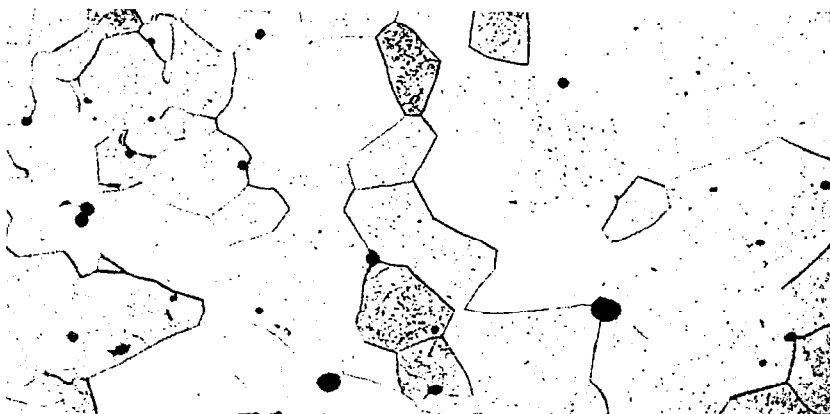
FIGURE A59 - AS-55 Sheet Butt Weld, Top View Showing  
Slagging of Yttrium Oxides



Weld



Weld Edge



HAZ

FIGURE A60 - AS-55 GTA Sheet Weld Microstructure. Weld No. 2, 400X. Met. 9207

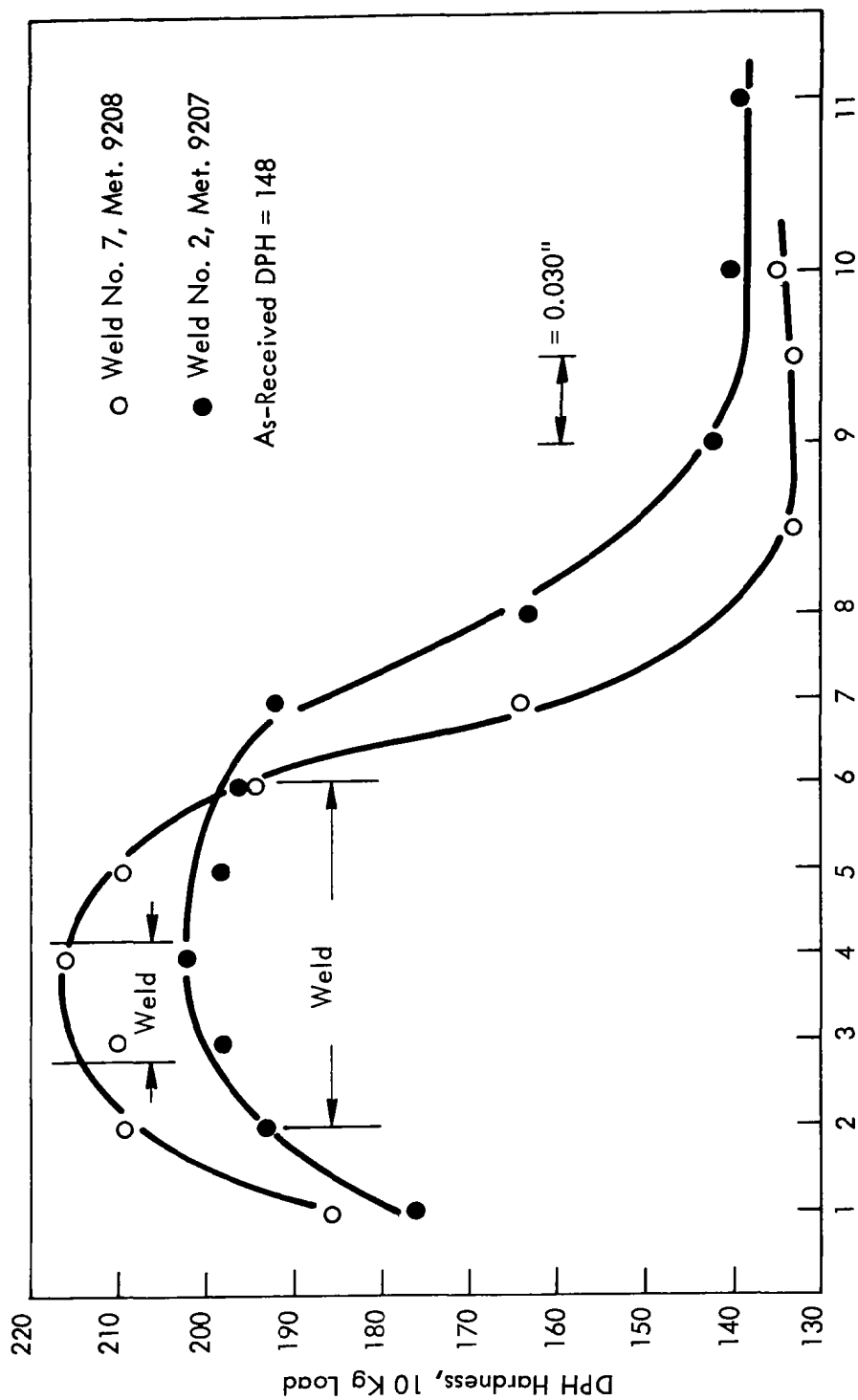
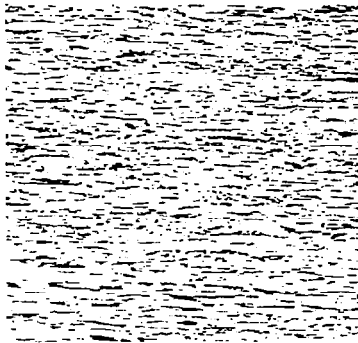
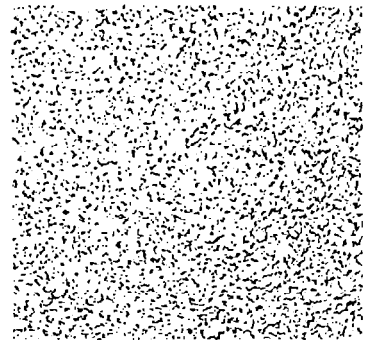


FIGURE A61 - Hardness Traverses of AS-55 GTA Sheet Butt Welds



2796

0.082" Wire



2797

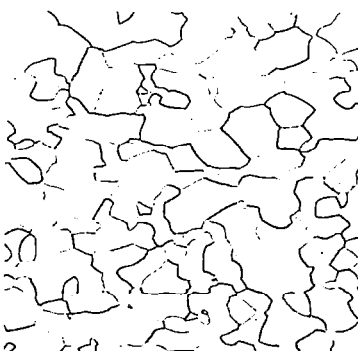


3628

0.035" Sheet

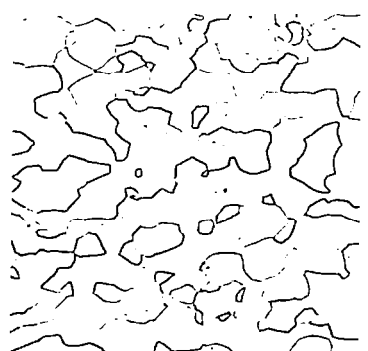


3629



3630

0.375" Plate



3631

Longitudinal

Transverse

FIGURE A62 - As-Received Microstructure of B-66 100X



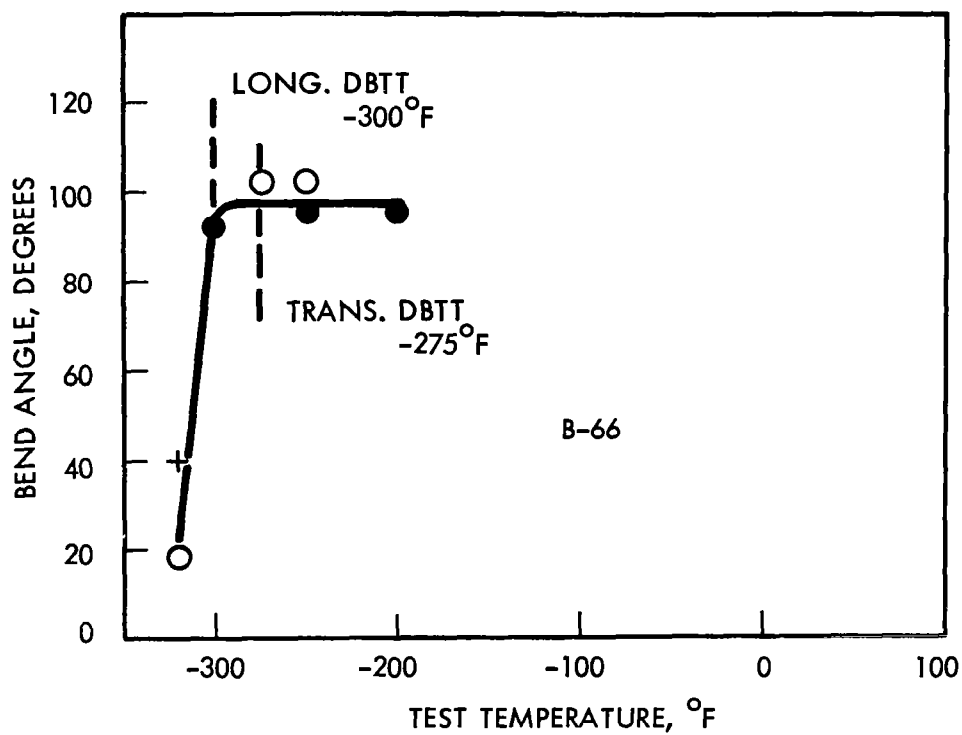


FIGURE A63 - B-66 Base Metal Bend Test Results

TABLE A11 - B-66 Sheet. GTA Butt Weld Record

Weld No.	Clamp Spacing (inch)	Speed (ipm)	Current Amperes	Weld Width Top/Bottom (inch)	Q Joules/Inch	Atmosphere Monitor Readings			Comments	
						O <sub>2</sub> (1) ppm	O <sub>2</sub> (2) ppm	H <sub>2</sub> O (3) ppm	Visual Inspection	Dye Check
1	3/8	15	50	0.11/0.07	3,400	--	3.5	2.3	Negative	Negative
2	3/8	15	70	0.13/0.08	4,750	--	4.5	0.5	Negative	Negative
3	1/4	15	80	0.135/0.110	5,420	5.0	5.4	0.05	1/2" Centerline Starting Crack	Positive
4	1/4	30	90	0.115/0.075	3,060	5.0	5.4	0.15	Edge Flash (4)	Negative
5	1/4	7.5	86	0.184/0.168	12,400	--	3.2	0.5	Starting Crack	Positive
6	3/8	7.5	60	0.136/0.100	8,380	1.0	3.5	0.35	Negative	Negative
7	1/4	15	113	0.200/0.196	8,140	0.7	2.5	0.1	Negative	Negative
8	3/8	15	86	0.190/0.180	6,020	0.3	2.4	0.1	Negative	Negative
9	1/4	30	170	0.231/0.228	6,460	2.0	2.4	0.05	Many Small Hot Tears	Positive
10	3/8	30	114	0.156/0.135	4,100	--	2.2	0.1	Negative	Negative
11	1/4	60	200	0.18/0.164	3,700	1.0	3.0	0.1	Many Small Hot Tears	Positive
12	1/4	60	165	0.138/0.090	3,050	1.0	2.0	0.2	Negative	Negative

(1) Westinghouse Oxygen Gage  
(2) Lockwood & McLorie Oxygen Gage

(3) CEC Moisture Monitor  
(4) Instantaneous Arcing to Weld Clamp Down

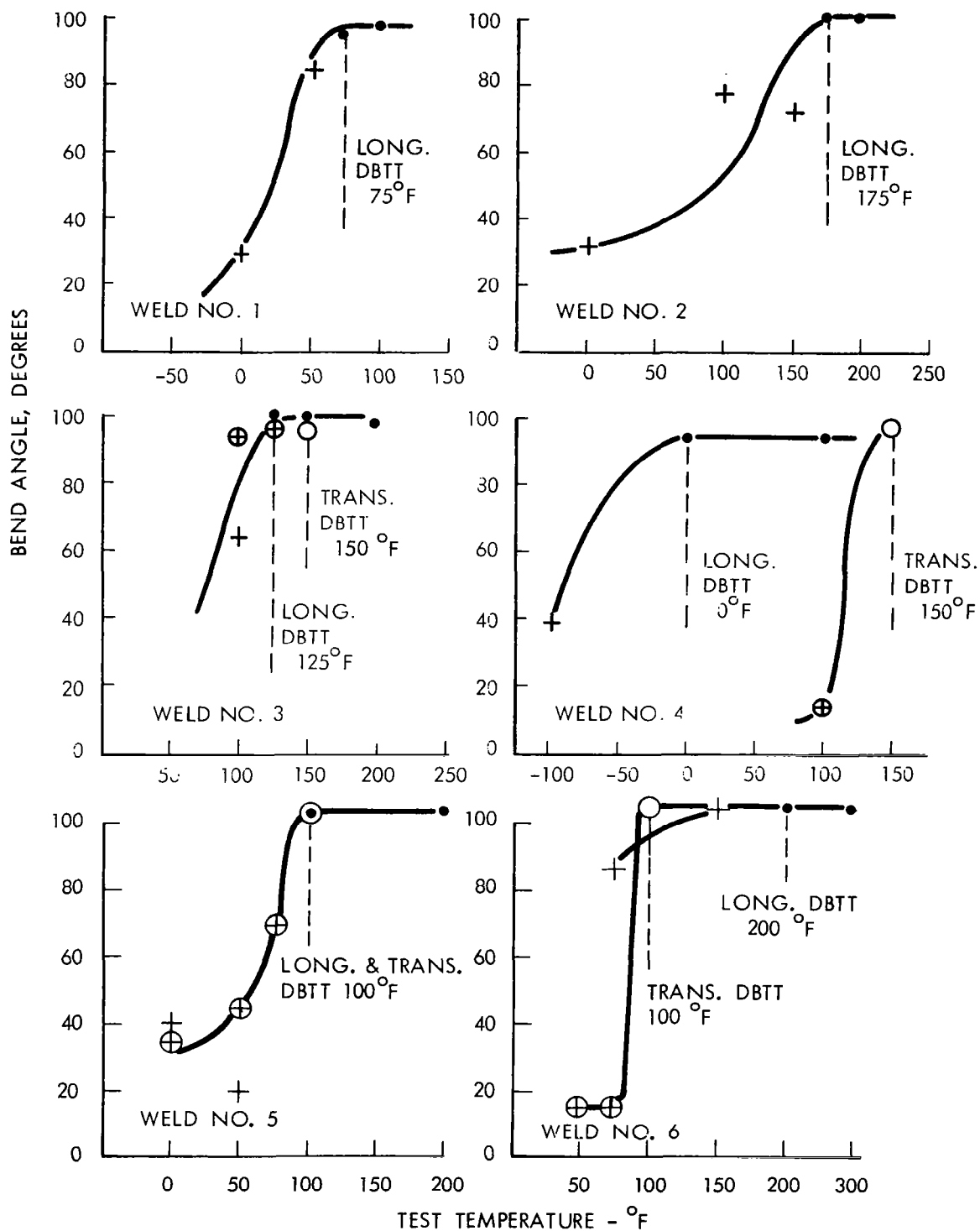


FIGURE A64 - Bend Test Results for B-66 GTA Welds  
1t Bend Radius

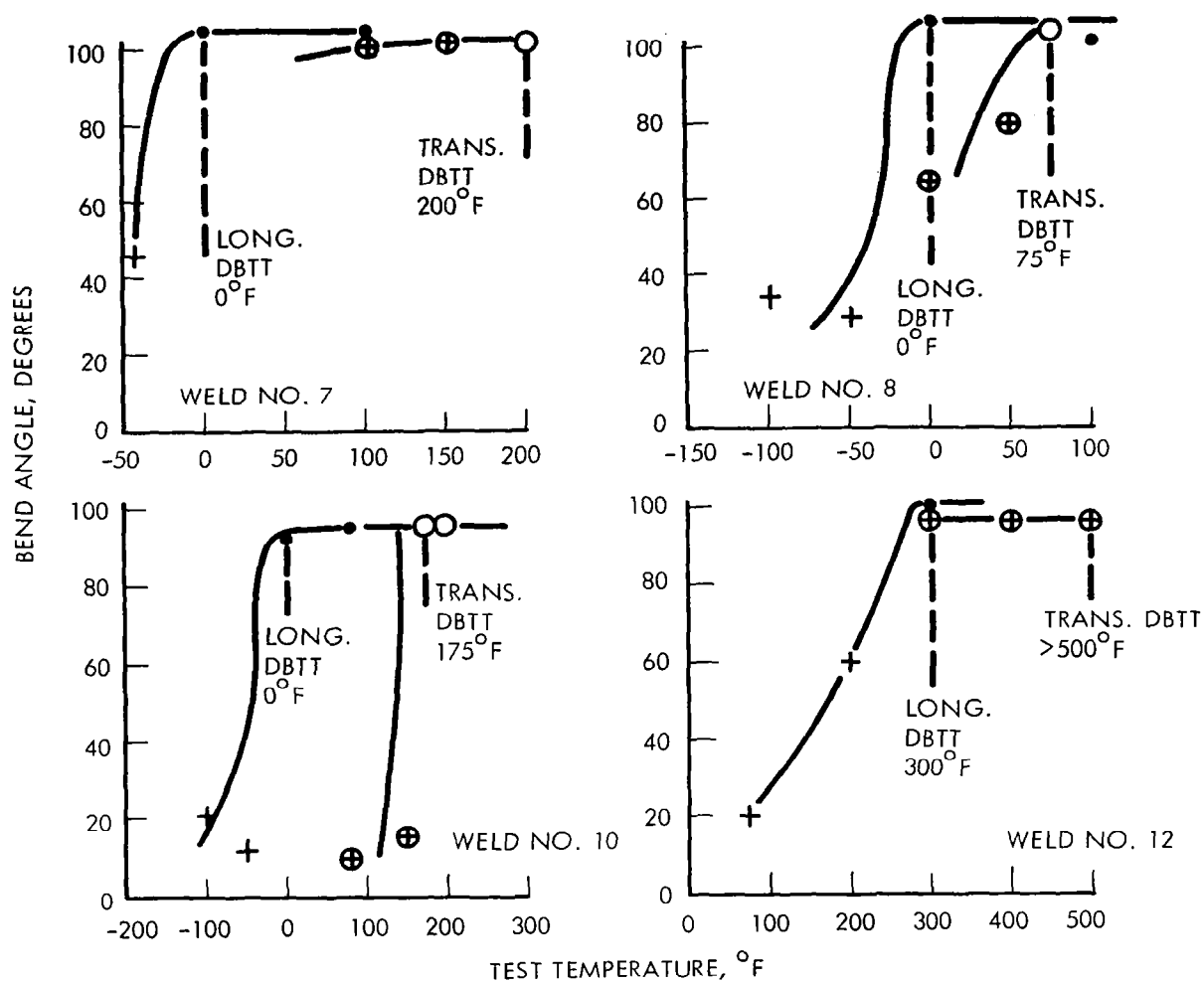


FIGURE A65 - Bend Test Results for B-66 GTA Welds  
1† Bend Radius

TABLE A12 - B-66 Sheet. EB Butt Weld Record

Weld No.	Speed (ipm)	Deflection <sup>1</sup> (Inches)	Current (ma)	Chill Spacing (Inches)	Power (watts)	Watt-Sec. per inch	Weld Bead Width (Inches)		Vacuum torr	Ave. Weld Bead Width
							Top	Bottom		
1	15	Zero	2.4	.094	360	1440	.027	.016	$1.7 \times 10^{-6}$	.022
2	15	L - .050	2.8	.250	420	1680	.040	.027	$1.7 \times 10^{-6}$	.034
3	50	L - .050	3.5	.250	525	630	.033	.022	$3.8 \times 10^{-6}$	.028
4	100	L - .050	4.6	.250	690	413	.027	.020	$3.8 \times 10^{-6}$	.024
5	15	L - .050	3.0	.094	450	1800	.034	.020	$3.8 \times 10^{-6}$	.027
6	15	T - .050	3.0	.094	450	1800	.056	.054	$3.8 \times 10^{-6}$	.055
7	25	L - .050	3.2	.094	480	1150	.036	.024	$3.8 \times 10^{-6}$	.030
8	50	Zero	3.4	.094	510	612	.022	.016	$4.0 \times 10^{-6}$	.019
9	50	L - .025	3.4	.094	510	612	.030	.018	$4.0 \times 10^{-6}$	.024
10	50	L - .050	3.8	.094	570	684	.031	.022	$4.0 \times 10^{-6}$	.026
11	50	L - .100	4.6	.094	690	829	.032	.027	$1.9 \times 10^{-6}$	.030
12	100	L - .050	5.0	.094	750	450	.033	.032	$4.7 \times 10^{-6}$	.032

All welds made at 150 KV.

1. L. is longitudinal

T. is transverse

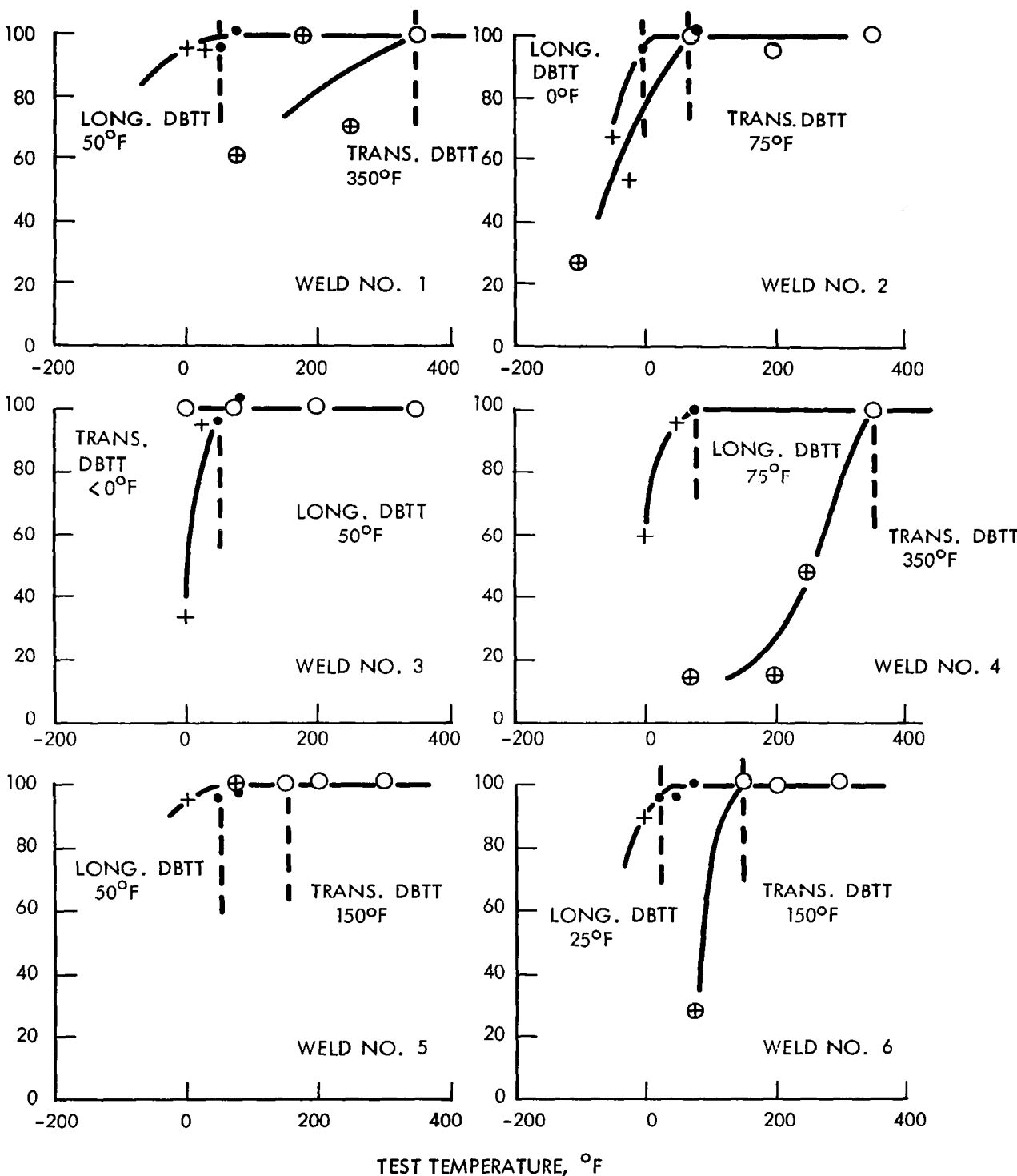


FIGURE A66 - Bend Test Results for B-66 EB Welds  
1t Bend Radius

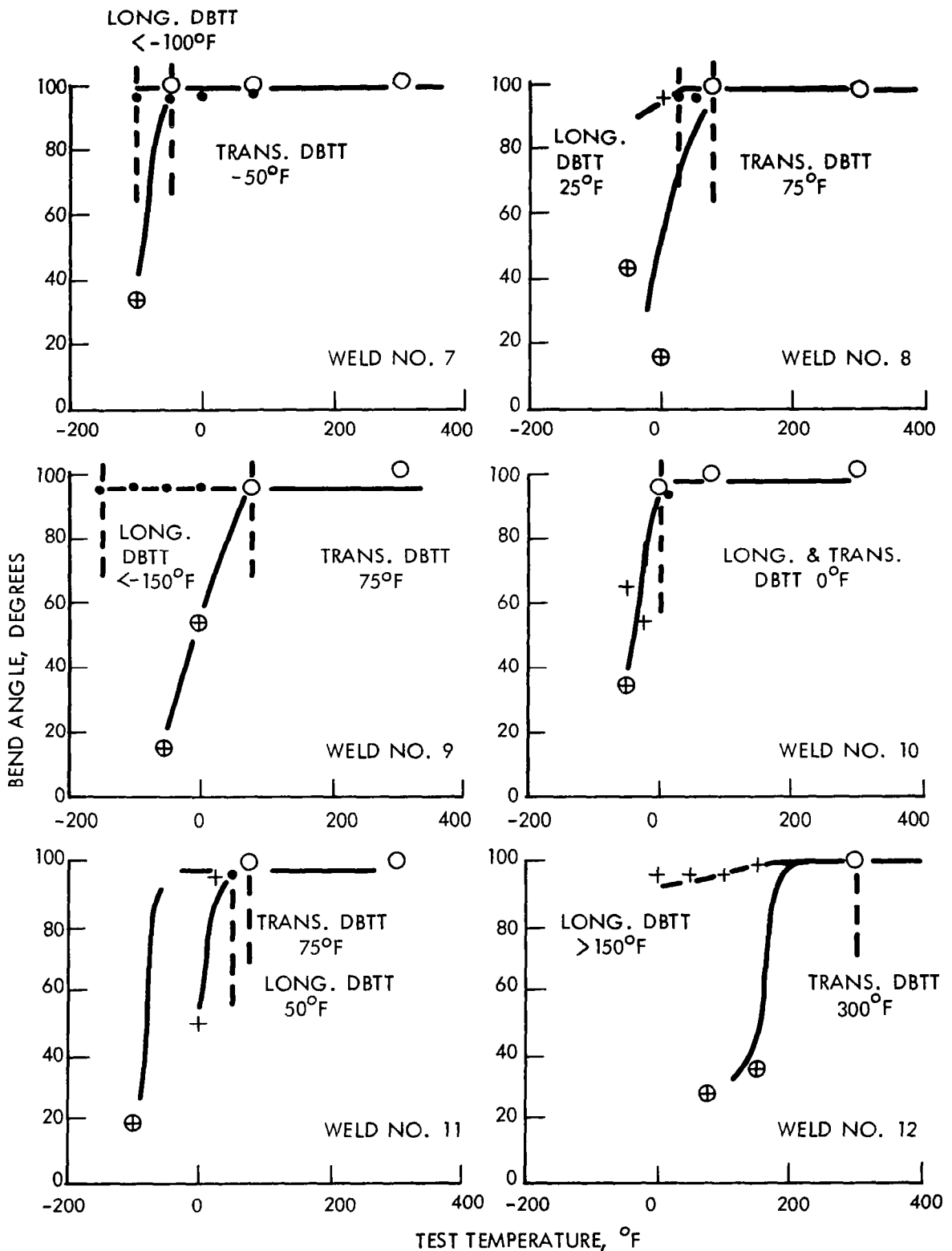


FIGURE A67 - Bend Test Results for B-66 EB Welds  
1t Bend Radius

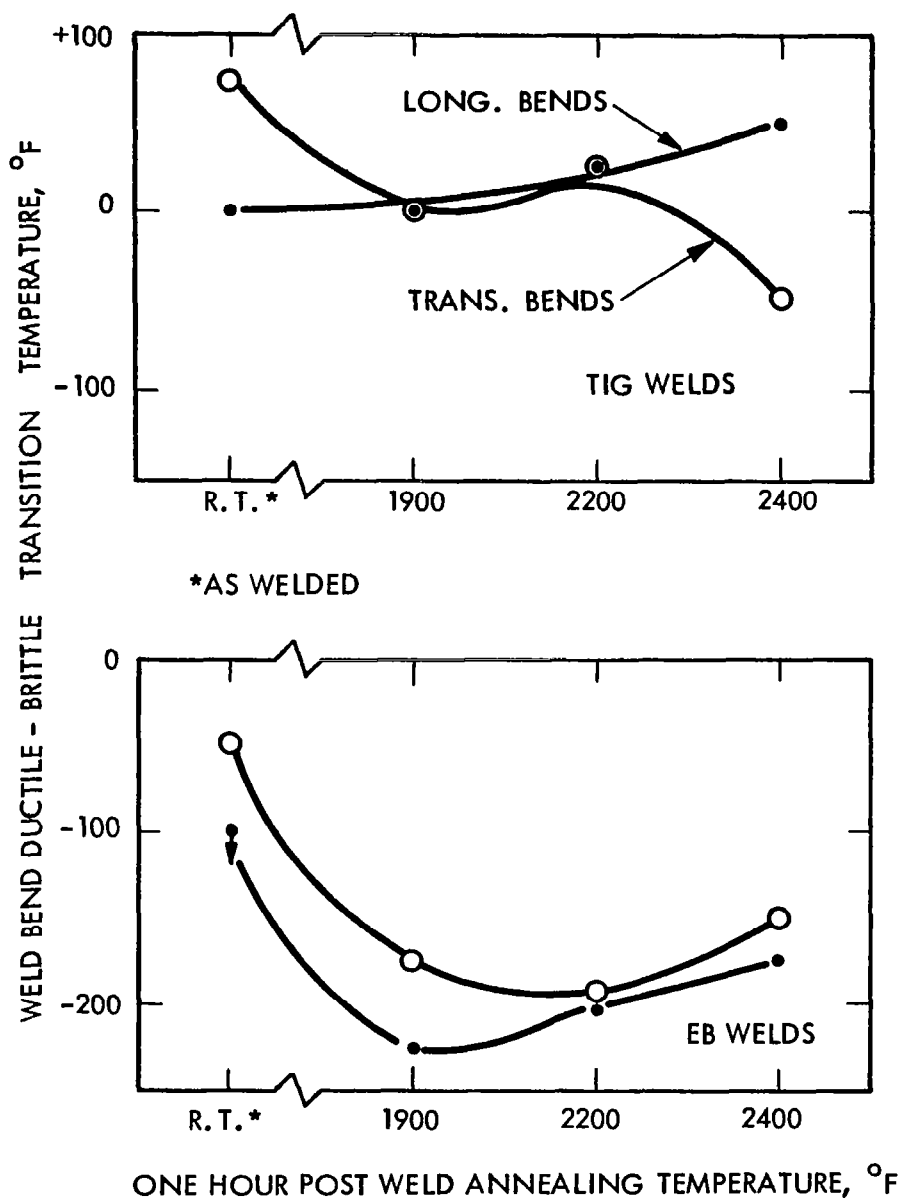


FIGURE A68 - Effect of Post-Weld Annealing on B-66 Sheet Weld Ductility



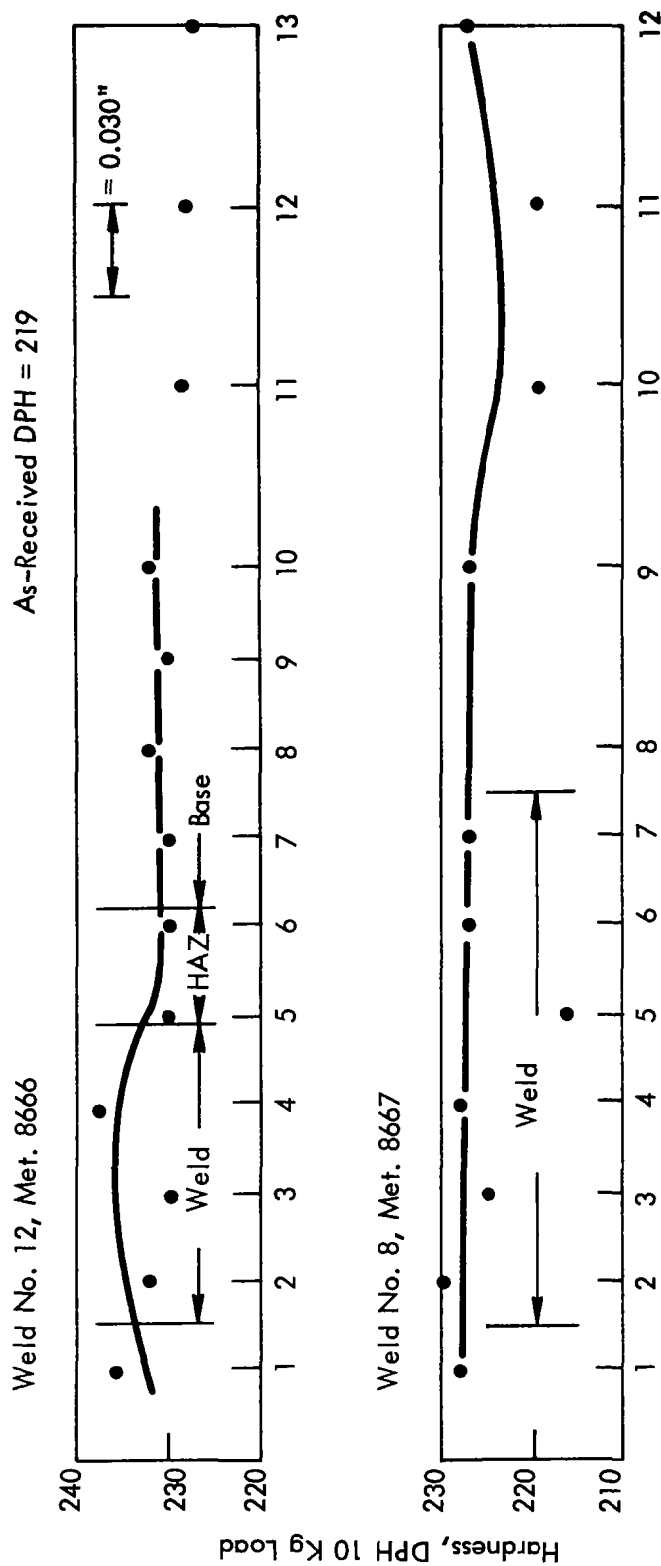
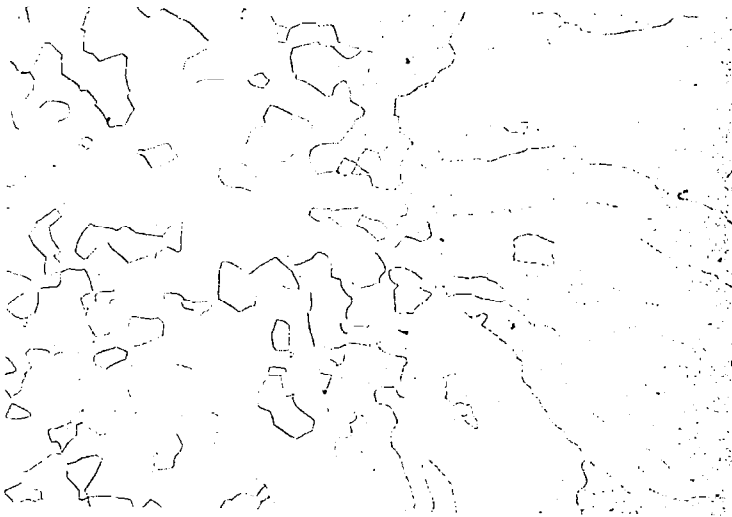
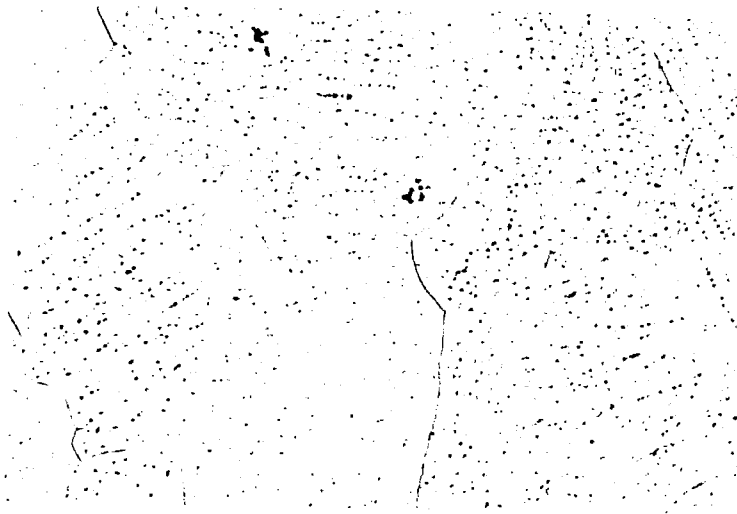


FIGURE A69 - Hardness Traverses, B-66 GTA Sheet Butt Weld



Weld Edge, 100X



Weld Center, 200X

FIGURE A70 - B-66 Sheet Butt Weld Microstructure. GTA Weld  
No. 8. Met. 8667

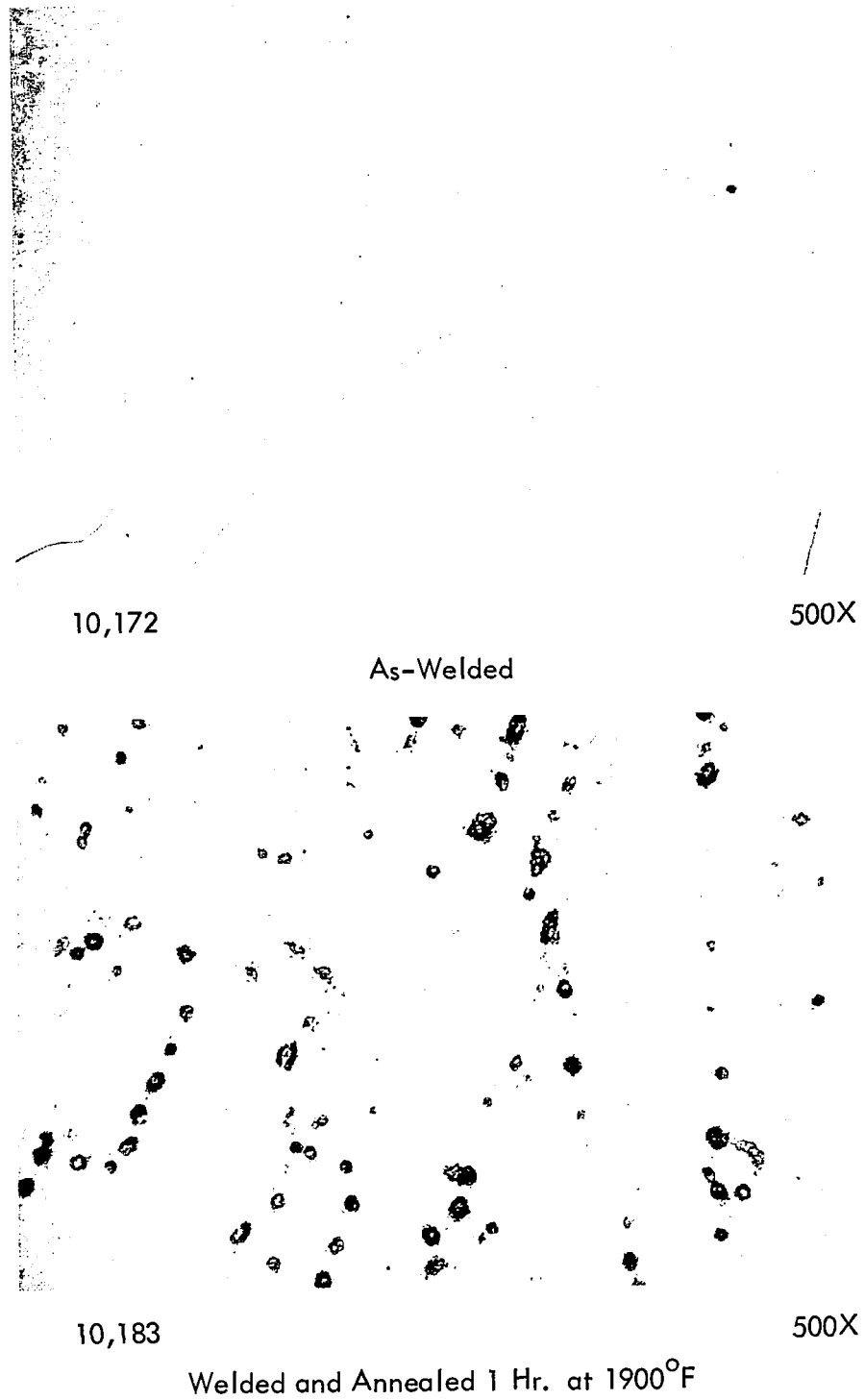


FIGURE A71 - B-66 Sheet Buttt Weld Microstructure

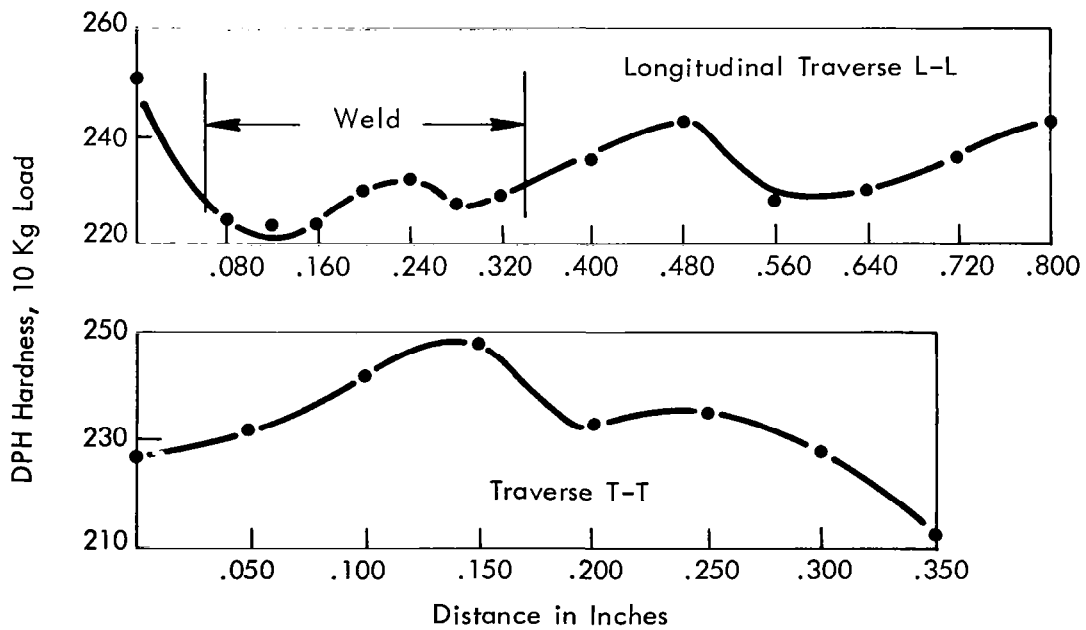
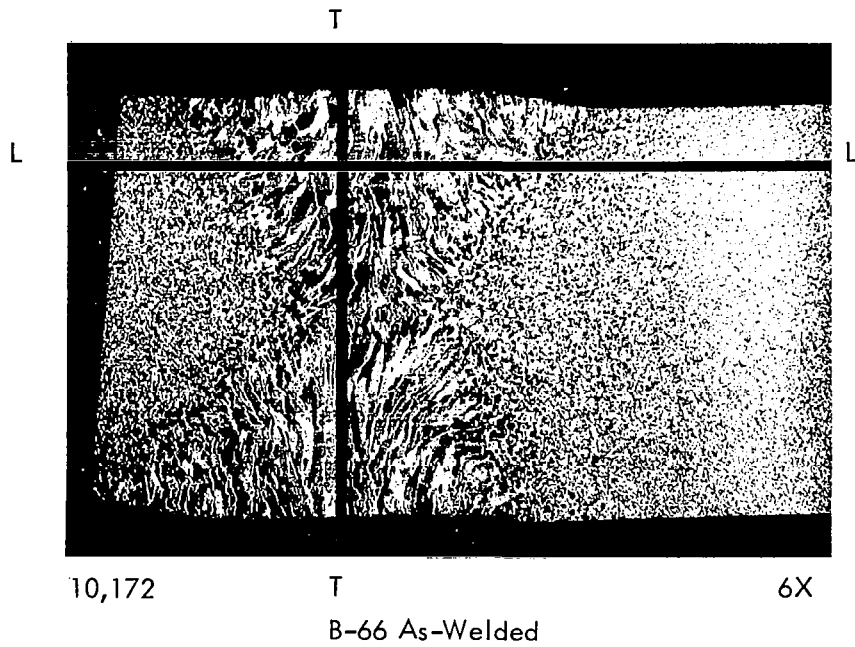


FIGURE A72 - B-66 Plate Weld Hardness Traverse

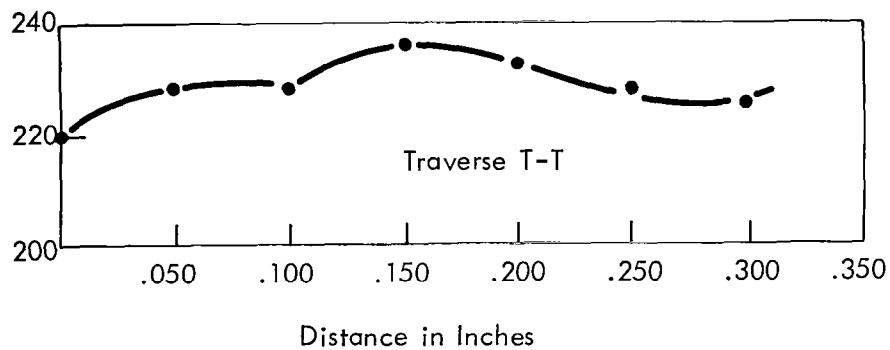
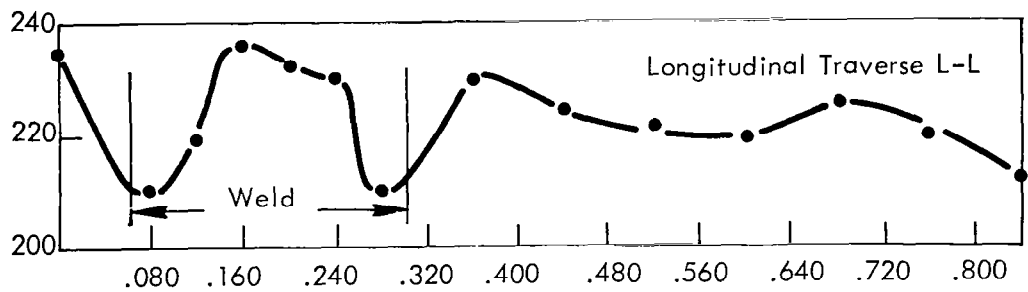
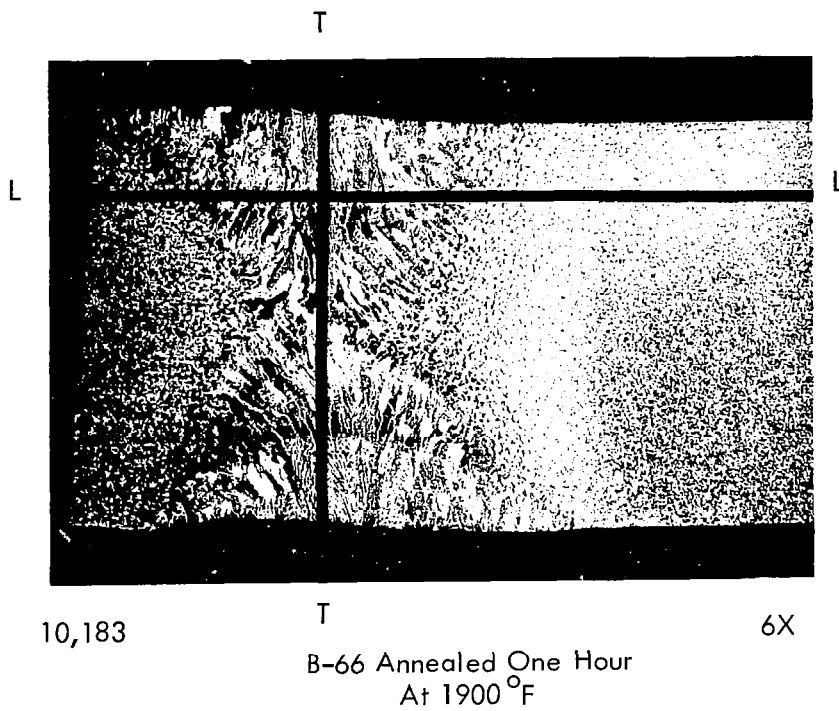
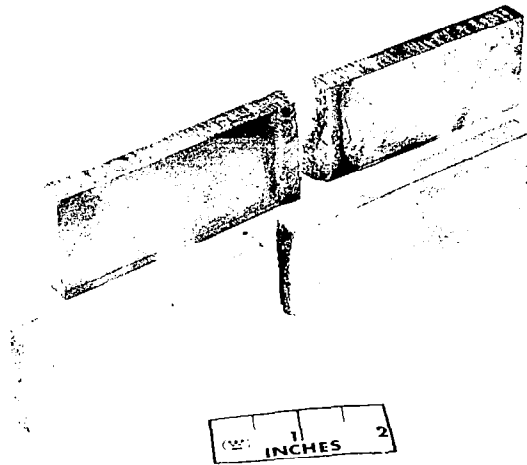


FIGURE A73 - B-66 Plate Weld Hardness Traverse



B-66

427-3

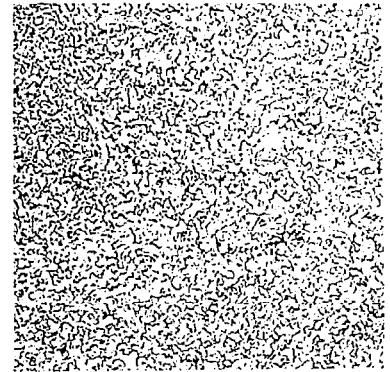
4° Longitudinal Bend  
4° Transverse Bend

FIGURE A74 - B-66 Plate Weld Bend Specimens

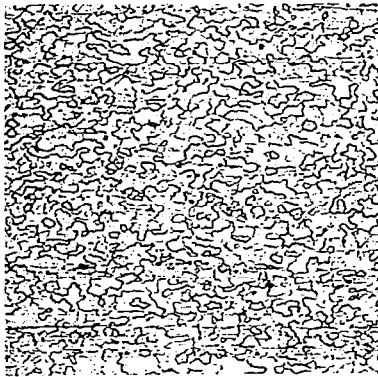


3744

0.082" Wire

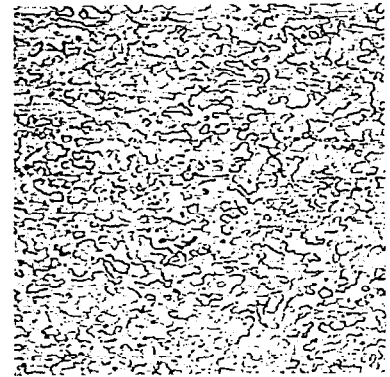


3745



2808

0.035" Sheet



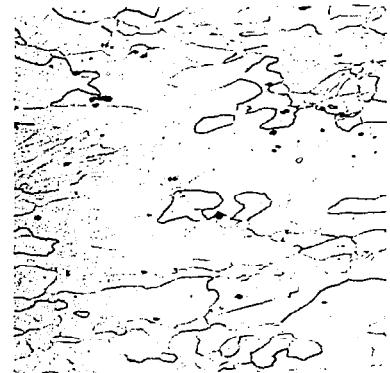
2809



3746

0.375" Plate

Longitudinal



3747

Transverse

FIGURE A75 - As-Received Microstructure of C-129Y, 100X

TABLE A13 - C-129Y Sheet. GTA Butt Weld Record

Weld No.	Clamp Spacing (inch)	Speed (ipm)	Current Amperes	Weld Width Top/Bottom (inch)	Q Joules/Inch	Atmosphere Monitor Readings			Comments	
						O <sub>2</sub> (1) ppm	O <sub>2</sub> (2) ppm	H <sub>2</sub> O (3) ppm	Visual Inspection	Dye Check
1	3/8	15	70	0.150/0.10	4,750	3.5	--	0.7	Negative	Negative
2	3/8	30	110	0.18/0.13	3,730	3.5	--	0.9	Negative	Negative
3	1/4	15	80	0.15/0.11	5,430	4.0	4.7	2.0	Edge Flash (4)	Negative
4	1/4	30	102	0.145/0.115	3,460	4.5	4.8	2.1	Edge Flash (4)	Negative
5	1/4	7.5	74	0.160/0.116	10,950	1.5	3.3	0.8	Negative	Negative
6	1/4	7.5	93	0.180/0.150	13,750	4.0	3.6	2.9	Negative	Negative
7	3/8	7.5	62	0.159/0.132	8,680	1.8	3.9	1.7	Negative	Negative
8	3/8	15	95	0.219/0.204	7,030	2.0	4.2	2.0	Negative	Negative
9	1/4	30	150	0.180/0.165	5,560	0.5	2.1	0.3	Negative	Negative
10	3/8	60	170	0.150/0.135	3,140	1.0	2.3	0.3	Negative	Negative
11	3/8	60	145	0.120/0.075	2,680	--	1.8	2.8	Negative	Negative
12	1/4	60	150	0.120/0.075	2,780	1.5	3.5	1.0	Negative	Negative

(1) Westinghouse Oxygen Gage  
(2) Lockwood & McLorie Oxygen Gage

(3) CEC Moisture Monitor  
(4) Instantaneous Arcing to Weld Clamp Down



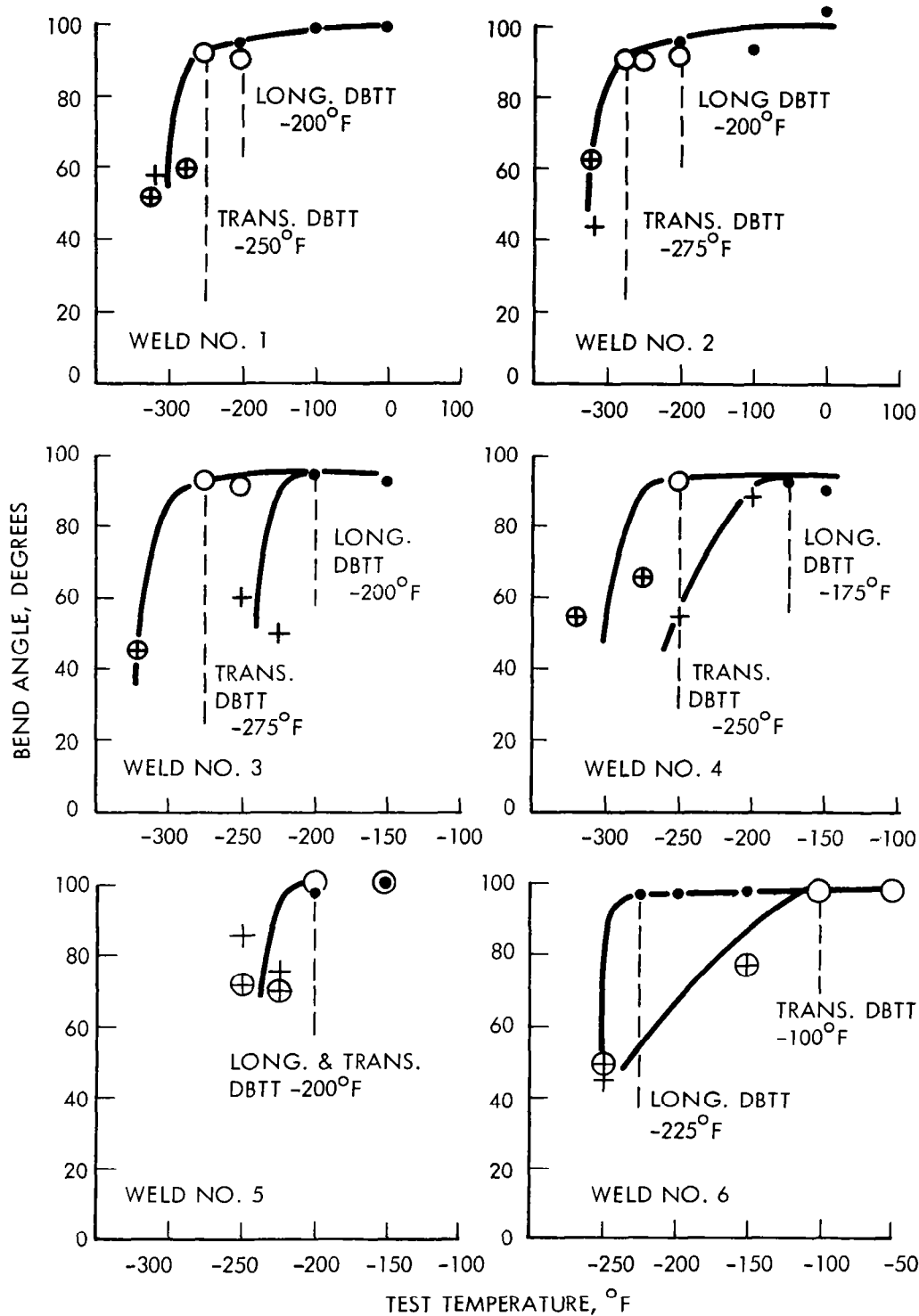


FIGURE A76 - Bend Test Results for C-129Y GTA Welds  
1t Bend Radius

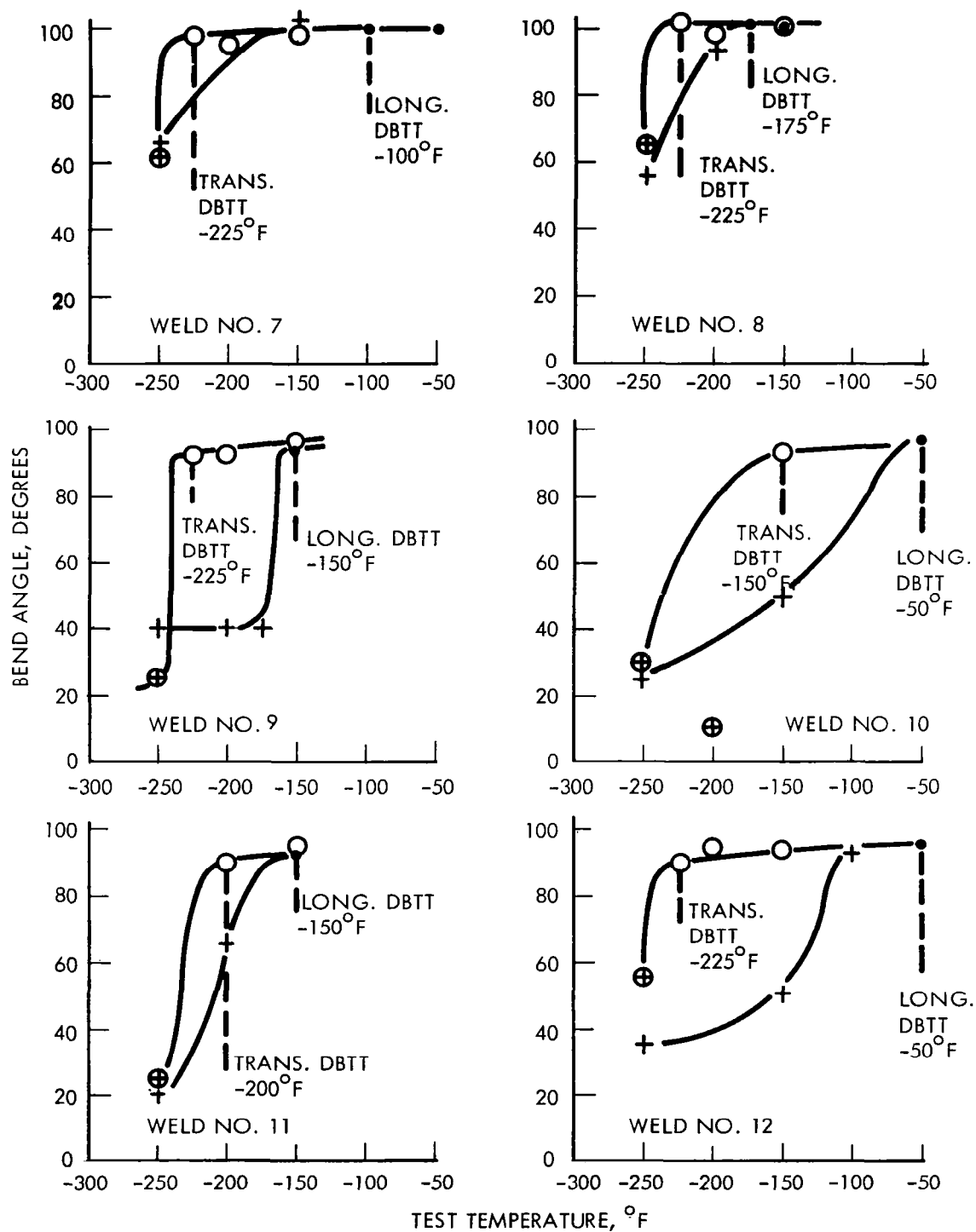


FIGURE A77 - Bend Test Results for C-129Y GTA Welds  
1t Bend Radius

TABLE A14 - C-129Y Sheet. EB Butt Weld Record

Weld No.	Speed (ipm)	Deflection <sup>1</sup> (Inches)	Current (ma)	Chill Spacing (Inches)	Power (watts)	Watt-Sec. per inch	Weld Bead Width (Inches)		Vacuum torr	Ave. Weld Bead Width
							Top	Bottom		
1	15	Zero	2.9	.250	435	1740	.040	.032	$2 \times 10^{-6}$	.036
2	50	L - .050	4.1	.250	615	738	.040	.026	$2 \times 10^{-6}$	.033
3	100	L - .050	4.6	.250	690	414	.038	.018	$2 \times 10^{-6}$	.028
4	15	Zero	2.8	.094	420	1680	.031	.025	$2 \times 10^{-6}$	.028
5	15	L - .050	3.1	.094	465	1860	.039	.027	$2 \times 10^{-6}$	.033
6	15	T - .050	3.2	.094	480	1920	.061	.054	$2 \times 10^{-6}$	.058
7	25	L - .050	3.6	.094	540	1290	.039	.030	$1.8 \times 10^{-6}$	.034
8	50	Zero	3.6	.094	540	648	.031	.019	$1.8 \times 10^{-6}$	.025
9	50	L - .025	4.0	.094	600	720	.036	.026	$1.8 \times 10^{-6}$	.031
10	50	L - .050	4.4	.094	660	792	.039	.025	(2)	.032
11	100	L - .050	5.0	.094	750	450	.032	.020	(2)	.026
12	15	L - .050	2.9	.250	435	1740	.043	.036	(2)	.040

1. L. is longitudinal  
T. is transverse

(2) Pressure not recorded.

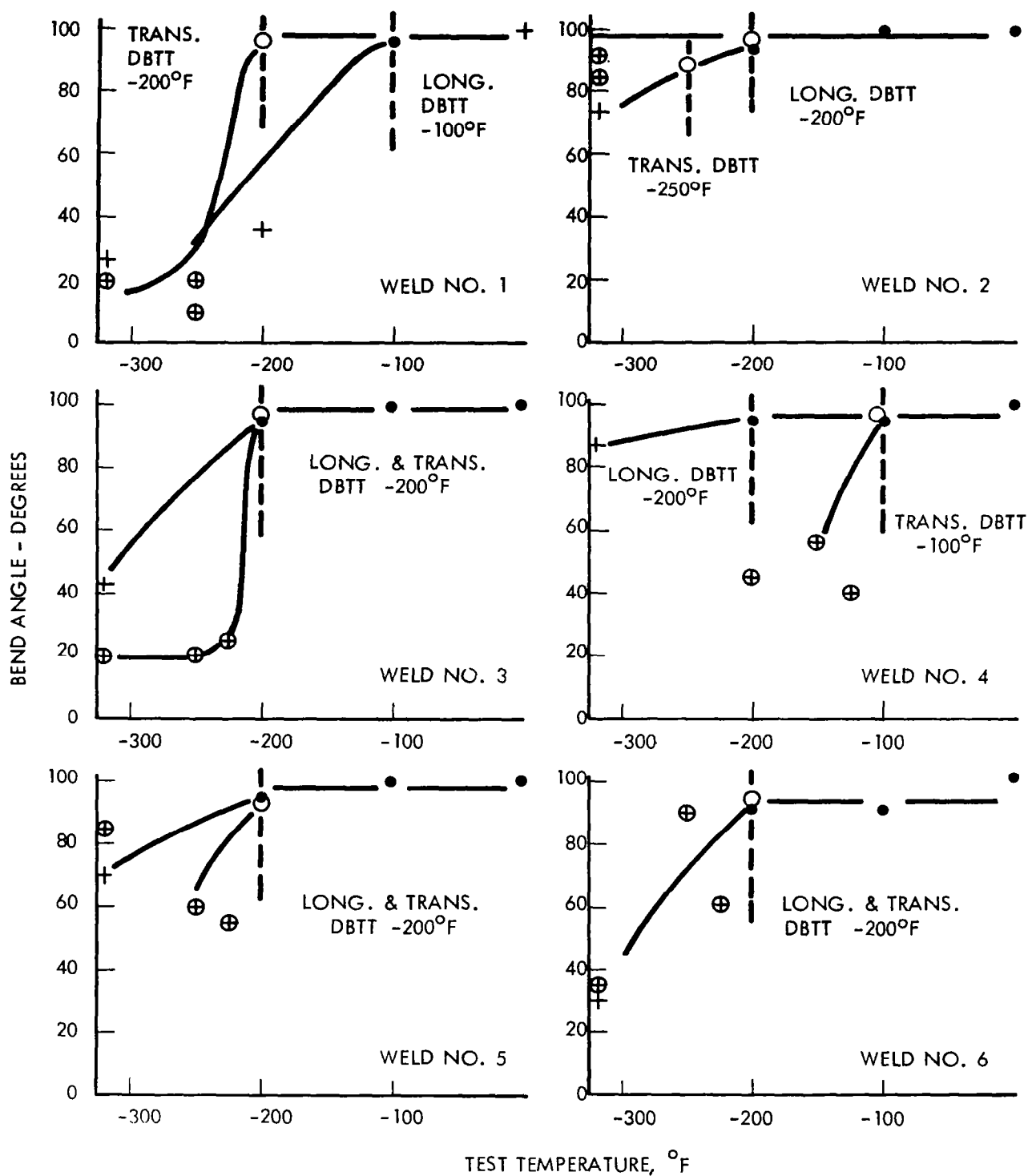


FIGURE A78 - Bend Test Results for C-129Y EB Welds  
1 $\frac{1}{2}$  Bend Radius

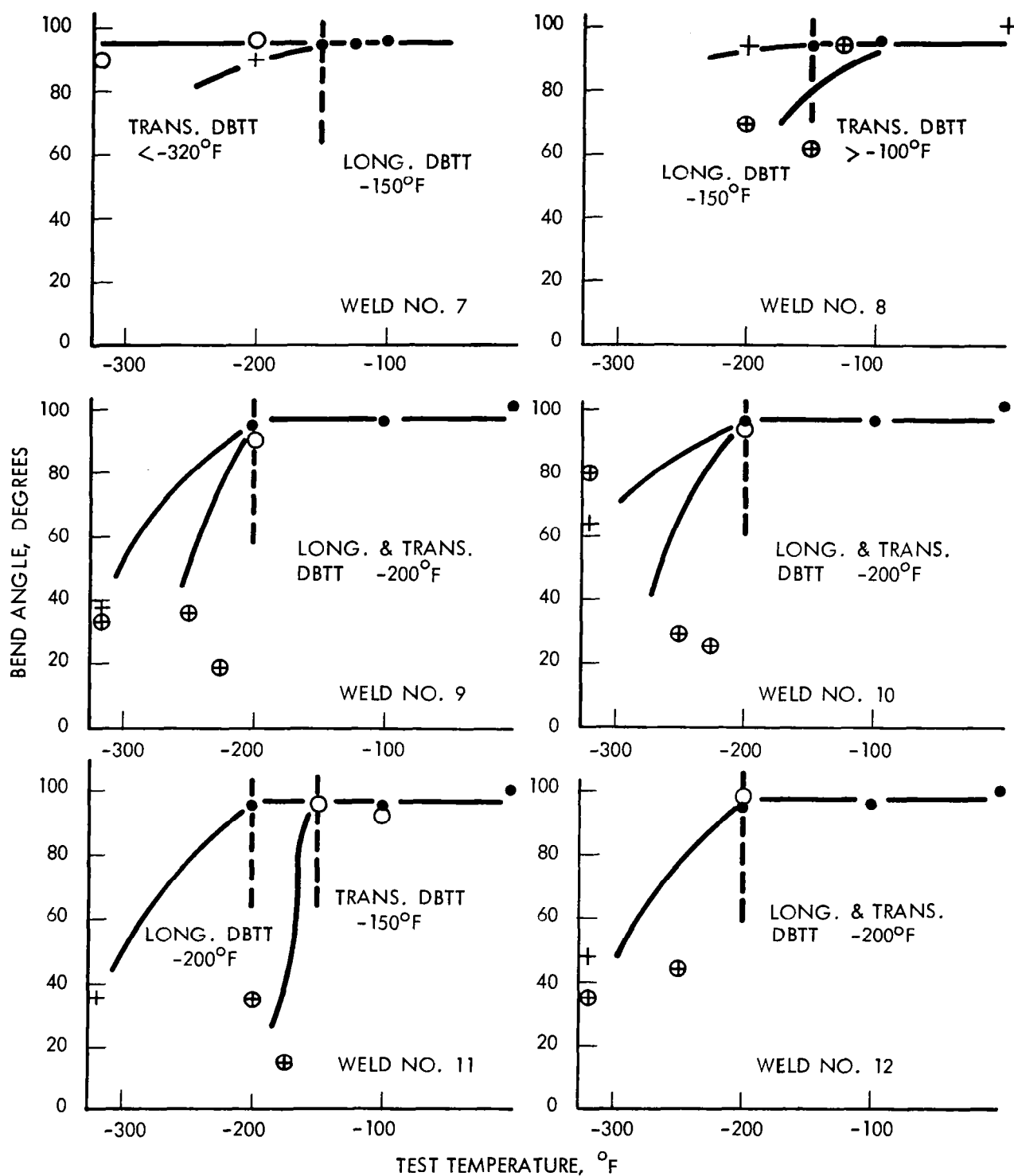
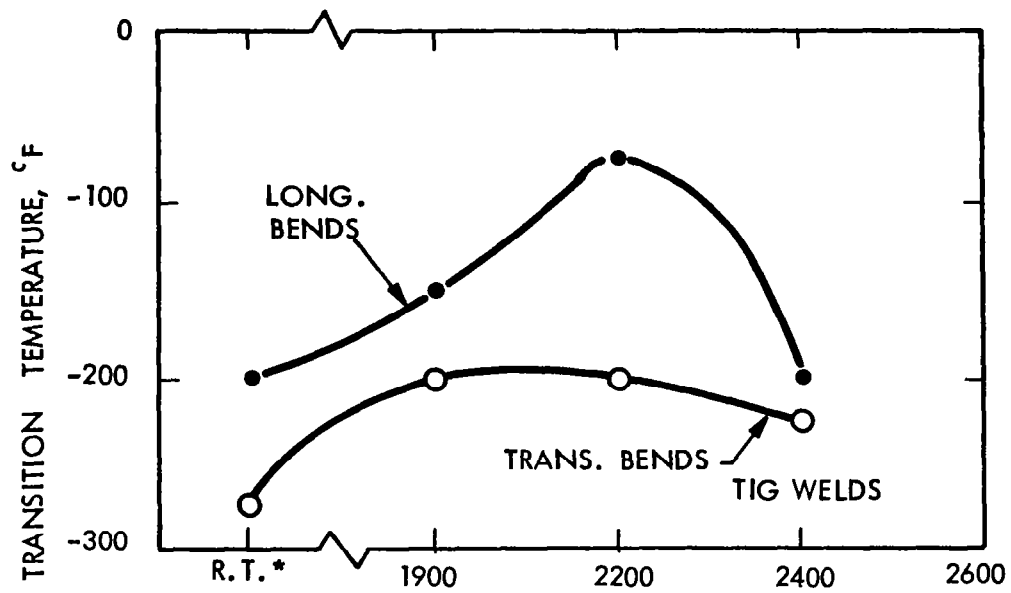


FIGURE A79 - Bend Test Results for C-129Y EB Welds  
1½ Bend Radius



\*AS WELDED

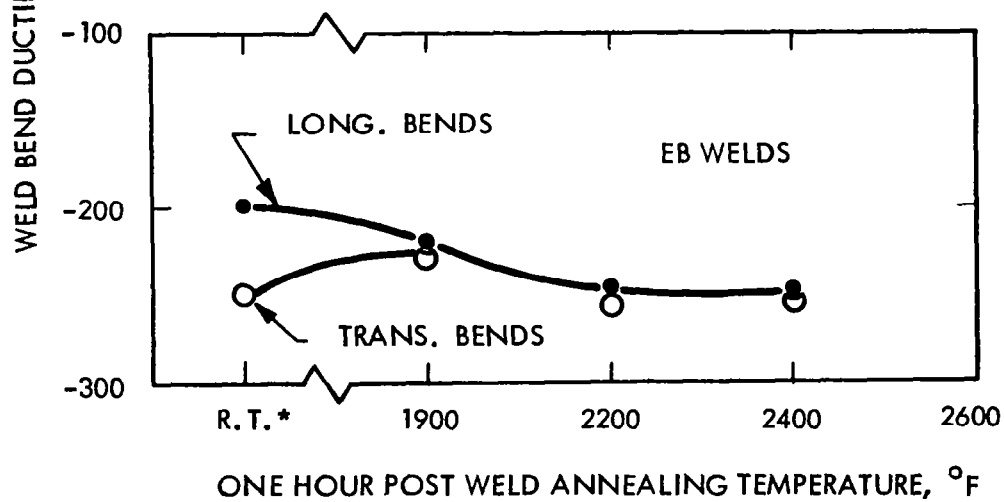


FIGURE A80 - Effect of Post-Weld Annealing on C-129Y Sheet Weld Ductility

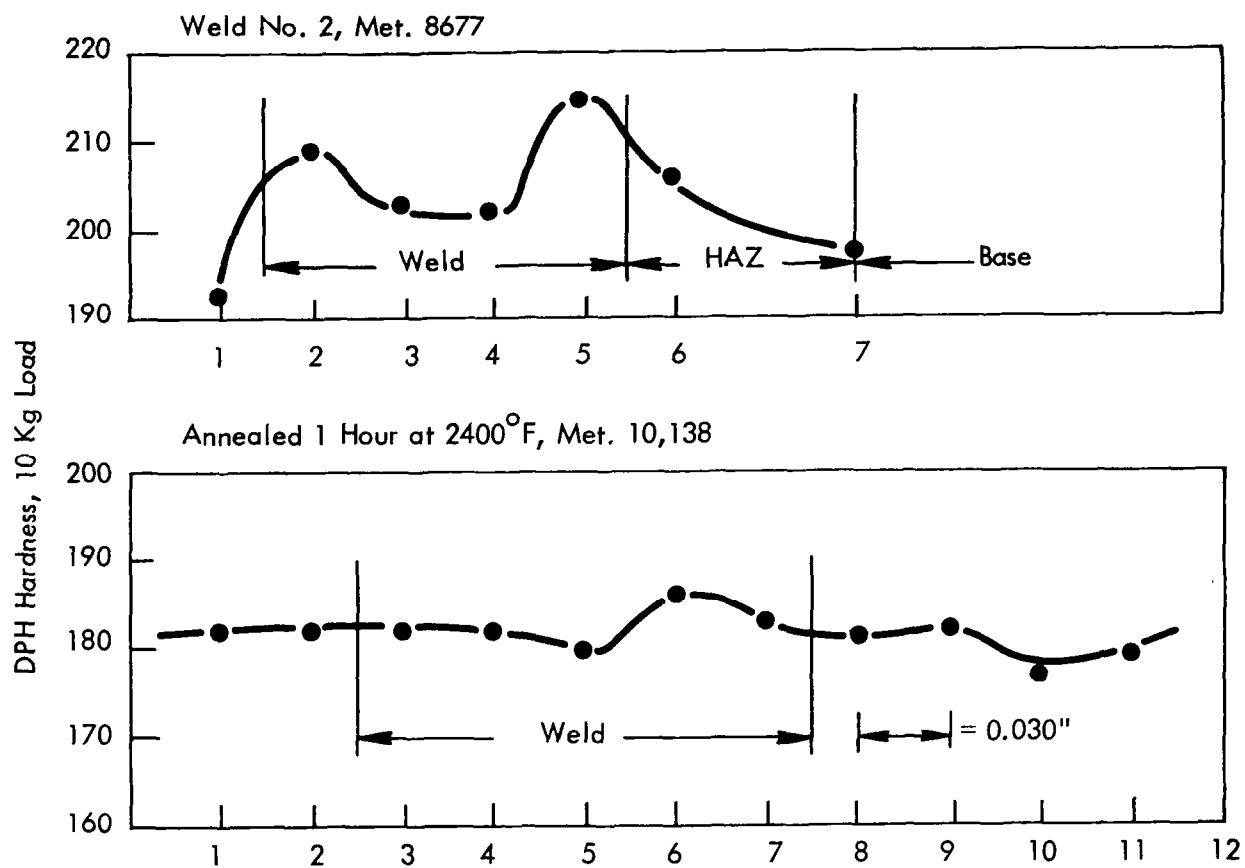


FIGURE A81 - Hardness Traverses on C-129Y GTA Sheet Butt Welds



9174-4

EB Weld No. 2, Interface

400X



8677

GTA Weld No. 2, Weld Center

200X

FIGURE A82 - C-129Y Sheet Butt Weld Microstructure



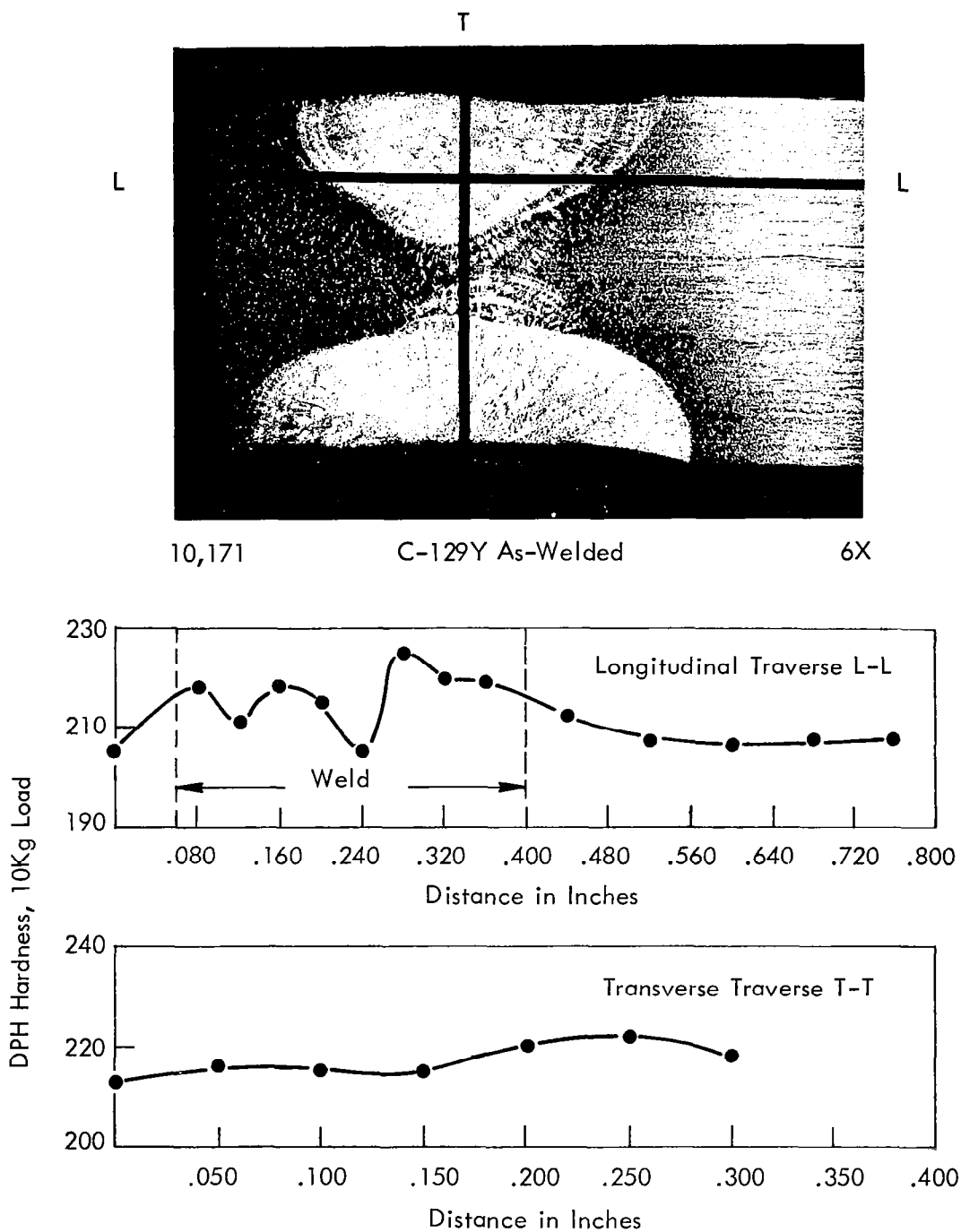
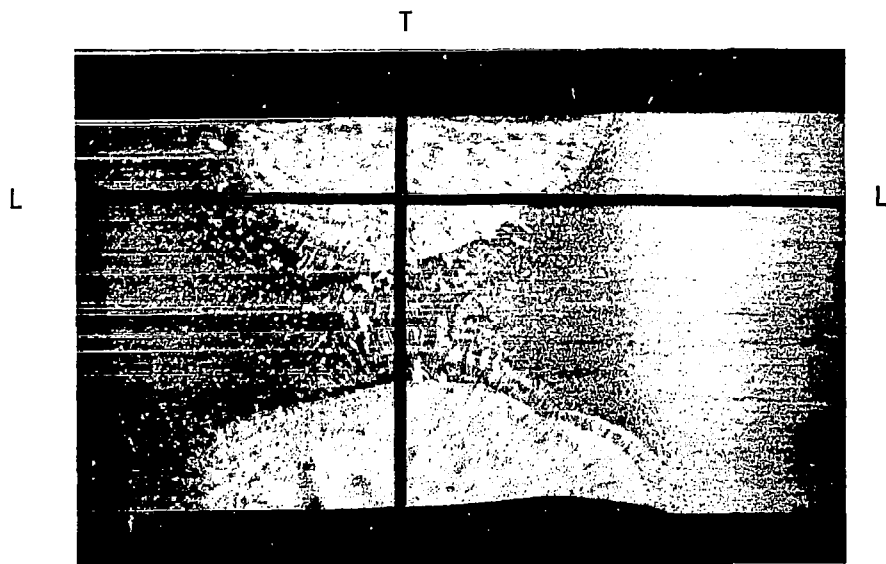


FIGURE A83 - C-129Y Plate Weld Hardness Traverses



10,178

C-129Y Annealed 1 Hr. at 2400°F

6X

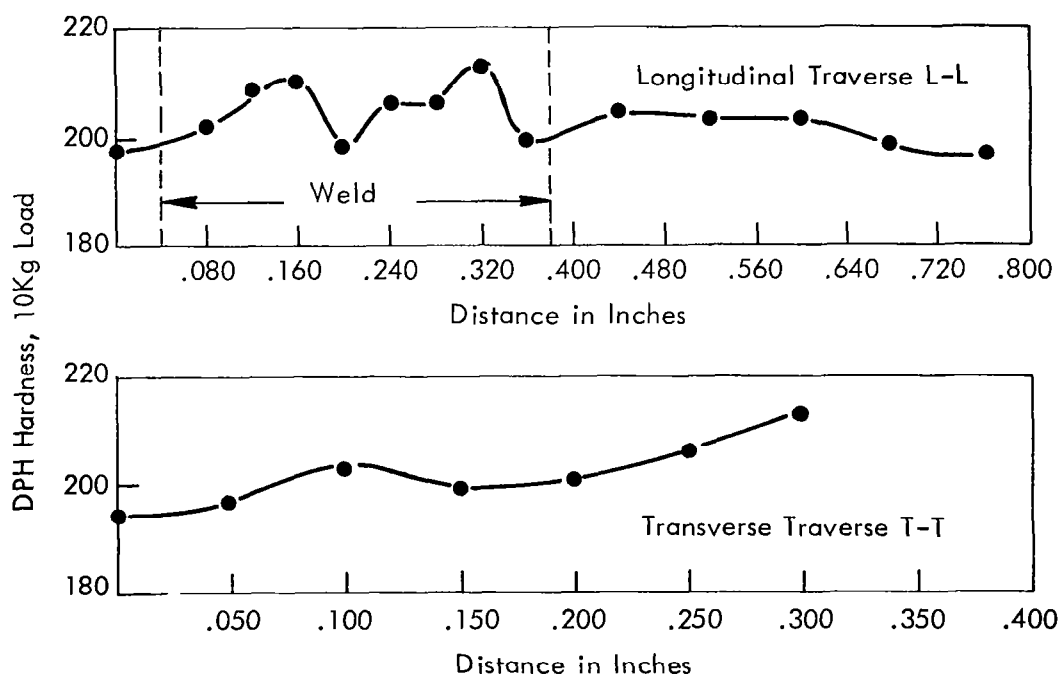
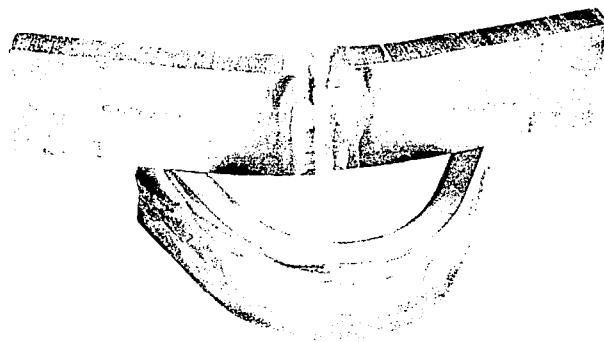


FIGURE A84 - C-129Y Plate Weld Hardness Traverses



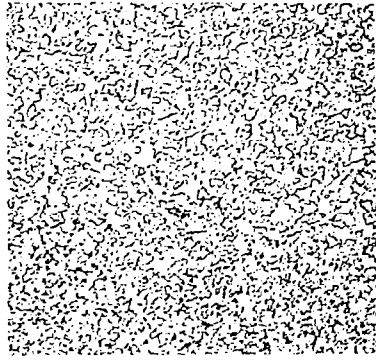
C-129Y

427-4

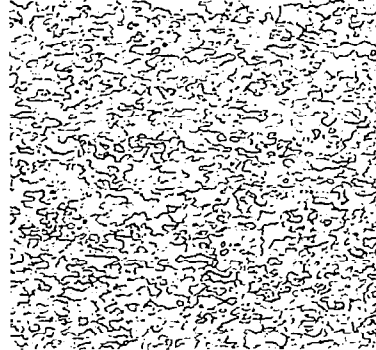
132° Longitudinal Bend  
27° Transverse Bend

FIGURE A85 - C-129Y Plate Weld Bend Specimens

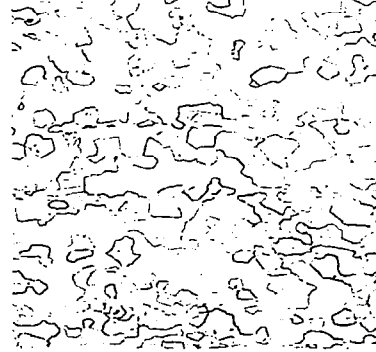
0.082"  
Wire



0.035"  
Sheet



0.375"  
Plate



Longitudinal

Transverse

FIGURE A86 - As-Received Microstructure of Cb-752, 100X

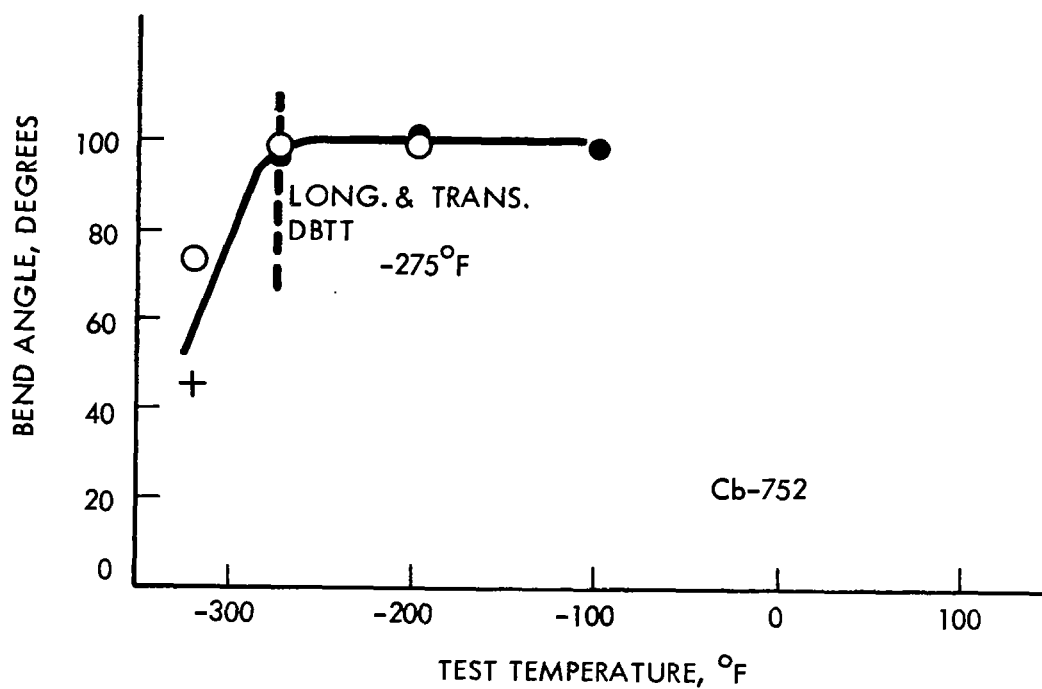


FIGURE A87 - Cb-752 Base Metal Bend Test Results

TABLE A15 - Cb-752 Sheet. GTA Butt Weld Record

Weld No.	Clamp Spacing (inch)	Speed (ipm)	Current Amperes	Weld Width Top/Bottom (inch)	Q Joules/Inch	Atmosphere Monitor Readings			Comments	
						O <sub>2</sub> (1) ppm	O <sub>2</sub> (2) ppm	H <sub>2</sub> O (3) ppm	Visual Inspection	Dye Check
1	3/8	15	70	0.130/0.080	4,750	--	4.8	0.8	Negative	Negative
2	3/8	30	110	0.160/0.140	3,730	4.0	--	0.4	1/8" HAZ Crack	1/8" HAZ Crack
3	1/4	15	80	0.155/0.120	5,430	3.0	3.9	0.1	Edge Flash (4)	Negative
4	1/4	30	100	0.135/0.100	3,390	3.0	3.7	0.2	Edge Flash (4)	Negative
5	1/4	7.5	60	0.114/0.060	8,880	0.5	2.8	0.1	Negative	Negative
6	1/4	7.5	86	0.200/0.190	12,000	--	3.2	0.5	Negative	Negative
7	3/8	7.5	64	0.174/0.135	9,460	--	3.2	0.05	Negative	Negative
8	1/4	15	92	0.174/0.150	6,820	--	2.8	0.05	Negative	Negative
9	1/4	30	149	0.192/0.180	5,520	--	1.0	3.1	Negative	Negative
10	3/8	30	87	0.129/0.090	3,310	--	2.6	2.2	Negative	Negative
11	1/4	60	170	0.141/0.090	3,230	--	2.9	2.4	Negative	Negative
12	1/4	60	215	0.156/0.138	4,090	--	3.2	0.5	Negative	Negative

(1) Westinghouse Oxygen Gage

(2) Lockwood &amp; McLorie Oxygen Gage

(3) CEC Moisture Monitor

(4) Instantaneous Arcing to Weld Clamp Down

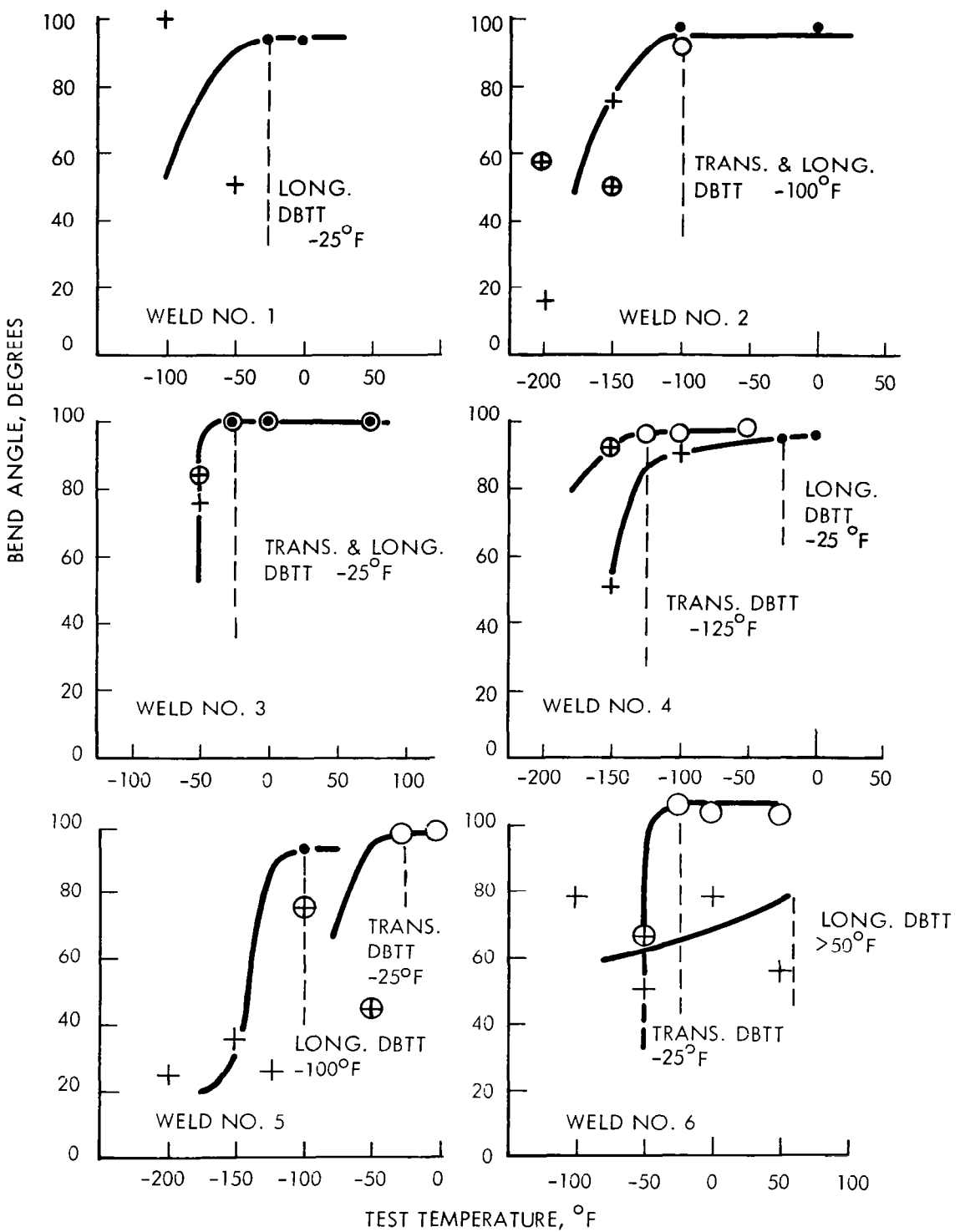


FIGURE A88 - Bend Test Results for Cb-752 GTA Welds  
1t Bend Radius

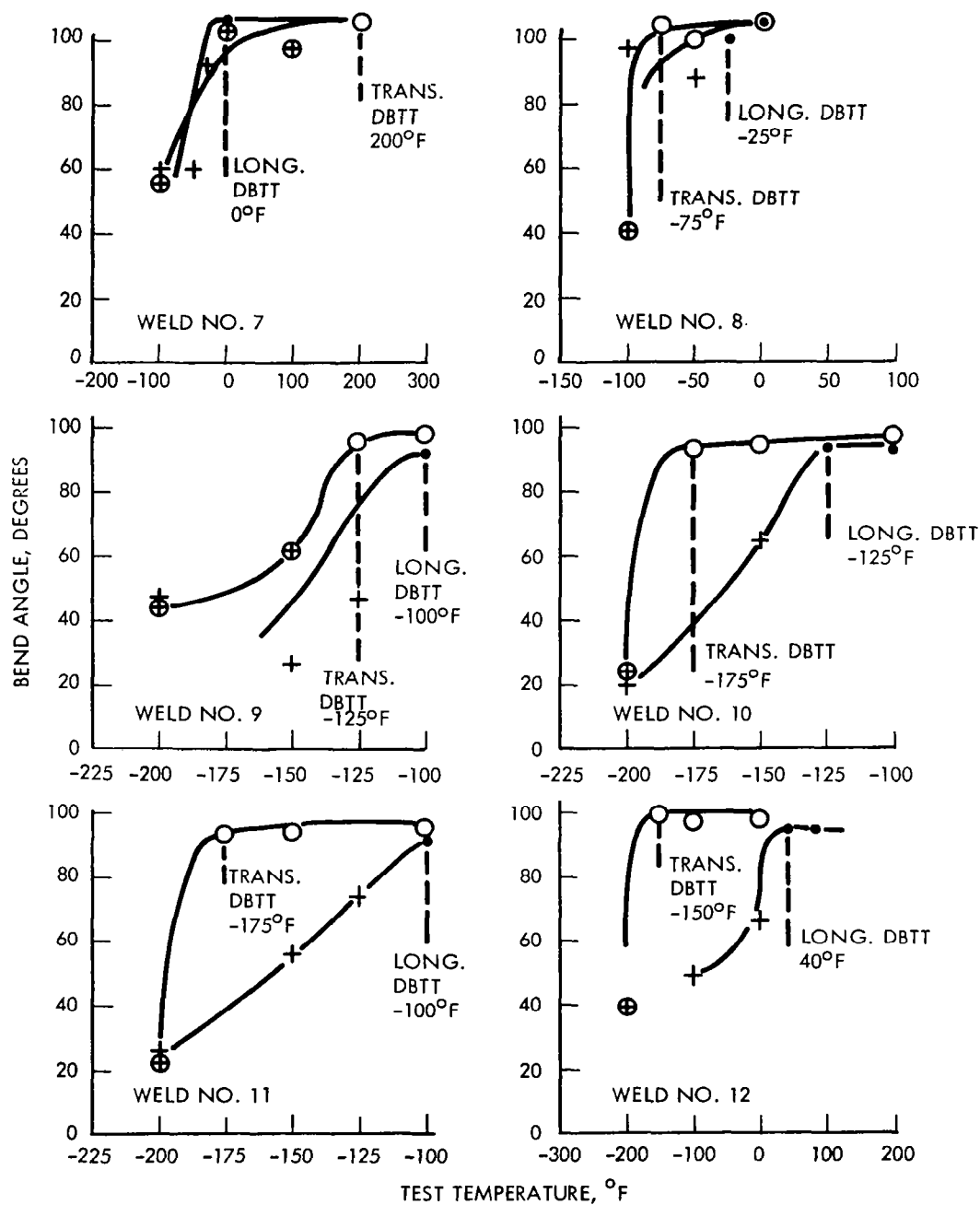
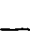




FIGURE A89 - Bend Test Results for Cb-752 GTA Welds  
1† Bend Radius



TABLE A16 - Cb-752 Sheet EB Weld Record

Weld No.	Speed (ipm)	Deflection <sup>1</sup> (inches)	Current (ma)	Chill Spacing (inches)	Power (watts)	Watt-Sec. per inch	Weld Bead Width (inches)		Vacuum <sup>2</sup> (Torr)
							Top	Bottom	
1	100	none	5.0	0.250	750	450	0.025	0.019	$6.5 \times 10^{-6}$
2	100	L-0.050"	5.0		750	450	0.035	0.022	$6.5 \times 10^{-6}$
3	50	L-0.050"	4.4		660	790	0.043	0.027	$6.5 \times 10^{-6}$
4	25	L-0.050"	3.8		570	1370	0.050	0.039	$6.0 \times 10^{-6}$
5	15	L-0.050"	3.3		500	2000	0.054	0.046	$6.0 \times 10^{-6}$
6	15	T-0.050"	3.3		500	2000	0.075	0.056	$6.0 \times 10^{-6}$
7	100	none	5.0		750	450	0.026	0.018	$6.5 \times 10^{-6}$
8	100	L-0.050"	5.0		750	450	0.035	0.022	$6.5 \times 10^{-6}$
9	50	L-0.050"	4.4		660	790	0.042	0.026	$6.5 \times 10^{-6}$
10	25	L-0.050"	3.8		570	1370	0.045	0.031	$6.0 \times 10^{-6}$
11	15	L-0.050"	3.3		500	2000	0.036	0.017	$6.0 \times 10^{-6}$
12	15	T-0.050"	3.3		500	2000	0.054	0.045	$6.0 \times 10^{-6}$

1. L. is longitudinal  
T. is transverse

2. Current evacuation practice provides pressures of  $1.5 \times 10^{-6}$  Torr

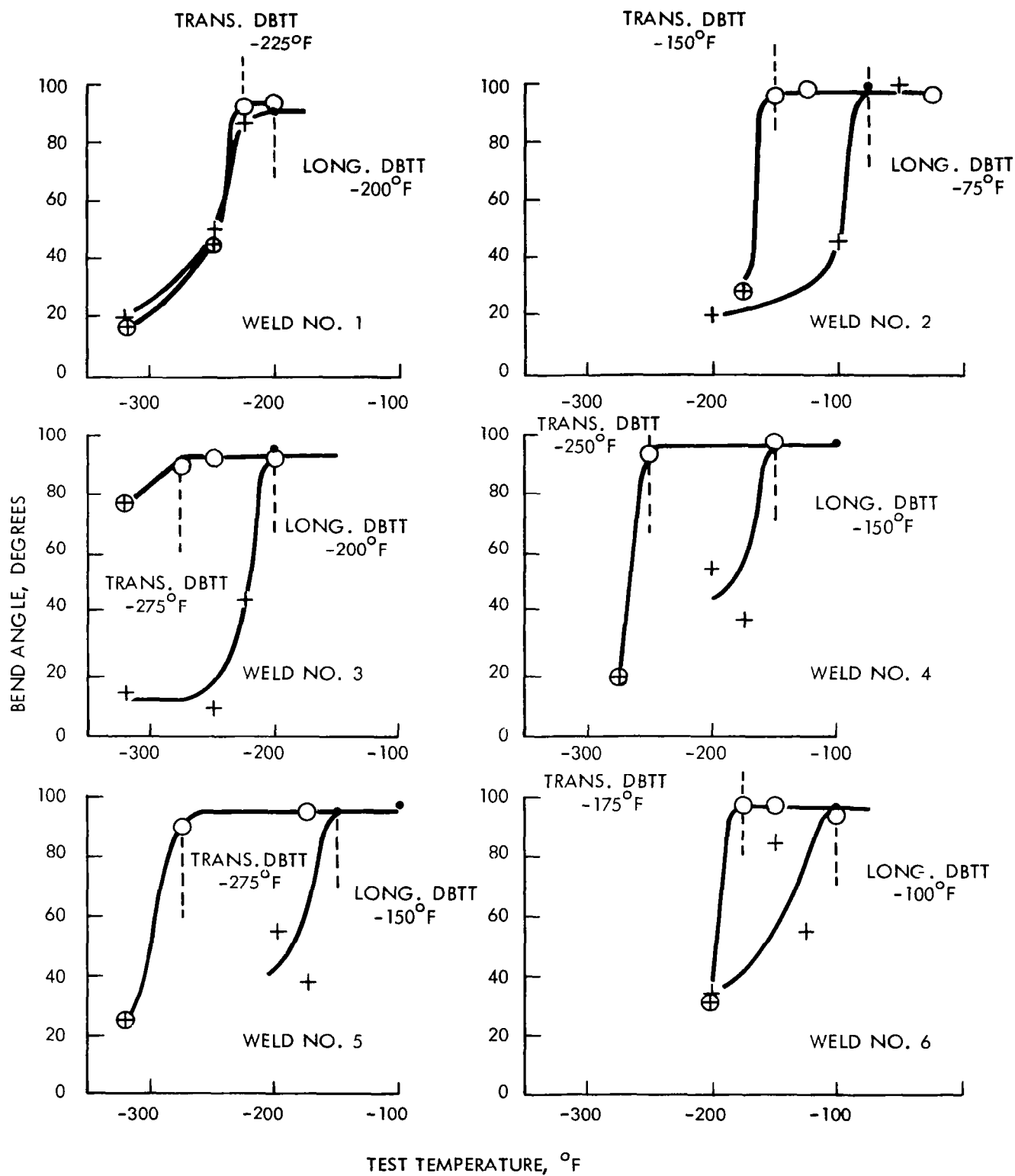


FIGURE A90 - Bend Test Results for Cb-752 EB Welds  
1t Bend Radius

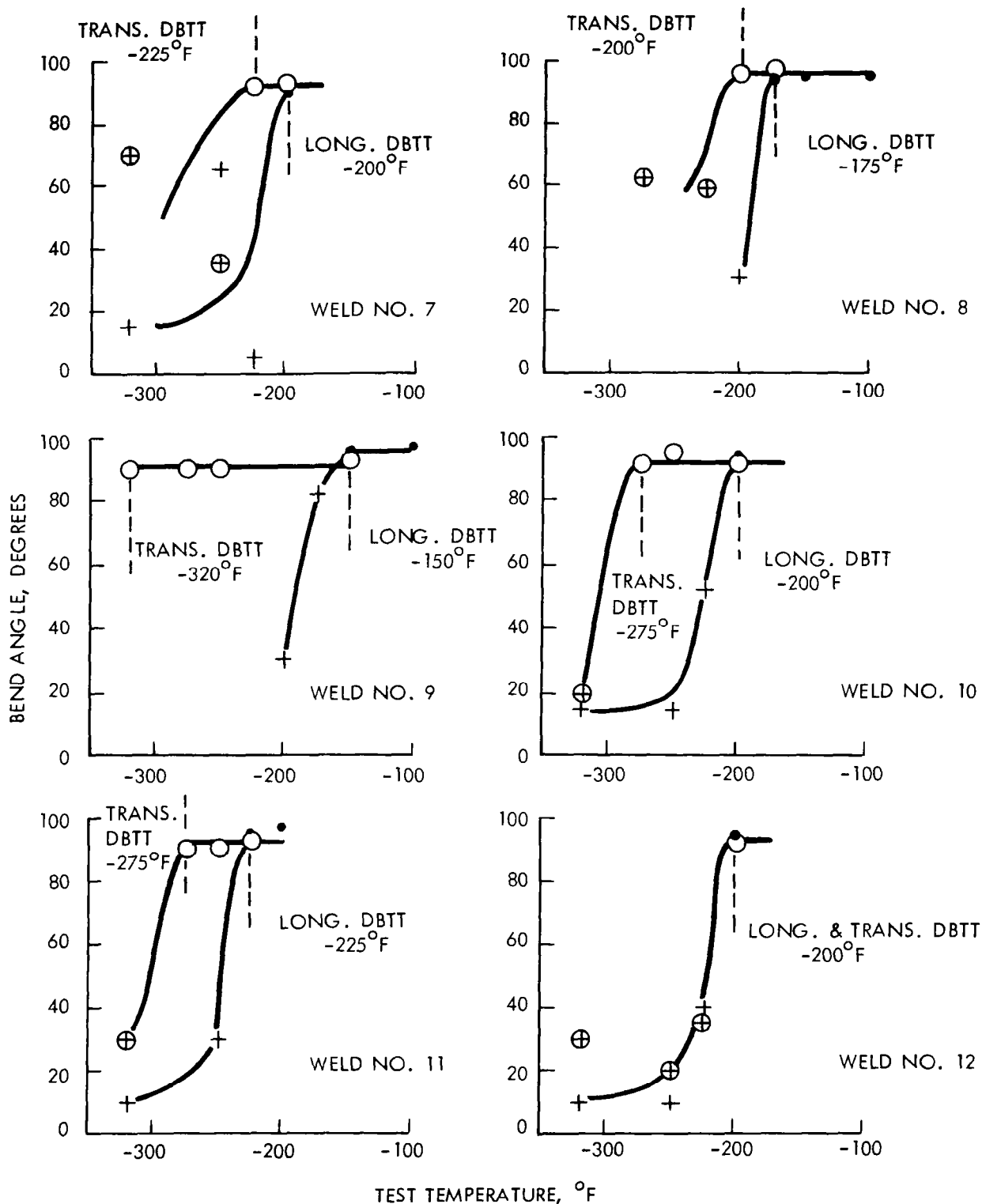


FIGURE A91 - Bend Test Results for Cb-752 EB Welds  
1t Bend Radius

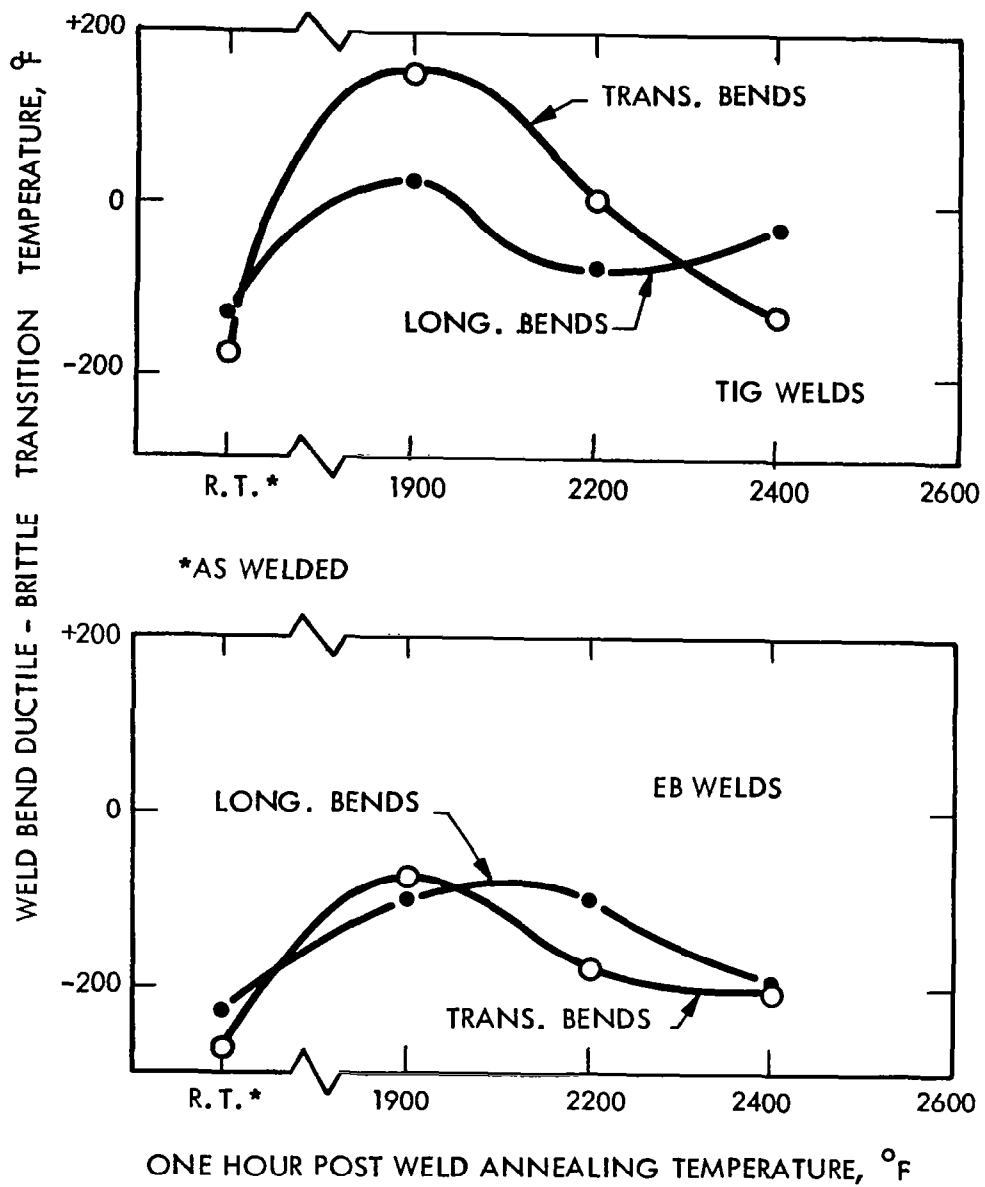


FIGURE A92 - Effect of Post-Weld Annealing on Cb-752 Weld Ductility

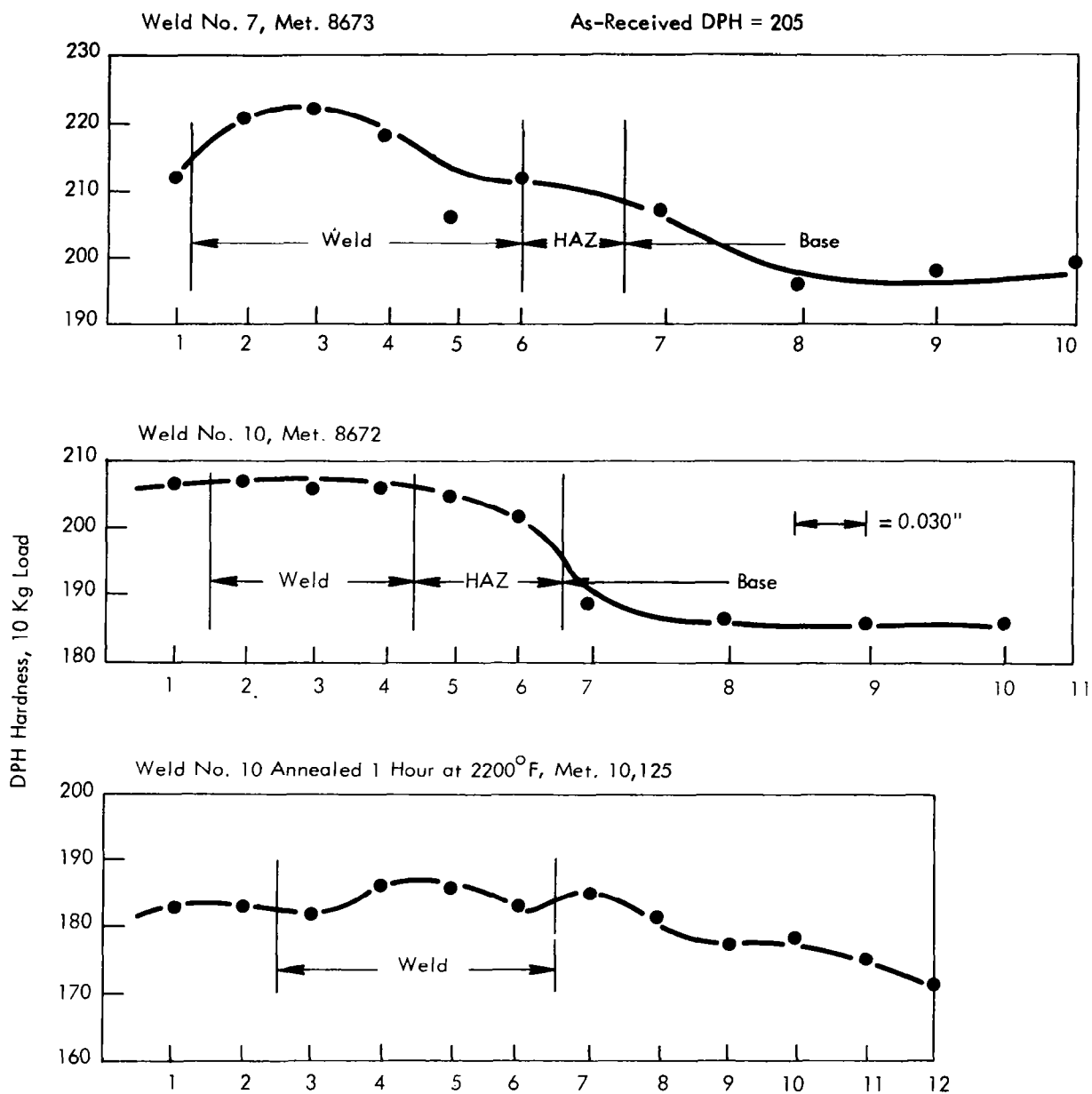
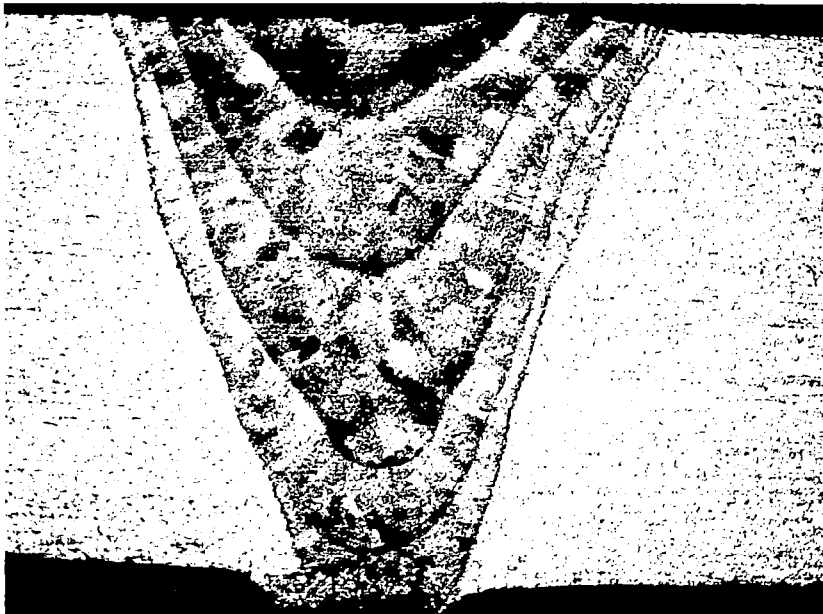


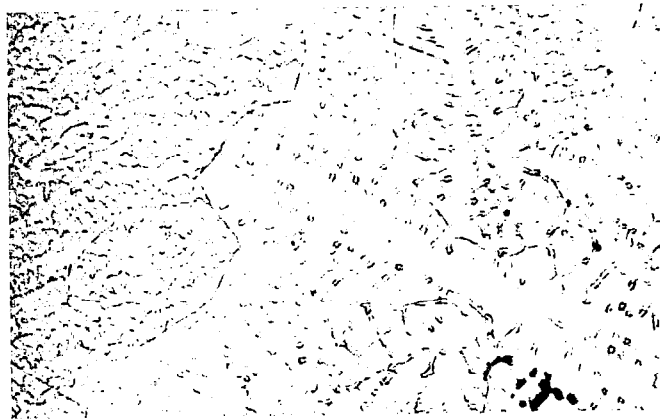
FIGURE A93 - Hardness Traverses, Cb-752 GTA Sheet Butt Welds



9167-1

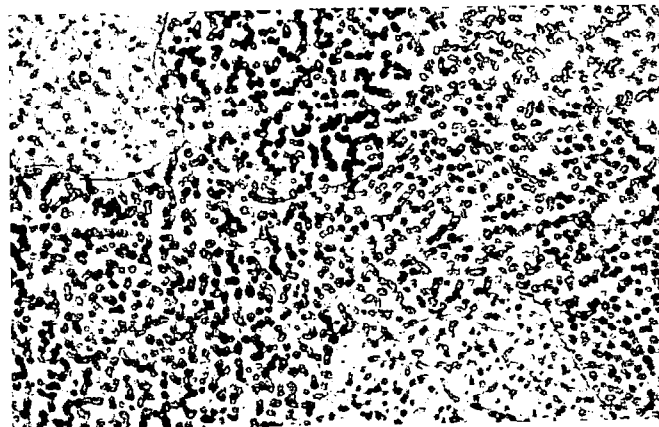
80X

FIGURE A94 - Cb-752 EB Weld No. 11



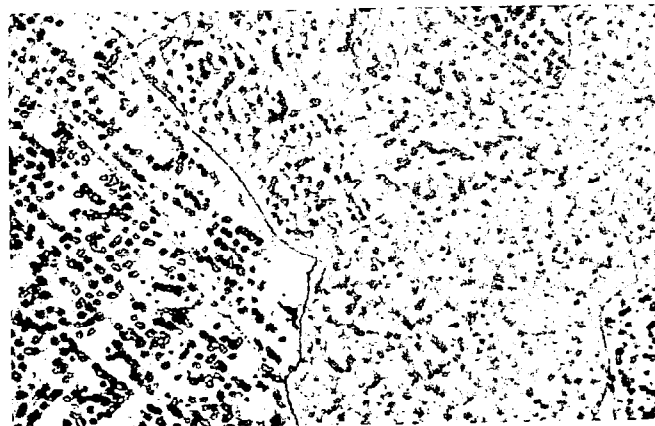
8672

As-Welded



10,125

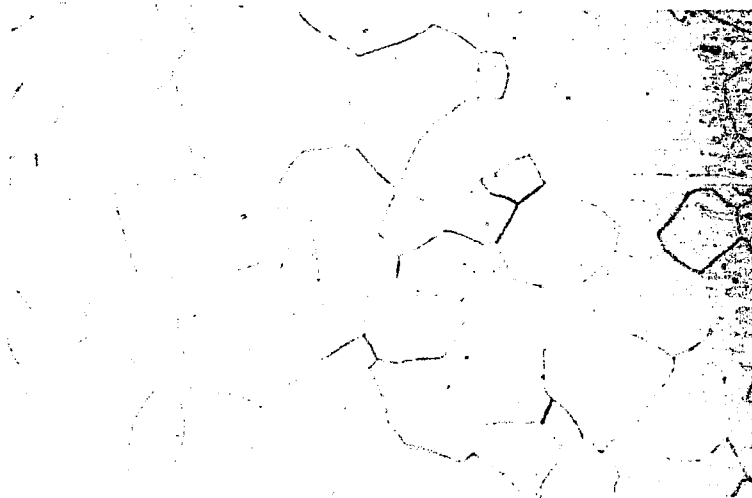
Annealed 1 Hour at 2200°F



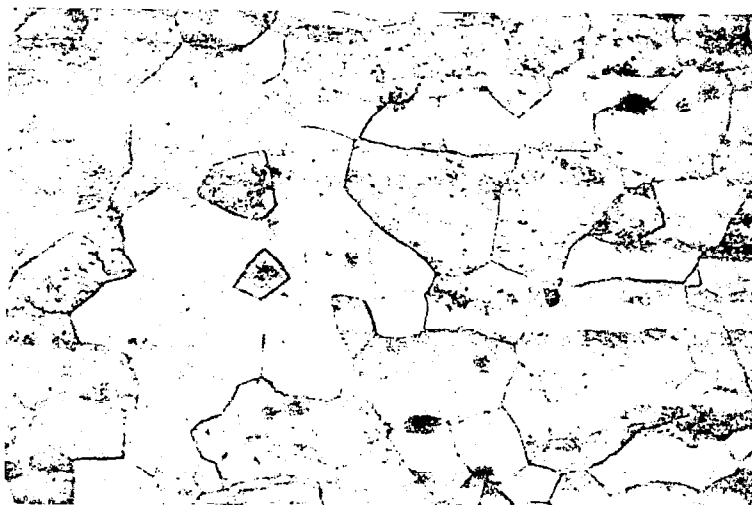
10,126

Annealed 1 Hr. at 2400°F

FIGURE A95 - Cb-752 GTA Sheet Weld Microstructure



10,124 HAZ, Annealed 1 Hour at 1900°F



10,125 HAZ, Annealed 1 Hour at 2200°F

FIGURE A96 - Cb-752 GTA Sheet Weld Microstructure, 400X





10,177

As-Welded



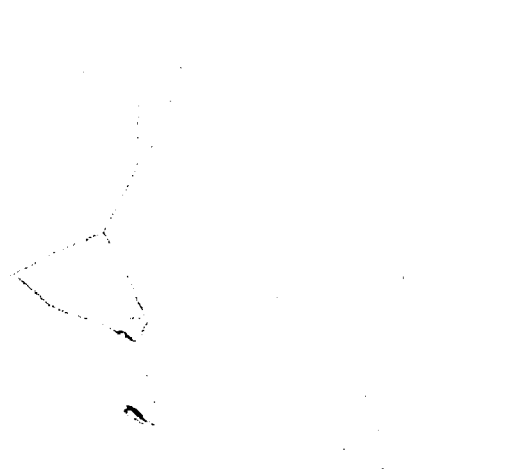
500X

10,180

Annealed 1 Hr. at 2200°F

500X

Weld Area



10,177

As-Welded



500X

10,180

Annealed 1 Hr. at 2200°F

500X

Heat Affected Zone

FIGURE A97 - Plate Weld Microstructure of Cb-752

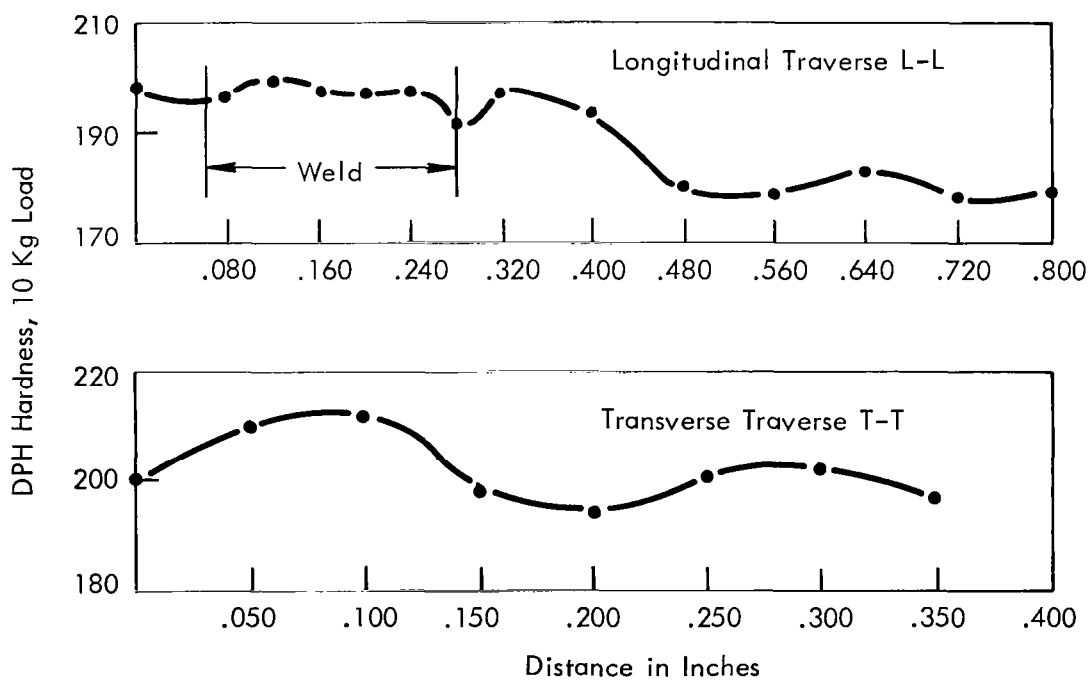
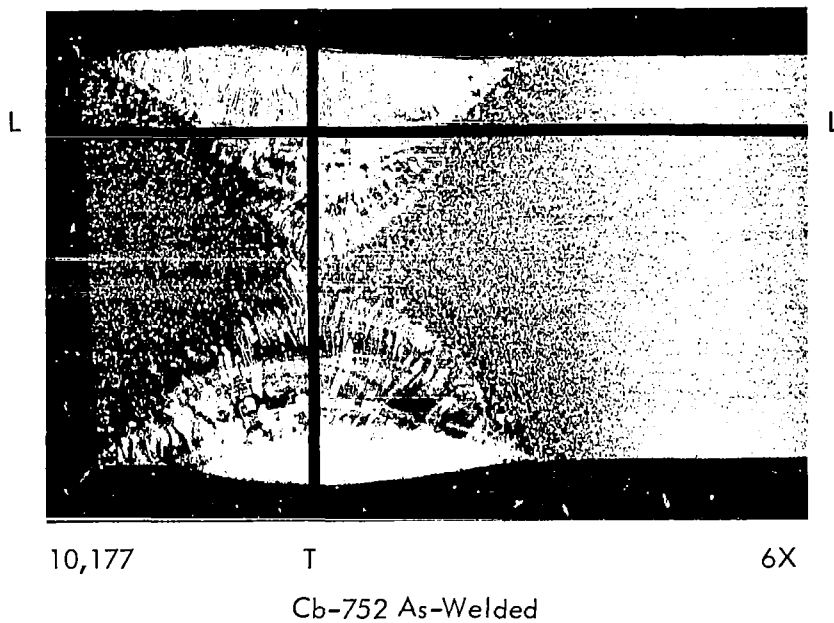


FIGURE A98 - Plate Weld Hardness Traverses of Cb-752

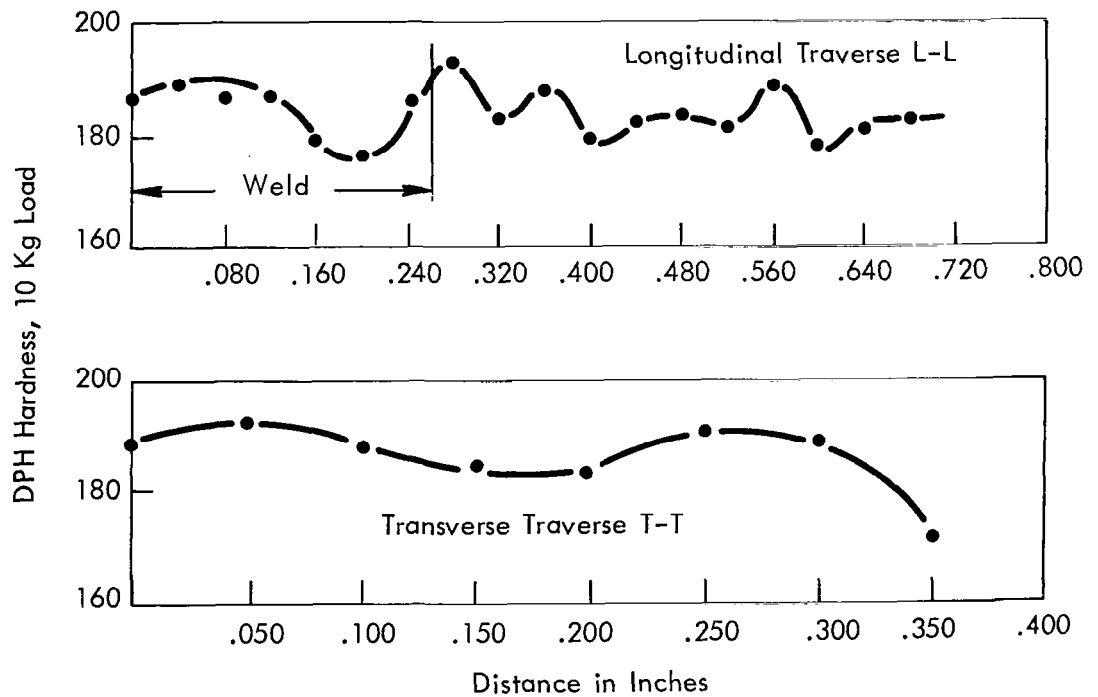
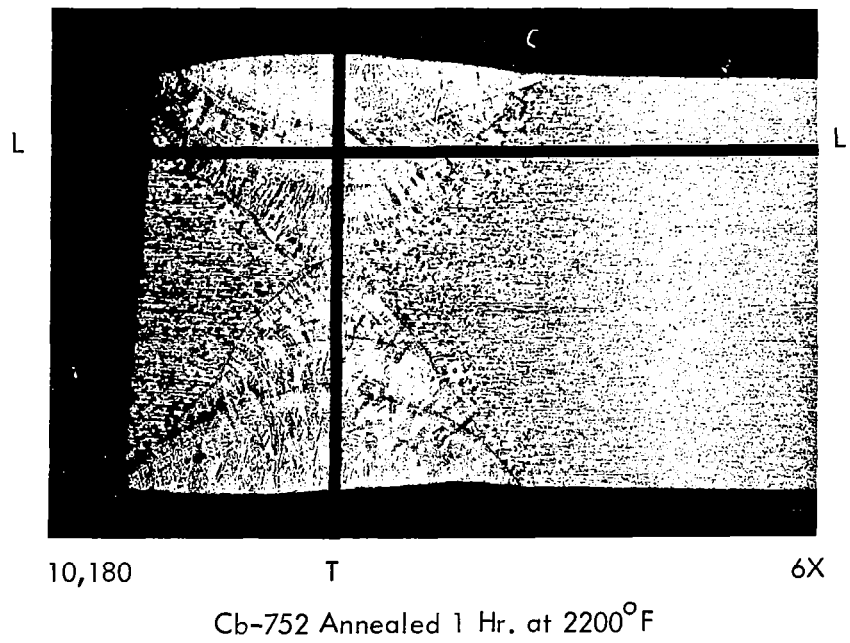
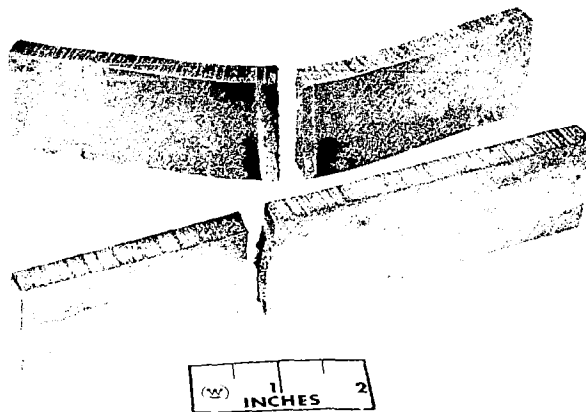


FIGURE A99 - Plate Weld Hardness Traverses of Cb-752

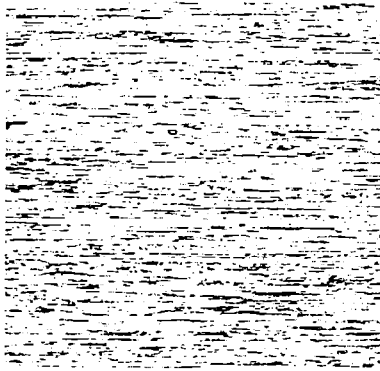


Cb-752

427-2

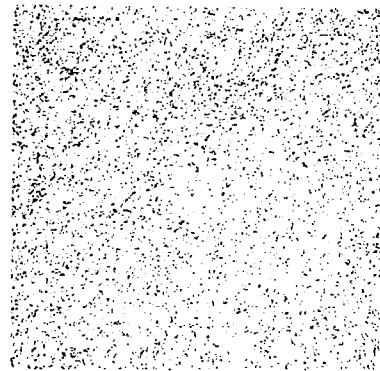
29° Longitudinal Bend  
45° Transverse Bend

FIGURE A100 - Plate Weld Bend Specimens of Cb-752

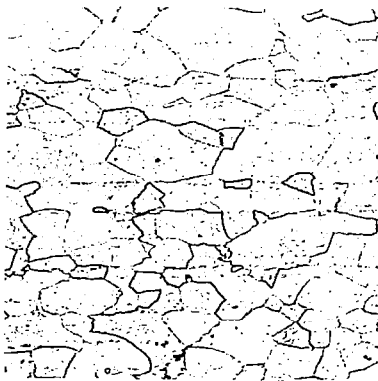


3322

0.082" Wire



3323

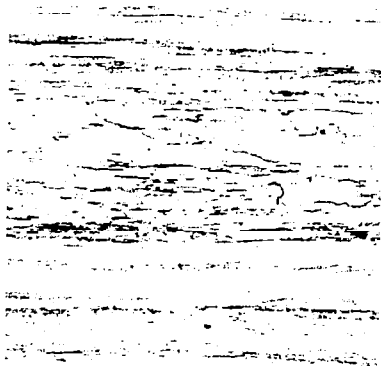


2800

0.035" Sheet



2801



200X

2624

0.375" Plate

Longitudinal



50X

2625

Transverse

FIGURE A101 - As-Received Microstructure of D-43, 100X

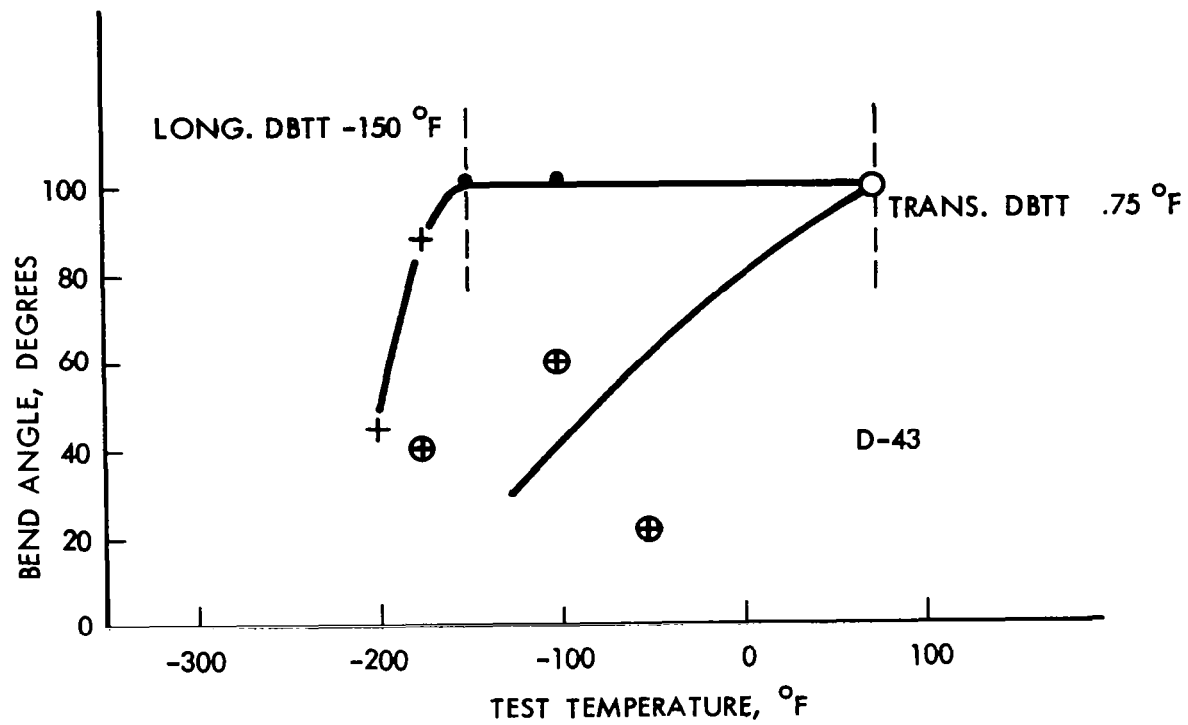


FIGURE A102 - D-43 Base Metal Bend Test Results

TABLE A17 - D-43 Sheet. GTA Butt Weld Record

Weld No.	Clamp Spacing (inch)	Speed (ipm)	Current Amperes	Weld Width Top/Bottom (inch)	Q Joules/Inch	Atmosphere Monitor Readings			Comments	
						O <sub>2</sub> (1) ppm	O <sub>2</sub> (2) ppm	H <sub>2</sub> O (3) ppm	Visual Inspection	Dye Check
1	3/8	15	60	0.10/0.02	4,080	--	4.3	0.17	Negative	Negative
2	3/4	15	80	0.18/0.18	5,420	--	4.3	0.40	Negative	Negative
3	1/4	15	75	0.14/0.12	5,100	5.0	5.5	0.20	Edge Flash (4)	Negative
4	1/4	30	100	0.135/0.09	3,390	6.0	5.9	0.40	Negative	Negative
5	1/4	7.5	65	0.120/0.09	9,340	3.5	4.4	2.2	Negative	Negative
6	1/4	7.5	82	0.190/0.190	11,800	4.0	4.6	2.4	Negative	Negative
7	1/4	15	122	0.240/0.240	9,020	0.5	2.4	0.15	Negative	Negative
8	1/4	30	135	0.165/0.150	5,000	--	2.0	0.5	Negative	Negative
9	3/8	30	114	0.159/0.144	4,550	0.5	2.2	0.30	Negative	Negative
10	3/8	30	72	0.099/0.024	2,590	0.5	2.1	0.40	Negative	Negative
11	3/8	60	155	0.129/0.075	2,865	0.5	2.7	0.30	Negative	Negative
12	1/4	60	215	0.180/0.165	4,090	2.0	3.2	0.10	Negative	Negative

(1) Westinghouse Oxygen Gage  
 (2) Lockwood & McLorie Oxygen Gage

(3) CEC Moisture Monitor  
 (4) Instantaneous Arcing to Weld Clamp Down

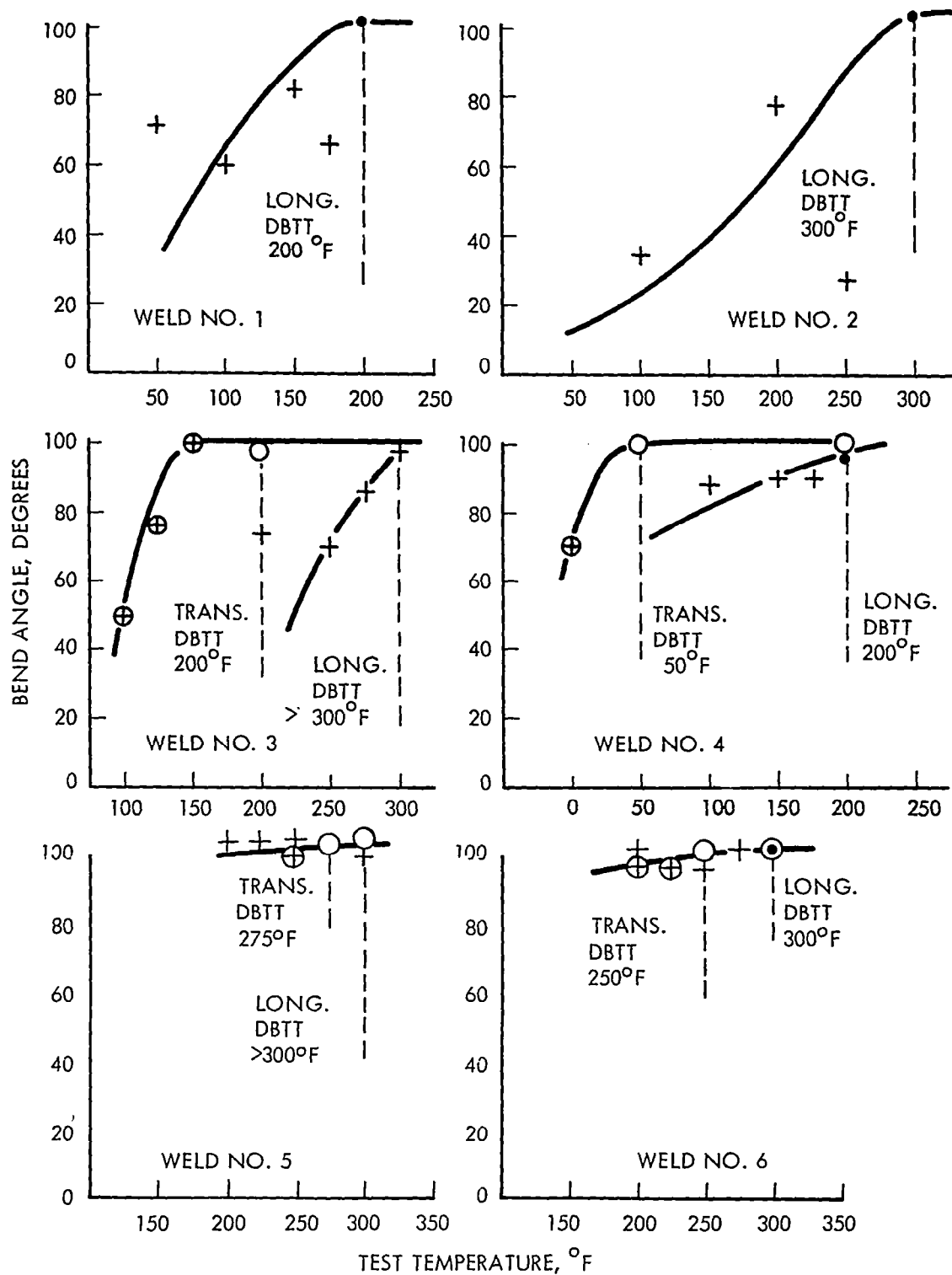


FIGURE A103 - Bend Test Results of D-43 GTA Welds  
1t Bend Radius



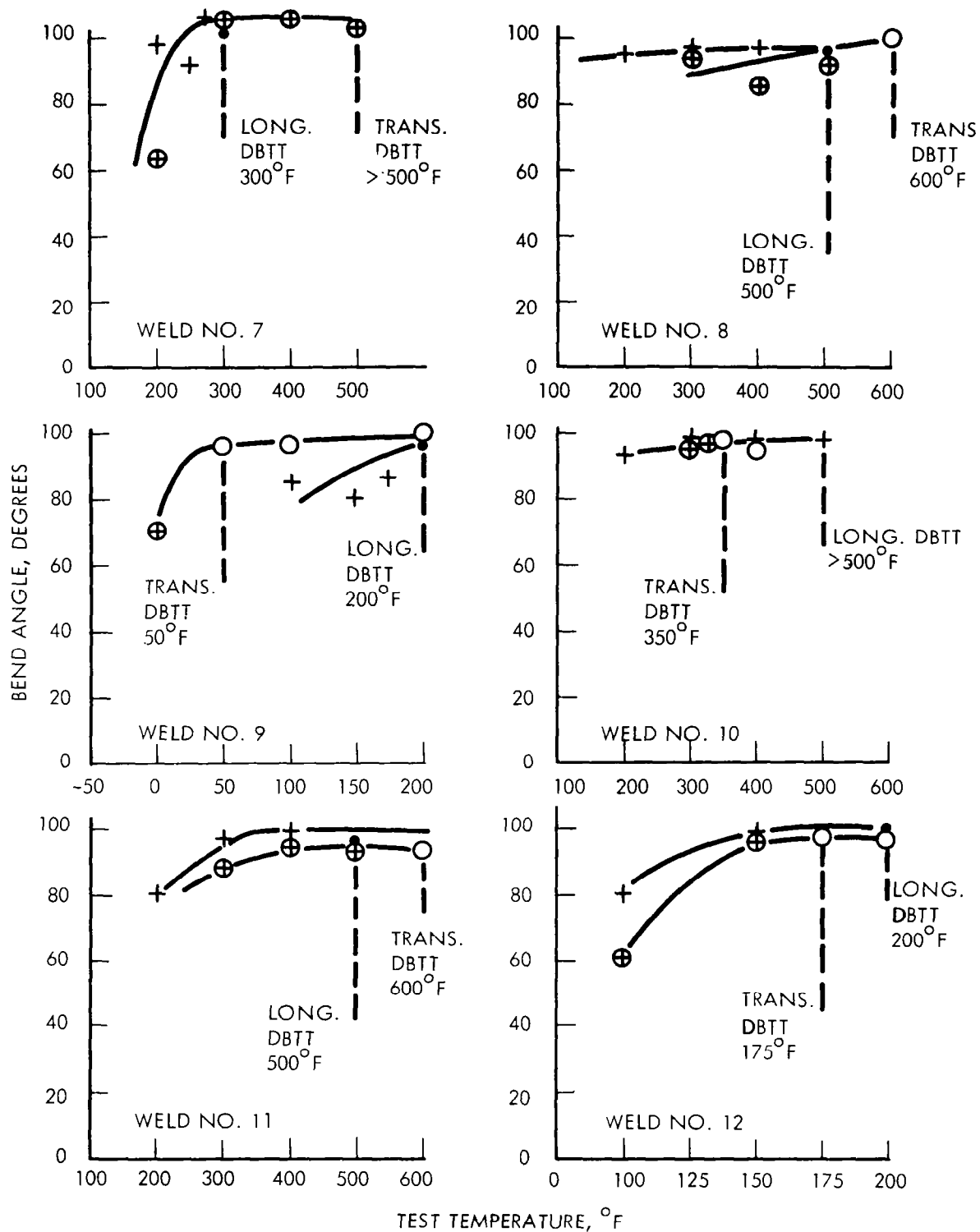


FIGURE A104 - Bend Test Results of D-43 GTA Welds  
1t Bend Radius

TABLE A18 - D-43 Sheet EB Weld Record

Weld No.	Speed (ipm)	Deflection <sup>1</sup> (inches)	Current (ma)	Chill Spacing (inches)	Power <sup>2</sup> (watts)	Watt-Sec. per inch	Weld Bead Width (inches)		Vacuum Torr
							Top	Bottom	
1	50	zero	4.2	0.094	630	758	0.036	0.024	$2.0 \times 10^{-6}$
2	100	L-0.050	6.0	0.094	900	540	0.034	0.029	$2.0 \times 10^{-6}$
3	50	L-0.025	4.8	0.094	720	865	0.036	0.027	$2.0 \times 10^{-6}$
4	15	L-0.050	3.3	0.250	496	1980	0.045	0.037	$2.0 \times 10^{-6}$
5	50	L-0.050	4.4	0.250	660	793	0.040	0.027	$2.0 \times 10^{-6}$
6	100	L-0.050	5.5	0.250	825	495	0.037	0.024	$2.0 \times 10^{-6}$
7	50	L-0.050	4.8	0.094	722	868	0.040	0.027	$2.0 \times 10^{-6}$
8	50	L-0.100	5.4	0.094	812	976	0.040	0.026	$2.0 \times 10^{-6}$
9	15	zero	3.0	0.094	450	1800	0.039	0.029	$2.0 \times 10^{-6}$
10	15	L-0.050	3.6	0.094	540	2160	0.044	0.027	$2.0 \times 10^{-6}$
11	15	T-0.050	3.6	0.094	540	2160	0.060	0.050	$2.0 \times 10^{-6}$
12	25	L-0.050	4.2	0.094	630	1510	0.040	0.035	$3.0 \times 10^{-6}$

1. L. is longitudinal  
T. is transverse

2. All welds made at 150KV.

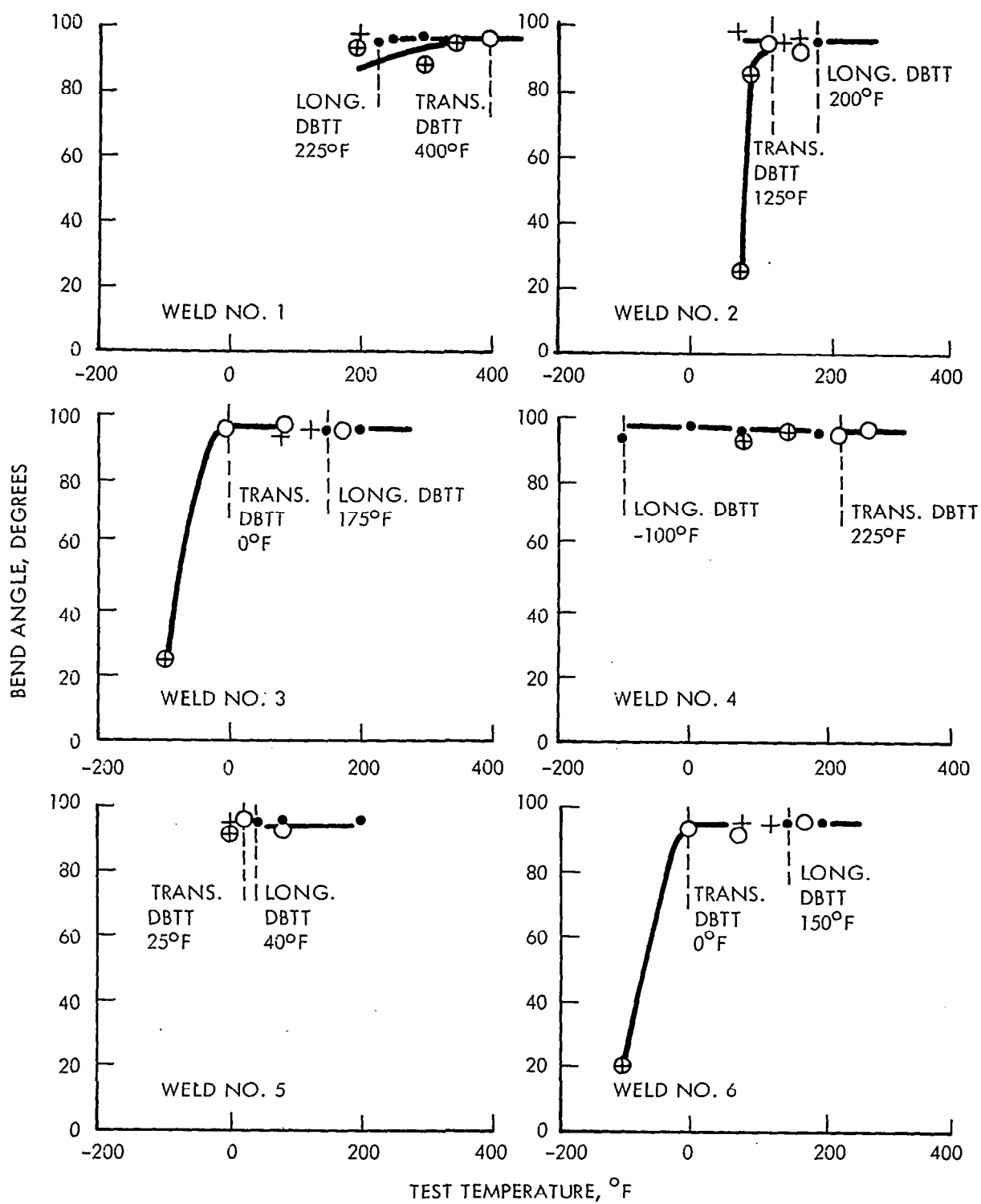


FIGURE A105 - Bend Test Results of D-43 EB Welds  
1t Bend Radius

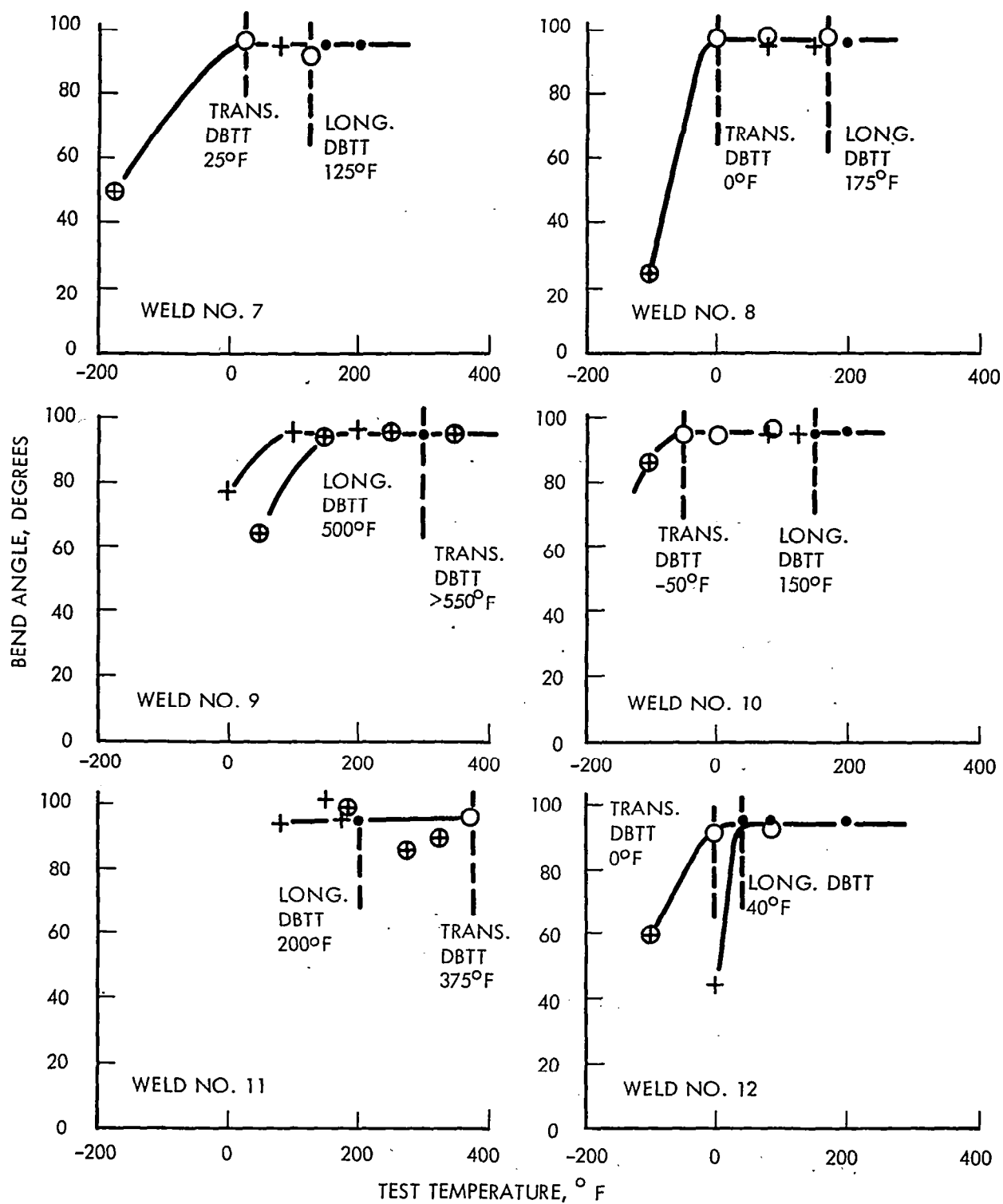


FIGURE A106 - Bend Test Results of D-43 EB Welds  
1t Bend Radius

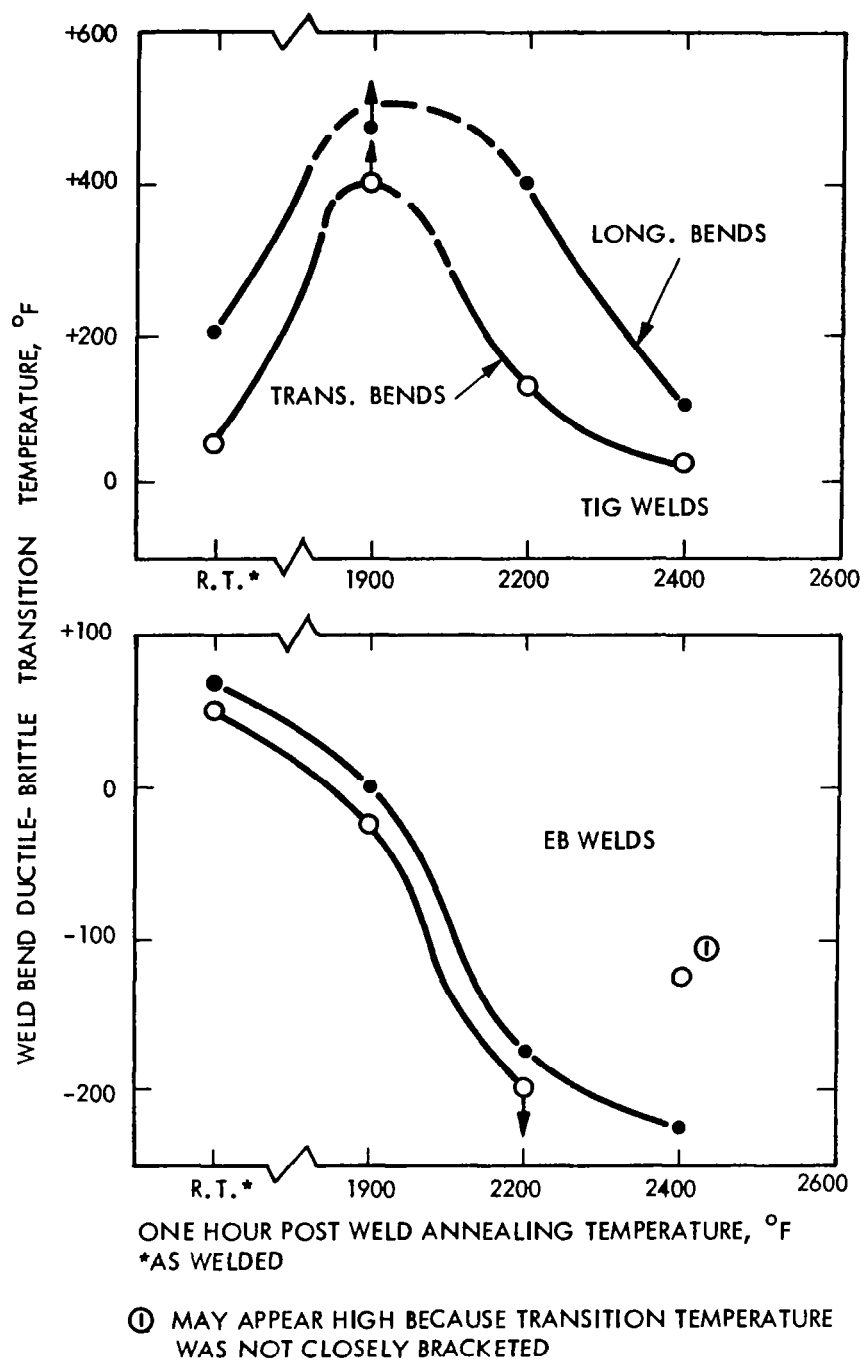


FIGURE A107 - Effect of Post Weld Annealing on D-43 Weld Ductility

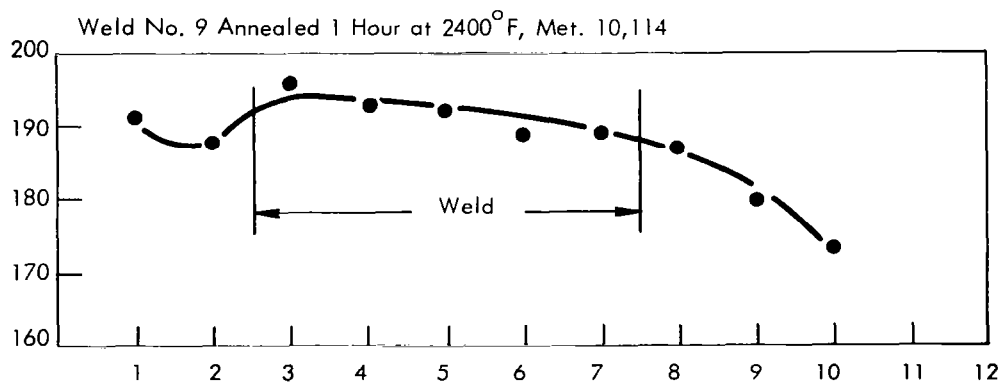
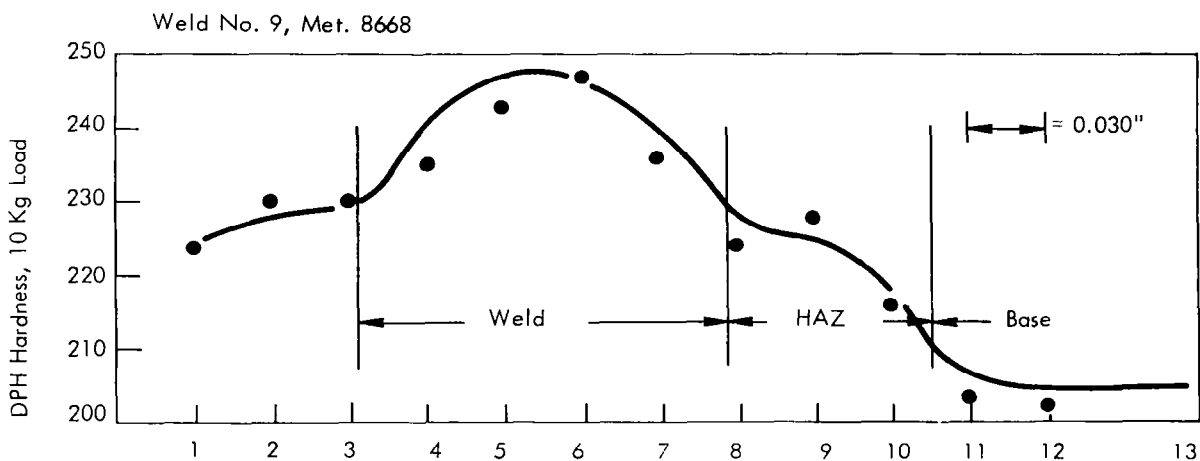
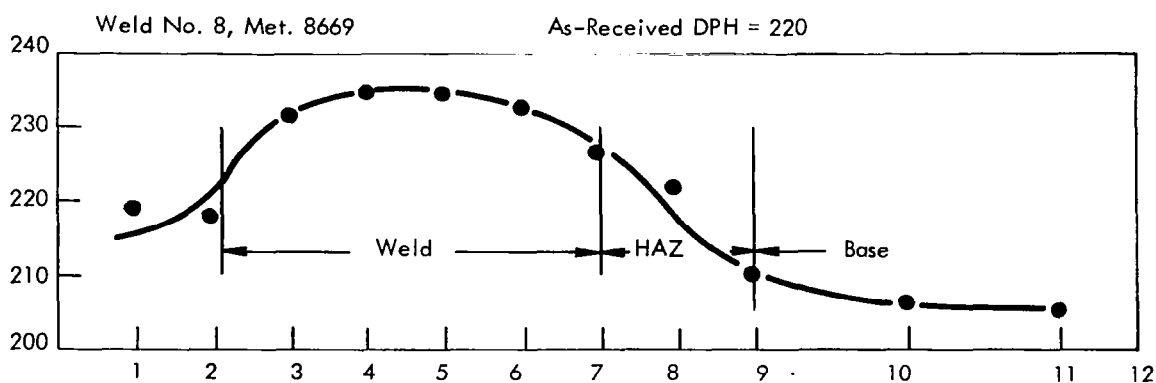


FIGURE A108 - Hardness Traverses, D-43 GTA Sheet Butt Welds



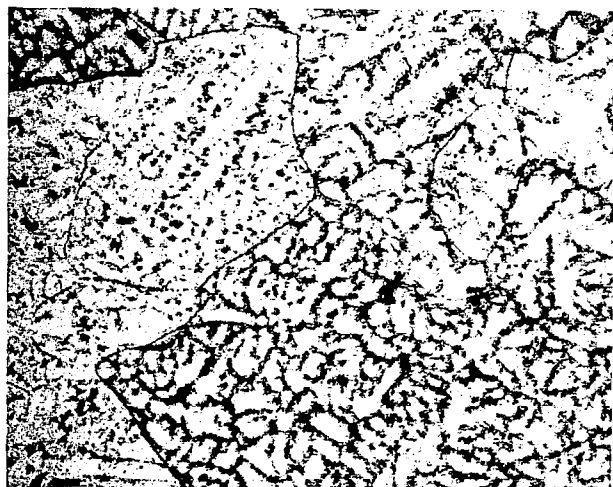
8668

As-Welded



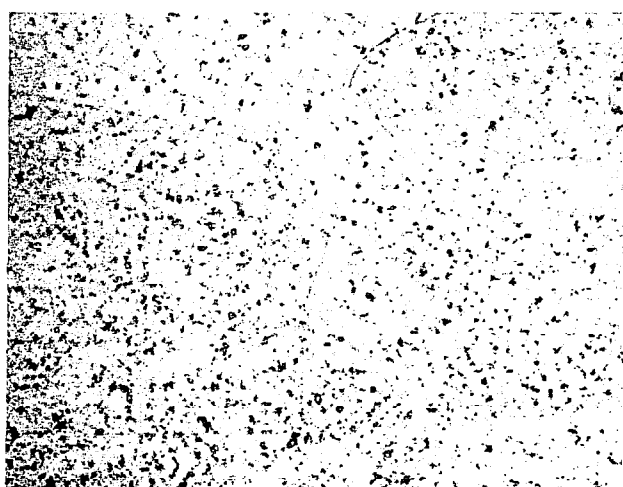
10,112

Annealed 1 Hr. at 1900°F



10,113

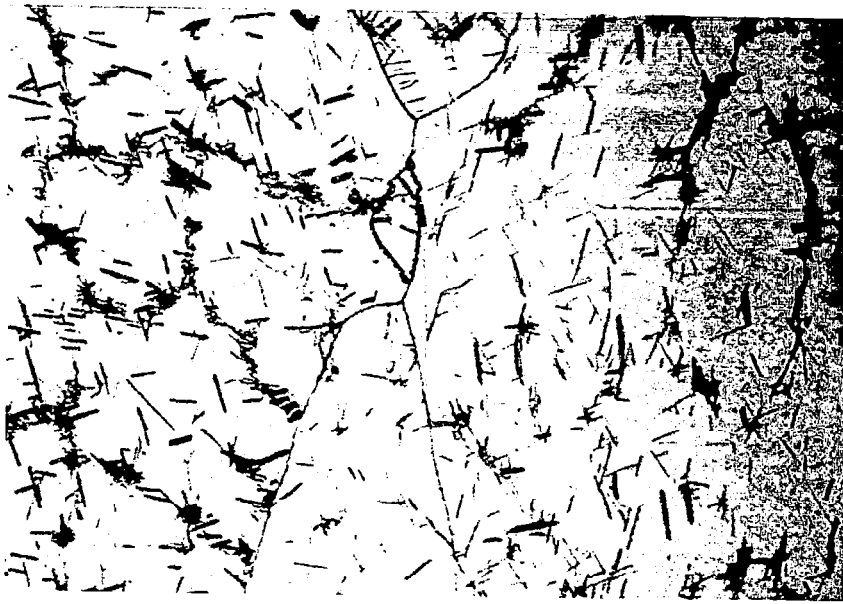
Annealed 1 Hr. at 2200°F



10,114

Annealed 1 Hr. at 2400°F

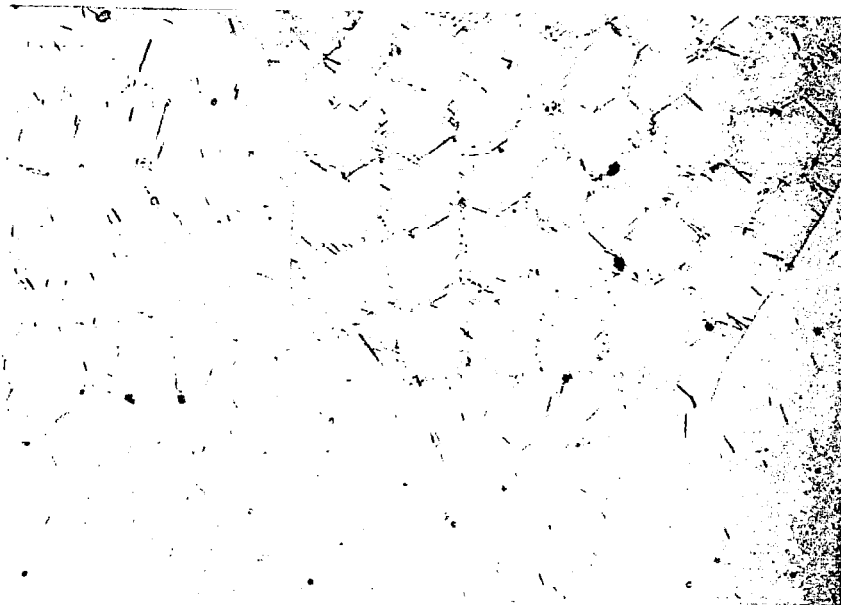
FIGURE A109 – Weld Microstructure in D-43 GTA Sheet Butt Welds, 400X  
All Weld Structure.



10,175

As-Welded

500X



10,179

Welded and Annealed for 1 Hr. at 2400°F

500X

FIGURE A110 - D-43 Welded Plate, Weld Microstructure



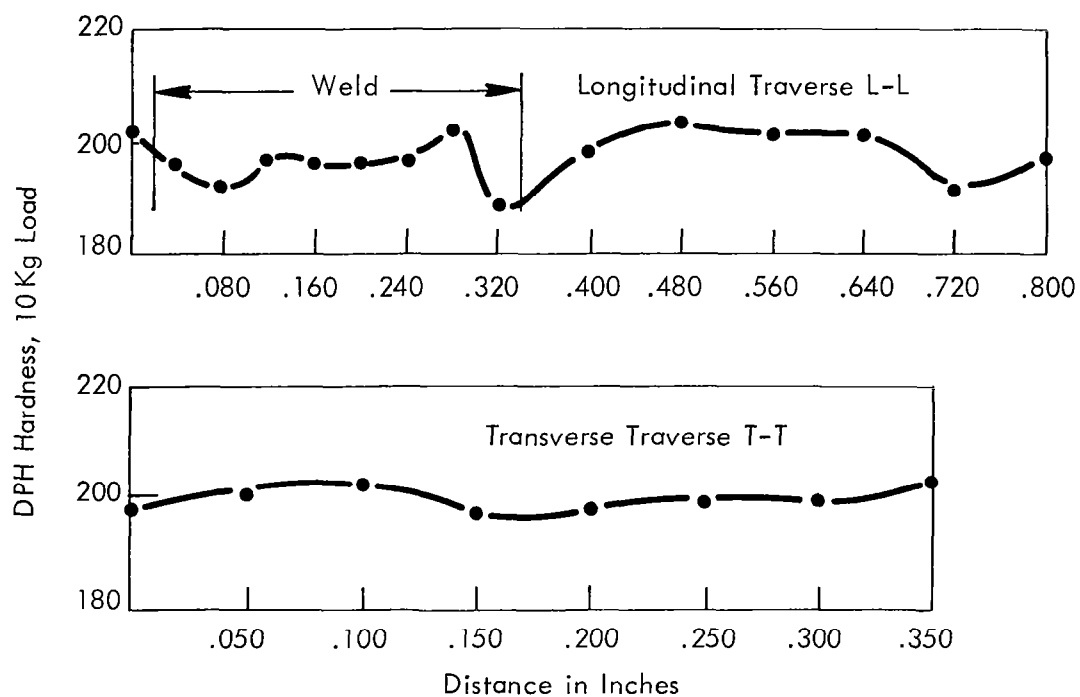
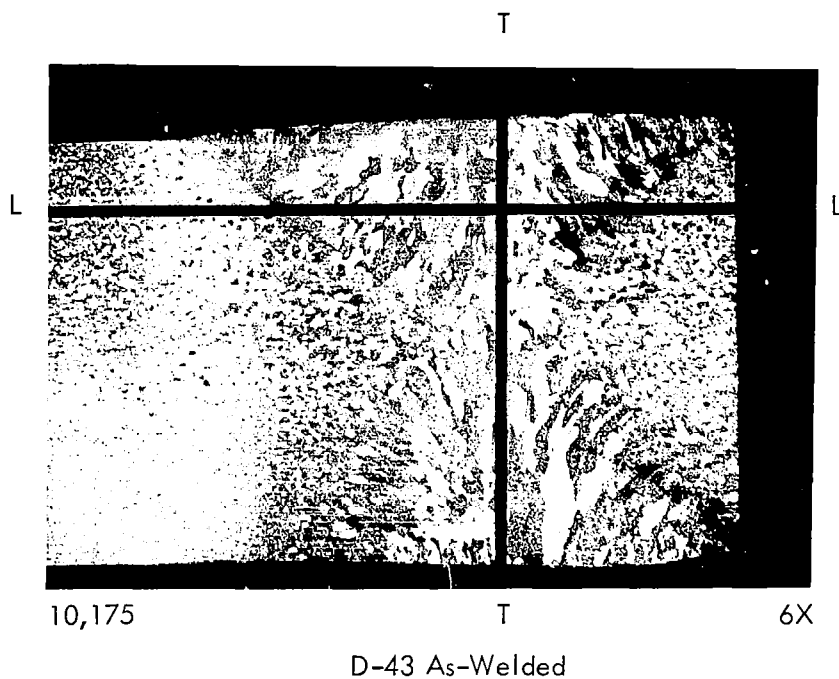
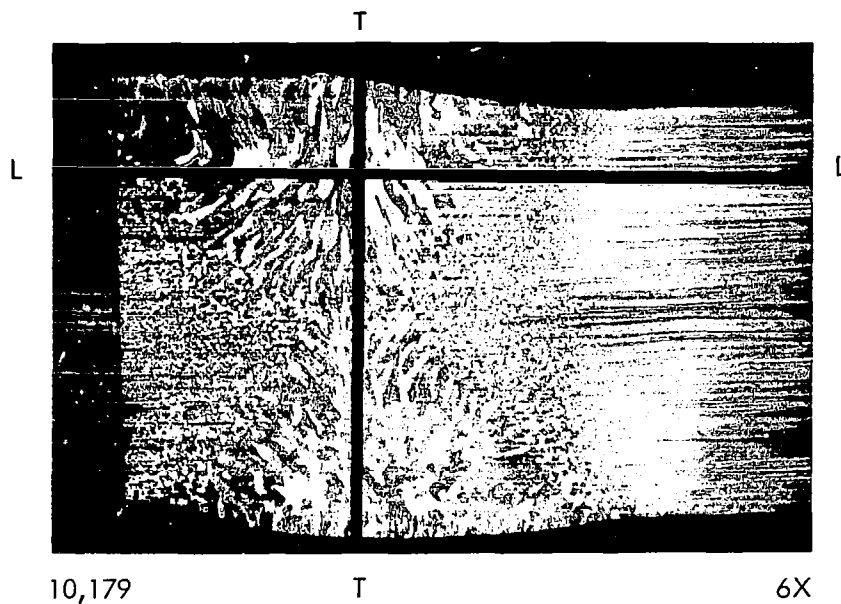


FIGURE A111 - D-43 Welded Plate Hardness Traverses



D-43 Annealed 1 Hour at 2400°F

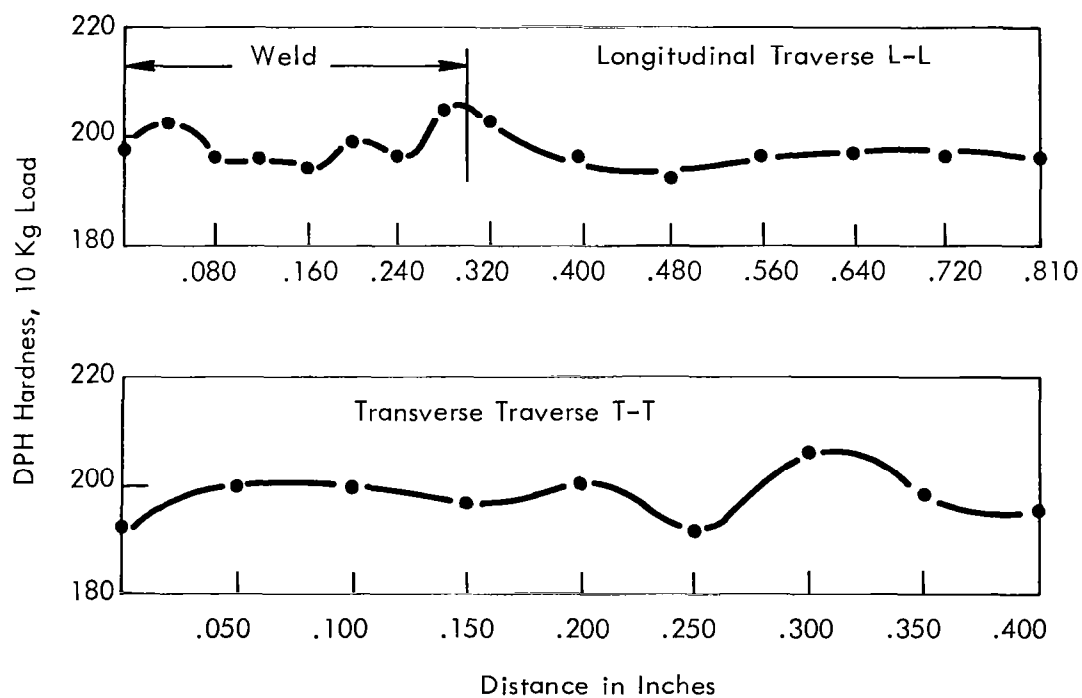
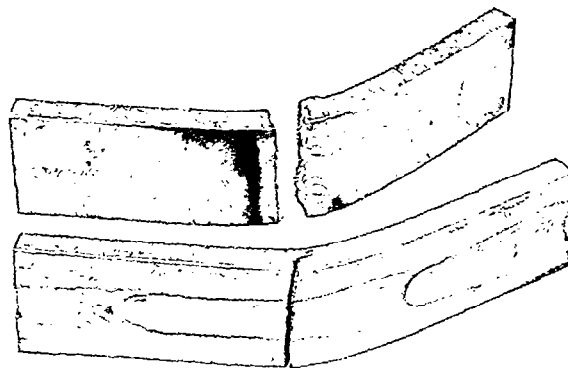


FIGURE A112 - D-43 Welded Plate Hardness Traverses

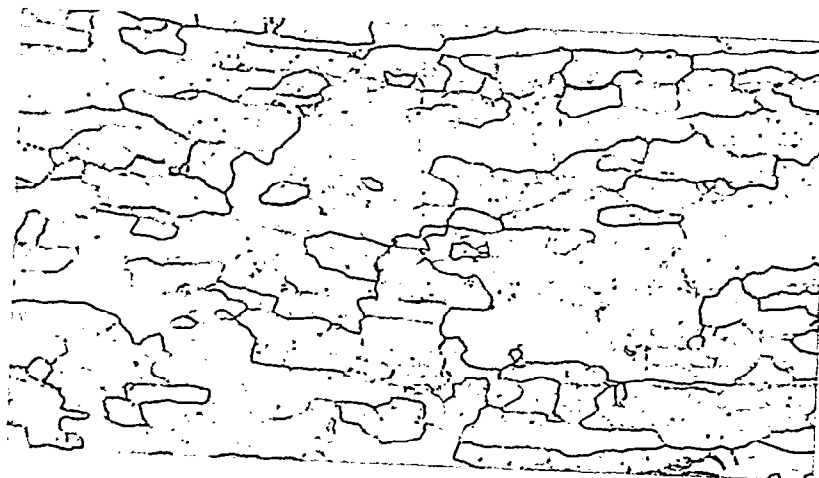


D-43

427-5

39° Longitudinal Bend  
47° Transverse Bend

FIGURE A113 - D-43 Plate Weld Bend Specimens



400X

9209

D-43Y

FIGURE A114 - As-Received Microstructure of D-43Y Sheet

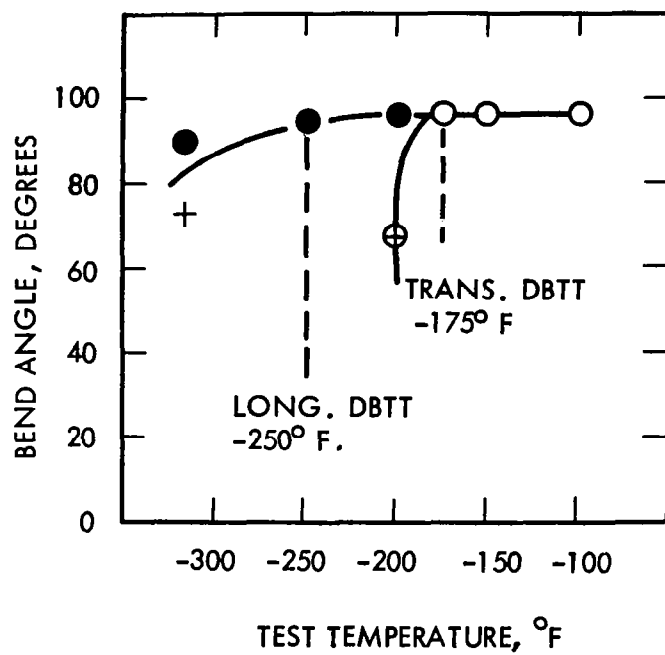


FIGURE A115 - D-43Y Base Metal Bend Test Results  
1t Bend Radius

TABLE A19 - D-43Y Sheet. GTA Butt Weld Record

Weld No.	Clamp Spacing (Inch)	Speed (ipm)	Current Amperes	Weld Width Top/Bottom (Inches)	Q Joules/Inch	Atmosphere Monitor Readings			Comments		
						O <sub>2</sub> (1) ppm	O <sub>2</sub> (2) ppm	H <sub>2</sub> O (3) ppm	Visual Inspection	Dye Check	Radiography
1	1/4	7.5	65	0.114/0.100	7800	--	2.4	0.1	Negative	Neg.	Slight Porosity
2	1/4	7.5	82	0.150/0.135	9200	--	1.9	0.15	Negative	Neg.	Negative
3	1/4	15	72	0.105/0.075	4320	--	1.9	0.19	Negative	Neg.	Negative
4	3/8	15	65	0.120/0.075	3640	--	2.2	0.20	Negative	Neg.	Porosity (5)
5	1/4	15	117	0.195/0.180	7010	--	3.0	2.9	Negative <sup>(4)</sup>	Neg.	Negative
6	1/4	30	100	0.099/0.090	3000	--	2.4	0.2	Negative	Neg.	Negative
7	1/4	15	117	0.165/0.150	7010	--	1.3	0.1	Negative <sup>(4)</sup>	Neg.	Negative
8	3/8	30	78	0.090/0.036	2180	--	3.8	0.3	Negative	Neg.	Porosity <sup>(5)</sup>
9	3/8	15	83	0.165/0.150	4980	--	4.0	0.3	Negative	Neg.	Negative
10	1/4	30	128	0.135/0.120	4090	--	3.0	2.9	Negative <sup>(4)</sup>	Neg.	Negative
11	3/8	60	160	0.111/0.105	2880	--	4.3	0.4	(6)	(6)	(6)
12	1/4	60	215	0.180/0.159	4090	--	3.0	3.0	Negative	Neg.	Negative

(1) Westinghouse oxygen gage.

(2) Lockwood &amp; McLorie oxygen gage.

(3) CEC moisture monitor.

(4) Rerun, first try hot tore severely along weld centerline.

(5) Welds rejected for further test, porosity attributed primarily to edge preparation rather than material characteristics.

(6) One transverse crack through weld.

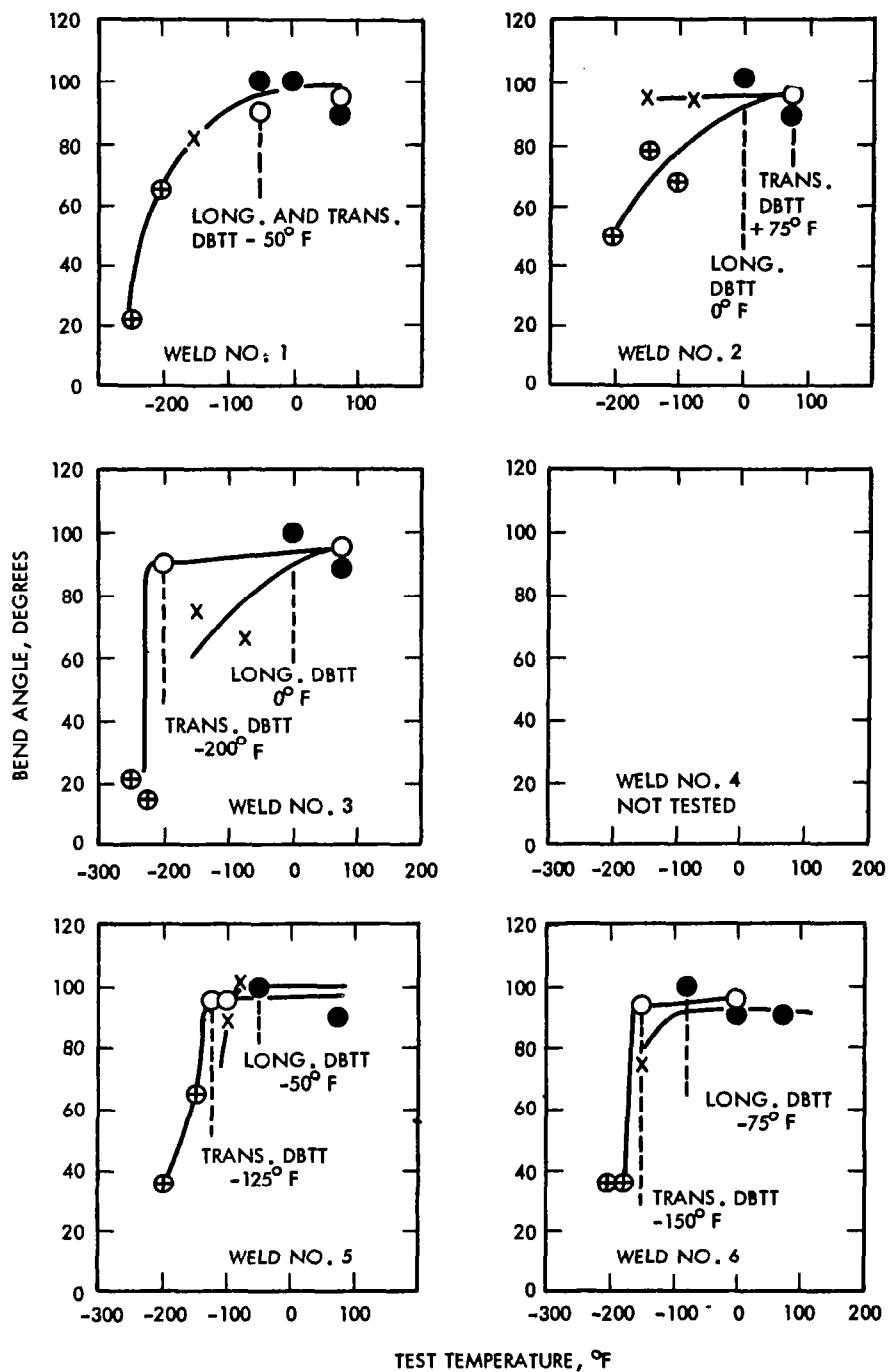


FIGURE A116 - Bend Test Results of D-43Y GTA Welds  
1t Bend Radius

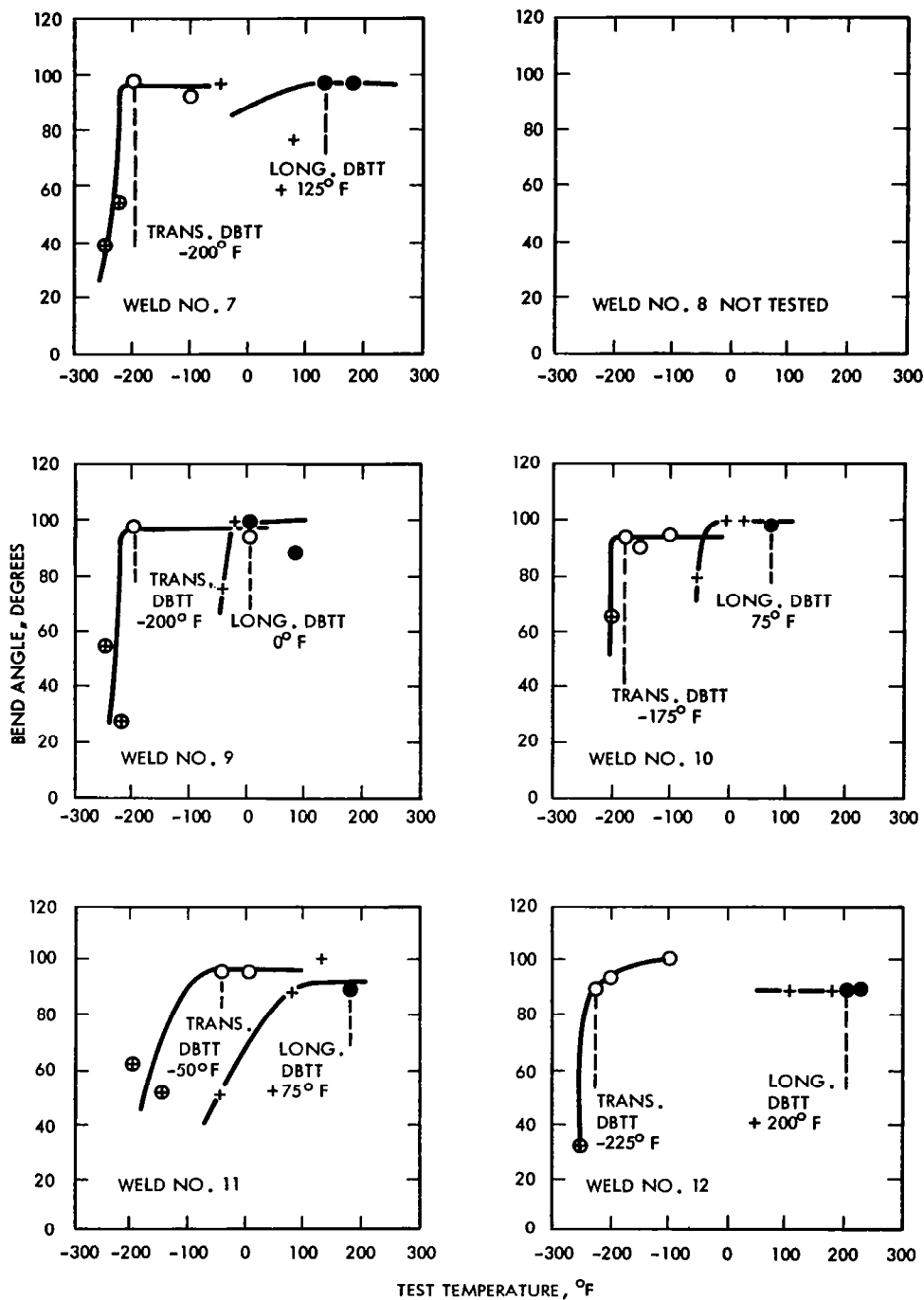


FIGURE A117 - Bend Test Results of D-43Y GTA Welds  
1t Bend Radius



TABLE A20 - D-43Y Sheet, EB Butt Weld Record

Weld No.	Speed (fpm)	Deflection <sup>(1)</sup> (Inches)	Current (ma)	Chill Spacing (Inches)	Power (Watts)	Watt-Sec. Per Inch	Weld Bead Width (Inches)		Average Weld Bead Width (In.)	Vacuum Torr
							Top	Bottom		
1	15	0	2.4	3/16	360	1450	.027	.020	.023	$3.4 \times 10^{-6}$
2	15	L-.050	3.6	3/16	540	2160	.026	.016	.021	$3.4 \times 10^{-6}$
3	15	T-.050	3.6	3/16	540	2160	.044	.040	.042	$3.4 \times 10^{-6}$
4	25	L-.050	3.6	3/16	540	1300	.041	.025	.033	$3.4 \times 10^{-6}$
5	15	L-.050	3.3	1/2	495	1980	.030	.024	.027	$3.4 \times 10^{-6}$
6	25	L-.050	3.3	1/2	495	1190	.041	.031	.036	$3.4 \times 10^{-6}$
7	50	L-.050	4.0	1/2	600	720	.036	.022	.029	$3.4 \times 10^{-6}$
8	100	L-.050	5.2	1/2	780	468	.034	.022	.028	$3.4 \times 10^{-6}$
9	50	L-.050	4.3	3/16	645	775	.034	.027	.030	$4.1 \times 10^{-6}$
10	50	L-.050	4.8	3/16	720	865	.041	.031	.036	$4.1 \times 10^{-6}$
11	50	L-.100	5.5	3/16	825	990	.038	.027	.032	$4.1 \times 10^{-6}$
12	100	L-.050	6.1	3/16	915	550	.031	.027	.029	$4.1 \times 10^{-6}$

All welds made at 150 kv.

1. L is longitudinal

T is transverse

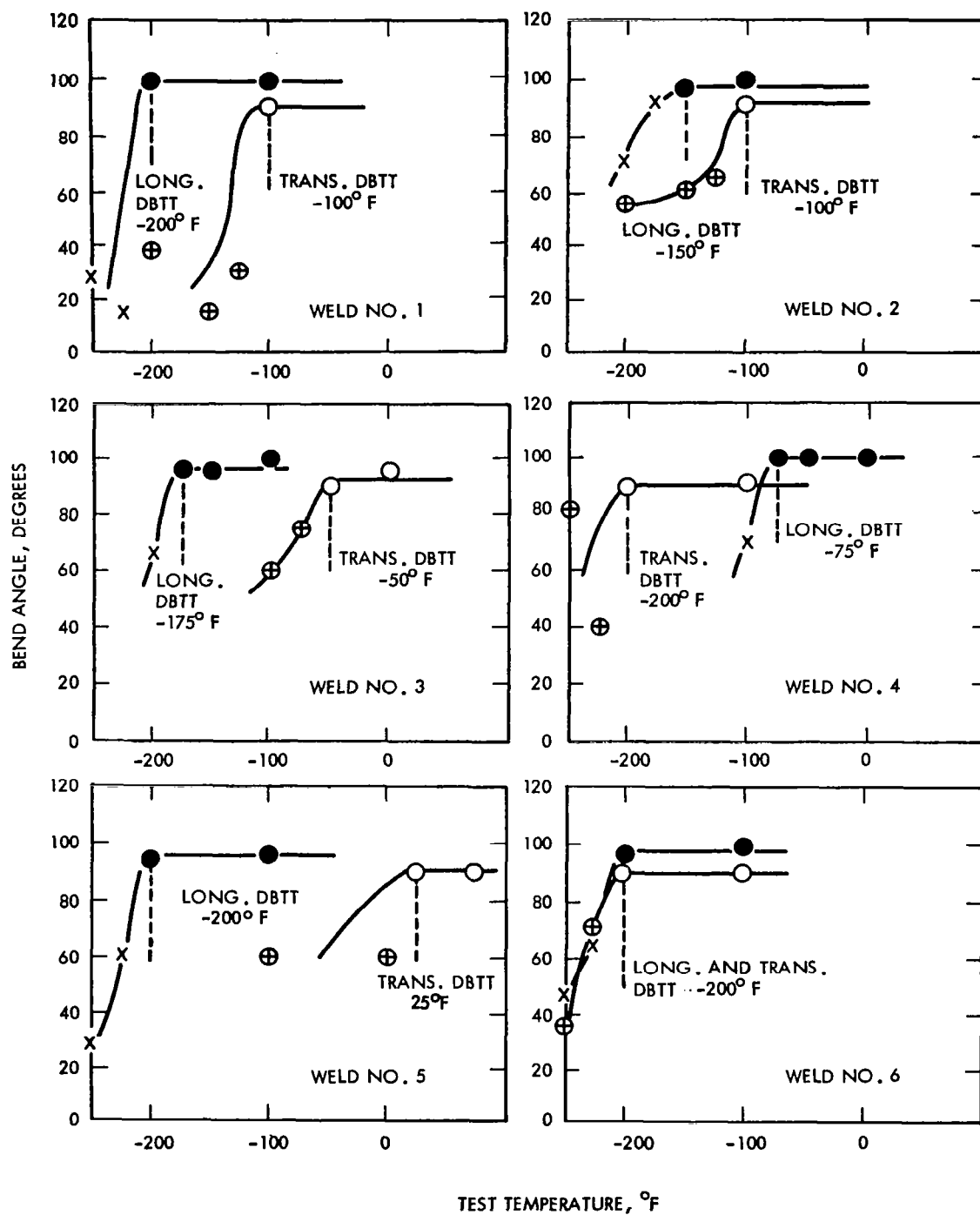


FIGURE A118 - Bend Test Results of D-43Y EB Welds  
1½ Bend Radius

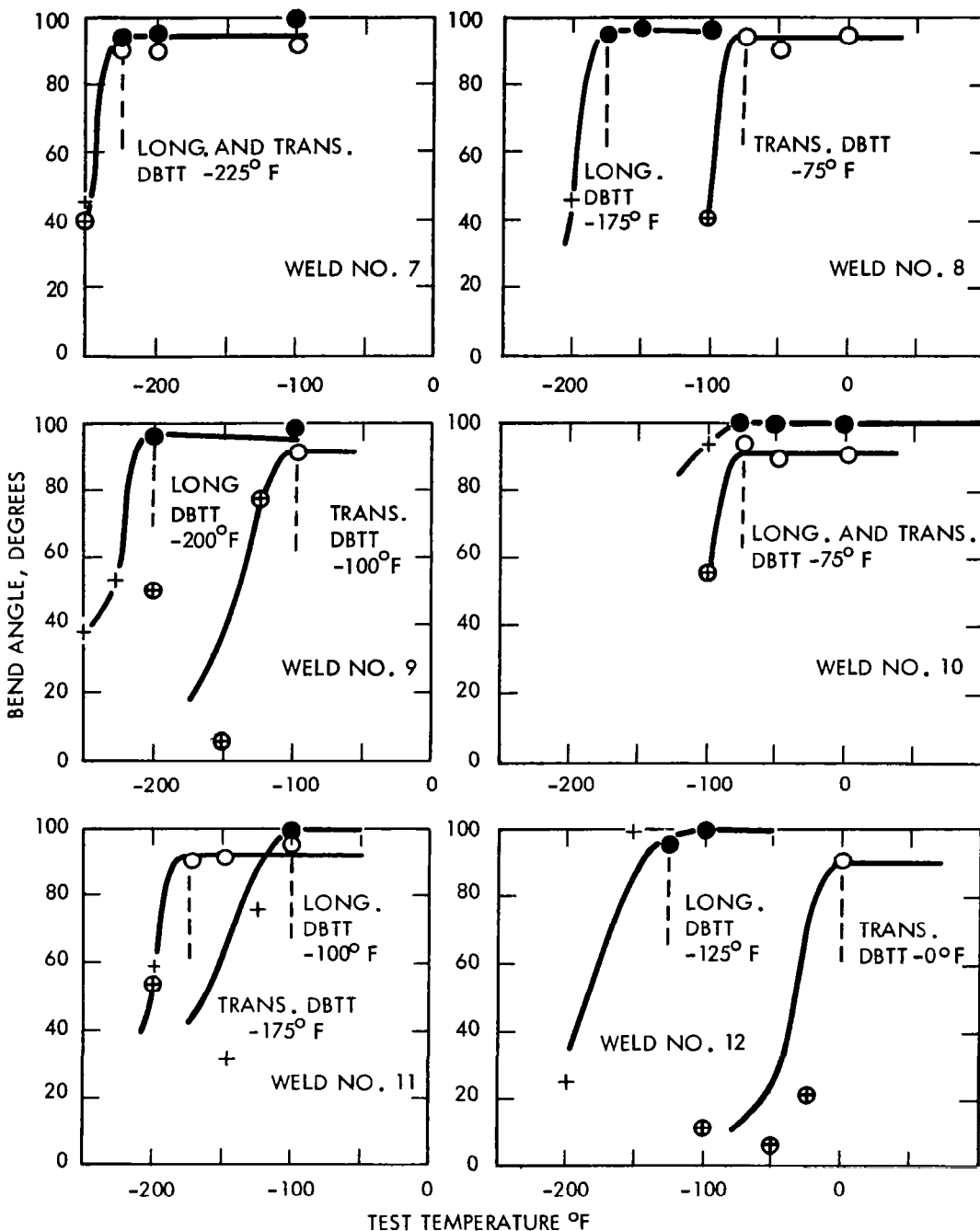
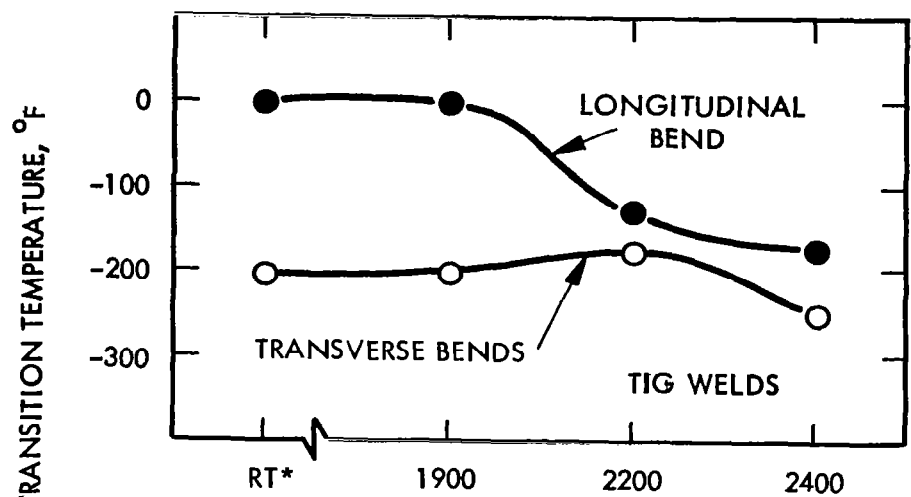
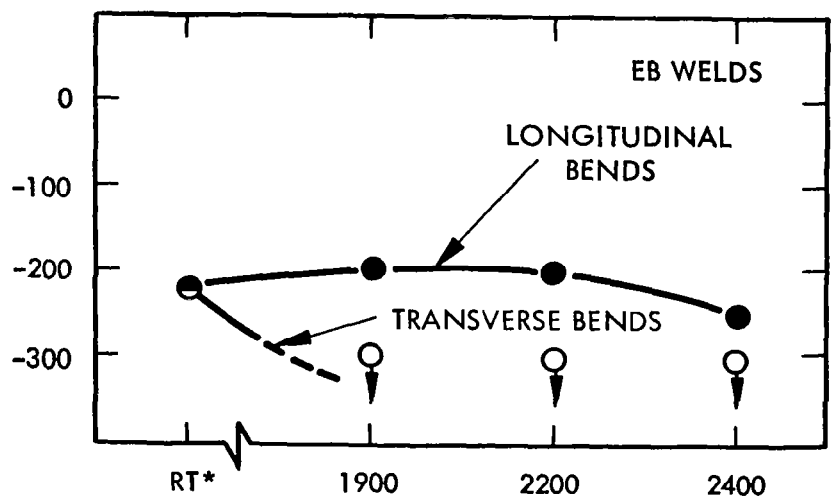


FIGURE A119 - Bend Test Results of D-43Y EB Welds  
1t Bend Radius



\* AS WELDED



ONE HOUR POST WELD ANNEALING TEMPERATURE, °F

FIGURE A120 - Effect of Post Weld Annealing on D-43Y Weld Ductility

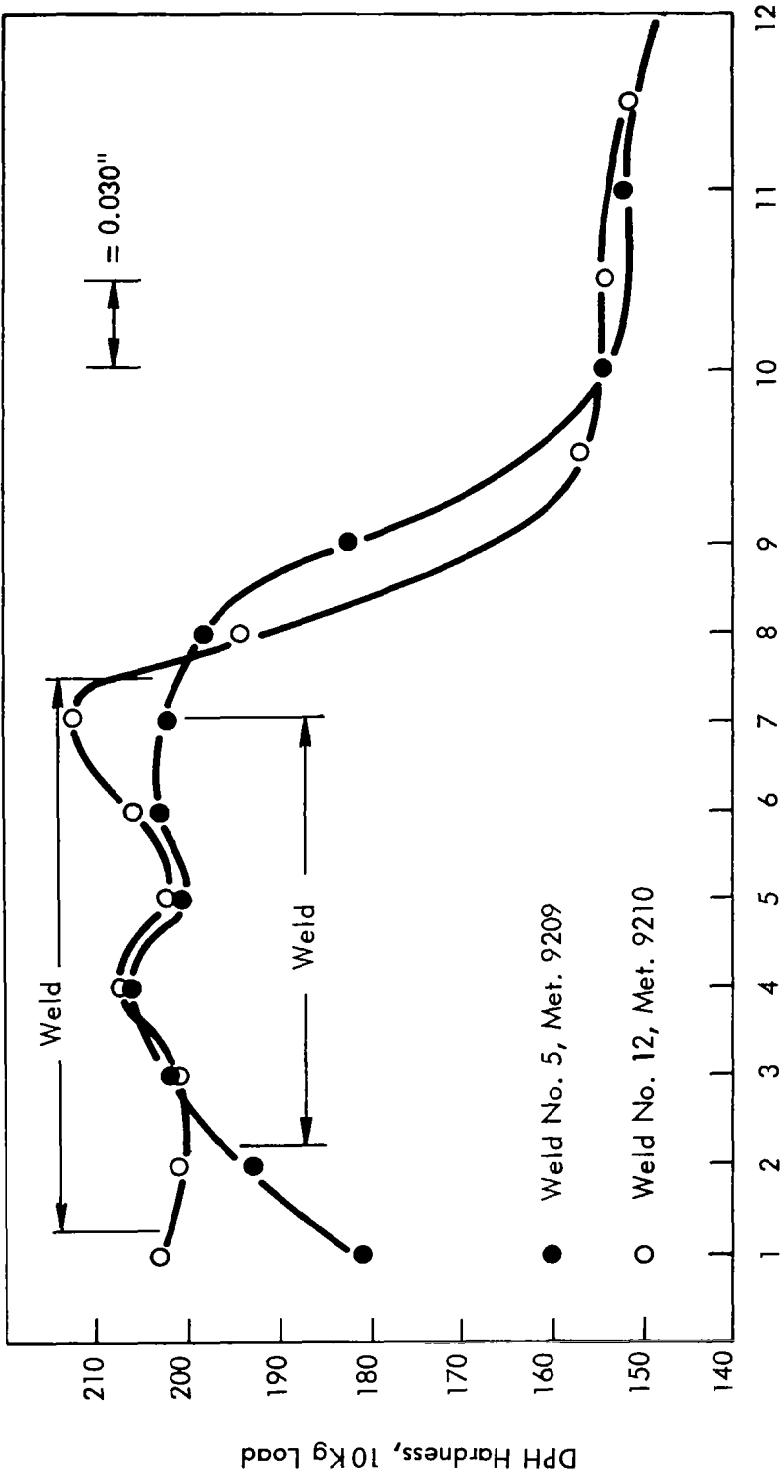
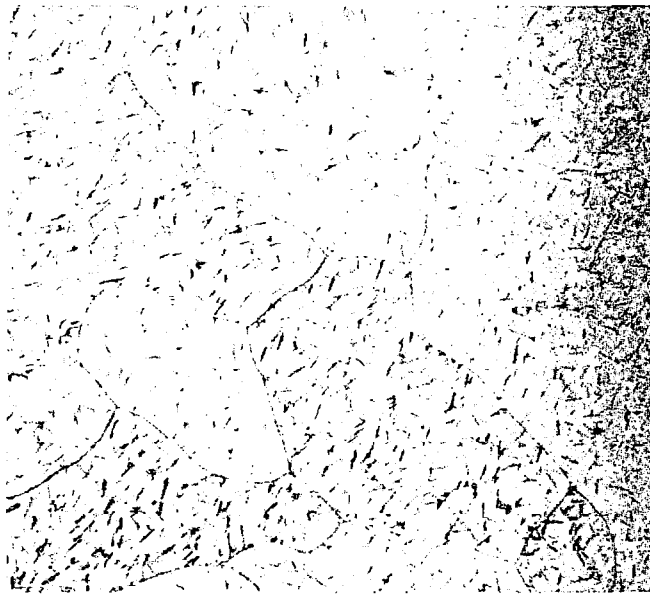


**FIGURE A122 - Hardness Traverses, D-43Y GTA Sheet Butt Welds**

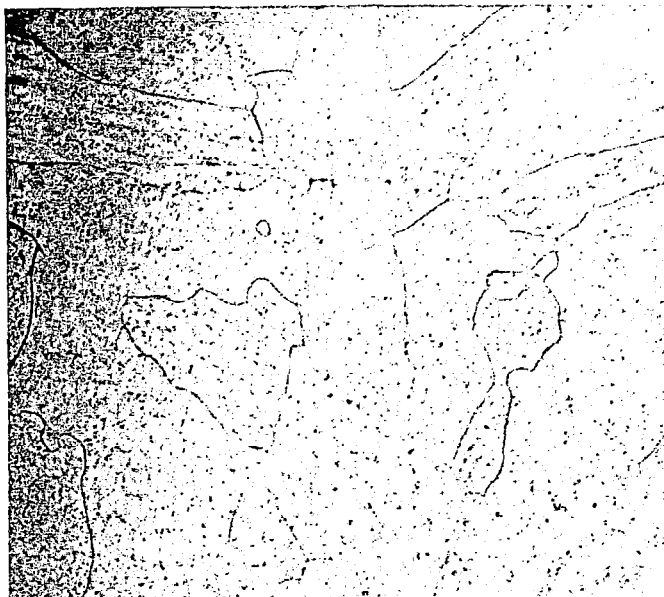


Weld

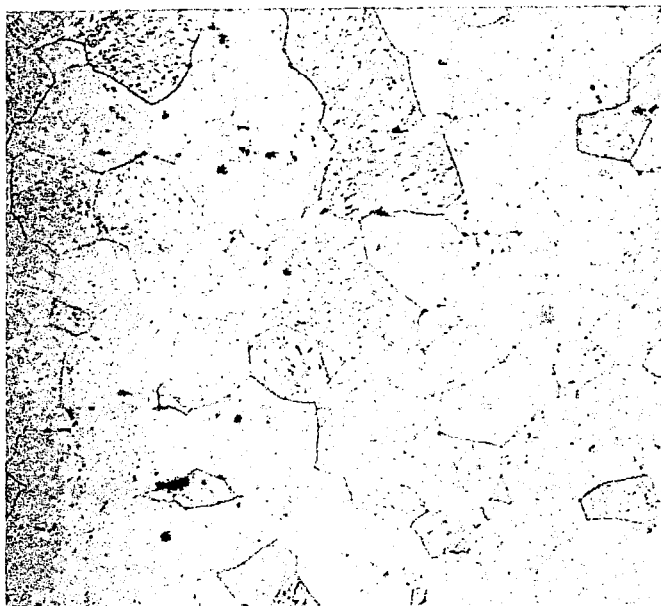


HAZ

FIGURE A122 - D-43Y GTA Sheet Butt Weld Microstructure Weld  
Number 9. 500X. Met. 9740

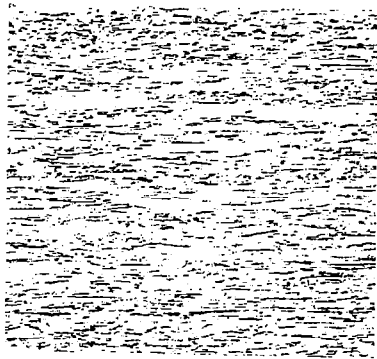


Weld



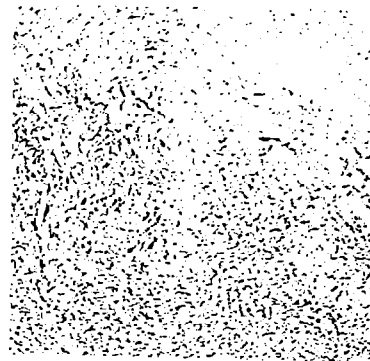
HAZ

FIGURE A123 - D-43Y GTA Sheet Butt Weld Microstructure Annealed  
1 Hour at 2400°F, 400X. Met. 10,144

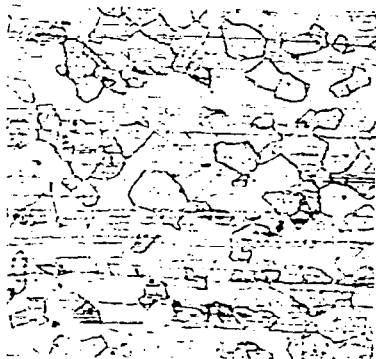


2806

0.082" Wire



2807

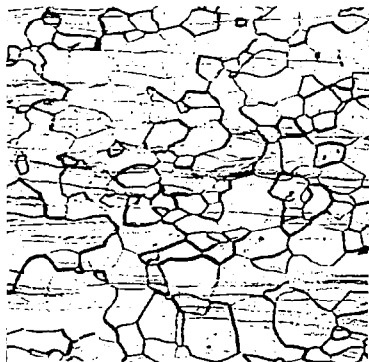


2802

0.035" Sheet



2803



3326

0.375" Plate

Longitudinal



3327

Transverse

FIGURE A124 - As-Received Microstructure of SCb-291, 100X



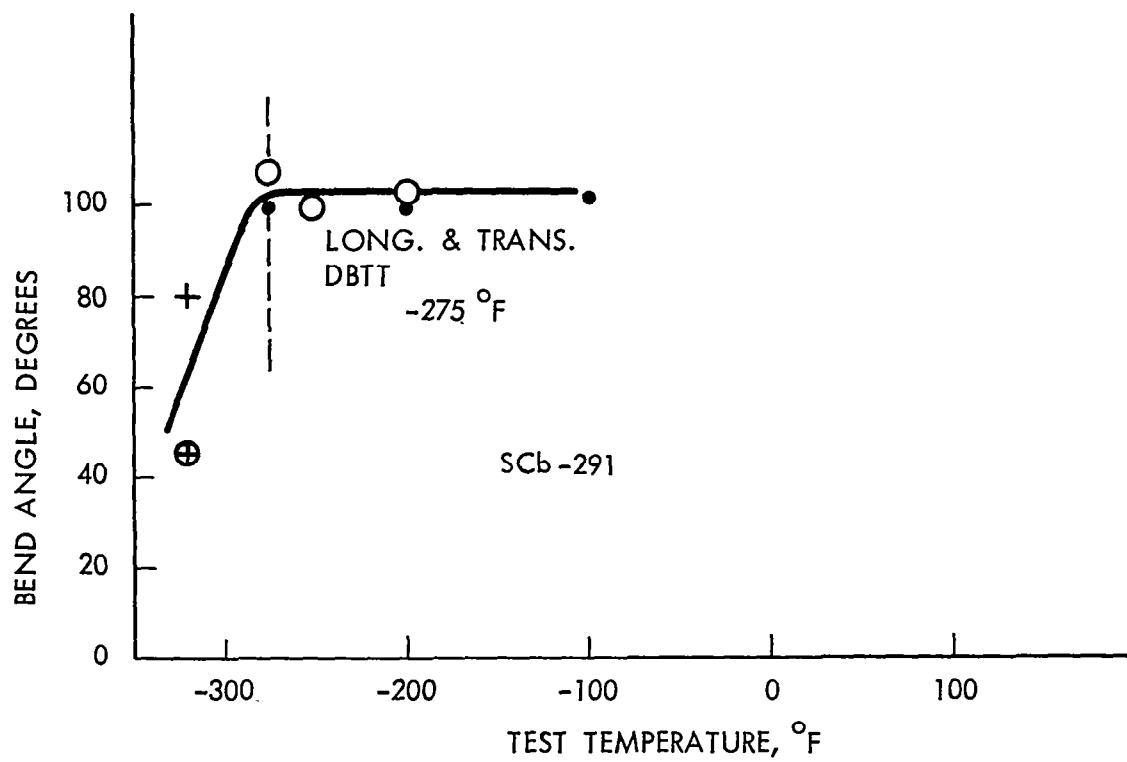


FIGURE A125 - SCb-291 Base Metal Bend Test Results

TABLE A21 - SCb-291 Sheet. GTA Butt Weld Record

Weld No.	Clamp Spacing (inch)	Speed (ipm)	Current Amperes	Weld Width Top/Bottom (inch)	Q Joules/Inch	Atmosphere Monitor Readings			Comments	
						O <sub>2</sub> (1) ppm	O <sub>2</sub> (2) ppm	H <sub>2</sub> O (3) ppm	Visual Inspection	Dye Check
1	3/8	15	70	0.15/0.13	4,770	3.5	--	0.9	Negative	Negative
2	3/8	30	115	0.18/0.16	3,900	3.5	--	0.9	1/8" HAZ Crack	1/8" HAZ Crack
3	1/4	15	83	0.16/0.15	5,640	2.5	3.6	0.4	Edge Flash (u)	Negative
4	1/4	30	100	0.125/0.110	3,400	4.0	4.6	1.6	Edge Flash (u)	Negative
5	1/4	7.5	56	0.136/0.114	8,050	2.0	3.5	0.2	Negative	Negative
6	1/4	7.5	72	0.150/0.140	10,650	1.5	3.4	0.4	Negative	Negative
7	1/4	15	75	0.120/0.090	5,400	--	2.5	0.1	Negative	Negative
8	3/8	15	88	0.216/0.210	6,510	1.6	3.6	1.5	Negative	Negative
9	1/4	30	160	0.198/0.192	6,080	0.5	2.1	0.2	Negative	Negative
10	1/4	60	166	0.135/0.084	3,155	--	3.1	2.6	Negative	Negative
11	3/8	60	145	0.120/0.045	2,680	1.0	3.0	0.9	Negative	Negative
12	3/8	60	185	0.180/0.156	3,520	1.5	2.8	1.5	Negative	Negative

(1) Westinghouse Oxygen Gage

(2) Lockwood &amp; McJorie Oxygen Gage

(3) CEC Moisture Monitor

(4) Instantaneous Arcing to Weld Clamp Down

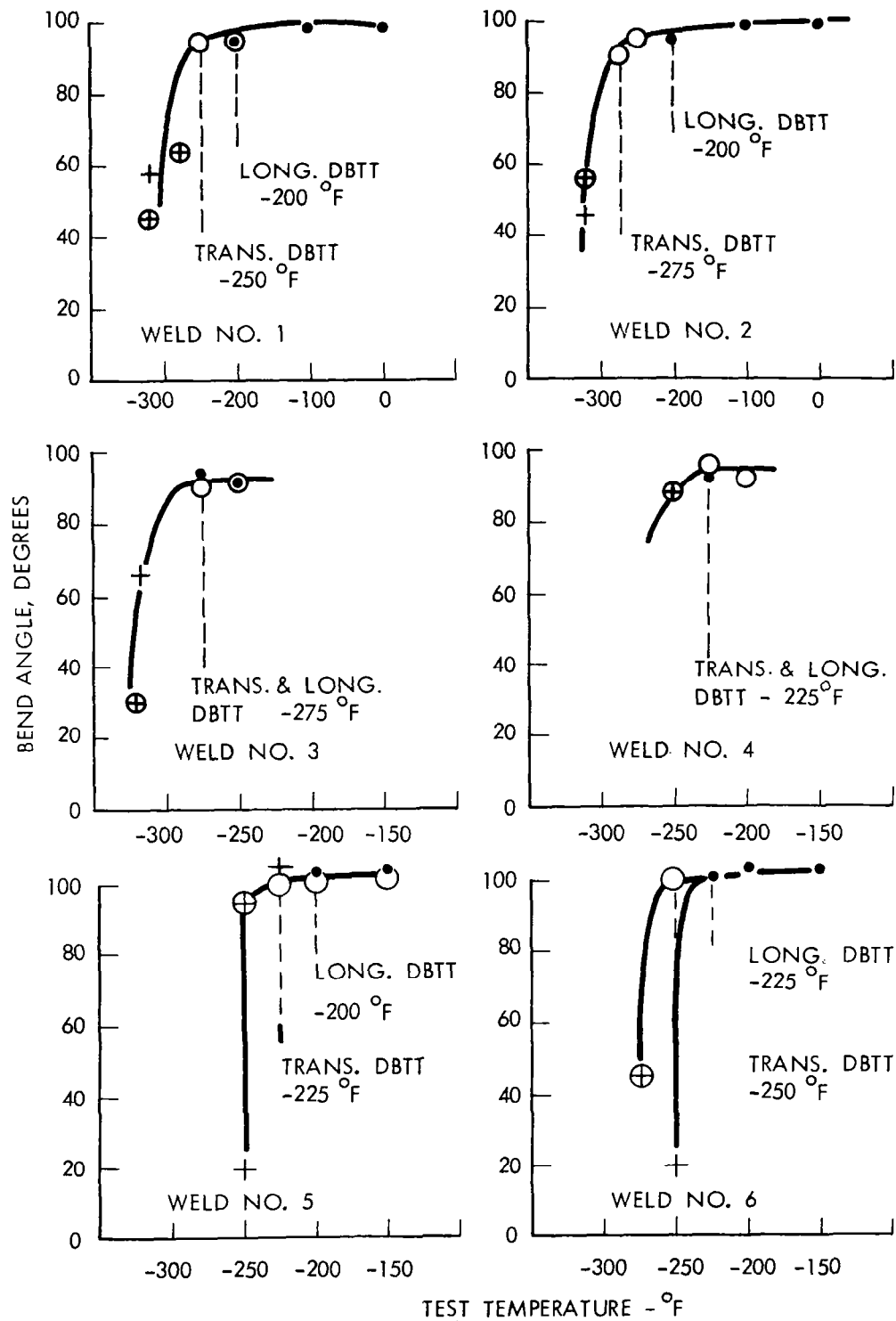


FIGURE A126 - Bend Test Results for SCb-291 GTA Welds  
1½ Bend Radius

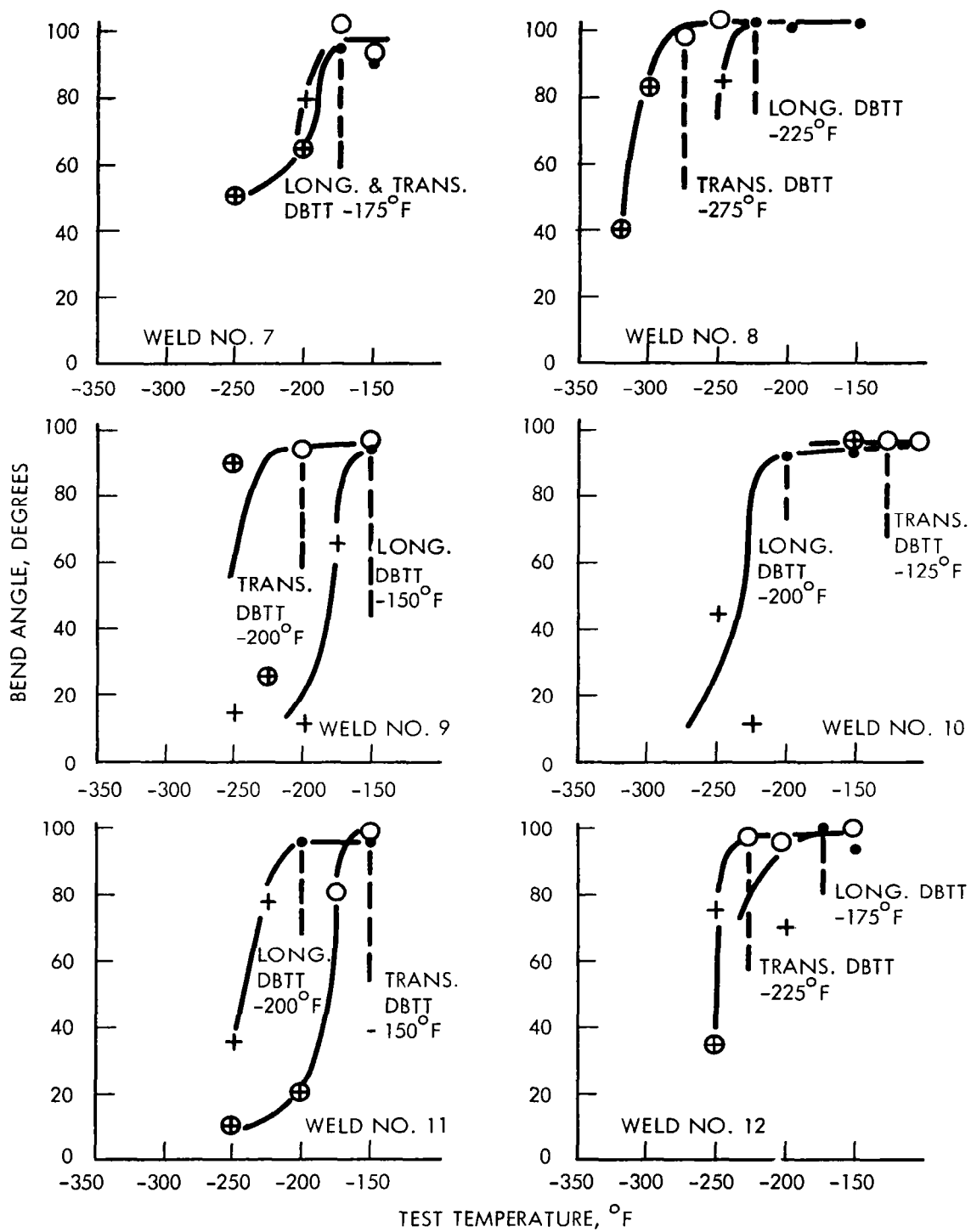


FIGURE A127 - Bend Test Results for SCb-291 GTA Welds  
1½ Bend Radius

TABLE A22 - SCb-291 Sheet. EB Butt Weld Record

Weld No.	Speed (ipm)	Deflection <sup>1</sup> (inches)	Current (ma)	Chill Spacing (inches)	Power (watts)	Watt-Sec. per inch	Weld Bead Width (inches)		Vacuum <sup>2</sup> (Torr)
							Top	Bottom	
1	100	none	5.0	0.250	750	450	0.028	0.018	$4 \times 10^{-6}$
2	50	none	4.0	↘	600	720	0.035	0.022	$4 \times 10^{-6}$
3	50	L-0.050"	4.4		660	790	0.038	0.027	$4 \times 10^{-6}$
4	25	none	3.1		465	1100	0.038	0.029	$5.5 \times 10^{-6}$
5	25	T-0.050"	3.9	↘	585	1400	0.070	0.060	$5.5 \times 10^{-6}$
6	15	none	2.5		375	1500	0.030	0.021	$5.5 \times 10^{-6}$
7	100	none	5.0	0.094	750	450	0.028	0.016	$4 \times 10^{-6}$
8	50	none	4.0	↘	600	720	0.033	0.020	$4 \times 10^{-6}$
9	50	L-0.050"	4.4		660	790	0.040	0.025	$4 \times 10^{-6}$
10	25	none	3.1		465	1100	0.033	0.024	$5.5 \times 10^{-6}$
11	25	T-0.050"	3.9	↘	585	1400	0.065	0.050	$5.5 \times 10^{-6}$
12	15	none	2.5		375	1500	0.023	0.016	$5.5 \times 10^{-6}$

1. L. is longitudinal  
T. is transverse

2. Current evacuation practice provides pressures of  $1.5 \times 10^{-6}$  Torr

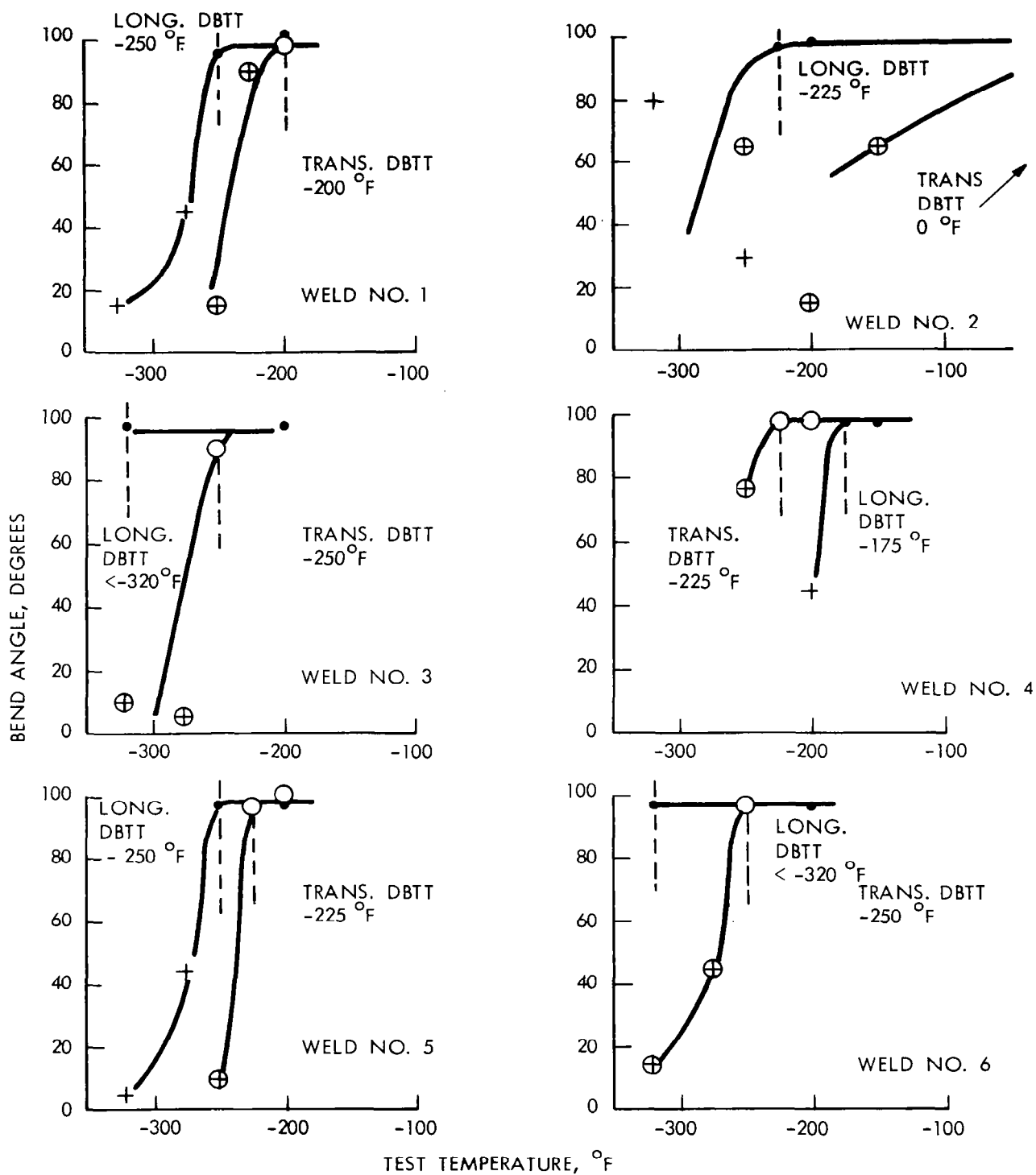
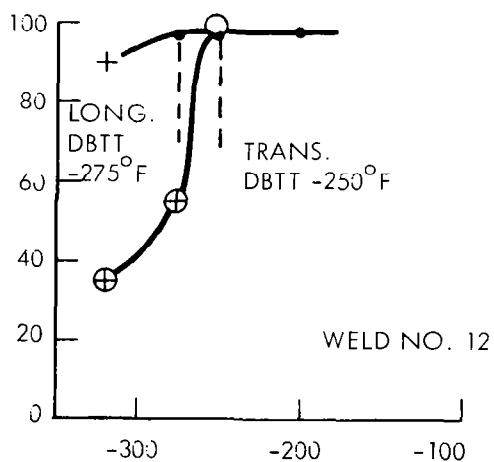
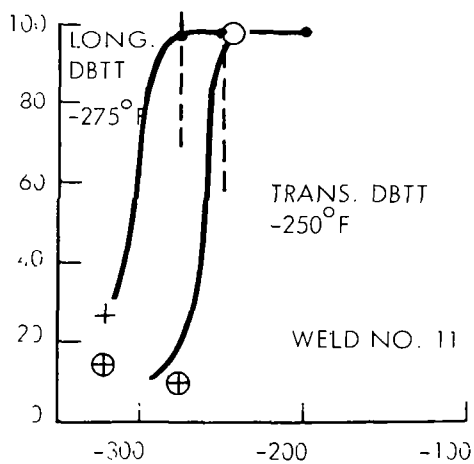
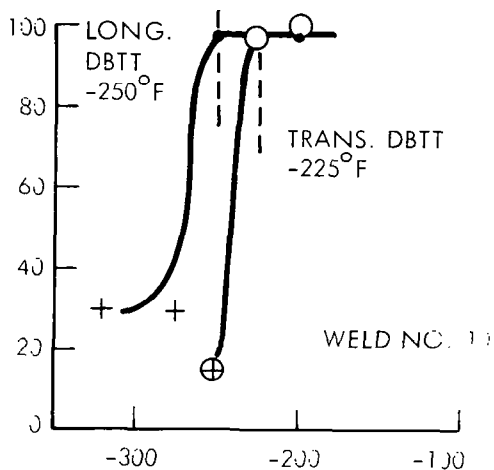
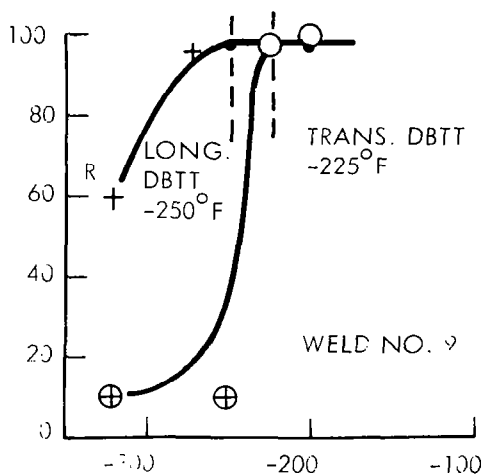
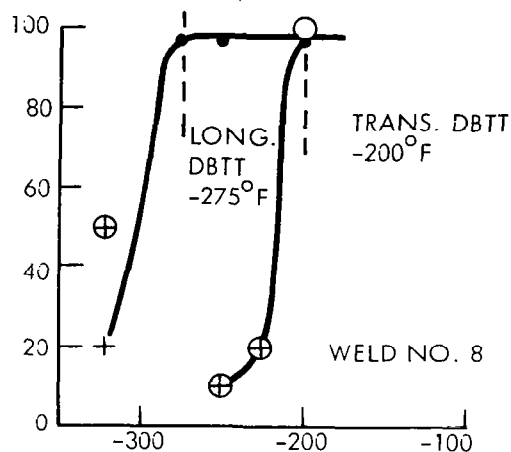


FIGURE A128 - Bend Test Results for SCb-291 EB Welds  
1½ Bend Radius



TEST TEMPERATURE, °F

FIGURE A129 - Bend Test Results for SCb-291 EB Welds  
1t Bend Radius

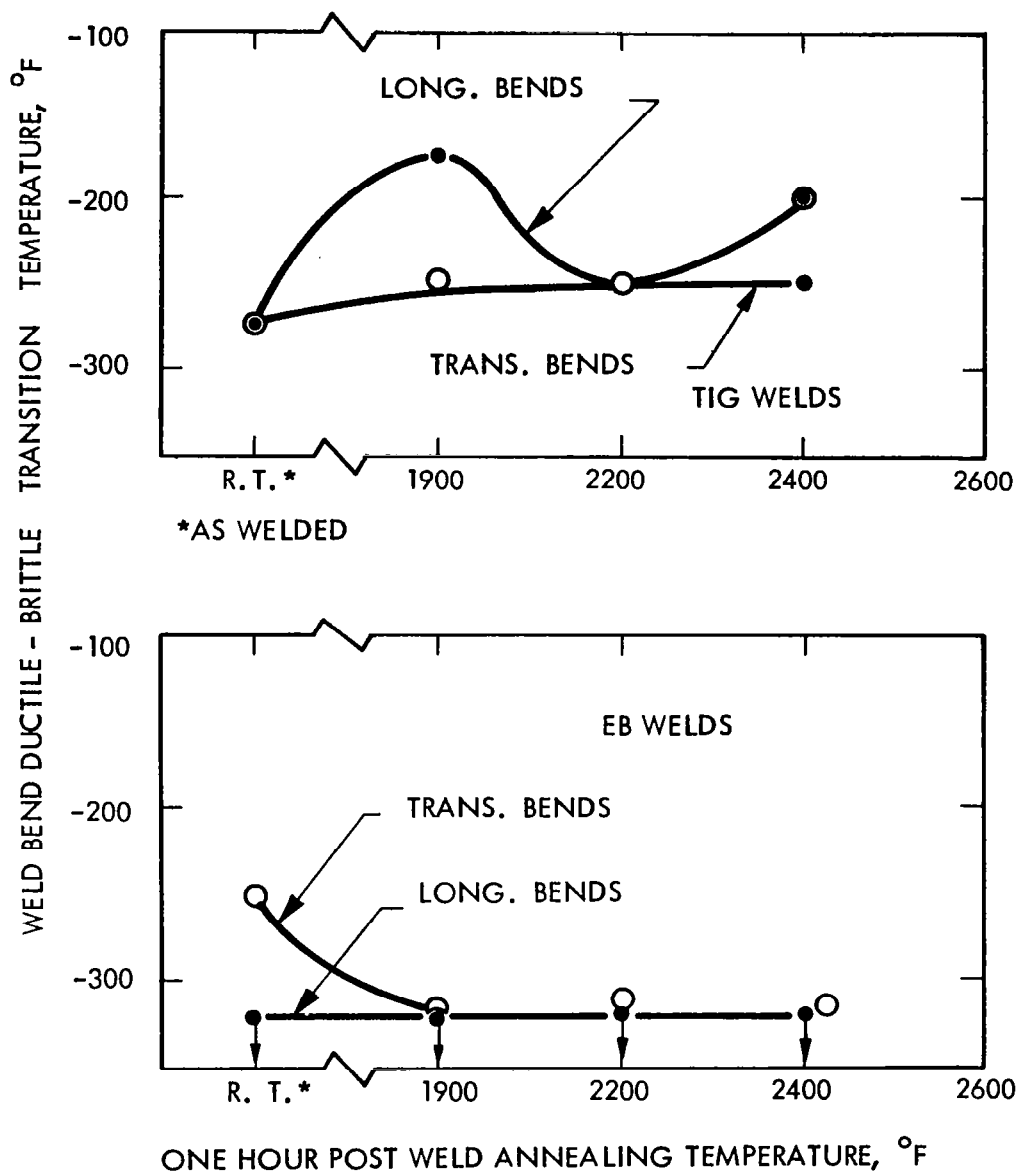


FIGURE A130 - Effect of Post Weld Annealing on SCS-291 Weld Ductility



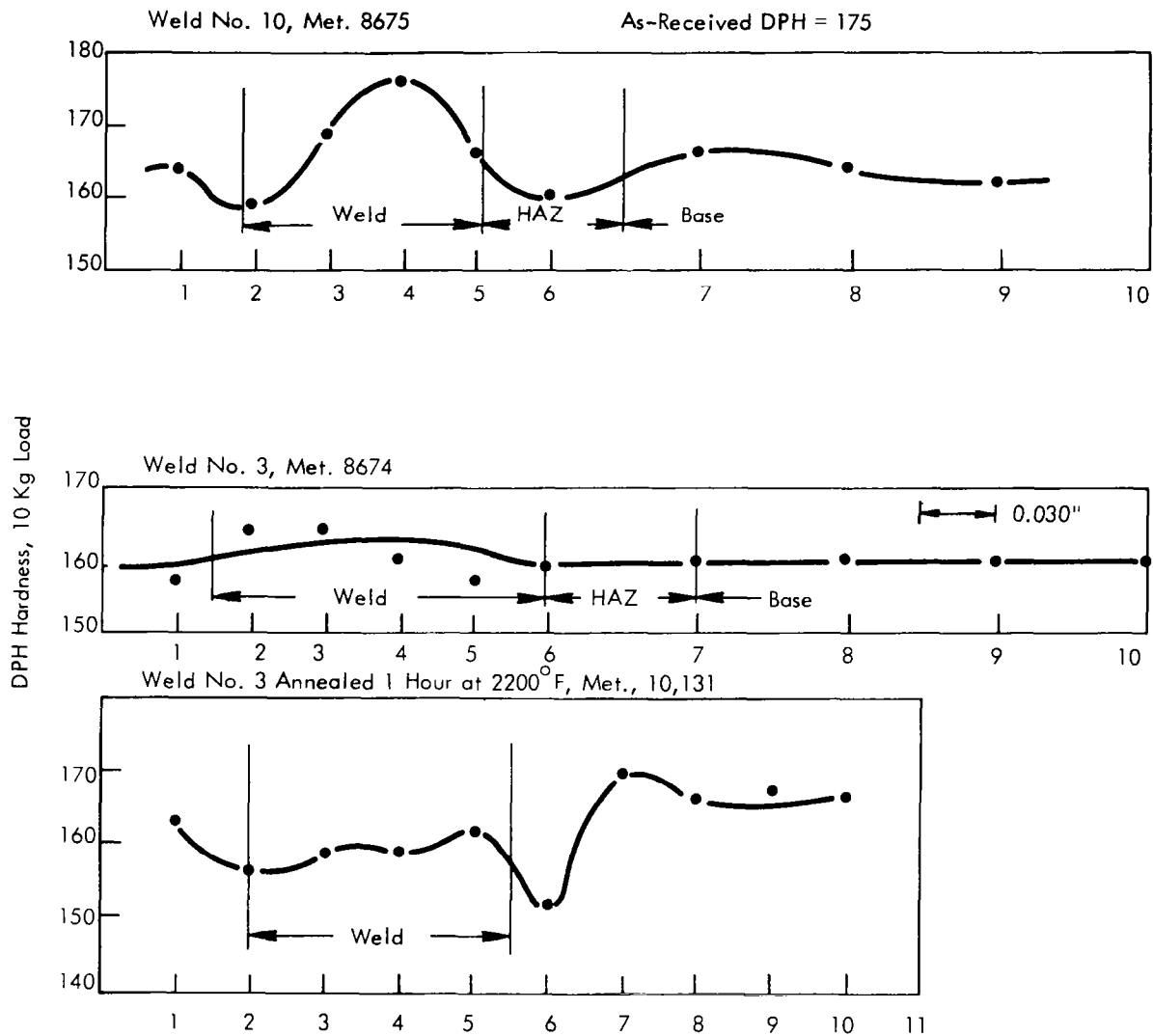
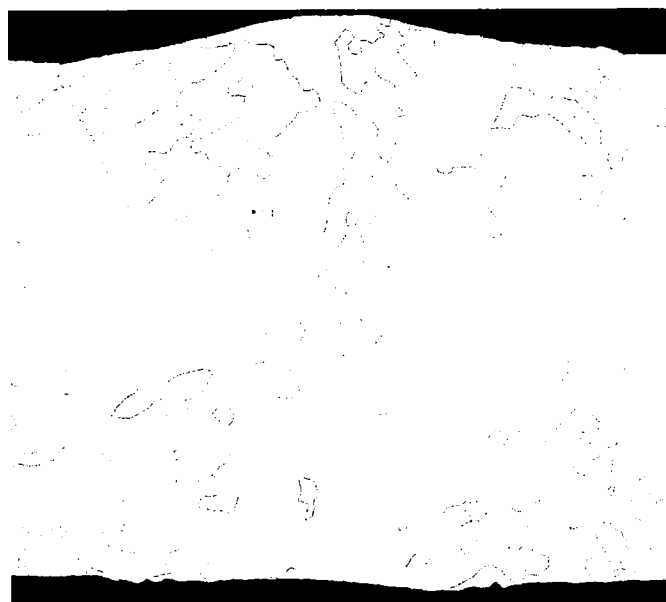


FIGURE A131 - Hardness Traverses, SCb-291 GTA Sheet Butt Welds



Weld Edge

400X



Weld

80X

FIGURE A132 - SCb-291 EB Sheet Butt Weld Microstructure. Weld Number 3. Met. 9169.

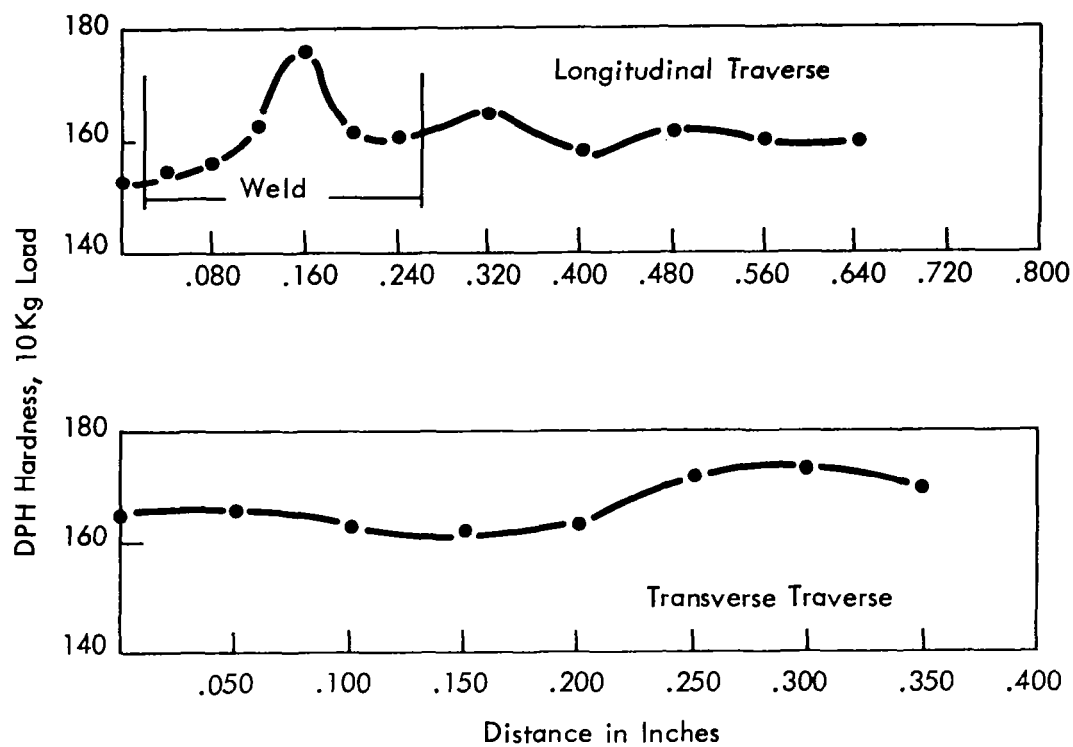
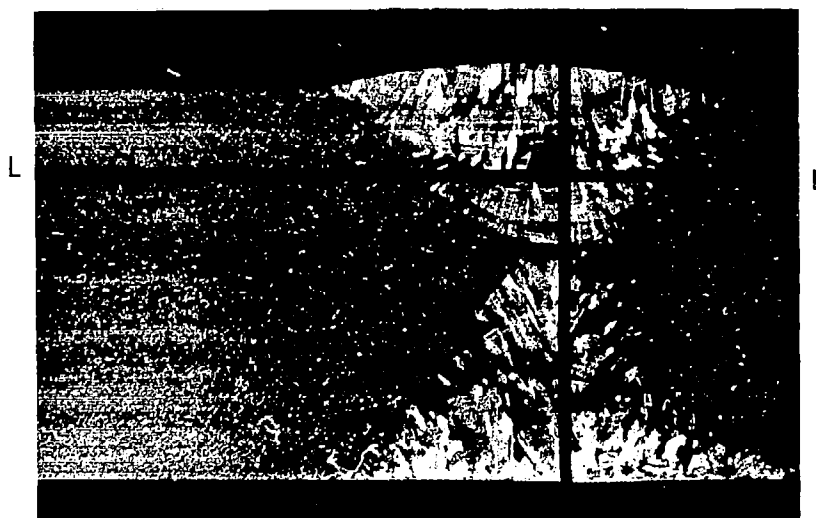


FIGURE A133 - SCb-291 Welded Plate Hardness Traverses



10,182 SCS-291 Annealed 1 Hr. at 1900°F 6X

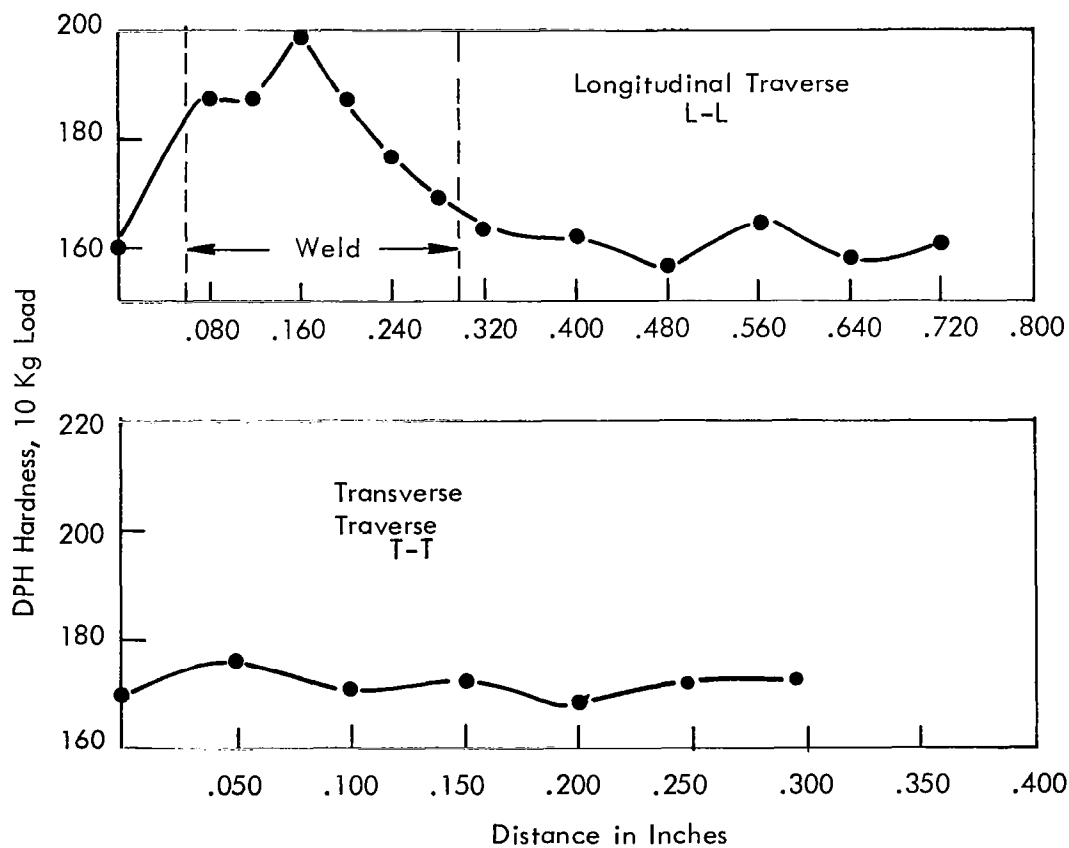
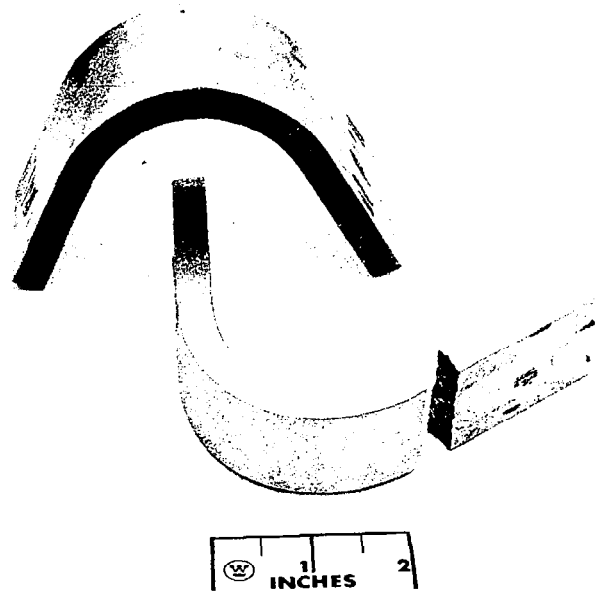


FIGURE A134 - SCS-291 Welded Plate Hardness Traverses



SCb-291

435

160° Longitudinal Bend  
132° Transverse Bend

FIGURE A135 - SCb-291 Welded Plate Bend Specimens

TABLE A23 - Unalloyed Arc Cast Tungsten Sheet, GTA Weld Record

Weld No.	Type (1)	Clamp Spacing (inch)	Speed (ipm)	Current (amps)	Pre-Heat (°F)	Weld Width Top/Bottom (inch)	Q Kilojoules (per inch)	Comments - Visual, Dye Penetrant and Radiographic Inspection
1	Butt	3/8	7.5	155	--	.160/.140	21.10	Good Weld
2	BOP	3/8	7.5	163	550	.190/.175	22.15	Good Weld
3	Butt	3/8	7.5	115	--	.100/.040	15.62	Centerline crack, 1-1/2" long
4	BOP	3/8	7.5	121	550	.115/.050	16.45	Good Weld
5	Butt	3/8	15	176	--	.170/.150	11.90	One transverse (weld + Haz) crack
6	BOP	3/8	15	184	550	.200/.190	12.52	Good Weld
7	BOP	3/8	15	158	--	.140/.115	10.75	Good Weld
8	BOP	3/8	15	147	550	.130/.095	10.00	Good Weld
9	Butt	3/8	30	235	550	.180/.170	7.95	Propagated crater crack + Trans. (weld + Haz) crack.
10	Butt	3/8	30	220	--	.135/.100	7.45	Propagated crater crack + trans. (weld + Haz) crack.

(1) Fusion butt weld or bead-on-plate (BOP)

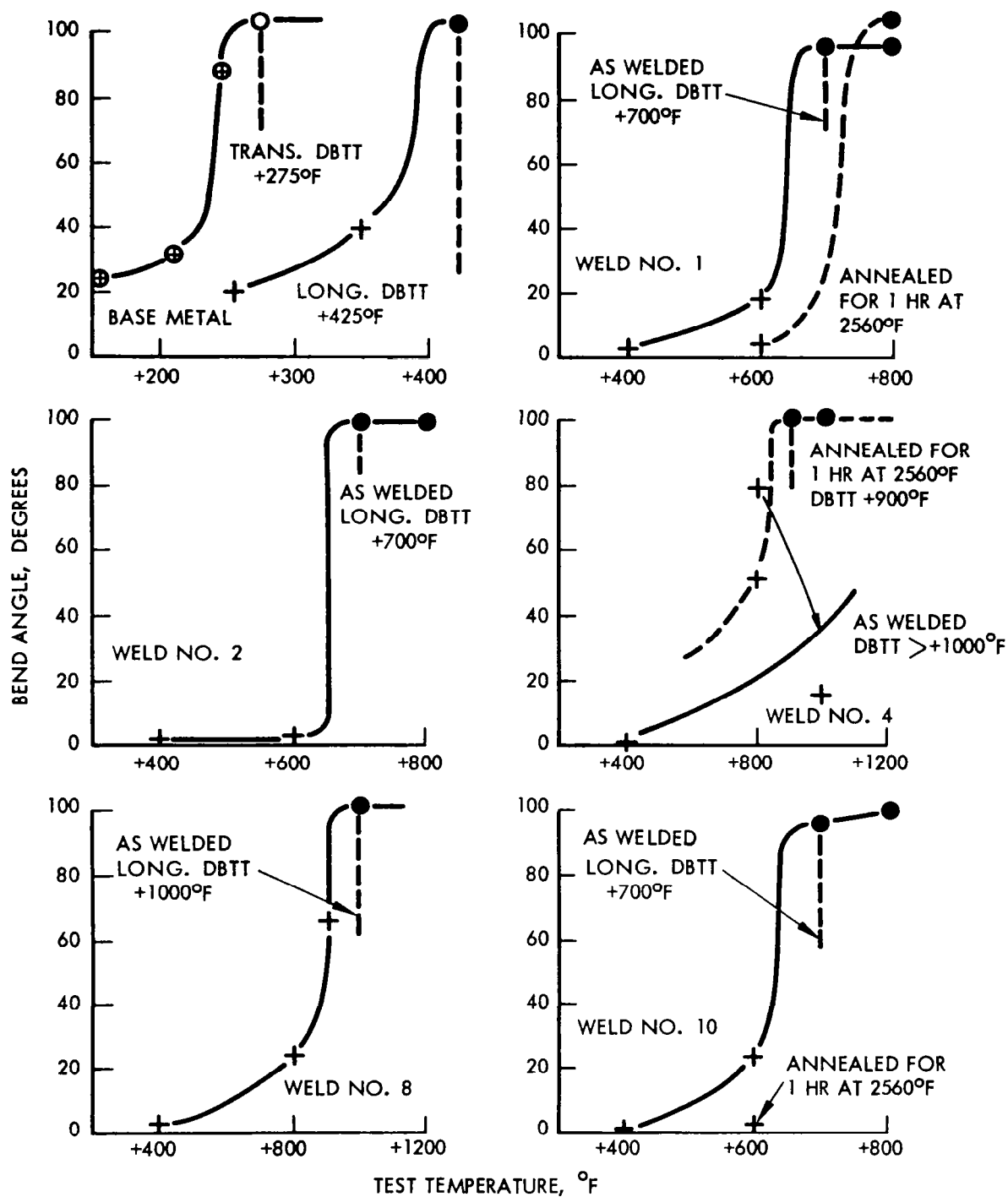
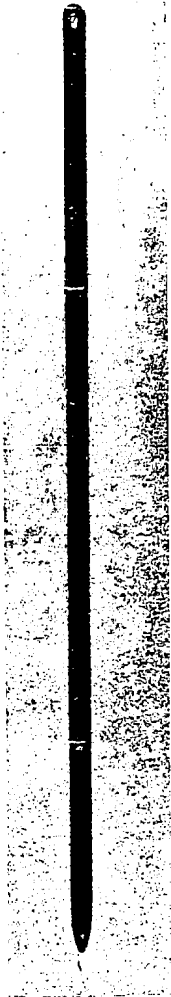


FIGURE A136 - Bend Test Results for Base Metal and GTA Welds in Unalloyed Arc Cast Tungsten (4t Bend Radius)



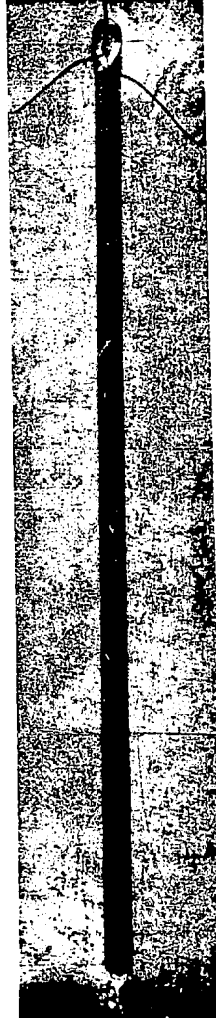
W, Weld No. 1  
155 Amp at 7.5 ipm  
21.1 Kilojoule/inch  
No preheat.



W, Weld No. 8  
147 Amp at 15 ipm  
10.0 Kilojoule/inch  
550°F preheat.



W, Weld No. 7  
158 Amp at 14 ipm  
10.75 Kilojoule/inch  
No preheat.



W, Weld No. 10  
220 Amp at 30 ipm  
7.45 Kilojoule/inch  
No preheat.

FIGURE A137 - Typical GTA Welds in Unalloyed Arc Cast Tungsten



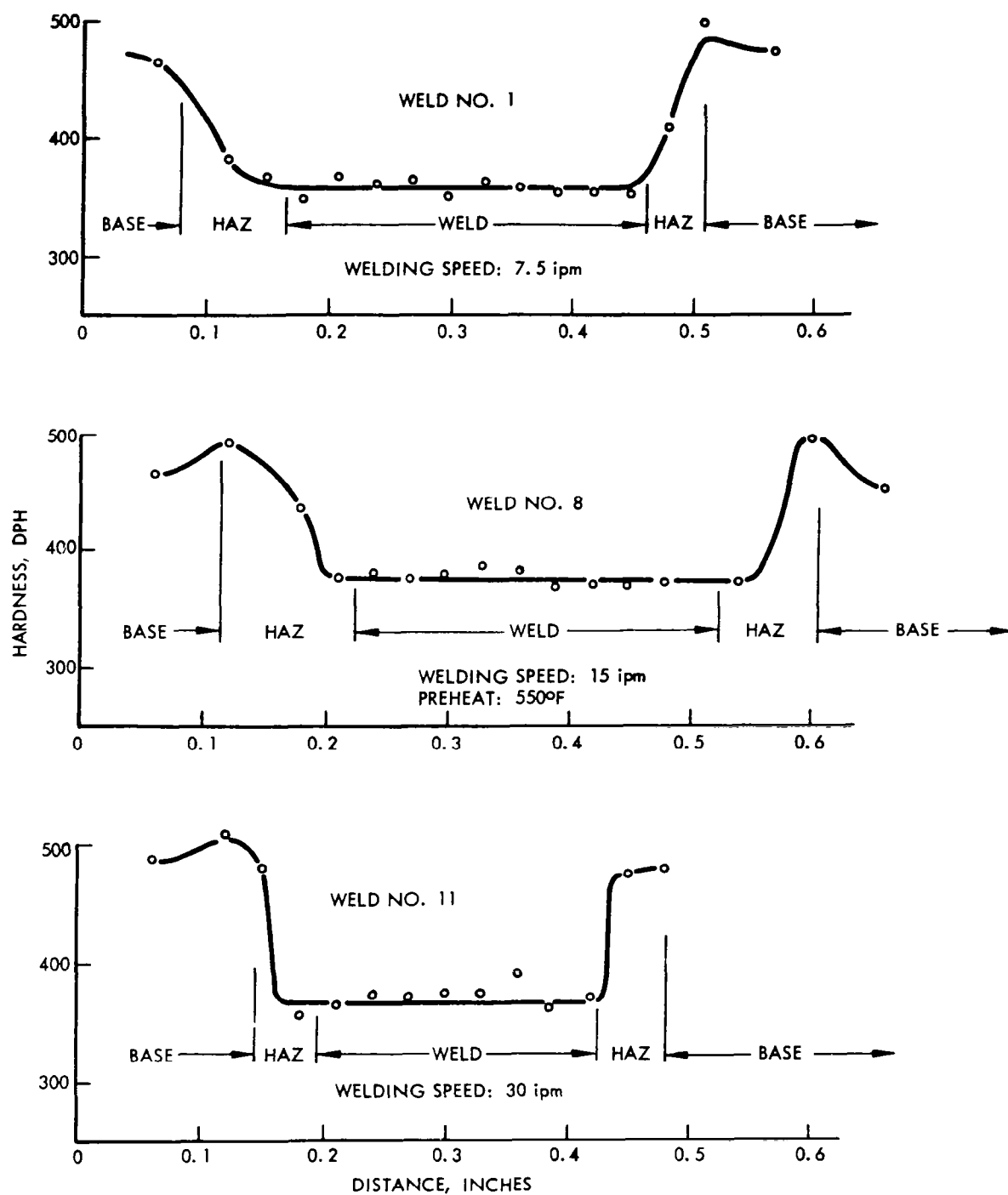


FIGURE A138 - Hardness Traverses for GTA Welds in Unalloyed Arc Cast Tungsten

TABLE A24 - Unalloyed Arc Cast Tungsten Sheet, EB Weld Record

Weld No.	Speed (ipm)	Deflection (inches)	Current (Ma)	Chill Spacing (inches)	Power (Watts)	Watt-Sec. (Per inch)	Weld Bead Width (inches)		Vacuum (Torr)	Comments (3)
							Top	Bottom		
1	15	.050"-L	4.95	1/2	745	2980	.028	.012	$4.4 \times 10^{-6}$	Bend tested
2 <sup>(1)</sup>	15	.050"-T	$\frac{4.40}{4.80}$	1/2	$\frac{660}{720}$	$\frac{2640}{2880}$	.040	N.P. <sup>(2)</sup>	$5.0 \times 10^{-6}$	Bend tested
3	25	.050"-L	4.95	1/2	745	1800	.025	N.P. <sup>(2)</sup>	$4.4 \times 10^{-6}$	Bend tested
4	15	.050"-L	5.40	3/16	810	3240	.025	.015	$4.4 \times 10^{-6}$	Bend tested
5	25	.050"-L	5.40	3/16	810	1940	.022	.010	$4.4 \times 10^{-6}$	Bend tested
7	50	.050"-L	6.60	1/2	990	1190	.017	.015	$5.0 \times 10^{-6}$	
8	100	.050"-L	7.80	1/2	1170	700	.017	.010	$5.0 \times 10^{-6}$	
9	100	Zero	7.20	1/2	1080	650	.015	.010	$5.0 \times 10^{-6}$	
10	15	.050"-T	5.20	3/16	780	3120	.040	.030	$5.0 \times 10^{-6}$	Bead on Plate
11	50	.050"-L	7.20	3/16	1080	1300	.020	.020	$5.0 \times 10^{-6}$	
12	100	.050"-L	8.50	3/16	1270	760	.020	.020	$5.0 \times 10^{-6}$	Bead on Plate
13	100	Zero	7.80	3/16	1170	700	.015	.012	$5.0 \times 10^{-6}$	Bead on Plate

(1) Rewelded because of lack of penetration on first pass.

(2) Bottom delaminated and bulged, no visible fusion.

(3) All welds defected as per dye penetrant.

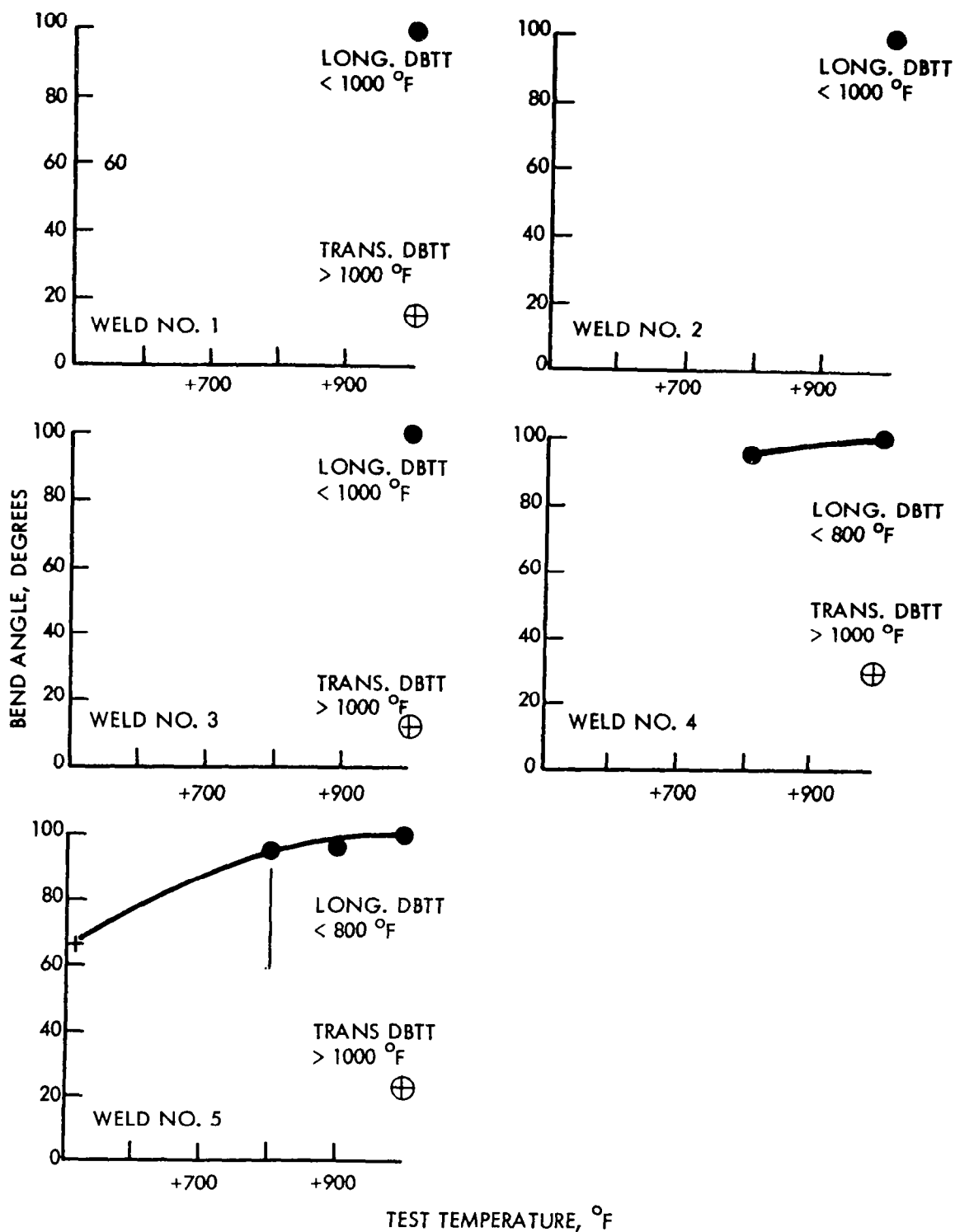


FIGURE A139 - Bend Test Results for EB Welded Unalloyed Arc Cast Tungsten  
4t Bend Radius

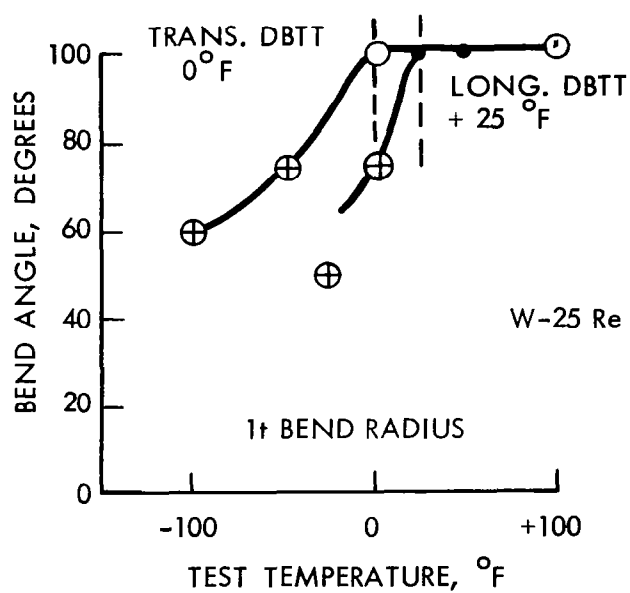
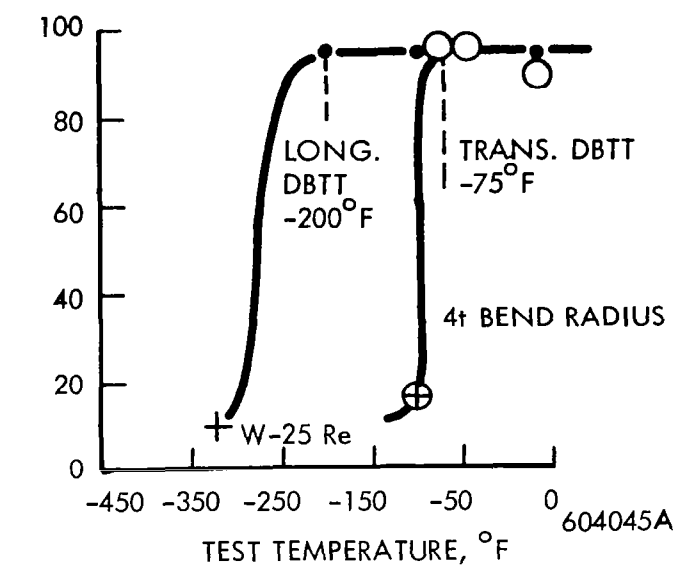


FIGURE A140 - Base Metal Bend Test Results for W-25Re  
4t Bend Radius

TABLE A25 - W-25Re Sheet. GTA Weld Record

Weld No.	Type (I)	Clamp Spacing (inch)	Speed (ipm)	Current (amps)	Pre-Heat (°F)	Weld Width Top/Bottom (inch)	Q Kilojoules (per inch)	Comments - Visual, Dye Penetrant and Radiographic Inspection
1	Butt	3/8	7.5	121	--	.170/.150	16.45	Good weld
2	Butt	3/8	7.5	109	450	.180/.170	14.83	Centerline weld crack 3" long
3	Butt	3/8	7.5	100	--	.150/.110	13.60	Good weld
4	Butt	3/8	7.5	83	550	.110/.055	11.29	Good weld
5	Butt	3/8	15	139	--	.180/.160	9.44	Three transverse cracks thru weld + Haz
6	Butt	3/8	15	131	450	.170/.150	8.90	Good weld
7	Butt	3/8	15	102	--	.120/.075	6.93	Good weld
8	Butt	3/8	30	204	--	.185/.160	6.93	Six transverse cracks thru Weld + Haz
9	Butt	3/8	30	185	450	.180/.160	6.28	Five transverse cracks thru Weld + Haz
10	BOP	3/8	30	147	550	.125/.110	5.00	Four transverse cracks thru Weld + Haz
11	BOP	3/8	3	95	--	.150/.110	32.30	Good weld
12	BOP	3/8	3	90	550	.150/.120	30.60	Good weld

W-25Re, Weld No. 2  
109 Amp at 7.5 ipm  
14.83 Kilojoule/inch  
450° F preheat.



W-25Re, Weld No. 7  
102 Amp at 15 ipm  
6.93 Kilojoule/inch  
No preheat.



W-25Re, Weld No. 11  
95 Amp at 3 ipm  
32.30 Kilojoule/inch  
No preheat.



W-25Re, Weld No. 12  
90 Amp at 3 ipm  
30.60 Kilojoule/inch  
4550° F preheat.



FIGURE A141 - GTA Welds in W-25Re

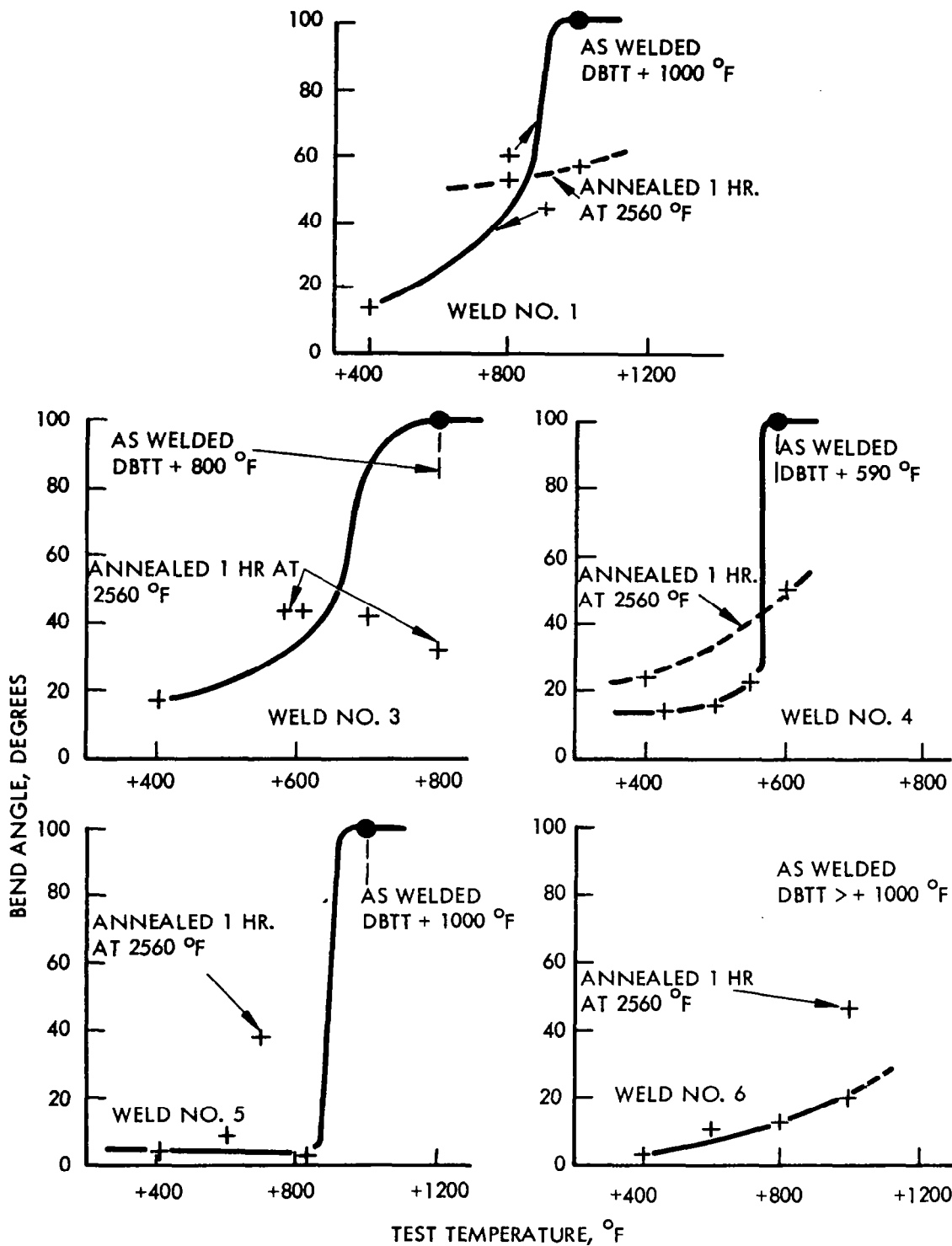


FIGURE A142 - Bend Test Results for W-25Re GTA Welds  
4t Bend Radius

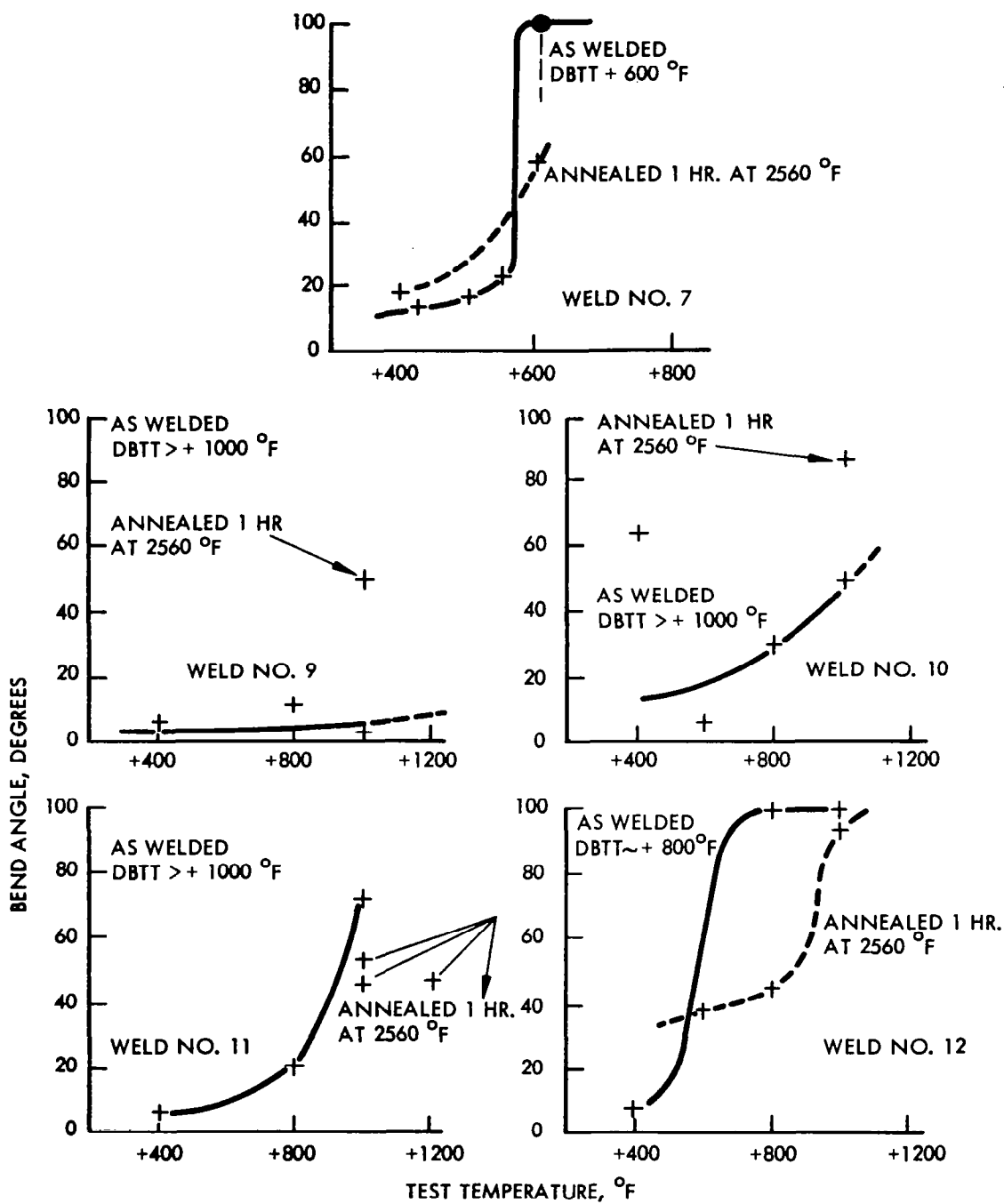


FIGURE A143 - Bend Test Results for W-25Re GTA Welds  
4t Bend Radius



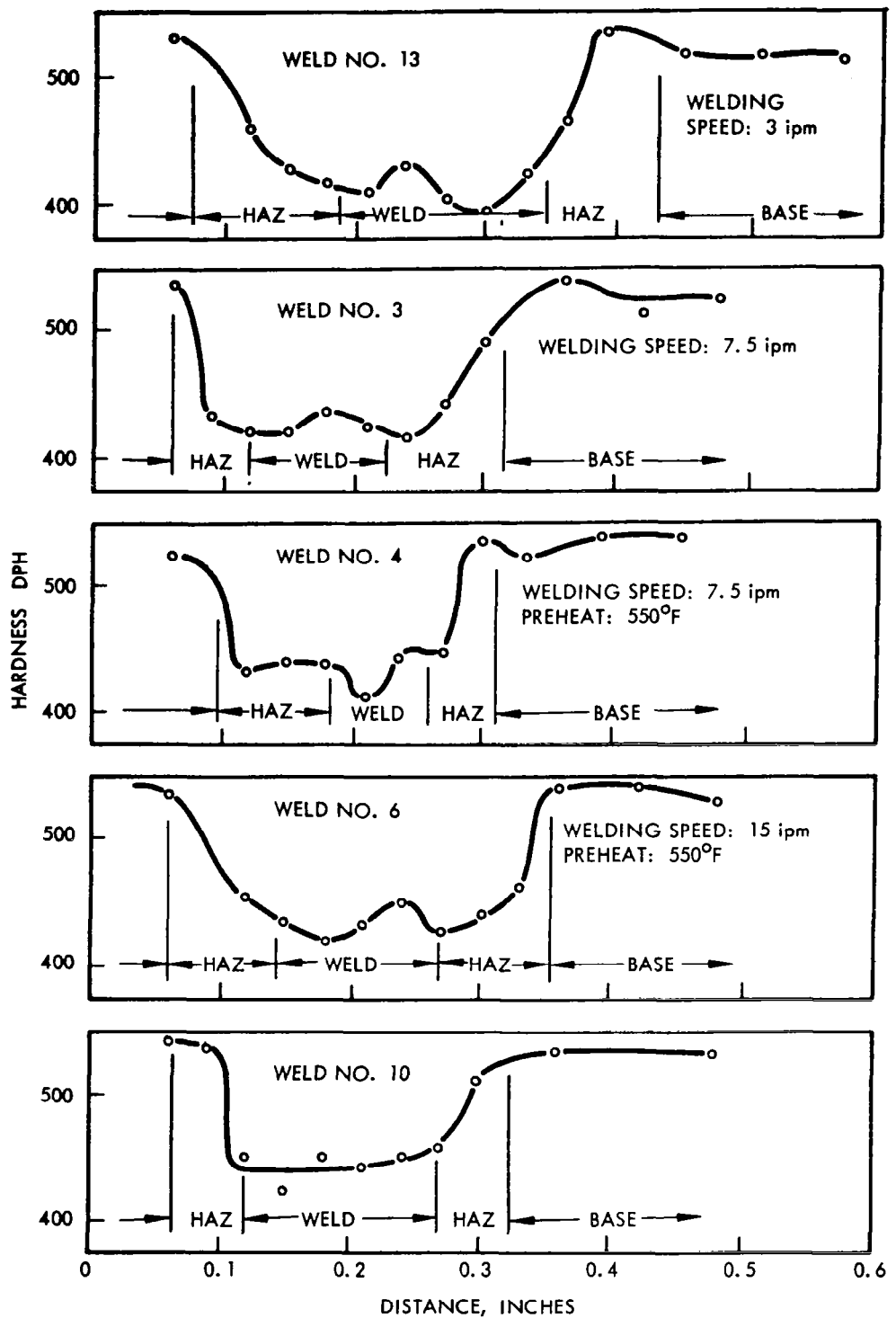


FIGURE A144 - Hardness Traverses of GTA Welds in W-25Re

TABLE A26 - Electron Beam Welding Parameters for W-25Re

Weld <sup>3</sup> No.	Speed (ipm)	Deflection <sup>1</sup> (inches)	Current (ma)	Chill Spacing (inches)	Power <sup>2</sup> (watts)	Watt-Sec. per inch	Weld Bead Width (inches)		Vacuum (torr)
							Top	Bottom	
1	100	L-0.050	7.5	0.250	1125	675	0.028	0.018	5.0x10 <sup>-6</sup>
3	50	L-0.050	6.3	0.250	945	1130	0.035	0.023	5.0x10 <sup>-6</sup>
4	100	L-0.050	7.2	0.094	1080	650	0.029	0.017	5.0x10 <sup>-6</sup>
5	50	L-0.050	6.0	0.094	900	1080	0.035	0.022	5.0x10 <sup>-6</sup>
11	50	zero	5.6	0.094	840	1010	0.027	0.020	1.7x10 <sup>-6</sup>
12	25	L-0.050	6.0	0.094	840	2010	0.040	0.032	1.7x10 <sup>-6</sup>
13	15	L-0.050	4.6	0.250	690	2860	0.036	0.022	2.0x10 <sup>-6</sup>
14	50	L-0.100	7.2	0.094	1080	1300	0.031	0.022	2.0x10 <sup>-6</sup>
15	50	L-0.025	6.0	0.094	900	1080	0.030	0.022	2.0x10 <sup>-6</sup>
16	15	L-0.050	5.1	0.094	765	3020	0.038	0.027	2.0x10 <sup>-6</sup>
17	15	zero	4.8	0.094	720	2880	0.032	0.023	2.0x10 <sup>-6</sup>
18	15	T-0.050	5.7	0.094	855	3420	0.060	0.050	2.0x10 <sup>-6</sup>

1. L. is longitudinal  
T. is transverse
2. All welds made at 150 KV
3. 18 welds were made to produce 12 acceptable welds because of a welding problem mentioned on Pages 13 and 14.

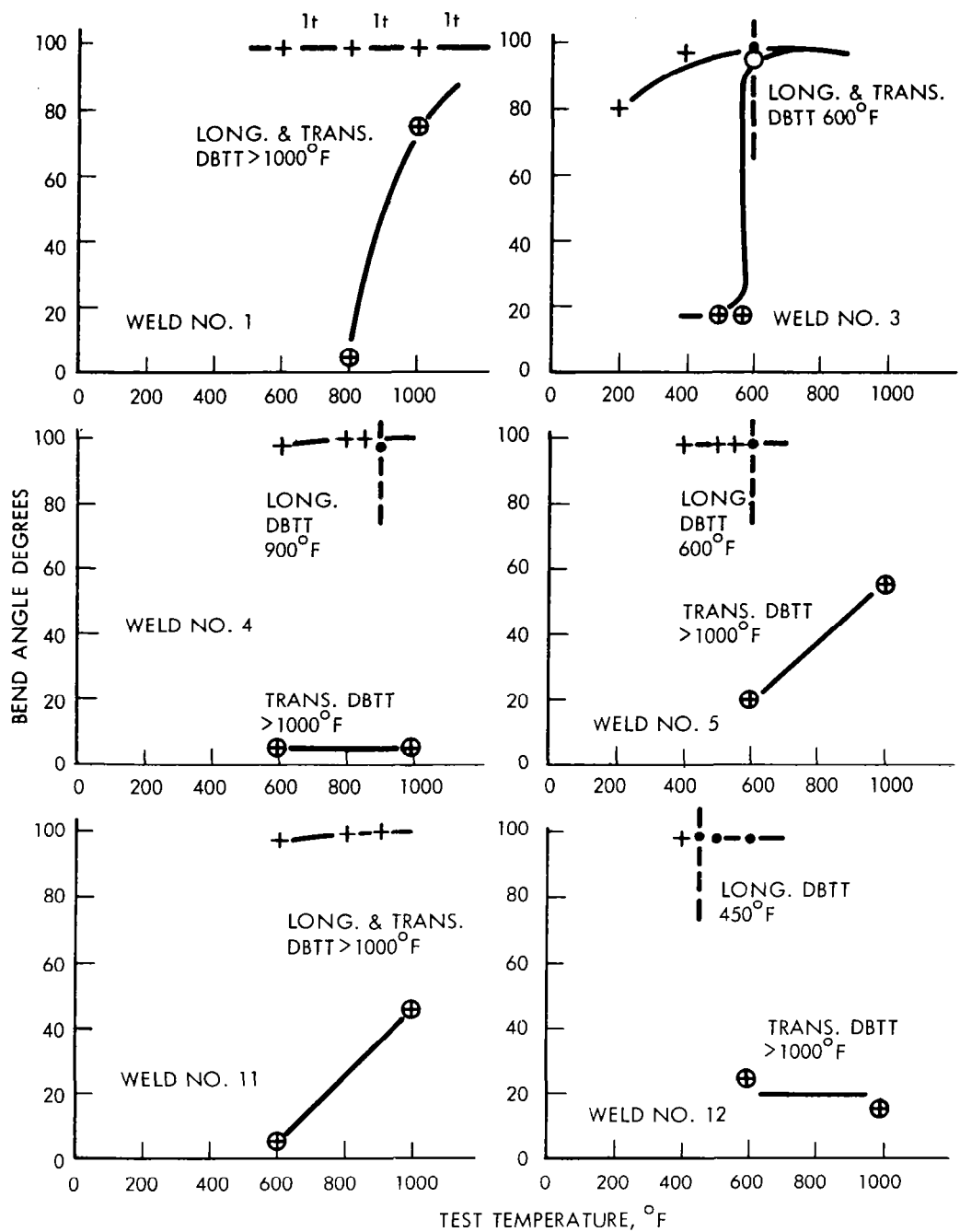


FIGURE A145 - Bend Test Results for W-25Re EB Welds  
4t Bend Radius

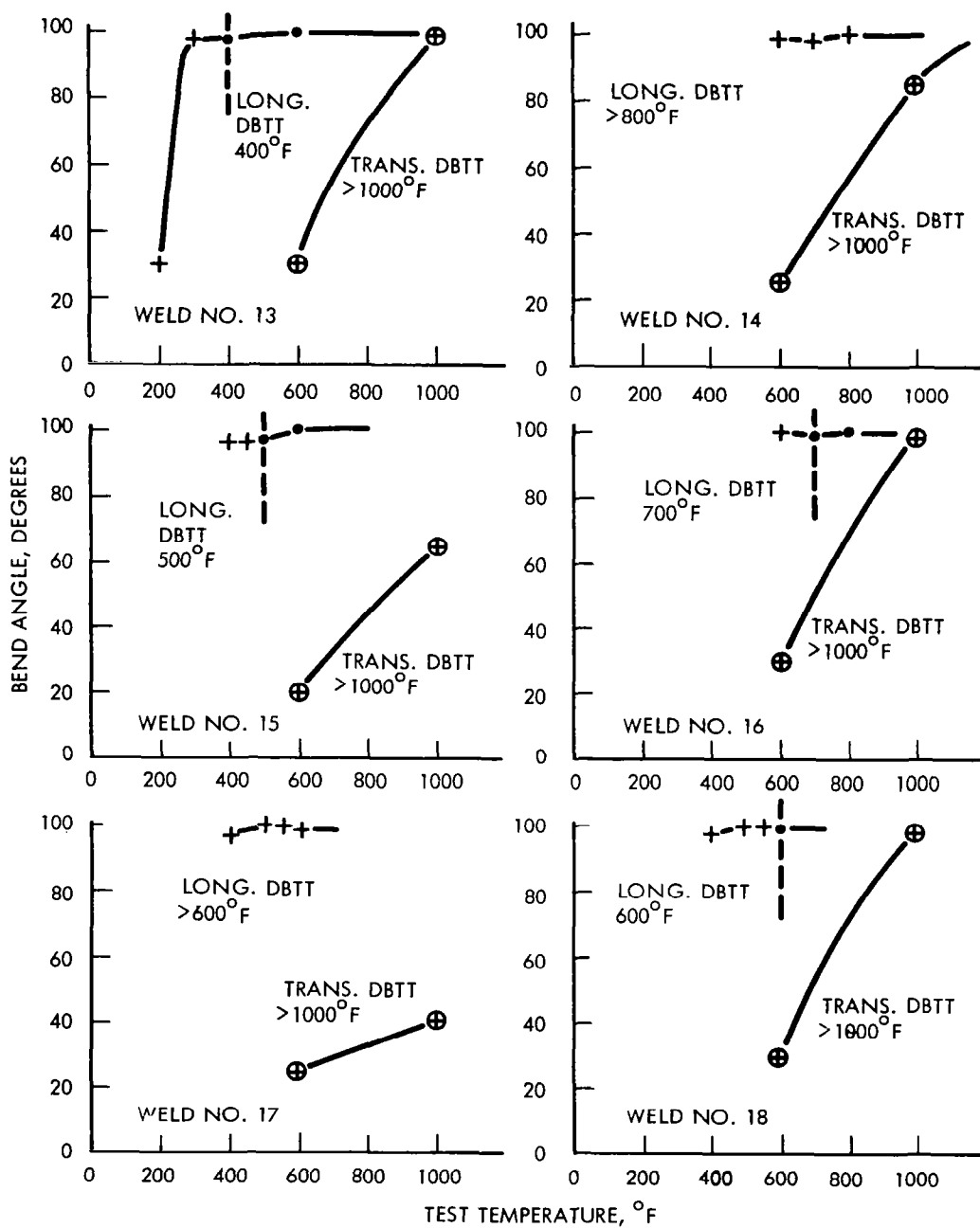


FIGURE A146 - Bend Test Results for W-25Re EB Welds  
4t Bend Radius

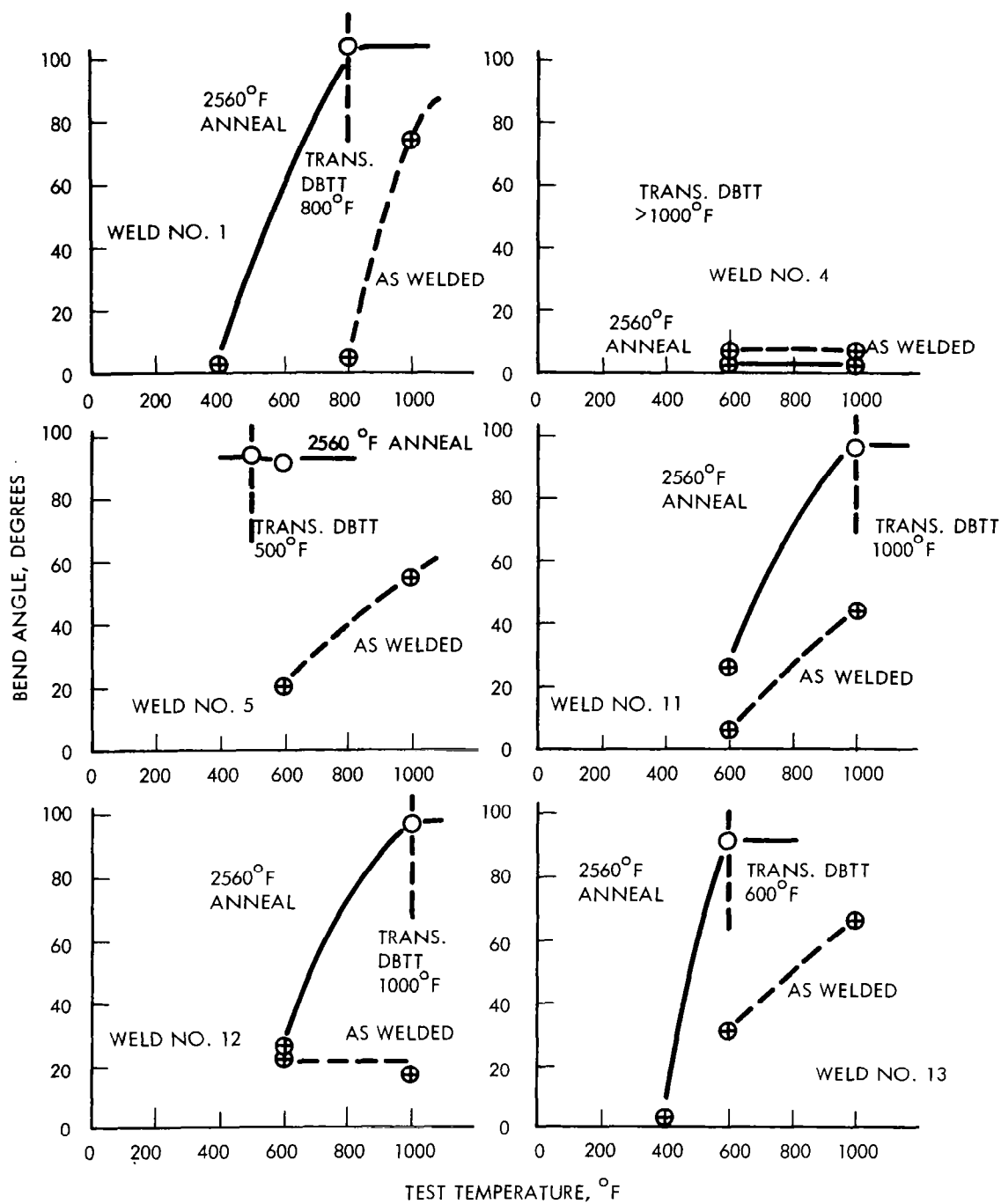


FIGURE A147 - Bend Test Results for W-25Re EB Welds, Stress Relieved 1 Hour at 2560°F 4t Bend Radius

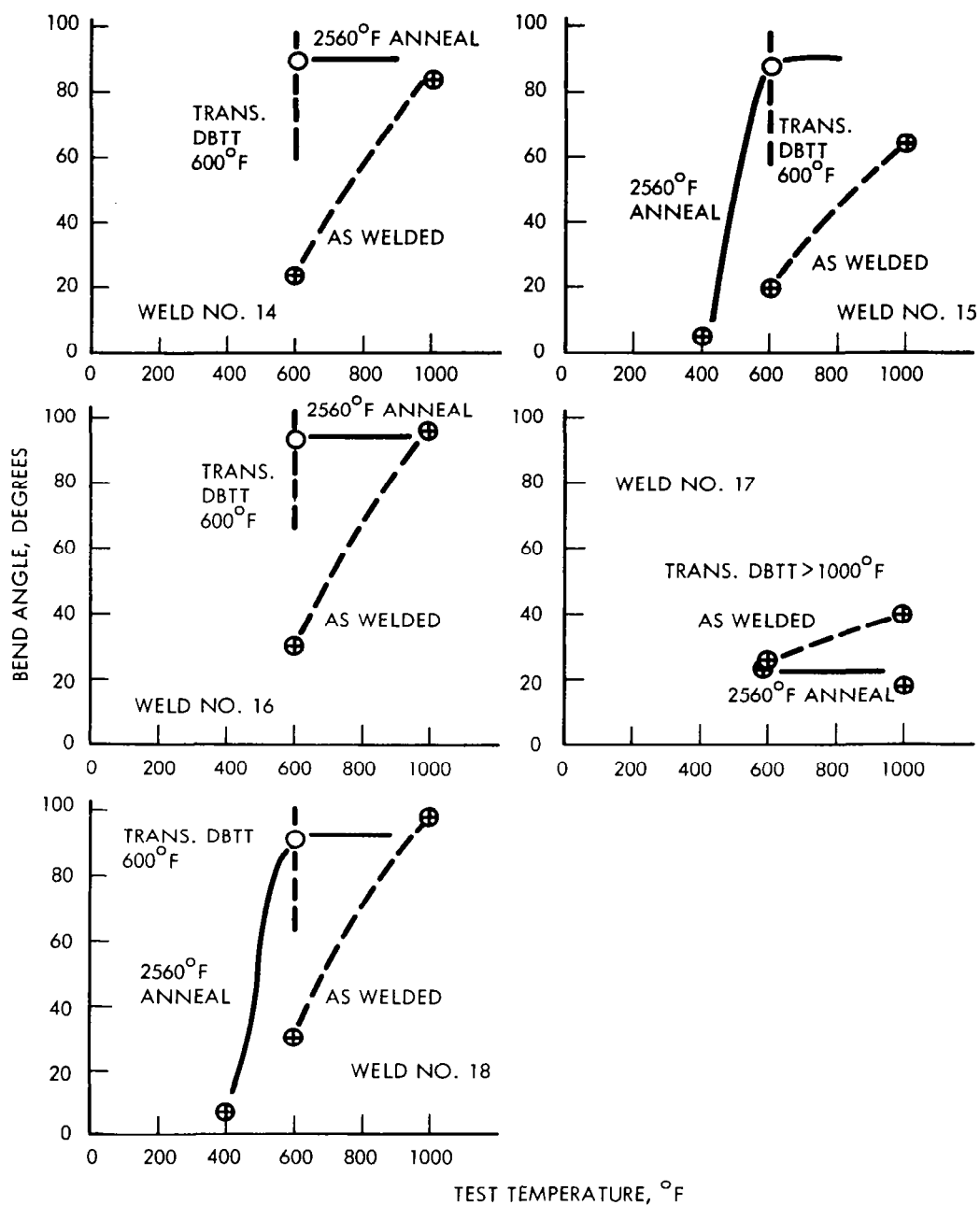
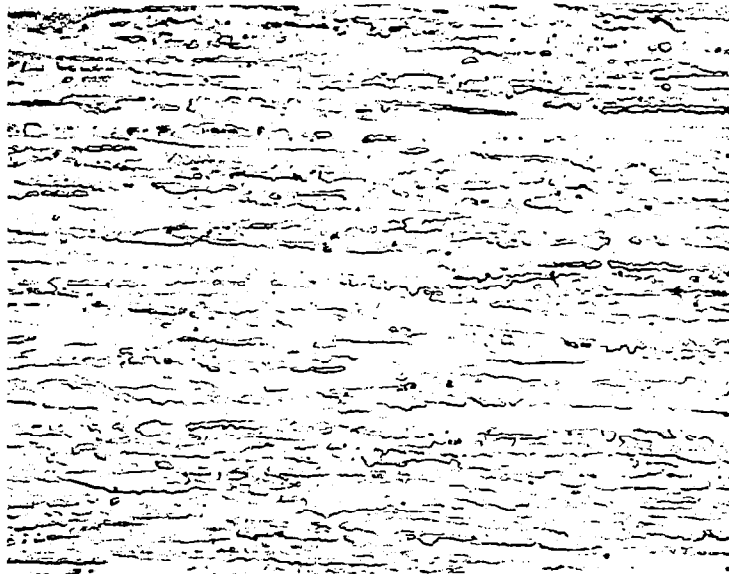
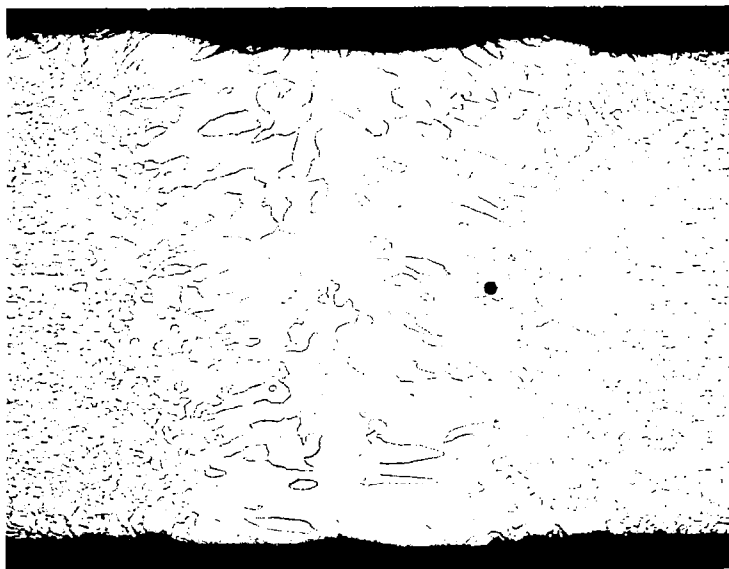


FIGURE A148 - Bend Test Results for W-25Re EB Welds, Stress Relieved 1 Hour at 2560°F 4t Bend Radius



Base Metal

400X



EB Weld

80X

FIGURE A149 - W-25Re EB Weld and Base Metal Microstructure

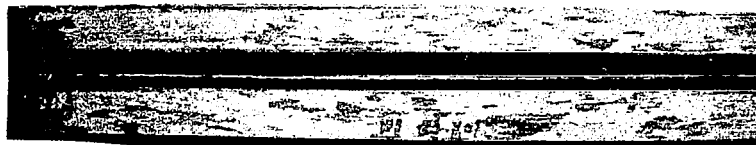
TABLE A27 - Sylvania "A" Sheet, GTA Weld Record

Weld No.	Type	Clamp Spacing (inch)	Speed (ipm)	Current (amps)	Pre-Heat (°F)	Weld Width Top/Bottom (inch)	Q Kilojoules (per inch)	Comments - Visual, Dye Penetrant and Radiographic Inspection
1	Butt	3/8	7.5	163	550	--	--	Badly cracked
2	Butt	3/8	1.5	176	--	.170/.170	11.9	Badly cracked
3	Butt	3/8	3	130	--	.150/.140	44.2	Badly cracked
4	Butt	3/8	3	125	500	.170/.160	42.5	Badly cracked





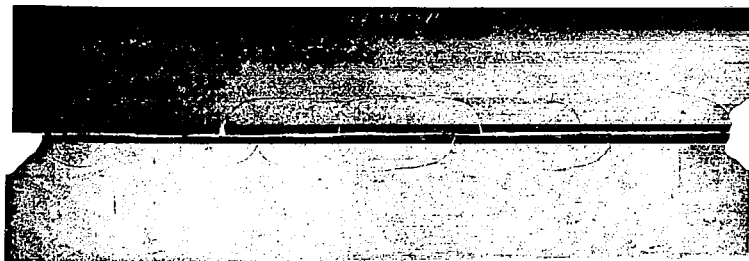
Weld No. 1 First Try; Preheated 550°F; 7.5 ipm 871-2



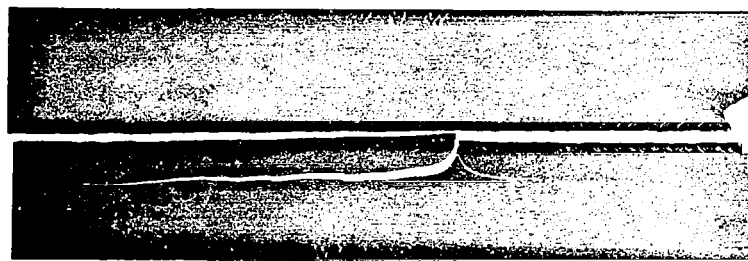
Weld No. 1 Second Try; Preheated 550°F; 7.5 ipm 871-2



Weld No. 2 No Preheat; 1.5 ipm; 119.8 Kilojoules/inch 871-2



Weld No. 3 No Preheat; 3 ipm; 44.2 Kilojoules/inch 6023



Weld No. 4 Preheated 550°F; 3 ipm; 42.5 Kilojoules/inch 6023

FIGURE A150 - Sylvania "A" GTA Welds

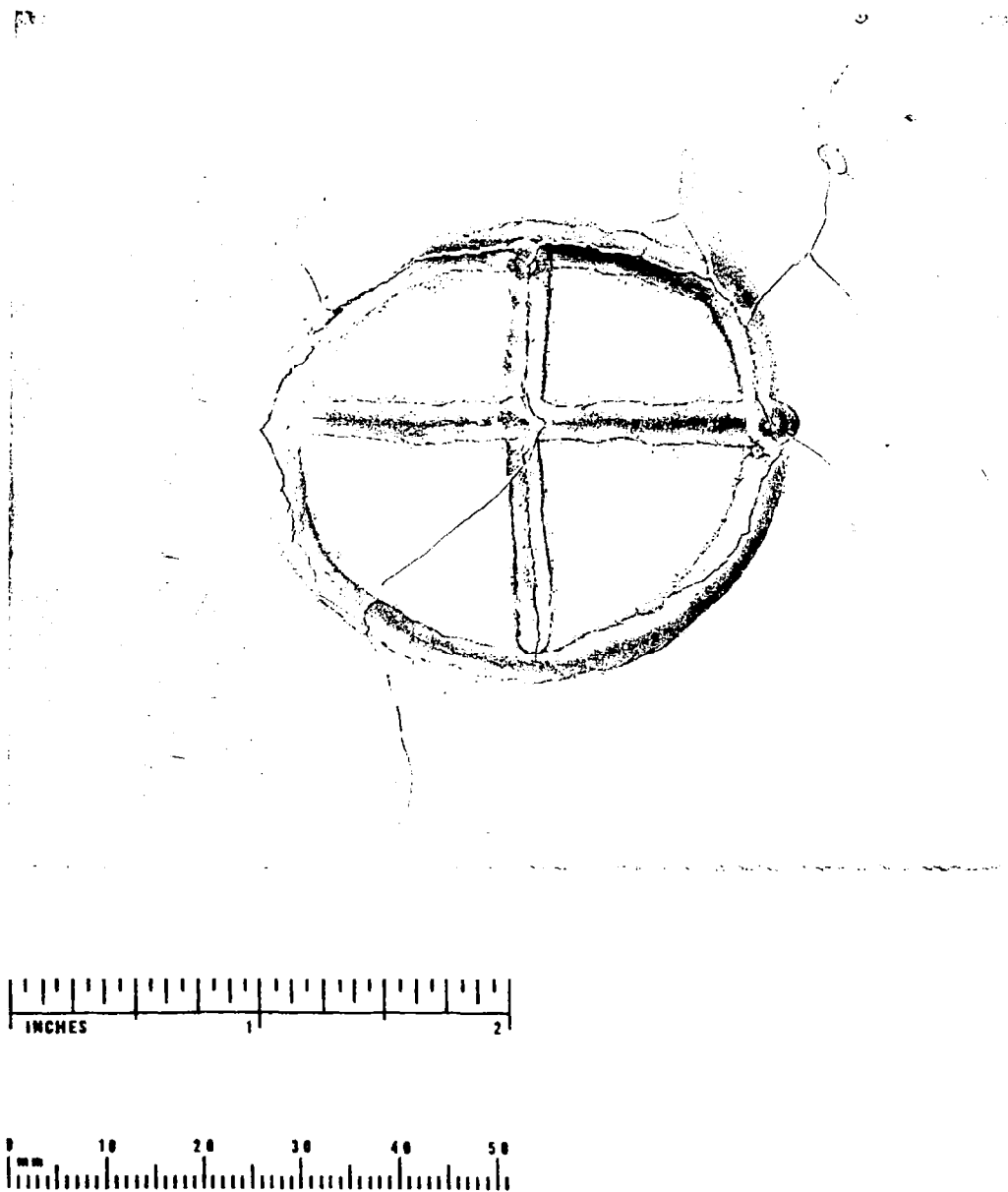


FIGURE A151 - Sylvania "A" GTA Bead-on-Plate Patch Test